FAILURE MECHANISMS IN SURFACE TREATED TOOL STEELS

BY

ISAKPOBEJE EWERE

A thesis submitted for the degree of Doctor of Philosopy

at the UNIVERSITY OF ASTON in Birmingham

OCTOBER 1979.

TITLE: FAILURE MECHANISMS IN SURFACE TREATED TOOL STEELS

NAME: ISAKPOBEJE EWERE

DEGREE: Ph.D

DATE: OCTOBER 1979

S Y N O P S I S

An investigation of the failure mechanisms associated with cyclic and static stressing of hot work tool steels has been undertaken. The materials used were BH13 and Ni-Cr-Mo (No.5) die steels, both were evaluated in the hardened and tempered conditions and after the application of various surface treatments. Five test procedures were employed, namely - wear, thermal fatigue, mechanical fatigue, impact, and slow bend. The surface treatments employed were plasma nitriding, Tufftriding, brush plating of a Co-Mo alloy, electroless deposition of a Ni-P alloy and electrodeposition of hard and Micro-cracked chromium.

Simple upset forging tests, aided by microscopic examination of die surface and subsurfaces were performed:-

(1) to establish the wear mechanisms of both steels during dry hot forging.

(2) to assess the effect of surface quality on wear.

Four main mechanisms (oxidation, erosion, abrasion, delamination) were observed, while it was shown that die wear is a sensitive function of surface quality.

Thermal fatigue test results indicated that plasma nitriding and brush plated Co-Mo alloy may delay craze-cracking of dies during hot forging and die-casting.

Semi-range S-N curves for three-point bend fatigue conditions were established for No.5 die steel in the hardened and tempered condition, and after coating with electrodeposited hard and Micro-cracked Cr, brush plated Co-Mo alloy and electroless Ni-Palloy. The mechanisms observed on the fracture surfaces included, brittle and ductile failure, void coalescence and cleavage facets.

Standard Izod impact test results indicated reductions in Notch-toughness of between 1.7% to 12.3% for similar coatings to those applied to fatigue testpieces above. The failure mechanisms were also similar to those observed on the fatigue testpieces.

Finally slow bend test results showed that, all except hard Cr improved ductility of the composites.

I N D E X

DIES
WEAR
FATIGUE
DUCTILITY
TOUGHNESS

LIST OF CONTENTS

LIST OF TABLES

LIST OF FIGURES

Fig. 59 Effect of machining on subsurface hardness of dies before forging.

(a) and (b) show the variations in No.5 die, while

(c) and (d) show the variations in BH13

FG: Finish ground. RG: Rough ground

RT: Rough turn EDM: Electro-discharge machining.

Fig. 60 Effect of thermal cycling on plasma nitrided BH13 die after

(a) 500 cycles at 500°C, mag x 249

(b) 1000 cycles at 750°C, Mag x 123

(c) 2000 cycles at 750°C, Mag x 123

(d) Co-Mo alloy brush plated No.5 die after 1000 cycles at 500°C. Mag. X345.

(e) bath plated Co-Mo alloy No.5 die after 1000 cycles at 500°C. Magnificant including taper x 1000 (after still and Dennis[24]).

Fig. 61 S.E.M. fractograph showing a mixture of void coalescence and cleavage near the notch root of a hard Cr plated No.5 die steel impact testpiece.

Fig. 62 S.E.M. fractograph showing large and small dimples in the core of a hard Cr plated No.5 die steel impact testpiece.

Fig.63 S.E.M. fractograph showing a mixture of dimples and tearing near the notch root of a hard Cr plated No.5 die steel impact testpiece.

Fig. 64 Three views of the fracture surface of a hard Cr plated No.5 die steel impact testpiece showing -

(a) the edge of the restpiece

(b) a mixture of cleavage plus tearing

(c) an enlargement of one of the tear ridges.

Fig. 65 Two views of the fracture surface of a hard Cr plated No.5 die steel impact testpiece showing -

(a) several large and small dimples

(b) an enlargement of the central dimples together with the inclusions associated with them taking ahead of the rear ridges in fig. 64.

1. GENERAL INTRODUCTION

The cost of dies used for drop forging is of frequent, practical concern to both the design and production engineer since it constitutes about one-tenth of the total cost of a forging. Thus, due to the present world economic climate drop forgers are constantly searching for die materials which are cheap to fabricate and heat treat, but which also possess mechanical and thermal properties to make them stand up to the severe service conditions experienced in the industry.

In the past this search led to the use of die materials which vary considerably from cheap, low alloy to expensive highly alloyed steels. The most commonly used dies are BH13 and a low alloy Ni-Cr-Mo grade referred to as No.5 die steel in BS224. This is probably because of their intermediate cost.

More recently, however, research within the university and industry has been directed towards both structural modifications (i.e. by varying chemical composition) and improved surface technology to lengthen die life. In the latter situation a wide range of diffusion and surface coatings have been formulated and applied on industrial dies. The results of such application have not all been fully successful. In some instances it has been reported that die life may be increased considerably (about 80% improvement) while in others the improvement has been less.

Despite these claims dies are still reported to fail either through fatigue or the malpractice of operatives on the shop floor. It is generally recognised that the forge Manager may trace damage of his dies to one or a combination of the following four basic phenomena although not all their failure mechanisms are exactly known.

(1) Wear.

(2) Mechanical Fatigue.

(3) Thermal Fatigue.

(4) Plastic Deformation.

All these phenomena can be complicated since they may occur in different forms (either separately or together) and at a variety of sites in the die, each of which can lead to eventual die failure. For example, wear may be erosive or fatigue orientated, although in either case this may lead to the production of out-of-tolerance forgings and an increase in down-time required for tool setting.

As a result of the above it seems logical that interest has grown in recent years to investigate all the modes of failure in some detail together with the thermo-mechanical properties of the die steels, before and after surface treatment, with a view to understanding their basic failure mechanisms.

2. LITERATURE REVIEW

Information and data reviewed in this section are orientated towards understanding the current knowledge of service failures of BH13 and Electem No.5 die steels, although much of this information may apply to other die steels. This section is divided into three general parts. The first two deal with wear in forging dies and other thermo-mechanical properties of die steels. Finally, the third part is devoted exclusively to surface treatments and their effects on the service failures of die steels.

2.1 WEAR

2.1.1 INTRODUCTION

Practically wear is not necessarily catastrophic, although it may reduce operating efficiency, increase power losses and perhaps double die replacement rates. Die wear is not entirely an intrinsic material property, but is also a characteristic of the engineering system. A number of conditions may cause wear, with many mechanisms contributing to the damage caused. The solution of a particular problem requires precise identification of the nature of the problem. Care must therefore be exercised in applying general solutions to individual problems.
In the past an empirical approach coupled with conventional wear tests was adopted in an attempt to understand the mechanism of wear in forging die steels, and so relate the severity of wear to material properties and enviromental conditions. Unfortunately, most of the earlier conventional tests were aimed at conventional wear processes, e.g. adhesive and abrasive wear. However, for a wear test to be of significance it must be simulative of the actual forging conditions, e.g. impact blow, temperature gradients across die, loading frequency and test geometry. No conventional wear testing machine (e.g. falex, pin and disc,

block and disc, or amsler) can accommodate all the experimental conditions experienced during forging. The present trend, however, is to perform the test in a real hammer or press [1,2,3]. So far emphasis has been placed on (a) characterising materials (b) determining the effects of variables and (c) selecting materials for specific applications, e.g. coating dies. Little evidence therefore exists of the true nature of the wear process in die steels during upset forging.

This work attempts to fulfill this need by examining the wear phenomenon of both steels, using the same press used by Dennis and Still.[1]

In general, the four main modes of failure of a forging die steel may be collectively grouped into deformation, erosion thermal and mechanical fatigue, although their causes may be intermingled. Information presented in the forepart of the following discusses only the first two modes and other related topics, whilst the last two failure modes are dealt with under the general heading of "thermo-mechanical properties".

2.1.2 TYPES OF WEAR

2.1.2.1 ADHESIVE WEAR

Extensive investigations have already been done on this subject. Work by several authors [4,5,6] are available. However, the process of wear particle formation has not been clearly established. Bowden and Tabor [7], Tabor [8] Landheer and Zaat [9], have put forward their theories. There is no unilateral agreement as to what occurs, even though they all agree that when two surfaces come into contact they meet at their asperities. Wear by adhesion occurs when surfaces slide against each other, and the pressure between the contacting surface asperities is high enough to cause local plastic deformation and adhesion. Asperity deformation occurs until such time when the real area of contact has increased enough

to support the load, thus causing an increase in the area over which adhesion can take place as sliding continues. Eventually, the adhesively formed junctions rupture at their weakest points, usually resulting in metal transfer from one surface to the other. However, if particles remain undislodged from their adhesive junctions they can act as agents for subsequent abrasive wear.

Several factors may affect asperity deformation (elastic plus plastic). For example deformation may be affected by temperature, sliding speed, load, strengths of the contacting metals, surface cleanliness and oxidising conditions. Unfortunately, there does not exist, as yet, any mathematical relationship containing combinations of more than three of these factors. According to Archard [6], wear (V) may be expressed by the relationship

$$V = \frac{K\,Lx}{Lm}$$

Where L = Load, X = distance of sliding

Lm = flow pressure of the wear surface

K = a dimensionless constant.

The flow pressure may be regarded as hardness according to Hirst [10]. The accuracy and completions of this relationship is not generally accepted upon. According to the above equation wear rate would generally decrease as hardness increases if the other factors remain constant. Load and sliding distance are not the only factors that would affect wear. Microstructure and the distribution of hard particles can affect hardness values. Thus the dimensional constant (K) would vary from material to material. Also K would change as the load or sliding speed is changed according to this equation. Unfortunately, these changes in K value, argue against the constancy generally expected of a constant of proportionality in a mathematical equation. Therefore, there must be

some factors missing from the equation. For example the equation excludes an apparent area term, and thus suggesting that test geometry is unimportant in determining wear. This is untrue since test geometry can affect subsequent wear by abrasion due to the presence of undisloged wear particles.

Wear under adhesive conditions, unlike abrasive wear, is subject to sharp transitions in behaviour. Variations in load and speed may bring about marked thermal changes which proceed and cause wear changes. Welch [11] examined the idea of mild wear (oxidation) and severe wear (oxidative + metallic) and the sharp transition between them. He referred to this as T_1 and T_2 transitions as shown in fig.1.

Below T_1 wear occurs by the removal of oxide debris from an oxidized surface of a work hardened substrate. T_1 is a transition to severe wear initiated by the breakdown of the protective surface oxide produced at lower loads. Plastic deformation of the substrate then ensues, caused by a higher bulk temperature due to sliding such that the wear rate increases considerably and leading to the production of metallic debris. Between T_1 and T_2 severe wear occurs. At T_2 the surface temperature is high enough for phase hardening to produce a hard "white layer" which prevents deformation and helps to establish an oxidized surface once more.

In hot forging, the situation encountered is quite different from that described above. The least forging load applied by the 10 - Ton press at Aston is probably in the region of 4 tons for a single cycle. Thus any oxide forming on the die surface may easily be broken, thus creating room for metal - to - metal contact. Also die surface temperature is elevated well above room temperature, as against the room temperature condition used by Welch. On the above basis it would

appear that mainly severe (oxidative plus metallic) wear would occur during hot forging.

Finally it should be noted that although adhesive wear theory appears to be well documented in the literature, understanding falls short of the effects of microstructure on wear. Both Archard [12] and Rabinowicz [13] have elaborated on the inability of this theory to explain the effects of microstructure. It certainly does not account for processes such as subsurface deformation, crack nucleation and propagation, which depend very much on material structure. The knowledge is certainly incomplete, but this is the present situation.

2.1.2.2 A B R A S I V E W E A R

One of the very first real attempts to examine abrasive wear scientifically were made by Kruschov [14], and Kruschov and Babichev [15]. Commercially pure metals (Fe, Cu, Pb, Nl, W, Mo, AL) were examined in their annealed conditions and it was found that their wear resistance (reciprocal of wear volume) decreased linearly with load and sliding speed but increased with bulk hardness. Fig.2. shows the results obtained for wear resistance against bulk hardness, percentage carbon and carbides. A number of steels (as indicated by the varying %C steels in fig 2a) heat treated to different hardness levels showed linear relationship between hardness and wear resistance, but the slopes of their graphs were found to be less than that for pure metals. This indicates that wear resistance also varies with microstructure.

Serpik and Kanton [16] have also shown that wear resistance varies with carbon content, for steel, and also as the microstructure varies for a given carbon content (fig 2b). Popov [17] similarly demonstrated (Fig.2c) that in steels both volume and composition of carbides are important. This results conforms with those obtained for die steels (e.g. 5% Cr steel)

in which vanadium carbides are claimed to be superior to chromium carbides in improving the wear resistance of BH13.

Work by Kruschov [14] and his co-worker [15] mentioned above has certain important implications which must be closely examined. First it concluded that at a given hardness value, the wear resistance of a heat treated steel is less than that of a pure metal treated to the same hardness. Second, it concludes that steels of different compositions heat treated to the same hardness do not possess the same wear resistance. Finally, the linear relationship for the pure metals has its origin at zero, where as the relationships for alloy steels show positive intercepts when they are extrapolated. This indicates that the behaviour of alloy steels cannot be described by the simple equation of the form

$$\text{Wear resistance } (\varepsilon) = K H_v \qquad (1)$$

Published tests [18, 19] on the simple theory of abrasive wear do not agree with the above observations. For example, the usual model considers a single hard conical asperity of known included angle (θ) to contact a metal specimen under known load (L) as the indenter in a hardness test. If the asperity (particle) is made to traverse the specimen, the volume of metal can be obtained from

$$V = \int_0^x \frac{L \tan \theta}{\pi H_v} \, dx \qquad (2)$$

where $\frac{L \tan \theta}{\pi}$ is constant and H_v is the metal hardness. Thus equation (2) is equivalent to (1) with $K = \frac{L \tan \theta}{\pi}$ since it predicts that, for constant grading conditions (θ, L are constant), the wear resistance ε will be directly proportional to the metal hardness. Equation (2) therefore allows the results for the pure metals to be explained if the gradients of the line is assumed to be equal to $L \tan \theta/\pi$ but it does not explain the

other implications of the work by Kruschov and his co-worker. After Kruschov, Badse [20] studied and plotted wear resistance against bulk hardness and obtained a relationship better fitted by two lines rather than one, but which also showed sudden increasing change. He then suggested that to obtain results similar to those of Kruschov, surface rather than bulk hardness should be used in the ε Vs H_v plot for heat treated steels. Unfortunately, it has been demonstrated recently that in this modified plot, the linear relationship is only followed in a general sense. However, further work on white cast iron, nodular iron and steel has shown that abrasive wear rate depends on the hardness of the worn, rather than the unworn surface. For white cast irons which do not work harden, there appears to be a good correlation between wear volume and hardness of the worn and unworn surface. With steel, increased hardness was observed on the worn surface. This is because the surface of the steel is work hardened due to high stresses set up. The worn surface considered above is itself a subsurface. Thus the subsurface of the steel is work hardened during abrasive wear, implying that the abrasive wear mechanism would depend amongst other things on subsurface hardness. That is, the subsurface hardness would affect the rate of plastic deformation and surface traction by each asperity during subsequent sliding abrasion. These results may well apply to some die steels, although it is not clear whether surface treated and untreated H13 and electron No.5 die steels would work harden during hot forging. It is worth noting that the rate of plastic deformation and surface traction at each asperity may also influence the subsurface deformation, crack nucleation and propagation processes. Unfortunately, the present level of understanding of abrasive wear mechanism (as indicated by the simple abrasive wear model) does not permit an explanation for these

material-dependant subsurfaces processes which may account for micro-chip formation. However, the inability of the simple model to explain the results for heat treated steels together with the contradictory nature of some of the previous work [21], suggests that wear by abrasion is strongly affected by factors other than hardness.

2.1.2.3 EROSIVE WEAR

Wear by erosion, of a solid surface can occur in a fluid stream with or without the presence of another phase, e.g. solid particles. Sometimes the particles may be fluid droplets which implies that a single-phase erosive wear phenomenon is in operation. However, when the particles are solid or some phase different from the carrying fluid, then a multiphase flow system is operative. In both cases, wear is provoked by a fluid flow which carry particles that impact the surface to be worn. Sometimes erosion may occur simply due to the high temperature of a fluid running over a surface. In this section, however, attention is only focused on erosive wear by particle impact phenomena. In the multiphase flow system (particle impact) metal removed is due to the imposition on the surface of shear or normal stresses of sufficient size to cause failure, either through single blow effects or fatigue type effects. These contact stresses arise from the kinetic energy of the particles in the fluid. Whatever the fluid may be, the particle speed and impact angle (which of course depends on fluid viscosity) combined with abrasive size gives a measure of the kinetic energy. Erosive wear scans produced by such a system have a fine granular appearance similar in nature to brittle fracture.

Erosive wear rate varies with the impact angle of the hard particles, as well as type of material. For example when impact angles are small,

e.g. the normal stress component is negligible, cutting wear similar to cutting abrasion occurs as opposed to ploughing. In such a case, the hardness of the surface resisting wear is the critical factor, but certainly not the only one. However when the angles are large, i.e. shear stress component is negligible, ploughing prevails and vertical deformation occurs.

In a forging situation both effects are quite possible since scales and wear debris are squeezed and made to flow radially by the approaching press ram. The important factor, however, is that both effects of cutting and ploughing can lead to surface and subsurface deformation.

2.1.2.4 DEFORMATION - TYPE WEAR

Rabinowicz [18] has suggested that the basic wear mechanisims of adhesion, abrasion, mechanical fatigue, chemical wear and thermal wear may be observed in impact wear as well as in sliding wear. As discussed above, erosive wear may also be classified as a deformation-type wear.

Finally, the most recent delamination wear theory [22] also invokes deformation in the process of metal removal.

2.1.2.5 DELAMINATION THEORY OF WEAR

This theory was first proposed by Suh [22] to explain the nature of sliding wear. It is based on dislocation theory and the plastic deformation and fracture of metals near a surface. It therefore departs completely from the classical adhesion theory which completely ignores the physics and physical metallurgy of metal deformation even at the near-surface which is very vital to wear particle formation during sliding.

Extensive analytical and experimental work has confirmed the validity of the theory and several of the postulated processes involved. It has been shown that rubbing wear particles appear as thin flakes of metal with highly polished surfaces and not as the hemispherical fragments generally proposed by the adhesion theory.

As pointed out above this theory is based on the behaviour of dislocations at the near surface, subsurface, void and crack formation, and the subsequent joining of cracks by shear deformation of the surface. Fig.3 shows the mathematical model used in deriving a wear equation for this theory. It has been shown that for the case of a hard surface sliding against a softer one, wear volume can be represented by

$$W_T = K^1 LS \qquad (1)$$

where K^1 is a wear factor given by

$$K^1 = \frac{b}{4\pi}\left[\frac{K_1 G_1}{\sigma_{f_1} S_{o_1} (1-\nu_1)} + \frac{K_2 G_2}{\sigma_{f_2} S_{o_2} (1-\nu_2)}\right] \qquad (2)$$

ubscripts 1 and 2 represent the soft and hard metals respectively.

o = critical sliding distance required for the removal of a layer (i.e. N wear sheets)

= poisson's ratio.

= shear modulus.

= friction stress.

= Burgers vector.

= a constant which depends primarily on surface topography.

= the distance slid at any instance.

= load

is wear equation has certain physical and metallurgical implications.

(1) the wear rate (or volumetric wear) depends on or is influenced by the surface topographical features of the metals in contact.

(2) Wear rate is proportional to the normal load.

(3) Minimum wear rate is achieved when G/σ_f ratio is small and S_o is large.

(4) Wear rate does not depend directly on hardness.

(5) Above all, wear rate depends on material structure.

According to equations (1) and (2) wear rate is minimum when G/σ_f is small and S_o is large, for most commercial metals σ_f is proportional to G, although σ_f can change drastically at constant G, if the metal is extremely pure initially with only few dislocations and/or impurities. Thus in forging die steels, where solid solutions hardening together with hardening by secondary phase particles may occur due to heat treatment, the G/σ_f ratio may decrease. As will be discussed later, 5% Cr die steel, for example, consist of ferrite plus M_7C_3 or ferrite with M_7C_3 plus M_3C_3 carbide mixture. In the presence of carbide forming additions such as vanadium, chromium and molybdenum, secondary hardening takes place on tempering due to precipitation of carbides other than M_3C. In addition, hardening on tempering may also occur by the breakdown of any retained austenite.

The critical sliding distance S_o would therefore be expected to decrease with an increase in dislocation density and density of hard particles formed due to heat treatment and sliding during forging. Hence the wear rate may, according to delamination wear theory, decrease due to increase in hardness caused by the formation of solid solution. However this may not be the case due to hardening by inclusion of secondary phase particles. The effects of such particles can be influenced by their distribution.

This bulk material hardness in itself is not the controlling factor in wear.

Finally, it has been shown in addition to the above that it is the delamination wear theory and not adhesion theory which satisfies the thermo-dynamic requirements of the frictional and wear behaviour of metals. The ultimate formation of thin flake-like sheets (wear particles) depends on two mechanisms, i.e. void formation and crack propagation. For materials having medium tensile strengths and good fracture toughness, in which void can nucleate easily, it has been reported that crack propagation may be the controlling factor. However for materials of relatively high tensile strength but low fracture toughness, in which void nucleation can be difficult and crack propagation can be easier it is the former that is the controlling mechanism.

.1.3 METAL DEFORMATION DUE TO REPETITIVE LOADING

ne of the reasons for die rejection in service is due to damage caused the relative impacting of the mobile top die on the stationary ttom die via the slug. Mechanical wear arising due to loading is lled deformation or impact wear.

ll and Prandtl have suggested theoretical solutions to explain the haviour of a metal when indented by a flat punch [23]. Hill believed at the metal is instantaneously displaced adjacent to the punch, and ter slides horizontally relative to the punch with the slip lines eting the punch at 45°. Prandtl solution however, requires a dead cap metal over the punch head such that the slip lines radiating from the ch corners meet at 90° on the angle of symmetry. This dead cap of al may well correspond to the central die region often observed on flat

dies during upset forging [24]. However, as shown by this reference, cracking occurs in the central die region indicating separation of die materials. Thus after a finite amount of deformation the dead cap region would become altered, and a pile-up of uncertain shape will occur which may enhance deformation wear.

Jahanmir and Suh [25] have recently examined the plastic deformation of an elasto-plastic surface layer which was subjected to normal and tangential loads exerted by a hard asperity. They demonstrated that plastic deformation occurs in such a way that the shear strain component in planes at right angles to surface accumulates incrementally every time a hard asperity passes over the surface. However, it is suggested that the surface traction determines the depth of plastic deformation and plastic strain. The size of plastic strain accumulated over a given cycle remains constant when the size of the surface traction is unchanged. This result appears to indicate that plastic deformation can accumulate indefinitely when two surfaces slide over each other, perhaps as in forging.

2.1.4 DISLOCATION GENERATION BENEATH SLIDING CONTACT WITH A FLAT CYLINDERICAL DISC

The sources of engineering material weakness could be many. One such source is the formation of dislocations when relative sliding occurs between two metals under the influence of a normal load plus abrasive hard particles.

With the exception of tiny whiskers, dislocations are inherently present in all metal due to the mechanism of growth of crystal from the melt. In addition they may be introduced through collapse of vacancies or due to high local stresses set up at second phase particles.

Thus during forging, where compound impacting occurs due to normal ram load and material flow, the last mechanism above would be a suitable candidate for the generation of dislocations in the dies. As discussed previously the slip direction and surfaces are not constant after a short time [23], they may be of any form. Hence the slip field or dislocation stress field may extend outside the area orginally bounded by the slug.

With coated metals, the occurence of further dislocations at the interface has long been known [25].

2.1.5 VOID NUCLEATION AND CRACK FORMATION DURING DEFORMATION

Void nucleation may occur either by particle - matrix separation or by particle fracture. If the particles are equiaxed particle-matrix separation is likely, whereas if the particles are elongated before deformation, particle fracture may occur.

Void nucleation around an equiaxed particle may occur in three ways depending on the criterion used for its formation. The three criteria used for their formation are - energy, local stress and local strain. Gurland and his co-worker [27] proposed an energy criterion for the formation of voids around inclusions. They suggested that voids can form at the interface between sliding members when the locally concentrated elastic strain energy, which may be released as a result of decohesion, becomes comparable with the energy of the new surface generated. Additionally, in a study of cavity formation at the interface of a spherical inclusion in a plastically deformed matrix, Tanaka et [28] showed that in a purely elastic system the energy criterion is always satisfied for particles larger than 250^{o}A when the stress almost reaches

its yield value. In many other instances, however, much larger particles have been observed to remain attached to the matrix even when the strains far exceed the yield value. Furthermore, the presence of inclusions less than 250^{o}A argues against the Tanaka et al [28] suggestion. Therefore the energy criterion can be regarded as a necessary but insufficient condition for void formation.

However, in the late forties, Zenner [29] proposed the idea of dislocation pile-up at inclusions or other obstacles. This was then followed by Stroh's theory of crack formation [30]. Zenner suggested that the leading dislocation of the pile-up may coalesce as it hits an obstacle since the stress at the head of the pile-up is $n\gamma$, where n is the number of dislocations in the pile-up and γ is particle-matrix shear strength. Stroh analysed void formation by considering local stress concentrations due to dislocation pile-up at an obstacle. Unfortunately the mechanism proposed by Stroh does not satisfy the conditions experienced in metals with moderate flow stress at moderate temperatures. This is because the generation of a high stress can be difficult due to the ease of secondary slip. However, in the late sixties, Ashby [31] improved the level of understanding of void formation. By using a stress criterion based upon a dislocation model for void formation he showed that the dislocations generated by primary slip interacted with those generated by secondary slip of particles. Consequently reverse pile-ups are formed which may in turn result in a large tensile interfacial stress being set up at the particle-matrix interface. This dislocation model appears to be similar to a second theory [26] of crack formation due to a double pile-up by two attracting sequences of dislocations. This latter theory suggest that the leading dislocations of the two pile-ups react with each other to form a "compound" dislocation, which would then coalesce if the constituent

slip planes are not subjected to a shear stress.

Since Ashby, a new energy term has been added by Brown and his co-worker[32] to the dislocation model for void formation.

The third and final criterion is that of local strain. Work by McLintock[33] suggests that large strains concentrations may develop around rigid inclusions in a non-hardening matrix. This work was based on the stress distribution around cylindrical inclusions in anti-plane shear. From this he suggested that a mixture of local interfacial shear strain and a local interfacial tensile stress may be responsible for void formation around inclusions.

From the above review it would appear that for void nucleation the energy criterion must be satisfied and that a tensile stress capable of separating the matrix from the inclusions must be developed. In a recent paper[34], it was shown that there is very little difference between the molar surface energies of solid and liquid pure metals. This paper recommends surface energy values for solid transition metals such as Ni, Cr, V, Fe, Mn, Co, and Mo, which are comparable with their liquid conterparts. However, since the present state of knowledge does not permit prediction of surface energies for solid alloys, it will suffice to assume that any alloy consisting of these metallic elements would possess energies similar to their liquid counterparts.

Hence during hot forging, the surface energies of local melts (probably produced either by welding or due to slug resting on die) would be comparable with those for the freshly produced die subsurface due to wear. However, since the energy criterion is satisfied only for large particles, the stress criterion may then become the necessary and sufficient criterion for void formation in die steels during hot forging.

1.6 THE EFFECT OF DIE MATERIAL ON WEAR

In practice, most dies are used in the tempered martensitic condition and the tempering treatment is adjusted to give the required combination of hot strength and toughness. The alloying constituents are used to promote increased resistance to tempering, increased hardenability, grain growth restrictions and also to vary the amount and composition of both austenite and carbide at the hardening temperature. Improved resistance to softening, can improve high temperature erosion while secondary hardening effects can greatly alter the abrasion resistance of tool steel.

The strength of an alloy steel in the hardened and tempered condition will depend upon the strength of the matrix and the extent to which the matrix is hardened by the precipitated phases, e.g. carbides. There is abundant evidence that the wear resistance of a tool is not only determined by the amount of carbide but also by the nature of that particular carbide. Thus the coarsening rates of carbides and rates of going into solution at higher temperature will have marked effect on the wear resistance of a particular alloy. This also implies that the strength of a die steel will depend upon the amount and type of carbide formers present.

Molybdenum, vanadium, chromium, manganese and silicon are the elements common to BH13 and Electem No.5 die steels. All alloying elements move the eutectoid to a lower carbon percentage and thereby increase the amount of undissolved carbide in the hardened steel. Apart from silicon, their relative ability for meeting this task is related to the carbide forming tendency of the alloy. Molybdenum and Vanadium cause the greatest

increase in undissolved carbides. Chromium and Manganese, on the other hand are intermediate while nickel (present in No.5 die steel) has the least effect. Carbides formed by these elements are generally designated by M_3C, M_6C, $M_{23}C_6$, M_7C_3, M_2C and MC.

Drapal [35] has shown that the equilibrium carbide phase in a straight 5%Cr steel is M_7C_3. However, in practice this alloy may be comprised of ferrite plus M_7C_3 or ferrite with M_7C_3 plus M_3C carbide mixture. According to Goldschmidt [36], M_3C is an iron-rich carbide while M_7C_3 and $M_{23}C_6$ are chromium rich. Kuo [37] has also suggested that Fe_3C can dissolve up to 18%C whilst Cr_7C_3 and $Cr_{23}C_6$ can dissolve as much as 50% and 35% of iron respectively. Thus in chromium steels M_7C_3 carbides only dissolve partially during heating for hardening, leaving some excess which makes the steel abrasion resistant.

M_6C and M_2C are molydenum rich carbides [36]. Secondary hardening is achieved if 2-5% Mo is present in a die steel, and according to Kuo [37] this is due to M_2C which precipitates as needles in 500 - 600°C range. The effect of M_2C only influences the hardening with molybdenum contents greater than 1.25% although a lower level of molybdenum increases the hardness and slows the rate of softening [35]. On further tempering, M_2C tends to disappear giving way to the formation of M_6C and/or $M_{23}C$. M_6C resists dissolving on heating for hardenings leaving excess hard particles in the structure.

Vanadium is the most effective element in producing secondary hardening. This is due to precipitation of M_4C3 at vanadium contents greater than 0.2 to 0.5%. The Vanadium content in BH13 is about 0.9 - 1.1 According to Smith and Nutting [38], maximum secondary hardening is achieved with vanadium in 5%cr steel if tempering is done at 500°C for 5hr. V_4C_3

is a good secondary hardening carbide because of its low diffusivity, its wide dispersion and slow coalescence. However the growth rates of other carbides are relatively slow compared with chromium carbides in BH13 and No.5 die steels. Crafts and Lamonts [39] have demonstrated that in the presence of vanadium the growth rates of chromium carbides will, however, decrease. Thus in BH13 where the vanadium content is well in excess of the amount required for the precipitation of M_4C_3, the growth rate of chromium carbides may be markedly affected. Vanadium is not present in No.5 die steel, and so this effect is excluded. Therefore chromium carbide may grow faster in the latter steel. It should be noted however, that the coarsening rate of chromium carbides decreases in the order of Fe_3C, M_3C, $M_{23}C6$ and M_7C3.

From the above it seems that the most effective carbides in promoting hot strength and hence wear resistance in tool steels are in the decreasing order of Mc, M_6C and M_7C3. Thus Vanadium is the most effective element, followed by molybdenum and then chromium. But as indicated earlier, Vanadium is absent in No.5, while the only other element present in No.5 which is absent in BH13 is nickel. This element has the least effect in forming carbides, therefore it may be assumed that molybdenum and chromium effect the wear resistance of No.5 die steel in the order shown above for BH13. Tests results reported by Aston et al [2] indicate that electem No.5 would wear more than VMC (BH13)

HE EFFECTS OF SURFACE TOPOGRAPHY AND INTEGRITY ON WEAR

enerally, when two surfaces are in contact they meet first at their sperities, and some form of local welding between the asperities may cur due to the interatomic force of attraction between them. If such rfaces are then made to slide relative to each other, normal and tangential

loads are transmitted through the contact points by adhesive and ploughing action. The tangential force (traction) must be in excess of the static force for sliding to occur. The ploughing force is negligible however in a metal-to-metal contact, but related to the flow properties of the materials in contact as well as the size and shape of the asperities [41].

Surface topography and integrity are two major surface characteristics which affect the wear behaviour of machined and surface treated parts. Surface roughness is a topographical parameter which describes the short range geometrical deviations of a surface from the nominal geometric shape, whilst surface waviness describes the long range deviations. Surface integrity, on the other hand, characterises the quality of the surface and subsurface material in terms of plastic deformation, cracks, structural heterogeneity by phase transformations, and residual stresses, all of which may be affected by surface preparation methods.

Queener et al [42] have shown that under lubrication conditions run-in wear is dependent on the original surface roughness. Rowe et al [43] have also shown that run-in wear occurs in dry wear testing, and that sliding surfaces become smoother during running-in.

Apart from surface roughness, the quality of a machined or surface treated part is related to the degree of damage generated in the surface layer. Abrahanson et al [44] have demonstrated that subsurface damage introduced during machining increases the initial wear rate.

Forging dies may be of varying profile, from simple flat to quite complicated shapes. Die blocks or inserts may be supplied already

forged by the manufacturers. They may also have been heat treated with machined faces dovetailed in accordance with customer requirements, and even sometimes finish ground on impression faces. Instead of being forged, they may sometimes be supplied in the form of rolled bars in the annealed condition. These bars may then require further heat treatment and machining before they are ready for use as forging dies. Thus a forging die experiences surface and subsurface deformation before been put into use.

Surface integrity of a part may be affected during grinding and turning by the type, size and wear land of wheels and cutters.

The use of a sharp tool and a moderate speed may lead to very little subsurface damage, but when a worn tool or a high speed is used, subsurface damage may be increased considerably. In turning high strength steels, three clear defined behaviours can be observed since phase transformation near the surface depends on the temperature generated during machining, and also on the speed of cutting. Cutting at low speed with a worn tool causes microstructural defects. If machining is done at moderate speeds with a worn tool, a surface layer softer than the bulk, is generated due to thermal effects. However, machining at higher speeds with a worn tool generates a harder surface but a softer subsurface. The hard surface layer is generated by the high rate of heating and cooling near the surface which produces untempered martensite. The softer subsurface is overtempered martensite.

Similarly high temperature generated in grinding may cause surface cracks or grinding burns. Usually the burn causes metallurgical damage in the subsurface.

With electric-discharge machining (EDM) no mechanical damage is done to the subsurface, since the tool and work are often maintained about 25μm

away from each other. However the work may be cracked due to thermal effects in the tempered martensitic state. Each discharge and consequent removal of metal particles occurs between a high point of the workpiece and the tool. The surface finish is of the order of 750μm or less. The lay of the finish, is multidirectional, which is advantageous in applications involving friction wear. From the above it would appear that the surface topography and integrity, obtained on dies due to the application of the various machining techniques, would affect the wear phenomenon and the rate of wear by delamination.

2.1.8 THERMO-MECHANICAL PROPERTIES

2.1.8.1 THERMAL FATIGUE

Thermal fatigue cracking occurs due to repeated application of stresses which are thermal in original. These stresses arise in the case of forging dies as a result of the restricted degree of freedom of expansion or contraction of the die surface due to repeated heating (by slug) and cooling by air or other coolants. The thermal stresses generated by heating or cooling depend on both cooling or heating rate as well as the size of die insert. As the cooling rate decreases, the maximum thermal stress increases for increasing diameter of die insert or bar. Child [56] recently reported that for a 50mm diam. round whose air cooling rate is $0.312^{\circ}C$/sec at $500^{\circ}C$, the maximum thermal stress generated will be $15N/mm^2$. Several investigators [57,58] have published reports on a number of applications in which thermal fatigue is primarily responsible for terminating the life of a component.

Apart from operating parameters (i.e. component size and shape, stress and strain concentrations), material and environment may affect the nature and size of thermal fatigue cracking. Manson [57] has pointed out that owing to the influence of environment thermal fatigue testing becomes a test not of the orginal material but of the resultant surface layer. In

practice high temperature oxidation often occurs during each thermal cycle. The weak brittle oxidation products can readily disintegrate and induce cracks in the material.

Although thermal endurance is a function of the composition, microstructure and mechanical properties of any material, many investigators have reported only the effect of variation in chemical composition. Baron and Bloomfield [59] noted that alloys based on additions of Cr, W and other elements conferring hot strength, tend to give greater resistance to cracking than alloys based primarily on nickel additions. Thus BH13 may have a greater thermal fatigue cracking resistance than electem No.5 die steel since the latter is based on 1.5%Ni while the former is essentially a 5%Cr die steel.

Apart from the effect of material composition, die manufacturing method plus surface preparation technique may affect grain size and hence the boundary strength or endurance of the material. Betteridge [60] has noted that final forging operations for turbine blades may impose 10 - 20% reduction since repeated heating followed by small deformation may lead to undesirable grain growth. This can have deleterious effect on boundary strength or fatigue strength.

The influence of surface treatments to improve wear [24] has been investigated to some extent. Chromizing increases thermal fatigue life from 50 to 80 or 100 cycles in a typical thermal fatigue test. Bengtsson [61] also reported that nitriding of die-casting dies could be advantageous in prolonging thermal fatigue life by increasing hot tensile properties particularly at their edges.

2.1.8.2

FATIGUE CRACK NUCLEATION

Fatigue failure starts in some small region which probably consists of only a few thousands of individual atoms. The ability of such a region to resist fatigue damage must therefore be related to its internal structure, which in turn depends on the size and arrangement of crystals and their grain boundary properties. Also within the crystal, the distribution of subcrystalline units and disconntinuities, as well as the atomic arrangements and spacing can be expected to play a part. However, for failure to occur, internal structure change must occur. This is often produced by the complex stresses (internal or external) imposed upon the region by its surroundings. Thus there are two basic ingredients for the understanding of fatigue failure - information on the internal structure and the stress systems.

One of the earliest theories on crack initiation was that of metallic crystallisation. But this was soon discounted when it was suggested that fatigue failure was preceded by the formation of slip bands from which cracks eventually initiated [45]. Some twenty years later, this theory was developed further by Gough and his co-workers [46-48]. They demonstrated that slip bands were generated below the fatigue limit. It was further shown that slip occurs along certain crystallographic orientations on crystal planes, and that slip depends on the resolved shear stress and is in dependent of pressures normal to the plane [49, 50].

However, it was Orowan [51] who postulated the first generally accepted theory which assumes that certain areas of a part would deform more readily than the rest when stressed. Such areas may contain inherent stress raisers e.g. inclusions, or may simply be a preferred orientation

for active slip systems to operate. Orowan demonstrated that these areas of localised plasticity would experience a fall in strain due to continued strain hardening, when subjected to controlled cyclic stresses. This theory sets the basis for the explanation of the shape of S - N curves. However it depends on heterogeneous deformation only.
Years later, electron microscopy revealed that a slip band was infact a packet of small slip steps. Using this knowledge, Wood [52] suggested that crack initiation may not require localised strain hardening to enable it to start. He suggested that the to and fro fine slip movement in fatigue could result in the formation of ridges or notches at the metal surface. These notches act as stress concentration sites. Furthermore a group of researchers [53] showed that as the number of loading cycles increased, the slip lines broadened into bands in which cracks formed. The penetration of slip bands into the free surface varies from one band to another. Those which remained visible after slight electropolishing of the surface, were called persistent slip bands. Cracks constantly occur within the persistent slip bands, and it was thought that this makes a fatigue testpiece susceptible to initiation of failure. Another theory was that of formation of extrusions and intrusions on surface peaks and valleys during fatigue [54]. It was suggested that metal ribbons were extruded from the persistent slip bands, and intruded in the reverse motion of fatigue. This forms the basis of a number of other crack initiation theories. For example Cottrell and Hull [55] postulated a theory for the formation of extrusions and intrusions (surface micro cracks) on the surface based purely on the mechanical movement of atoms by supposing that two intersecting slip bands operate sequentially during both the tensile and compressive halves of the stress cycle.

Thus from the above it is certain that crack nucleation may start at the surface or near-surface of a metal. Nevertheless the above theories were based on single crystals. They can therefore be expected to vary, i.e. suppressed or enhanced in polycrystalline materials. The presence of inclusions may affect crack initiation.

2.1.8.2.1

EFFECT OF SURFACE ROUGHNESS, GRAIN SIZE AND SECOND PHASE PARTICLES ON FATIGUE STRENGTH

Surface roughness can have appreciable effect on fatigue strength. The fatigue strength increases as the quality of a polished surface is improved and, in general, is higher when the direction of polishing is parallel to the direction of the applied stress than when it is perpendicular to it.

The fatigue strength of many metals (e.g. steels) increases with decreasing grain size. Generally a material's resistance to plastic deformation (yield stress and hardness) increases as the grain size decreases, and thus the cyclic stress to cause continuing slip might also be expected to increase. For a particular material the grain size may also affect the cyclic stress necessary for a microcrack to develop beyond the grain in which it formed. If this is so, then the fatigue strength can be expected to increase with decreasing grain size because, with a small grain size, a microcrack may not be able to penetrate to a sufficient depth before encountering a grain boundary. However it will be able to do so if the grain size is large. If the metal is such that the microcracks change into macro cracks at smaller sizes, any change in grain size above this has no effect on the subsequent fatigue strength.

The presence of second phase particles in the form of non-metallic inclusions

leads to a stress intensification. Stress and strain concentrations around inclusions in alloyed metals, having a complex microstructure preventing slip, can result in microcracks forming by void coalescence or fracture of inclusions at the inclusion-matrix interface before the stress necessary to cause cyclic slip in a surface grain is reached. The degree of influence of an inclusion on fatigue strength depends on its index of deformability, its size, spacing volume fraction, and matrix-inclusion coherency.

2.1.9

SURFACE TREATMENTS AND THEIR PHYSICAL AND MECHANICAL PROPERTIES

It is not the aim in this section to detail the methods leading to the production of the surface treatments, but it is intended to review some of their important properties which influence the mechanical behaviour of the resulting composites. Several sources of information on the former already exist in the literature [62, 63].

2.1.9.1

ELECTROLESS N_1 - P alloy

Electroless N_1-P alloy plating involves a controlled autocatalytic chemical process which leads to the reduction of nickel cations by means of hypophosphite anions on certain catalytic surfaces in the presence of water.

Electroless N_1-P alloy deposits of varying compositions, structure and properties are attainable, depending on the type of bath and its operating conditions. As plated deposits are lamellar in structure and electron transmission diffraction patterns showed them to be super saturated solid solutions of phosphorus dissolved in fine-grained nickel. They appear as a metastable intermediate state between that of a mixture of Ni + P and the equilibrium system of Ni(p) + Ni_3P.

Variations in phosphorus content of the deposits have a significant effect on the mechanical properties of the coatings. But the phosphorus content of the deposits is strongly influenced by the bath PH. Baldwin and Such [64], and Parker and Shah [65] have all reported that phosphorus content increases with decrease in Ph. Acid baths in common use produce deposits containing about 7 to 10% P, and alkaline baths about 5 to 7% P. The phosphorus content of deposits from a bath of given PH can be increased by increasing the concentration of hypophosphite. Parker and Shah [65] also reported that the phosphorus content of deposits is affected by both bath temperature and PH.

Baldwin and Such [64] showed that as - deposited alloys may have varying degrees of ductility depending on the amount of phosphorus in the coating. Using an acid bath they reported that an alloy having a phosphorus content of 5.5% is the most ductile. In addition they showed that as solution acidity increased from 4 to 5.6 PH, the ductility also increased but later decreased as PH6 was approached.

The stresses in as - plated electroless Ni-P alloy are usually low and tensile in nature, although, increasingly PH may affect the stresses produced by changing them from low compressive to high tensile values [64]. For example it was reported that a linear increase occurs, from ($5kg/mm^2$) compressive to ($11.2kg/mm^2$) tensile stress, with increasing PH at a plating temperature of between 70 - 90°C for a coating thickness of 12.5μm. It is believed that the change in the type of stress is due to the variations of phosphorus content with PH of the solution [65].

As - plated deposits have a vickers hardness of about 500 which remains constant irrespective of initial phosphorus content before any heat treatment.

2.1.9.2 ELECTRODEPOSITED HARD CHROMIUM

As - plated hard chromium usually has a lustrous appearance. Typical formulations for their deposition are contained in the literature [62]. Hard Chromium (Cr) deposits have high internal tensile stresses and are therefore invariably macro-cracked. their elongation is considered to be much less than 0.1%. The fatigue limit of a high tensile steel plated with Cr may be reduced by about 40% when the composite is heated to about 150°C or 400°C, with the maximum reductions occuring between these temperatures. However, if the composite is heated at 450° to 500°C for 1hr, the fatigue strength then becomes the same as the unplated steel [66].

Very little information is available for the performance of hard Cr plated steel under high impact loads as in hot drop forging. In the past, only two types of wear measurements were made - abrasive wear with relatively light loads similar to grinding, and rubbing or frictional wear under higher pressures against a harder material. Recently however, Still et al [67] showed that the volumetric wear of chromium coated (75μm) flat dies after forging 1000 slugs is $0.2 \times 10^{-3} CM^3$, while that for the unplated die is $4.37 \times 10^{-3} CM^3$. In both cases the steel used was Electem No.5 die steel.

The static and sliding coefficients of friction of cr-plated steel on steel are 0.17 and 0.16 respectively, compared with 0.30 and 0.20 for steel on steel.

The high hardness and abrasive resistance of chromium electrodeposits can be retained at temperatures up to 200°C, but will suffer some reduction between that temperature and 400°C, and even more at higher temperatures.

2.1.9.3
ELECTRODEPOSITED MICRO CRACKED CHROMIUM

Micro cracked Cr are produced from chromic acid baths in much the same way as for hard chromium except that in the former the dilute solutions contain mixed sulphate/fluoride or silicofluoride catalysts. The catalyst enables a continuous and uniform network of cracks to be formed. These cracks are produced by high tensile stresses which are developed in the coating as the thickness increases [68].

One of the many advantages of this type of chromium is that these cracks dissipate crack propagation energy at their tips, and thus help to delay crack propagation into the substrate. In general the residual stresses in micro-cracked chromium tend to be less than for hard chromium. The cracks also act as reservoirs for lubricants on the surface of a plated part in certain situations [69], although such a coating may be suspect in areas where cyclic loading or impact occur.

The hardness of the as - plated deposits are generally as hard as hard chromium.

2.1.9.4 BRUSH PLATED CO MO ALLOY

Brush plating is a high speed electrodeposition process in which a component is plated without using conventional vats. The plating tool or stylus consist of an inert electrode (carbon) covered with a suitable absorbant material (e.g. cotton wool), which is then enveloped in a highly wear resistant 75% polypropelene - 25% nylon weave material. The cotton wool acts as a reservoir for the cleaning or plating solution which helps to prevent burning or stressing of deposits. During cleaning or etching the electrode is made the cathode of an electric circuit, and the anode whilst plating. The recommended current/voltage for brush plating is 10 - 20A at 10 - 20v D.C. using a low rectifier capacity of approximately $4A/dm^2$.

A report by Jones [70] details some of the important merits and pitfalls of this process. Rubinstein [71] has claimed that improved adhesion may be achieved by this process providing extreme care is taken in preparing and precleaning the substrate [70].

Presently, very little is known of the mechanical and physical properties of brush plated Co-Mo alloys. However, Dennis et al [72] recently examined the properties of Co-Mo electrodeposits plated from baths having certain constituents similar to those employed in brush plating. (A conventional bath consist of 100/l sodium heptonate, boric acid (40 g/l), 3.15 g/l sodium molybdate, 28 g/l sodium chloride 150 g/l cobalt sulphate heptahydrate. In brush plating the proportions of some of the constituents employed are generally much higher and may also contain a concentration of about 0.7M carboxylic acid). They reported that deposits containing low concentration of Molybdenum had columnar structures. For deposits having higher molybdenum content, lamellar structures were claimed. Thus, although the structures of brush plated Co-Mo alloys have not yet been directly investigated, it is thought that they may be lamellar and fine-grained from the above.

On steel substrate the coating has a semi-bright finish. When the substrate is ground before plating, stressed and cracked deposits may be obtained. Brush plated Co-Mo alloy deposits generally improve the surface hardness of a steel substrate.

2.1.9.5 PLASMA NITRIDING

Edenhofer [63,73], Tibbetts [74], and Jones et al [75,76] have published excellent reports on this subject. By careful adjustment of treatment parameters, plasma nitriding can be used to produce a case consisting of a

compound layer and a diffusion layer. The former usually consists of iron nitrides while the latter represents the area where nitrogen has mainly been incorporated into the existing iron lattice as interstitial atoms or as finely dispersed alloy nitride percipitate. Occasionally only the diffusion layer may be produced (as in high alloy tool steel) but more often both layers are produced as in heat treatable steels, nitriding steels and BH13. Nitrided BH13 has a γ^1 white layer 2.54 - 5.1μm thick, a case 254-381μm and a surface hardness of 900 -1150 Hv. The depth and hardness of the diffusion layer depends on the amount of nitride forming elements in the steel, e.g. vanadium, and chromium.

The mechanical properties of these layers - such as anti-scuffing, ductility, wear resistance and fatigue strength - stem from the structures described above. Generally the residual stress present in plasma nitrided case is compressive. Jones and Matin [77] recently determined the residual stress distribution as a function of case depth of a 'nitralloy' type of EN41B steel after plasma nitriding at 525°C for between 0.5 and 24 hrs. to produce different case depths. They showed that a triaxial tensile stress was in operation in the core while conditions of high biaxial compression existed in the case. The greatest core stress been in the longitudinal directions. They also reported that the magnitude of the core stress depends on nitriding time since for times less than 2 hrs. the stress was influenced by the extent to which the compressive surface stress had developed, whereas for times in excess of 2 hrs. the core stress increased as the case depth increased relatively slowly.

From the above it seems that nitriding should be beneficial in increasing fatigue strength at all times. But this is not always the case. Work by Sutton [78] and Bardgett [79] indicates that nitriding can sometimes have very

little, if any, effect on the fatigue limit of steels.

Industrially forging dies similar to BH13, plasma nitrided for 20 hrs at 530°C to produce γ' compound layer of about 5.1μm thick, have been shown to give longer service lives than parts subjected to 40 - 60 hr gas treatment [80]. Also high wear resistance has been claimed for plasma nitriding treatments [73], but this depends on the structures of the case, its hardness, core, material, relative ductility of case and core, and the service conditions. The ductility of the case decreases with increasing thickness.

2.1.9.6 TUFFTRIDE

This is a cyanide salt bath ferritic nitro-carburising treatment applied to ferrous materials to improve their anti-scuffing and wear resistance - usually abrasive wear. The principle of treatment has been recently outlined by Astley [81].

The compound layer formed consist mainly of carbon rich mono-phased ε-iron nitrides, particularly when the treatment temperature is between 570 - 580°C.

3. EXPERIMENTAL

This section is divided into two major parts - the first part relates mainly to wear investigation, although some of its standard procedures also apply to the second group of tests. The latter group deals with investigations into the thermo-mechanical properties of Electem No.5 die steel.

3.1 STUDIES OF WEAR MECHANISMS

3.1.1. EXPERIMENTAL PLAN

Generally, the selection of a wear test depends not only on the mode of wear being investigated but also on the test objective. For example, wear tests may be performed for one or a combination of the following reasons: determination of the effects of directly or indirectly dependent variables, characterisation of materials and lubricants, fundamental understanding of wear processes, and the selection of materials for a specific application. In the present work the aim is twofold:

(1) to establish the wear mechanisms in surface treated and untreated BH13 and No.5 die steels during hot forging.

(2) to determine the effect of surface topography on wear.

From the onset it was realised that in order to meet the aim in (1), a test rig was needed capable of simulating service conditions during hot forging. Four areas were examined in the selection process, i.e. loading (work geometry and applied load), motion, environment and the wearing medium (surface finish of parts in contact). Based on experience within the Department [82], and elsewhere [3], it was decided that the experimental forging press at Aston is as close a test rig as one would expect in practice. Thus, conventional test apparatus such as pin and disc, with unidirectional or reciprocating sliding, do not qualify.

Most of the work done previously was centred around a standard 1000 cycles forging test. Although this showed familiar cracking on the die surface [24], it did not indicate the processes leading to crack initiation and propagation. Initial metallographic work done on some of the polished samples obtained from the previous workers did not therefore reveal any more useful information other than that already published. Consequently, it was decided that the earlier stages of forging should be examined, e.g. 1, 2, 5, 7, 10, 100 and 1000 cycles.

In the past, dies were sectioned for subsequent topographical examination after forging. But as will be explained later, sectioning may introduce undesirable stress fields at the edge of the section and is thereby likely to lead to misleading results at the near-surface. The use of scanning electron microscopy (S.E.M.) in the study of die surface topography without sectioning the as-forged and descaled dies was therefore chosen.

Although considered, it was impracticable to perform the forging test in a vacuum. To minimize oxidation after forging, the cooling dies should be stored in a desiccator. This would facilate approximate identification of oxides formed during forging.

Surface integrity of finished dies may considerably affect subsurface crack propagation rate and hence influence mode of failure. To account for this effect, it was decided that the grinding and turning parameters should be maintained constant for the establishment of wear mechanisms. Also the dies should be heat treated in accordance with industrial practice.

Finally, because it was difficult to identify the true effects of temperature stresses in previous investigations, it was decided that rather than perform only simulated thermal cycling tests, cold forging

tests were also needed. It was thought that this would offer an effective means of comparing the patterns and origins of cracks arising from each of the cyclic stressing processes, i.e. impact loading and thermal stresses acting separately or together.

3.1.2 DIE PRODUCTION

Typical chemical compositions of the two steels used in this investigation are shown in table 1.

Both steels were obtained in their annealed conditions. The Ni - Cr - Mo grade designated as No. 5 was obtained from Walter Somers Ltd., hence the propriety name Electem. BH13 was obtained from Uddeholm Ltd., Headed inserts (fig. 4) were machined from round bars, leaving a suitable tolerance for grinding after subsequent heat treatment for hardening. Headed inserts were used to enable direct S.E.M. examination of worn die topography after forging without sectioning.

3.1.3 DIE HEAT TREATMENT

BH13 inserts were pre heated to 840^{o}C and quickly transferred into I.C.I. cassel salt baths at 1030^{o}C. They were then oil quenched for about 30 mins and finally tempered at 550^{o}C. On the other hand, No.5 die inserts were quenched in oil from 840^{o}C, air cooled to approximately 200^{o}C and then finally tempered at 480^{o}C. In both cases, the heat treatments produced industrially accepted surface and bulk hardness. That is, 47-52 Rc (487-587 VPN) for BH13 and 41.5 - 43 Rc (411-427 VPN) for electem No. 5 die steel.

3.1.4 SURFACE TREATMENTS

After heat treatment the inserts were ground and some of them surface treated as shown in tables (2 & 3). In all, four surface treatments were employed for the purpose of wear investigation, i.e. plasma nitriding, Tufftride, electrodeposited hard chromium and a brush plated Co-Mo alloy.

3.1.4.1 PLASMA NITRIDING

After degreasing, BH13 inserts were nitrided in a plasma of 25/75 N_2/H_2 gas mixture for 20 hrs at 520°C and 5-9 torr. The temperature was controlled to within ± 5°C. The aim was to produce a case consisting of a diffusion layer plus a very thin wear resistant white layer made up of a predominately rich γ^1-nitride phase (Fe_4N) with a thickness of about 2.5 - 5μm. In addition, it was hoped in this way to obtain a case thickness of about 300μm having a surface hardness of about 1150 VPN which will be similar to that reported by Edenhofer [73].

A description of the Aston apparatus and a similar treatment procedure has been made elsewhere [83].

3.1.4.2 TUFFTRIDE

The present principle and practice of treatment has been outlined by Astley [81] BH13 dies indicated in table 3 were industrially treated at I.C.I. using a ferritic nitrocarburising cyanide salt bath. Treatments were carried out at about 580°C for approximately 1 - 1½ hrs, in order to obtain a compound layer consisting mainly of carbon rich mono-phase ε - iron nitride. For such treatment parameters the compound layer was 9μm.

3.1.4.3 BRUSH PLATED CO-MO ALLOY

The dies were given the following pre-treatments.

(a) Alkaline clean (solution as for hard Cr below) using normal current and 18 - 20v for a few minutes.

(b) Cold water swill

(c) Etch with a sodium salt activator solution using reverse current and 10 - 15v for a few minutes.

(d) Cold water swill.

(e) De-Smut with a tartaric acid activator solution, using reverse current and 20 - 25v for a suitable time.

(f) Cold water swill.

(g) Actuate with an ammonium salt activator solution, using normal current. No further swilling is required.

After the above pre-treatment, the flat die surface was gently swabbed by the plating stylus and the voltage gradually increased from zero to 18v. 1 A-hr/dm^2 was used to obtain deposits of 12.5µm - 2.5µm thick. Generally, as-plated deposits were swilled with water and rinsed with inhibisol to avoid surface stain.

3.1.4.4 ELECTRODEPOSITED HARD CHROMIUM

The following pre-plating treatments were employed to the die surface after stopping off the rest of the die.

(a) Hot alkaline clean (Macdermid Matex XDC2 cleaner) at 2 amps, 5 - 7 volt for a few minutes depending on degree of contamination.

(b) Cold water swill.

(c) Acid dip in HCL (50/50 v/v) for a few minutes.

(d) Cold water swill.

(e) Cyanide clean (Klenewell electrolytic cleaner) at 1 - 2 amp and 5 - 7 volts.

(f) Cold water swill.

(g) Electro-etch in 50% H_2So4, using lead as anode

(h) Cold water swill.

(i) cyanide clean.

(j) Cold water swill.

(k) re-activate die surface by dipping in 50/50 HCL

(l) Cold water swill.

After the above treatment, the dies were then plated. Hard Cr was deposited from a chromic acid bath catalysed with sulphuric acid in a 100:1 ratio. The solution composition and operating conditions were as follows:- 250g/L Cr_3O; 25g/L H_2So_4; 50A/dm^2 current density, bath temperature (55°C) and plating time (30 mins).
This treatment enabled bright hard deposits of about 12.5µm thick to be obtained.

3.1.5 FORGING TEST

A simulated forging test was employed in the evaluation of the wear resistance, and in the study of the wear mechanisms of the surface treated and untreated (hardened and tempered) die steels. A 10 - ton crank press was used [1, 2] as shown in fig. 5.

3.1.5.1 PRESS OPERATION

En3B slugs, 12mm by 18mm, are placed in a vibratory bowl feeder which feeds them, one by one, through a conduit to a double gate system leading to an induction heating coil. The slugs are supported in the coil by a refractory finger. On completion of heating the finger is lowered by air cylinder and the slug transferred by the feed tongs onto the die durface. The retaining arm is then withdrawn and the tongs returned under the heating coil leaving the slug in position on top of the die ready for forging. On return of the tongs a microswitch is tripped which operates a solenoid valve allowing high pressure air to enter the clutch cylinder and so engaging the clutch of the press.
All the air cylinders, except that operating the ejector, are controlled by cam activated air valves. The position of the cams on the drum and their lengths determine the timing of operation of the cylinders, and hence the press ram. The ejector is operated by air valves which are triggered by cams mounted on the ram of the press. The ejector

cylinder is timed to operate before the ram pressure on the forged slug is released. Thus the ejector pushes hard against the forging and ejects it forcibly as soon as the forging pressure is released. As the ram reaches the top of its stroke it activates two microswitches. One switch retracts the ejector, while the other introduces air to the other side of the clutch cylinder, disengaging the clutch and allowing the ram to stop at its top dead centre.

3.1.5.2 EXPERIMENTAL FORGING CONDITIONS

The conditions described below specify the stress systems produced by the experimental press at Aston which influence wear and its mechanism.

3.1.5.2.1 DIE PRE HEATING

Die pre heating is done by means of three cartridge type resistance heaters, each supplying 400 watts at 250v A.C. The heaters are inserted into both die holders. In order to achieve a more efficient heating, boxes made of a refractory material are fitted around the base and sides of the holders and filled with asbestos wool.

The dies are pre-heated to 130°C before the commencement of each forging operation and then raised to and maintained at 150°C throughout each forging cycle. Thermocouples which are inserted about 6.3mm below the working surfaces of both the bottom and top dies, are connected to recorders/ controllers which visually display the temperatures as well as controlling the electrical power to the resistance heaters and thereby keeping the die temperatures within $\pm$ 5°C of the preset temperature.

3.1.5.2.2. SLUG HEATING

Slug heating is achieved by an induction heating systems. The temperature of each slug immediately before forging is monitored by means of a Land optical pyrometer. The signal is then fed into an Ether controller which allows forging of only those slugs which are within the preset temperature

range of about 1050 - 1150°C.

3.1.5.2.3 DIE SURFACE TEMPERATURE

Still and Dennis [24] recently attempted to measure the surface temperature of untreated No.5 die steel, using both direct and indirect methods. They suggested that the die temperature varies from about 317°C at a depth of 500μm to about 485°C - 550°C at the die surface. However, the surface temperature for surface treated dies are not presently known but might be expected to be similar.

3.1.5.2.4 DIE AND SLUG SURFACE FINISH

The effect on wear of scale formed on slugs during hot forging, may be influenced by the surface finish of both die and slug particularly when the time for slug heating is very short. A rough slug would scale more than a smooth one. But, the more scale that is formed, the more abrasion is likely to occur at the slug-die interface. Hence standard EN3B steel slugs, used by previous investigators [24], were also used.

All the dies employed (table 2), in the first instance, were machine ground to a good finish taking off 12 - 25μm cut at a time. Dies which were surface treated were used in their as-plated or nitrided conditions.

3.1.5.2.5 PRESS BLOW ENERGY

The total energy supplied during the stroke of a crank press can be difficult to compute, particularly in the case of the Aston press where exact constructional information have not been compiled.

However, in general the forging press subjects the slug to a slow-speed compressive force such that as the slug is being deformed, the pressure

applied reaches its maximum value just before the end of the stroke. The ram velocity of a crank press can be of the order of 2.54 to 25.4 cm/sec. Accurate control of stroke length and rapid cycling rates can be achieved on the press. Stroke length can be adjusted by altering ram height. tightening the bolt.

In this investigation a constant condition was used to produce a 75% slug reduction.

3.1.5.2.6 DWELL TIME

This represents the actual time when the slug and die remain in intimate contact. Excluding other time elements, this time may represent the forging time. This time may be varied by varying blow energy. Work within the department suggest that this time is 0.105 secs per forging cycle (i.e. for 75% slug-reduction).

3.1.5.2.7 CYCLE TIME

The press has cam facilities for the control of cycle times between 6 and 10 secs. In addition, the cycle times may be adjusted by controlling the rate at which slugs are pushed through the heating coil by reducing the useful stroke length of the pusher. In this investigation, the 10 secs cam arrangement was used while maintaining other variables constant.

3.1.5.2.8 LUBRICATION

Dry conditions were employed throughout this investigation under laboratory air condition.

3.1.6 DIE SURFACE TOPOGRAPHY STUDIES AFTER FORGING

Die surface examinations were performed under two general conditions, i.e., in as - forged and descaled conditions. The aims of the study may be summerised as:

(1) to observe the general pattern of cracks present on the die surface after forging so that they could be matched with those observed in the subsurface.

(2) to study the morphology and surface features of wear debris and other general features of die surface which were absent before forging.

These general features include the presence of any plastic deformation and exposed subsurface imperfection.

The use of optical microscopy was initially attempted, but it was found that because of the heavily deformed nature of some of the dies, it was extremely difficult to observe the surface features in detail. Consequently S.E.M. was used.

Descaled dies were examined after wear evaluation. As a result these dies were stored in a desiccator to avoid further oxidation before S.E.M. examination. In addition, die surfaces were pickled in very dilute sulphuric acid before re-examination.

The dies were examined after forging without sectioning for the purpose of surface topography studies. Thus, because of size of die inserts used, only 17^{o} - 20^{o} tilt angles were used in S.E.M. examinations.

Table 2 shows the number of test pieces examined for the purpose of establishing wear mechanisms. It also indicates other supportive test conducted to establish the mechanism observed on die surfaces.

3.1.7 WEAR MEASUREMENT

Several methods exists for the evaluation of wear, some of which relate particularly to the test configuration being considered. For example wear scar volumes resulting from a Falex flat block-on-ring test may be determined from measurements of the average block scar width, projected area of the block scar, and change in weight of the block and ring. All these measurements are converted into volume losses by assuming that the cross section of the scar is circular and of the same diameter as the ring.

However, in a cross-cylinder abrasive dry wear test of some high-hardness tool steels (D2, M2), Steven and Catlin [84] demonstrated how wear volume can be derived as a function of depth of penetration.

All these methods have their pitfalls and relative merits. The use of weight change, for example, can be inaccurate because of material transfer in a configuration where adhesion wear occurs, or because of debris accumulation at the edge of the scar due to erosion and other wear modes. Contamination or oxidative products may also contribute to errors in weighing. The presence of jagged edges due to debris or scuffing sometimes discounts the use of scar width method. Finally the use of maximum wear depth for the derivation of volumes often involves too much mathematics and their associated assumptions.

The method that fulfils the requirements of the scars obtained in the investigation is the projected area method (planimeter method)

3.1.7.1 WEAR VOLUME EVALUATION

The amount of wear resulting form the forging test was determined from the profile trace of die wear scar. A Taylor Hobson Talylin surface analyser was used in producing the trace. The wear area determined from this trace, by means of a planimeter, was then converted into wear volume (see appendix 1). Before taking a profile, the die surface was descaled electrolytically. The descaling procedure involved the use of a carbon rod anode partly immersed in a solution of 5% H_2So_4, containing 0.1% by wt. of O-tolylthiourea as inbibitor. The solution temperature was maintained at about 75^{o}C while the die surface was cleaned cathodically. The applied current density varied between 20 - 25 A/dm^2 and the descaling time also varied depending on the extent of contamination.

Unlike previous investigators, it was considered that the use of only four trace positions in the evaluation of wear over a non-symmetric wear region was inadequate. The reasons for this are:-

(1) practically the drift in the press ram makes it impossible to map-out an exact plateau region which is equal to the slug diameter before forging. One or two diametral traces may show a plateau after a certain number of forging cycles for a particular die steel but it may not be so after eight or more traces even with unplated electem where the plateau affect appears to occur.

(2) The conversion of area into wear volume is based on the idea of rotating a vertical plane (i.e. the wear area) about a central vertical axis such that the area sweeps out a volume which can be estimated by multiplying the area by the path length of rotation. The length of this path is taken as half the circumference of an imaginary circle which lies mid-way between two imaginary concentric circles defined by two points on a diameter along which a trace was taken. Thus for each diameter there may be a different path length and wear area. Hence increasing the number of diametral traces from four to at least eight would improve considerably the accuracy of measurement. In the present work, twelve diametral traces per die were taken at 30^{o} to each other.

(3) It is often theoretically stated that during upsetting the degree of freedom of movement of the deforming slug is restricted or of zero flow in the region directly under the slug. In practice this is not true. The constraining frictional force is not uniform over the slug-die interface. Hence some minute metal flow occurs in this region. Therefore diametral wear traces taken over only four diameters may not be representative of the true volume.

Sometimes, in order to compare the wear behaviour of two or more materials subjected to a continuous test run for a constant sliding distance, wear rates are reported instead of volumetric wear. The use of wear rates calculated by simply dividing volume loss by total distance of sliding can be misleading. This is because the configuration of a wear scar may sometimes change in engineering systems where a number of wear mechamisms occur. In the case of incremental test runs, as in upsetting, this effect of changing scar configuration may be minimized if wear rates are calculated after each cycle. Sharp[85] has indicated the ability of this method to compare the wear rates of different materials at the same load per apparent unit area. But this may also be misleading since for different materials (e.g. BH13 and No.5) similar rates at a given load per apparent unit area may be reached after very different total distances of sliding.

In view of the above together with the fact that industrially, attention is focused more on die volume left for resinking rather than local volume loss per unit sliding distance, it was decided that only the total wear volumes be reported.

Wear volumes of each stage of the incremetal test were calculated where possible, as traces obtained for the first few forging cycles showed little or no measurable wear. Some of the traces showed some dishing probably due to ram loading. However this latter effect was eliminated by rotating a straight edge corresponding to the original die surface, but equal in length to the measured wear scar diameter, through a suitable angle such that it contacted the trace at points on the die (Fig. 57b).

3.1.8 SUBSURFACE STUDIES

After all non-destructive tests had been completed, the next stage was to undertake a study of the underlying subsurface and near-surface features of the worn dies. To do this a die block sectioning technique was required capable of revealing features at the interface between the worn surface and the rest of the die matrix. A taper sectioning technique was selected. However, apart from the experimental difficulties of viewing below the intercepting planes, this method has its advantages and drawbacks as indicated in the section under hardness measurement below. For example apparent depths of measurements below the intercept need to be corrected to obtain the true depth using equation.

$$d/d^1 = h/L$$

where d is the true depth (Fig. 6). However, when small taper angles are used, as in this investigation, the problem of polishing cracks is minimized. As a result of the above together with other points raised later, it was decided that taper sections should be used in conjunction with normal (conventional) sections in all the studies pertaining to die subsurface.

3.1.8.1 TAPER SECTION

The specific reasons for the use of taper sections in this work are as follows:-

(1) To observe cracks in the subsurface and near surface, and their links with those observed on the die surface.

(2) To observe the inclusions present in the steels and compare the influence (if any) of the polishing stress field on them with those observed in similarly polished vertical sections. That is, to show if cracks present in the subsurface were introduced by mechanical polishing.

(3) To produce an increased magnification of the coating and nitrided case of about 10:1 so that hardness impressions across and through them to

the base metal could be made.

(4) To determine near-surface and subsurface change in composition using electron probe micro analyser (E.P.M.A).

The steps involved in the production of taper sections are illustrated in fig. 6

3.1.8.2. CONVENTIONAL CROSS SECTIONS

Because of the approximate nature of the true depths of measurements on a tapered section, together with the fact that features (e.g. inclusions and hardness impressions) lying parallel to the surface but perpendicular to the edge appear thicker than they really are, the use of taper sections alone in a subsurface (near-surface) study is not always highly recommended. For a better interpretation of results obtained from taper sections, they need to be used in conjunction with conventional sections.

Conventional cross sections were used in the following areas of studies.

(1) Indentification of non-metallic inclusions using S.E.M. and optical microscopy.

(2) Revealing deformation and cracks in die subsurface before and after forging.

(3) Preliminary hardness measurements, e.g. to check core and case hardness after heat treatment.

(4) To determine if there were any grinding or heat treatment cracks.

(5) Powder x-ray diffraction analysis of heat-treated dies to establish structure of steels, i.e. presence of martensite and austenite (if any).

(6) Electron probe micro analysis to study compositional changes near the surface and below it.

(7) General metallography.

3.1.8.3 IDENTIFICATION OF NON-METALLIC INCLUSIONS

Non metallic inclusion in BH13 and No.5 die steels may arise either due to entrapped slag during solidification or by reactions leading to precipitation of non-metallic phases. Typical of the second group, are sulphide and silicate inclusions.

Conventional cross sections of forged and unforged die inserts were examined after polishing and etching in boiling 50% HCL for 5 - 20 mins. In the case of forged inserts, it was hoped that the direction of metal flow could be indicated by the direction of elongation of inclusions. Micrographs and x-ray micro-analysis of the elements present in the inclusions were taken using the x-ray attachment of the S.E.M.

3.1.8.4 ELECTRON PROBE MICROANALYSIS (E.P.M.A.)

A cambridge Scan 5 micro analyser was used, and operated at 15Kv and 0.5μA. The areas in which it was employed have already been mentioned. In general, specimens (tapered or conventional sections) were conventionally prepared and cleaned on a vibratory cleaner.

Trace records for the variations of the important oxidizing and carbide forming elements are shown in fig (7a, b). Also included in appendix 2, is a computer data for oxide scale formed on the slugs before forging.

3.1.8.5 SCANNING ELECTRON MICROSCOPY (S.E.M.) CAMBRIDGE 1Q

The areas in which this technique was used have already been mentioned. They include indentification of grinding or heat-treatment cracks, and the revealing of deformation. The presence of grinding (heat treatment) cracks before forging was examined in order to ensure that their presence after forging (e.g. on No.5 dies which were subjected to 1000 cycles of forging) were not due to

1. prior faulty grinding practice.
2. faulty heat treatment practice.

Two simple test procedures were adopted. Four die inserts (two for each materials i.e. BH13 and No.5) were produced for this purpose. Two of them were ground (without prior heat treatment) to a typical machine finish (25μm depth of cut), polished and etched in 50% HCL. The other two inserts (one for each material) were similarly ground, polished and etched after careful heat treatments as applied to inserts used in forging. It was also hoped that through these tests certain important information may arise concerning subsurface deformation due to grinding alone, and when it acts in conjuction with impact loading as in upset forging.

3.1.8.6 POWDER X-RAY DIFFRACTION TECHNIQUE

The reasons for the use of this technique are threefold.

1. To identify the oxides present on die surfaces after forging.
2. To identify the phases (e.g. martensite) present in the die matrix after heat treatment, but before surface treatment and forging.
3. To identify the phases present in the nitrided case.

A philips x-ray diffractometer was used. A tube with molybdenum target was operated at 40kv and 20mA current. The equipment has a pulse height analyser which reduces fluorescent iron K radiations generated in a specimen being examined. Permanent graphic records of intensity against diffraction angle were produced using a telecomputer interface attachment. No surface preparation was required for the first and third objectives above. However, for the second objective conventional cross sections were polished and pickled in H_2SO_4 to remove any oxide film. It is worth noting that before applying the x-ray technique to objective No.2, several other metallographic etching techniques were tried. Results obtained by the latter techniques proved inconclusive since it was difficult to distinguish between austenite and martensite under the microscope.

3.1.8.7 HARDNESS MEASUREMENT

Microhardness measurements on surface treated and untreated (hardened and tempered only) dies were made before and after forging, for the following reasons.

1. To check hardness conferred by heat treatment against industrially recommended standards.
2. To measure the degree and extent of change in hardness after forging (i.e. of coatings, nitrided case etc).
3. To determine coating and nitrided case hardness before forging, so as to compare their values with those recommended industrially for forging application.

Changes in hardness of a section taken from the die after forging may be due to a variety of factors which include:-

(1) Change due to heat treatment of dies at 150°C (i.e. die minimum applied temperature), and also at about 500°C (untreated die surface temperature according to Still and Dennis [24]).

(2) Damage due to intermittently repeated frictional contact between slugs and die via hard scales.

(3) deformation due to ram load, impact erosion etc.

(4) changes due to possible tempering.

(5) changes due to presence of oxidation products.

(6) changes due to specimen preparation for hardness testing.

To minimize the effects of some of these factors (5 and 6), it was decided that sufficient attention be paid to the experimental difficulties associated with near - surface metallography. The use of mechanical polishing and grinding to prepare sections through wear tracks may produce good results away from the edge of the section. However, at the edge where the section meets the wear track difficulties arise since the tensile stresses generated

in the surface of the section by the action of a polishing grit increases as the grit approaches the edge of the specimen. Away from the edge the force exacted by the grit parallel to the surface of the specimen is balanced by tensile stresses behind it and compressive stress in front of it. At the edge the compressive area is no longer contained by surrounding material, so that the compressive stresses may become relaxed by plastic flow in the case of ductile materials or by cracking in the case of brittle material.

Thus the edge of a die specimen prepared by polishing may be susceptible to additional damage after forging. Such a specimen section may be chipped and cracked when it is made of brittle coatings or other materials containing imperfections such as voids and non-metallic inclusions.

To protect the edges of specimens, the taper sectioning technique was employed so that the stress field ahead of a grit approaching the edge is always contrained to a certain extent, leaving the section with less chance of cracking. In addition the use of tapered sections would help obviate the difficulties of measuring hardness near the worn surface.

3.1.8.7.1 TEST

Micro-hardness measurements were made on a Leitz microhardness tester, while initial surface hardness measurements were made after heat treatment using Rockwell equipment.

Since it was possible to determine the maximum wear depth from each diametral wear trace, it was decided that taper sections be taken along the diameter containing the maximum wear depth (AB in Fig. 6a). In this way it was hoped that corrected values of measurements made below the maximum wear scar valley would indicate the degree and extent of change in hardness after a given forging cycle. But it must be remembered that measurements made below a particular maximum wear depth may not be exactly the same as those made

elsewhere in the matrix. This is because maximum wear depth may vary from one Talylin trace to the other. Fig. 6b shows a typical tapered plane on which measurement was made.

Before measurements all the ground sections were polished to about 1μm. In addition the nitrided and coated specimens were etched in 2 - 4% nital. By viewing along and below the line of interception of the two planes on the taper section, the line corresponding to the maximum wear depth was drawn and calibrated by means of a travelling microscope. Calibration was done in the following way. The section was set square with respect to the direction of movement of the calibrated table under the microscope, with one end of the section corresponding to the central die plane assigned zero co-ordinates. This end is represented by OB in fig 6b. This type of calibration was deemed necessary so as to obviate the guess work usually encountered when making measurements at interspacings in excess of 200μm in the measuring scale of the tester. However by making measurements along this line it became possible to establish the die surface zone which experienced the greatest change in hardness.

Measurements made below this line were made in three regions as indicated in fig. 6d: It should be noted that OB in fig. 6d is the same as in fig. 6b, but the wear track has been slightly exaggerated in the former. The three regions are denoted by heavy wear region (HWR), low wear region (LWR) and outside wear region (OWR). The latter measurements were made to enable comparision of the change in hardness between forged and unforged (but heat treated) areas. This would enable a qualitative assessment of the effect of heat treatment of the dies at 150°C. Also, since different modes of wear may occur at LWR and HWR (S.E.M. observations), it was considered that a knowledge of hardness variations below these regions after forging would be useful.

Naturally, the position of the line of interception (discussed above) may vary with type of surface treatment and number of forging cycles. An indication of the variation of this line is given in fig. 6. In addition photo micographs are included (Fig. 52) to show where hardness impressions were made.

3.2 THE EFFECTS OF SURFACE TOPOGRAPHY AND INTEGRITY ON WEAR

3.2.1 DIE MATERIALS AND PREPARATIONS

Twenty four dies (twelve of each material, BH13 and No. 5) were produced and heat treated as described in sections 3.1.2 and 3.1.3 respectively for this purpose. Table 3 shows a list of these dies together with subsequent surface treatments and finishes that were applied to them. In the case of dies which were surface treated the various surface finishing operations associated with them were applied before surface treatment. Details of surface treatment have already been discussed in section 3.1.4. However, unlike in the investigation of wear mechanisms, tufftrided BH13 dies were examined for wear in this section.

Both conventional and unconventional machining techniques were applied to the die surfaces in order to produce varying surface topographies and subsurface integrities. Two levels of each conventional technique (grinding and orthogonal turning) and a level of Electro-discharge machining were used. Grinding was done on a surface grinding machine (Jones-Shipman Model 540) using a wheel of type WA6Hv (178mm diam.). The wheel was not redressed for rough grinding after initial dressing for fine grinding. The depths of cut were varied for both fine and rough grinding while the wheel speed was maintained constant at 2880 rpm. The change in wheel diameter after fine grinding implied that a different cutting speed was used for rough grinding. Orthogonal turning was done

on a centre lathe, and the two levels of machining were achieved by varying cutter speeds and depths of cut. A servomet (Metals Research Ltd., Cambridge) electro discharge machine (E.D.M) was used, with a rotating planner as the anode of the electrical circuit. E.D.M. was conducted in paraffin at a feed rate designated by X3 on the machine.

3.2.2 ASSESSMENT OF SURFACE TOPOGRAPHY AND INTEGRITY

Metallographic studies including microhardness measurements and surface finish evaluation which form the basic data for this type of work [40] were used to assess the effect of the various levels of machining on the surface layers and service properties of both steels. Four samples of each steel prepared as described above were sectioned, lightly polished and examined microscopically after etching in boiling 50% HCL. These samples were not surface treated. It was hoped that in this way sub-surface imperfections such as micro-cracks, deformation etc., could be identified in addition to any surface features which may be observed near the surface of the section. Surface finish measurements were made using a Talysurf equipment. Microhardness measurements were conducted to identify possible areas of untempered martensite, overtempered martensite or retianed austenite.

3.2.3. F O R G I N G T E S T S

All dies were tested on the press described previously, using the same experimental conditions (section 3.1.5).

The numbers of forging cycles chosen were 10, 20, 50, 70 and 100. The reasons for this may be summarised as follows:-

1. to examine the effect of roughness and integrity on initial wear and steady state wear.
2. to examine the effect of surface treatment on initial wear.

3. to examine the effect of increasing forging cycles on initial wear.

Interest on the initial behaviour of surface treated and untreated dies grew from the observations made on die surfaces while investigating the mechanisms of wear. Because the predominant wear mechanism observed was both fatigue and subsurface orientated, it was considered that forging tests conducted at lower cycles may reveal further information on the influence on wear of the surface treatments.

3.2.4 WEAR EVALUATION

Unlike in the previous section, the planimeter was not used in wear evaluation. Instead, a weight loss method was employed. This was because of the extreme difficulty experienced in trying to evaluate wear areas on Talylin traces obtained for low forging cycles.
Weight measurements before and after forging were made on an oertling beam balance which has a measuring accuracy of 0.2mg.

3.3 THERMO-MECHANICAL PROPERTIES

3.3.1 THERMAL FATIGUE

The reasons for investigating this property were as follows:-

1. to determine the effect of thermal cycling on the lives of both BH13 and electern No. 5 die steels.
2. to determine the effect of surface treatments on the lives of both steels, with particular reference to hot forging and die casting applications.
3. to examine the nature of thermal fatigue cracking, so as to enable comparision with those cracks observed on die surface and subsurface during hot forging.

3.3.1.1 PRODUCTION AND PREPARATION OF TESTPIECES

Shouldered testpieces (appendix 3) were machined from bars of both steels which had been annealed as described in section (3.1.2). The smaller

diameter pegs at both ends of the testpiece were internally threaded to enable jigging of those testpieces requiring brush plating of Co-Mo alloy. On the other hand, one of the pegs was machined off in the case of testpieces which had to be plasma nitrided leaving the other for location during the thermal cycling test. All testpieces were hardened and tempered as described in section (3.1.3). Surface hardness for electem No. 5 was 40 - 41Rc, while that of BH13 was 49 - 50Rc.

3.3.1.2 SURFACE TREATMENTS

The pre-treatment and surface treatments applied to the thermal cycling testpieces were as described for plated Co-Mo alloy and plasma nitrided dies in section (3.1.4).

3.3.1.3 THERMAL CYCLING TESTS

The choice of testing temperatures was based on:

1. applications to which both steels are put in practice which often results in craze cracking.
2. past experience [24], so that present results could be compared with those in reference (24).

In die-casting the BH13 die surface temperature would depend on the melting temperature range of the metal or alloy to be cast. For example, typical melting temperature ranges for different magnesium die-casting alloys are 470 - 595°C (US.M11912) and 540 - 615°C (M10600). Apart from its use as a die, BH13 is sometimes used for the cores, sliders, and ejector pins of dies used for casting Zinc and Aluminium. These cores, dies and sliders are subjected to thermal cycling since they act as heat exchangers due to heat input from the casting metal and its subsequent loss through convection, radiation and cooling by water.

Similarly during hot forging heat is introduced to the die surface or cavity by hot slugs and lost through cooling by air or water. Again the

die surface temperature would depend on initial slug temperature and cooling rate. Work by Stilland Dennis [24] suggests that during hot upsetting, the die surface temperature may be in the region of 485 - 550°C. In the present programme the testing temperatures used were 500°C, 650°C and 750°C. A forging cycle range of 100 - 2000 was used in order to determine the effect of changing temperature stresses at both early and later cycles during forging and die casting. Timing of each cycle was based on the 10 sec cam setting of the experimental press. This time corresponds to 0.01 sec slug - die contact time during forging [24]. However, the time for producing one shot during die-casting may well vary depending on the material been cast. In this investigation, this time was assumed to be 0.01 sec, thus making it possible to use the same cam setting for both applications. A typical trace of the rise and fall in temperature is shown in fig. 8.

A description of the rig is included in appendix 3.

3.3.1.4 METALLOGRAPHY

After testing, each testpiece was sectioned, polished, etched in 2 - 4% nital, and then examined optically for cracking.

3.3.2 MECHANICAL FATIGUE

For several years metal fatigue has been regarded as the prime cause of about four-fifths of the failures in modern engineering components. Tool steels, in their own rights, have been no exception to this general belief. Liotard [86] once claimed that the main failure modes in dies during close-die forging are thermal fatigue, mechanical fatigue, deformation and erosive wear. Yet while attempts are been made to understand the causes of fatigue failures in constructional industries, a singular lack of information prevails in the forging industry as to the causes of mechanical fatigue of die steels.

In view of the above together with the dominant wear mechanism observed during upsetting (to be discussed later), it was considered that further investigation of fatigue may be advantageous. Electem No. 5 die steel was selected for this purpose, because it is cheap and favoured by drop forgers for use as a general purpose hot work die steel, even though it does not possess the ideal conditions of high wear resistance required for dies.

3.3.2.1 MATERIAL PREPARATION

Heats of No. 5 die steel, 38mm diam., were rolled to about 18mm diam and then annealed at 830°C for 2 hrs. to allow subsequent machining. A total of 36 (14mm + .05mm) plain testpieces (fig. 9) were machined from the batch, with 6mm flats cut at both ends to facilitate loading. All 36 testpieces were thoroughly mixed and labelled to ensure that no two testpieces had a common cross-section. This was done in order to randomize the effect of microstructure on subsequent fatigue data.

The testpieces were divided into groups and then given identical salt bath heat treatments as described for forging dies (3.1.3). This ensured that all testpieces had the same thermal history before surface treatment. After heat treatment, the testpieces were mechanically polished to 14mm diam. on a lathe to remove scale and to produce a smooth surface free from hardness cracks and pits. Using the order of labelling indicated above, the batch was divided into heats of 7 testpieces according to the surface treatment required. The remaining testpiece was used for the first trial run.

3.3.2.2 SURFACE TREATMENTS

Four surface treatments were employed namely - electroless Ni-Palloy, brush plated Co-Mo alloy, electrodeposited hard Cr and micro cracked Cr. With the exception of micro-cracked Cr and electroless Ni-P alloy, all other treatments were described in section (3.14). The pretreatments

applied here were as applied to the die inserts.

3.3.2.2.1 ELECTROLESS NI-P ALLOY

Canning "Nifoss 80" plating solution was used. A deionised water solution was made from 100 ml/l of "Nifoss 80" base solution and 250ml/l of "Nifoss 80" initial solution. The solution was operated at PH 5 and a temperature of 83 $\pm$ 2^{o}C, using a work area to solution volume ratio of 0.633 m^2/l. The immersion time was maintained at 1 hr so as to obtain deposit thickness of about 12.5µm on all testpieces.

3.3.2.2.2 ELECTRO DEPOSITED MICRO-CRACKED Cr.

A dilute solution of chromic acid containing a mixture of sulphate and silicofluoride catalysta was used to deposit micro-cracked Cr on the testpiece. The solution composition and operating conditions were as follows:- 150g/l Cro_3; 0.35g/l H_2So_4; 3g/l. H_2SiF_6; 17A/dm^2, solution temperature (45^{o}C), plating time (1 hr). This condition produced coating thickness of 12.5µm.

3.3.2.3 TEST EQUIPMENT AND METHOD

Fatigue tests were carried out on a 2-tonne load-controlled high frequency vibrophore (Amsler model) using a transverse beam and support arrangement as shown in fig. 10. A span-to-diameter ratio of 9.3 was used. A stress selector attachment was used for the automatic periodic changing of alternating load with steady mean load during testing. The ASTM step method of testing was employed. Assuming a stress ratio of 0.3 and using the tensile strength [87] of hardened and tempered electem No. 5 die steel as an estimate of its fatigue limit, a trial run was made at a stress level corresponding to 70% of this value. After a prescribed long life (10^6 cycles) failure did not occur in this particular testpieces. Thus this stress level was used as a reference for pre-assigning the first stress level for all other 35 testpieces.

An extremely low load of 2KN was used as the starting load for both surface treated, and hardened and tempered testpieces. In all cases if the testpiece survived the pre-assigned number of cycles, the stress was then increased by 5% until failure occured. Both the preceeding and maximum applied load were recorded together with the corresponding fatigue life.

The step method was used because of the limited number of testpieces which it requires. Infact, a single testpiece may be used, although the use of more testpieces gives more precise estimates of fatigue strength. Failure was considered to have occured when slow fracture had taken place as indicated by the significant drop of the load indication in the photo-electric cell attachment. All tests were ran at room temperature and in air.

3.3.2.4 HARDNESS MEASUREMENT

Micro hardness traverses were made on sections taken from all the testpieces.

3.3.3 NOTCH TOUGHNESS

During hot forging, the die surface is usually subjected to high impact loads. Since the results of wear investigations together with those of others [86, 82] suggest the occurrence of die deformation it was decided that further work was needed to substantiate the observed results. A toughness test was therefore needed which is capable of -

(1) indicating the impact resistance of a hardened and tempered No. 5 die steel.

(2) differentiating the effects of the various surface treatments on a comparative basis.

(3) revealing the types of failure mechanisms in operation under a high impact load, so that the origins of such failure may be

compared with those observed during hot forging.

The standard Izod V-notch test for notch toughness was selected for this purpose.

3.3.3.1 PRODUCTION AND PREPARATION OF TESTPIECES

The Izod testpieces (Fig. 11) were machined from heats of rolled electem No. 5 die steels as in the case of fatigue testpieces, leaving suitable tolerances for subsequent surface treatments. The conditions of surface treatment were the same as for fatigue testpieces. The dimensions of all testpieces were within the limits specified by BS131 parts 1 - 3: 1961.

3.3.32 T E S T I N G M E T H O D

Tests were performed on an Avery machine at room temperature. Using a standard gripping method and maximum potential energy (170 joules), the testpieces were broken as specified by British standard.

The energy absorbed by a testpiece on breaking was recorded (Table 5), and the nature of the fractured surface examined using scanning electron microscopy.

3.3.4 D U C T I L I T Y

Apart from surface hardness, it is the extent of the loss or gain in ductility of a composite, which is decisive for the treated part having to resist a certain mechanical stress. Therefore it is important to know the influence of the diverse structural variations which may be obtained due to the presence of surface coatings on the overall ductility of the part. It was considered that such a knowledge would assist in the understanding of wear, fatigue and impact behaviour of surface treated Electem No. 5 die steels.

3.3.4.1 PRODUCTION AND PREPARATION OF TESTPIECES

Round testpieces, 8mm diam. by 153mm long, were machined from rolled electem No. 5 die steel as described previously for fatigue testing. 19 testpieces were produced although results are reported for only 15 testpieces (Table 6). The other 4 testpieces were used for trials. Heat treatments and surface treatments were as described in sections (3.1.3, 3.1.4, 3.3.2.2).

3.3.4.2 TESTING METHOD

One way of determining the resistance to cracking of a composite is by the use of bend test. However methods of tension testing of metallic materials may be used depending on the relative ductility of the composite. If the coatings are too ductile and so require extremely small mandrel diameters to check the ductility, then tension testing methods may be used. From experience, the coatings employed are never too ductile. Hence bending, instead of tension, was used in accordance with BS1639 (1964) specifications.

A single (slow) bend test (mandrel and support method) was used since it was suitable for testing medium-to-thick testpieces for angles up to 120°. The test was conducted on a 50 tonne Denison machine using two fixed 76.2mm diam. steel rollers as supports. The distance between the two supports was adjustable, but was set at $D + 3a \pm a/2$ for this test - a, being the diameter of testpiece and D is twice mandrel radius.

A testpiece was bent by machine pressure applied midway between the supports via a 6mm radius mandrel. The test was stopped when the maximum angle of bend was attained, i.e. when multiple cracks were observed at the bend by means of an optical binocular. In addition failure was indicated when the load indicator on the machine gradually slowed down until it stopped. Typical bent testpieces are shown in fig. 12.

4. ANALYSIS OF RESULTS

4.1 STUDIES OF WEAR MECHANISMS

4.1.1 SURFACE TOPOGRAPHY STUDIES

The general features observed on as-forged and descaled dies (surface treated and untreated BH13 and No.5 steels) for most of the forging cycles were as follows:-

(1) Plastic deformation.

(2) erosive wear.

(3) exposed subsurface imperfections e.g. voids and inclusions.

(4) Numerous cracks, originating from observed voids which are located on or near inclusions. These cracks extend and join neighbouring ones to form polygons or metal islands.

(5) Sharp and parallel abrasion grooves.

(6) Scratch and ploughing marks. Transition from ploughing to cutting abrasion was observed in some cases.

(7) Heat checks, particularly in the die region underneath slugs before forging.

(8) Dislodged as well as loosely attached metallic flakes, some of which were covered with thick or thin layers of oxide.

(9) Wear edges showing crack paths and indicating separation of particles by a process involving removal of material in layers.

(10) Particle fragmentation and flow of material.

(11) Three distinct regions were revealed by the S.E.M., although in some case (e.g. after 1000 cycles) these regions may be identified with the naked eye. The amount of cracking and wear debris observed generally increased outwards from the die centre. These regions will henceforth be refered to as low wear region (L.W.R.), medium wear region (M.W.R.) and heavy wear region (HWR) as shown in fig. 13.

(12) Some characteristic grinding cracks were observed after descaling.

It should be noted that all the features listed above apply to Electem No. 5 dies inserts in their surface treated and untreated conditions, for both low and high forging cycles. However, in the case of surface treated and untreated BH13 inserts no ploughing or scratch marks were observed at the initial forging cycles (e.g. 1 and 2). Also, far more voids were observed on No. 5 die inserts than BH13 during hot forging. In the case of dies used for cold forging, only limited information was gathered.

1. Plastic deformation.
2. Polygonal cracks.
3. Scratch marks.
4. Collection of wear debris in the H.W.R.

4.1.1.1 N O. 5 D I E I N S E R T

Although generally observed at higher cycles, the occurence of some of these features (during hot forging) was localised and influenced by the number of forging cycles, irrespective of die material and surface treatment. For example after one, two and five cycles, only features like plastic deformation, ploughing and slight erosion were observed in unplated No. 5 die inserts (Figs. 14 - 16). After ten cycles slight cutting abrasion marks were observed (fig. 17), while after 100 cycles the occurence of cutting abrasion and voids forming at inclusions became evident (Figs 18, 19, 20). However, after 1000 cycles many of the features outlined above were collectively observed on the die surface (Fig, 21 - 27), although in some instances thick oxide layers hindered observation. It should be noted that because of the localised nature of some of these features, it is very likely that voids which may have formed and opened out as cracks elsewhere on the die surface at lower cycles (not investigated) no longer appeared

as voids after 100 or 1000 cycles. Instead they appeared as polygonal cracks. Furthermore it should be noted that there is no indication of flow of material around the edge of a crack once it has been formed (Figs. 19 - 20). This implies that any other form of deformation (e.g. due to ploughing, erosion) which probably occured in these cracked areas, did so before crack initiation and propagation and not during these processes (Fig 22).

Similar features were observed on coated No. 5 die inserts, although the occurrence of voids, material flakes (platelets) and polygonal cracks appeared to have been delayed to 100 cycles. Figs. (28 - 35) show micrographs of the worn surfaces of coated inserts. Fig (28) shows a view of an undescaled insert after 10 cycles cold forging. It can be seen that slight abrasion alone (scratch marks) occurred, while original micro-cracks in the Co-Mo alloy coating could still be seen. In addition, it would seem that little or no oxidation of die surface occurred during cold forging.

Figs. 29 (a - b) show the worn surface of a Co-Mo alloy coated insert after 10 cycles hot forging. It can be seen that the coating in this region of the die has been subjected to severe deformation. However, after 100 cycles a characteristic wear edge was observed. It shows multiple layers which suggest wear by a process involving material removal in layers (Figs. 30 a-b) Fig. 31 shows the linking of subsurface cracks with those in Co-Mo alloy coating after 1000 cycles hot forging. Figs. (33 - 35) illustrate the worn surface of a hard Cr plated No. 5 die insert. Figs. 33 and 35 show typical polygonal cracks and some loosely attached platelets. Fig. 33 was partially descaled to show that the features of the worn die surface can be shielded from vision by the thick oxide formed during hot forging. Fig. 34 shows a typical oxide smear.

4.1.1.2 BH13 D I E I N S E R T

In general the number of voids observed on surface treated and hardened and tempered BH13 inserts were limited, although polygonal cracks similar to those described above were also observed. This therefore suggests that these cracks were due either to particle fracture or the opening of pre-existing voids in the steel. In addition, abrasion marks were scant even after 1000 cycles of hot forging - mainly scratch and ploughing marks were observed on surface treated (plasma nitrided and Tuffrided) dies. Other general features observed on these dies have already been listed.

Fig. 36 shows a typical surface grinding marks before forging. Figs (37 - 38) show the worn surface of a hardened and tempered (but undescaled) insert after 100 cycles forging. Fig. 37 shows a wear edge with its characteristic layerlike appearance covered with smeared oxide, while Fig.38 shows a dislodged wear platelet sitting on a cracked and oxide smeared surface. Figs.(40 - 43)shows micrographs of nitrided (but undescaled inserts after hot forging. Fig. 40 shows two views of the worn surface covered with thick and thin oxide layers. It would seem that the crack in Fig.40b penetrated the underlying die material. Fig. 42 shows an area in which a void was suspected to have penetrated the oxide Layer after 1000 hot forging cycles. Fig. 43 shows an adjacent area with a similar void and cracks originating from it. However unlike in Fig. 42, the die surface was slightly exposed in fig. 43.

Fig. 5 (39 a-c) shows three views of nitrided (but descaled) inserts after 100 cycles hot forging. They show wear platelets and the gradual flattening of platelets which were probably fragmented in preceeding forging cycles. Fig. 44 shows the ploughing of another worn surface which appears to have been flattened in the manner previously described. Fig. 45 is a view of

a nitrided (but descaled) insert after 1000 cycles hot forging showing a dislodged platelet, cracks and slight erosion marks.

Fig. (46 - 49) show the worn surface of a Tufftrided (but descaled) insert after 100 cycles hot forging. Fig. 46 shows a void and a crack similar to those previously observed. Fig. 47 shows an enlarged view of the void in fig. 46, together with the crack originating from it: It would appear that the inclusion associated with it was fractured in the process of micro-crack nucleation. Fig. 48 shows a number of shallow voids in another area of the same die surface, while fig. 49 shows a long crack traversing the H.W.R.

4.1.1.3 FURTHER STUDIES

As would be expected the results outlined above unveiled fresh areas for further investigation. First, the results indicate the presence of loosely attached metallic flakes together with chipped oxide layers.

In order to explore this further, two simple experiments were performed. An area of the die (H.W.R.), known to contain loosely attached flakes but in which there was little evidence of dislodged flakes, was lightly marked. This area was "probed" with the edge of a compass and then re-examined under the microscope (Fig. 42). It was found that it now contained several dislodged flakes. In addition islands of metal (Below oxide layer) which had been surrounded by polygonal cracks, but which remained firmly attached to the underlying steel were found to have been only lightly scratched by the compass.

In the second test a plastic replica was stripped from a worn die surface in the HWR. On examination it was found that the replica had removed some of the loose particles or flakes. It should be noted that these tests were only successful on dies used for 100 and 1000 forging cycles (Figs 39, 35, 32 and 45).

From these tests, however, certain other significant information was revealed.

1. the underlying sides of the flakes removed from the worn surface had an appearance resembling that of the worn die (Fig. 45).
2. in some of the die areas where these flakes were removed, indications of the formation of further layer-like flakes were observed.

4.1.1.4 IDENTIFICATION OF OXIDES ON DIE AFTER FORGING

Powder x-ray diffraction analysis of the oxide layer on some of the dies showed that it contained a number of oxides of the elements of the die steel (BH13 or No.5 Electem). Details of such analyses are presented in tables (5 a-c) for unplated No.5 die and, plasma nitrided and Tufftrided BH13 die inserts. Figs. (55a - b) show x-ray traces for nitrided and Tufftrided BH13.

From the above it would seem that a flattened layer is formed on the die surface, which is comprised of compacted oxides of the elements of the steel plus fragmented metallic particles. Figs (39 a-c) indicate the process by which these particles are intermittently fragmented during successive forging cycles. Stott and Wood [89] have recently referred to such a layer as an oxide glaze. However, it is worth noting that the oxides identified in table 5 are by no means all the oxides that are likely to be present in the glaze. The use of x-ray diffraction techniques can be misleading since differing phases can easily be assigned the same d-spacing due to different orientation arising from plastic deformation during forging.

4.1.1.5 WEAR PLATELETS

The sizes of some of platelets (flakes) were measured on the grid of an optical projection microscope. The thickness was found to vary from about

25μm to 100μm, although smaller and even larger platelets may be measured if the limitation imposed by the measuring technique is obviated. Figs. (32, 39a, 45) show several wear platelets of varying dimensions. It can be seen that these platelets can be of many widths and depths.

4.1.1.6 IDENTIFICATION OF OXIDE FORMED ON SLUG BEFORE FORGING

Electron probe micro-analysis of scale formed on slugs before forging showed that the oxide was probably Fe_2O_3. These scales were collected and stored in a desiccator immediately after allowing the hot unforged slug to cool in a container. In this way it was hoped that further oxidation would be minimized, although it was realised that the oxide form of iron can change considerably with time in air from FeO to Fe_2O_3 and then Fe_3O_4. Computer data showing the scale to be Fe_2O_3 is shown in Appendix 2.

Micro hardness measurements of the scale were made after mounting and vibratory polishing. The average of three readings gave 510VPN.

4.1.2 S U B S U R F A C E S T U D I E S

4.1.2.1 EFFECT OF HEAT TREATMENT AND SURFACE GRINDING

Micrographs shown in Figs (53 a-b) indicate that before forging, but after heat treatment and fine grinding, no subsurface cracks were generated in both BH13 and No.5 die inserts. Only subsurface deformation was evident. BH13 and No.5 steel samples (taken from as-purchased bars) were heat treated and fine ground as described in sections (3.1.2, 3.1.3) and then lightly polished to remove surface oxides.

The result obtained implies that the long parallel cracks observed on some of the dies (e.g. fig 27) occurred during forging and may have been caused by cutting abrasion.

In addition, inserts which were heat treated only without grinding did not crack.

4.1.2.2. IDENTIFICATION OF SUBSURFACE INCLUSIONS

Two methods were used in identifying the inclusions observed during surface topography studies described above. First an x-ray dispersive technique was used to identify the elements associated with them. A typical trace is shown in fig. 50. The second method involved metallographic polishing of vertical sections taken from inserts of both steels after hot forging. Microscopic examination showed that silicates and manganese sulphides were present in both steels, with the former having a glassy appearance while the latter was dark grey. Fig. 51 shows an elongated sulphide inclusion after forging.

4.1.2.3 ELECTRON PROBE MICRO-ANALYSIS (EP.M.A)

Analysis of die sections (BH13 and No.5) for changes in chemical composition after forging showed that the distribution of the important oxidising elements was not significantly altered. That is, the ratios of the secondary hardening elements (e.g. Cr, Mo) remained virtually as they were before forging. This implies that even though oxidation had occured during forging, the oxides and metallic particles remained in the glaze (on the die surface). Thus they were not transfered to the slug - an indicator of the absence of metal transfer by adhesion. Figs. (7a-b) show the distribution of Cr and Mo in No.5 die insert before and after 100 cycles forging.

4.1.2.4 H A R D N E S S M E A S U R E M E N T

Results of microhardness traverses across and below the line of interception of the planes on the taper section are shown in table 6. The table shows results for both steels in their hardened and tempered and surface treated conditions after 100 and 1000 cycles. Some of these results are also shown graphically in figs (54 a-b). In addition the regions in which impressions were made are shown in fig. 52.

There appears to be a general increase in hardness in all the regions in

which measurements were made. Figs. 54 (b and d) show variations across one-half of the worn die surface (see fig. 6). For both steels hardness remained virtually constant at the die centre (but never fell below hardness in the area outside the wear region (OWR) after forging), and then increased again to a maximum in the HWR. It is worth noting that the hardness in OWR increased above the original hardness range due to heat treatment and/or surface treatment, even though it was unaffected by material flow during forging. The latter hardness range is represented by A, B, C, D, in figs 54 (a - d). The region (in figs 54 b,d) where the hardness profile changes direction corresponds to MWR, that is, it lies between LWR and HWR (Fig 13). Also from Figs (54 b, d) it appears that the increase in hardness in all three regions will be greater, the higher the forging cycles.

The results of measurements below HWR and LWR are shown in figs (54 a,c). Again an increase in hardness of the worn die surface is evident. Also it can be seen that this increase in hardness extends to varying depths below the worn surface depending on number of forging cucles, surface treatment and position of measurement. In the case of plasma nitrided BH13, the depth was greatest after 1000 forging cycles and for measurements below HWR (Fig 54C). Similarly for unplated Electem No. 5 die insert, the depth was greatest after 1000 forging cycles and for measurements below HWR.

The above results may be summarised as follows:-

(1) there is a general increase in hardness below and across the worn die surface after a sufficient number of forging cycles, although HWR appears to be harder than others.

(2) this increase in hardness appears to depend on the number of forging cycles and surface treatment.

In order to explain these results in terms of the possible causes of change in hardness listed in section (3.1.8.6), two tests were performed. Die inserts (BH13 and No.5) machined and heat treated (as in sections 3.1.2, 3.1.3), were sectioned, polished, etched and examined microscopically for retained austenite. Unfortunately it was not possible to distinguish between all the martensite and austenite regions. Consequently a second test was performed using an x-ray diffraction technique capable of decting 1 - 2% austenite.

The results of the latter test are shown in figs 56 (a,b) and table 7. It can be seen from figs 56(a,b) that the above dies contained retained austenite. To check further if the presence of retained austenite was due to faulty heat treatment practice, other testpieces prepared for use by Still and Dennis [24] were examined. Again, traces of retained austenite were observed (Fig 56c). These results are in agreement with that obtained by Crowther [92] in a similar salt bath heat treatment of forging dies (BH 13). However, specimens taken from dies after forging did not reveal any austenite regions when examined. It seems therefore that some transformation occured. Thus the increase in surface hardness may either be due to this transformation acting alone or in conjuction with any of the possible causes mentioned aboved.

Retained austenite is unstable and may transform into fresh martensite under the influence of deformation or during tempering, causing an unexpected increase in hardness. In other instances it may prevent the attainment of the desired increase in hardness because the austenite transforms to a product softer than martensite during subsequent tempering. The third possibility certainly does not explain the experimental results (Fig.54 a-d) Therefore it was thought that this transformation may be accounted for by the first two possibilities. Nevertheless it is worth noting that if

retempering of the die surface was to occur, sufficient time must be allowed for the transformation of retained austenite into martensite during the cooling half of the forging cycle. Unfortunately the die surface is only held at the reheating temperature (die surface temperature) for 0.105sec according to Still and Dennis [24]. This short slug-die contact time makes the second possibility doubtful [38].

From the above it would appear that the increase in hardness of hardened and tempered dies was probably due to -

1. austenite transformation due to deformation and -
2. heat treatment of dies at 150°C for the duration of forging (with subsequent air cooling after forging is complete).

The increase in hardness of the surface treated dies is very unlikely to be due to tempering. This is because, for example, the hardness of a nitrided case has good resistance to tempering [98]. Returning back to the list in section (3.1.8.6), it seems that there are only two other possibilities which would account for the increase in surface hardness of the dies. That is the increase may be due to -

1. intermittent frictional contact between the slug and die surface during forging.
2. Oxide products.

However since hardness measurements were made on taper sections taken from descaled dies, and the results of electron prolse micro analysis showed that there was no compositional change at the surface due to oxidation (section 4.1.2.3) it implies that the first possibility is most likely responsible for the increase in hardness. The intermittent frictional contact between slug and die results in the formation of a thin layer of fragmented wear debris (Figs 39a-c) on the die surface. Several authors [93,94,95] have identified metallic layers formed in such a manner to be hard, abrasion wear resistant and crystalline in structure.

4.1.3 WEAR MEASUREMENT

The result of wear measurements are presented in table 10. It can be seen that the bottom dies generally wore more than the top dies - a result which suggests that deformation plays an important role in the overall wear process.

The wear pattern consists of regions which correspond to LWR, MWR and HWR in fig. 13b. Thus the amount of wear across the die surface appears to be related to the hardness profile in figs. 54 (a, b), i.e. a region of heavy wear correspond to a region of high hardness. Figs. 57 (a-d) show typical wear traces for unplated, Co-Mo alloy plated No.5 die insert, unnitrided and plasma nitrided BH13 inserts respectively.

Irrespective of surface treatment, the results in table 8 show that wear may increase linearly with forging cycles. In addition the results suggest that wear decreased in the increasing order of unplated No.5, unnitrided BH13, Co-Mo alloy plated No.5 and plasma nitrided BH 13 die inserts.

4.2 EFFECTS OF SURFACE TOPOGRAPHY AND INTEGRITY AND WEAR

Table 3 shows the experimental surface and subsurface conditions of all the twenty four inserts tested together with the wear index associated with them. The index is arbitrary but increases with decreasing wear of the inserts.

Figs. 58 (a - f) show the results graphically, i.e. with die weight loss as a function of forging cycles. It can be seen that wear increased linearly with forging cycles in all cases after a sudden initial change in slope. For each die material (and irrespective of surface treatment), wear was found to be a sensitive function of surface profile. Thus the rougher surfaces had a slightly larger total weight loss than the smoother ones. Under increasingly high loads (as experienced during forging) the larger

primary asperities of the rougher die surfaces appeared to have been easily removed in comparison with those on the smoother surfaces. This is due to the high contact stresses (normal and tangential) generated. It is worth noting, however, that the small difference in weight loss shown on all the plots (for different surface treatment) may be due to the large weight of the primary asperities of the rougher surfaces. Thus, it seems that once the asperities have been removed and a steady wear condition is reached, the weight loss remains virtually the same as the number of forging cycles is increased. It is recognised that steady state wear can be affected by the initial wear if the initial wear particles are either returned or entrapped.

Figs. 58 (a - c) show wear results for unplated, Co-Mo alloy plated and hard Cr plated No. 5 die inserts, while Figs. 58 (d - f) illustrate the results for unnitrided, Tufftrided and plasma nitrided BH13 inserts respectively. The similarity between the two sets of results partly suggests identical wear mechanisms and also, that the effects on initial wear (running-in) of surface roughness and especially number of forging cycles are independent of die-material. If the prepared surfaces contained any surface or subsurface imperfections (e.g. deformation and microcracks) a large initial weight loss would be expected. This is illustrated in Figs. 58 (a - f) and figs. 59 (a-d), although it is worth realising that the effect of subsurface modification (integrity) cannot be separated from roughness and surface treatment effects. Thus, as demonstrated in Table 3, for the same substrate and machining (deformation index) but different surface roughness and treatment, the weight loss would differ. In addition it can be seen that dies (No.5 and BH13) which received the worst subsurface modification (deformation index 1) due to orthogonal turning, wore less than those which were spark machined (deformation index 2).

This was considered to be due to the countering effect of the smoother surfaces of the former group of dies.

However it should be noted that it is the difference in weight loss at each level of machining, rather than the shape of curves, that accounts for the difference in die materials. For example, a spark machined (hardened and tempered) BH13 insert showed less wear than its No. 5 die counterpart, even though their initial and steady state wear behaviour appeared similar. Thus this difference in weight loss may depend on the processes which lead to the formation of wear particles which in turn depend on die plus surface or diffusion coating material properties.

Figs. 53 (a, b) are S.E.M. micrographs of vertical sections of fine ground BH13 and No.5 die inserts showing the damage caused by grinding near the surface.

4.3 THERMO-MECHANICAL PROPERTIES

4.3.1 THERMAL FATIGUE

Thermal cycling test results are tabulated in table 9 , while the micrographs of some of the testpieces are shown in figs. 60(a-e). Fig. 60a was included in a previous publication by Still and Dennis [24]. It shows the thermal cracking of No.5 die steel which was plated with a much thicker deposit of Co-Mo alloy deposits. It is included here for the sake of comparison with cracks observed on testpieces plated with a similar coating but less thickness (12.5μm).

Table 9 shows that after 500 cycles (at 500°C) both plasma nitrided and unnitrided BH13 testpieces were uncracked. Fig. 60a shows a typical nitrided case after cycling at the conditions above. After 1000 cycles (at 500°C) it was observed that while the unnitrided testpiece was severely cracked, the nitrided case was only slightly cracked but unpenetrated. However, by increasing the temperature to 650°C and then 750°C (at the same number of

thermal cycles, i.e. 1000), the case became slightly penetrated by cracks. Fig. 60b shows a typical crack which penetrated the case at 750°C after 1000 cycles. Finally by keeping the temperature constant at either 650°C or 750°C, and increasing the number of thermal cycles to either 1500 or 2000, it was observed that the core of the nitrided testpieces became severely penetrated by cracks. It is worth noting that the severity of cracking increased with number of forging cycles. Fig. 60c shows a typical crack at 750°C after 2000 cycles.

Similar results for unplated and Co-Mo alloy plated No.5 die testpieces are also presented in table 9. Fig.60d shows several cracks observed on a coated testpiece after 1000 cycles at 500°C.

4.3.2 NOTCH TOUGHNESS

Table 10 shows that all the surface treatments reduced the notch toughness of the hardened and tempered No.5 die steel. The reduction in toughness due to each coating was as follows - electroless Ni-Palloy (1.7%), brush plated Co-Mo alloy (5.2%), electrodeposited micro-cracked Cr (7.9%) and hard Cr (12.3%). The average value of 16 joules for the hardened and tempered testpieces is in good agreement with results obtained by Bayliss [87].

The fracture mechanisms observed were void coalescence, cleavage, tearing and brittle failure. Figs. 61 - 73 show fractographs which illustrate these mechanisms.

4.3.3 DUCTILITY

The results for the slow bend tests are shown in table II. It can be seen that while hard Cr reduced the ductility of the hardened and tempered testpieces, all other coatings improved this property. The average percentage change in ductility due to each treatment was as follows: micro-cracked Cr (1.7), Co-Mo alloy (10.1), Ni-P alloy (22.2) and hard Cr (4).

In general failure occurred by a multiple crack initiation process, although limited cracks were observed on the hardened and tempered testpieces. Fig.12 shows two tested testpieces which indicate the relative maximum bend angles achieved for Co-Mo alloy plated and hardened and tempered testpieces.

4.3.4 MECHANICAL FATIGUE

The fatigue data are shown in table 12. It should be noted that not all the testpieces failed at half span length. Consequently the distance of one end of each testpiece to the fractured surface was measured to enable calculation of bending moment. An estimate of the fatigue strength for each testpiece was determined by taking the mean value between the stress value at which fracture occured and that of the preceding survival run.

Fig. 74 shows semi-range S-N curves for 50% survival run for all testpieces. It can be seen that the mean fatigue strength (at 10^6 cycles) of the hardened and tempered testpieces was reduced in varying proportions by the surface treatments - electroless Ni-P alloy (.115) brush plated Co-Mo alloy (.254), electrodeposited micro-cracked Cr (.309) and hard Cr (.381).

4.3.4.1 ANALYSIS OF VARIANCE

An analysis of variance of the fatigue strength estimates was undertaken for all the testpieces (appendix 4). The reason for this was twofold. First to establish whether the fatigue strength of the hardened and tempered testpieces was affected differently by each coating. Secondly, to determine the extent of their bias with respect to each other.

The estimated fatigue strengths denoted by A - E in table 13 were assumed to be normally distributed. Table 13d shows the sum of squares of the variability between and within the treatments (including hardened and tempered testpieces). Comparison of these variabilities indicated that each coating (B-E) affected the strength of (A) differently. However it did not

reveal how significantly different they affected (A).

Consequently, confidence limits were established for the sample means of each treatment at the 95% significance level. The results obtained are shown pictorially in fig. 75. It can be seen -

(1) that there is a bias between treatment, i.e. all the coatings (B-E) reduced the strength of (A).

(2) that the reduction was in the increasing order of electroless Ni-P alloy (B), brush plated Co-Mo alloy (C) electrodeposited micro-cracked Cr (D) and hard Cr (E).

(3) that there is a 95% confidence of the mean strength for each treatment lying in the range indicated.

However it is worth pointing out that the above analysis considers only the assignable causes of variation in the data (e.g. loading and testpiece geometry). Unassignable causes exist which may account for the effects of each coating as depicted in Fig. 75. For example there could be variations in the estimated strengths, of each of the seven testpieces per treatment, due to one or a combination of the following:

1. internal residual stresses.
2. micro-structural differences between coatings.
3. effective surface finish after coating.

This aspect would be examined further in section 5.

4.3.4.2 EXAMINATION OF FRACTURED SURFACES

Both macroscopic and microscopic examination of the fracture surfaces revealed that fatigue failure was initiated at the surface of the test-pieces. Fig. 92 shows photo macrographs of the fracture surface of a Co-Mo alloy plated testpiece. Figs (76-91) reveal further details of the fracture mechanisms, namely, cleavage, void coalescence, and brittle plus ductile failure.

4.3.4.3 HARDNESS MEASUREMENT

The results for hardness traverse are shown in table 4. These results are typical of the hardness of testpieces used for impact, slow bend and fatigue bend tests. The coating hardness were as follows: hard Cr (950 - 1010 vpn) micro-cracked Cr (893-960 vpn), Ni-P alloy (498 - 511 vpn) and Co-Mo alloy (561 -570 vpn).

5. DISCUSSION

The results of the above analysis will be discussed separately (as in section 4.1, 4.2, 4.3) and then collectively with particular reference to No.5 die steel. In addition a section on the practical implications and minimization of wear will be included.

5.1 WEAR MECHANISMS

Microscopic examination of worn die surfaces, subsurfaces and wear particle morphology suggests that several modes of wear operate during drop forging. These include abrasive, erosive, oxidative and delamination wear. The characteristic features observed on worn surfaces were similar for both BH13 and No.5 die inserts (irrespective of surface treatments) although their nature and extent of occurrence generally varied with forging cycles. However, due to this similarity, a general discussion of these features will be made for both steels in their hardened and tempered, and surface treated conditions.

5.1.2 ABRASIVE WEAR

Evidence of a number of abrasive wear mechanisms were observed on the worn surfaces. For example, it can be seen from figs (14 and 15) that ploughing of the surface of hardened and tempered No.5 inserts occured after the first and second forging cycles. This feature is revealed by the rough edges of the grooves caused by the lateral plastic flow of material. It was thought that this ploughing action may be due to hard scales from hot slugs since no wear particles were present on the die surface after the first forging cycle. However, the transition from ploughing to cutting abrasion shown in fig. 15 indicates that after a large number of forging cycles a high-stress grinding type of abrasion becomes operative. This may either lead to the generation of curled, smooth backed and continuous wear particles or the production of impressions due to plastic deformation (Fig. 18). It should be emphasised, however,

that the continuous and smooth backed micro chips which typify the former were not observed in this investigation. Instead the latter was observed, as shown in figs (17 and 18) for hardened and tempered No.5 insert after 10 and 100 cycles.

In general this type of abrasion occurs when the stress applied to the abrasives (hard scale and/or wear particles) exceeds their crushing strengths. During forging the stress generated due to ram loading is so high that the scales entrapped between the slug and die have little chance of sliding or cutting before they are fragmented. Consequently, their main effect may be due to the concentrated high compressive stress at the abrasive - die contact which may result in the formation of impressions referred to above. When a number of such impressions are formed close to each other the displaced materials may flow backward and forward until they fracture by fatigue giving rise to the formation of parallel grooves as shown in fig. 18. In addition, compressive stresses of the type mentioned above may be responsible for scales claimed to be embedded in local areas of the die surface [101].

Another type of abrasive mechanism observed on the dies irrespective of die material and surface treatment was scratching. In general, hardened and tempered BH13 as well as surface treated BH13 and No.5 die inserts had more scratch marks than hardened and tempered No.5 die inserts. This was probably because their surface hardness was higher than that of the scale. In this investigation the scale hardness was found to be about 510VPN which is low in comparison with that for hardened and tempered BH13 (550vpn).

All the types of abrasive wear mechanism discussed above can lead to die surface and subsurface damage. For example grinding or cutting abrasion may generate structural defects such as deformation, voids, microcracks, and as indicated above it may even lead to scale being embedded in die

subsurface. Subsurface changes produced in this way by grinding may set up residual stresses which will influence the fatigue strength of a metal alloy[90].

5.1.2 EROSIVE WEAR

Evidence of erosive wear marks observed on the surface of both steels in their surface treated and hardened and tempered conditions are shown in figs. (16, 22, 23 and 45).

During upset forging both high temperature and mechanical erosion may occur, but the occurrence of the former depends on the temperature induced on the die surface by the hot slug. If the temperature is high enough then some form of local melting may occur. Aston et al [2] put forward explanations which suggest possible local high temperature erosion even though the die surface temperature was unknown at the time. Measurements by Still and Dennis [24], however, suggest that the surface temperatures of hardened and tempered No.5 is about 485° - 550°C for this experimental situation. The tempering temperature for No.5 and BH13 inserts were 485°C and 560°C respectively, while the die-slug contact time was 0.105sec

In the present investigation, mechanical erosion was observed rather than high temperature erosion. The granular appearance of the damaged surface in the micrographs indicates that the engineering system involved during upsetting is such that a multiphase, solid-particle impingement erosion occurs instead of a single phase flow phenomena (as in high temperature erosion with no solid particles).

When corrosive effects are theoretically excluded from an erosive wear situation, then wear may be expected to be due to the imposition on the surface of normal or shear stresses of sufficient magnitude to cause metal fatigue either through single or cyclic blows. During hot forging corrosive effects (oxidation) can not be excluded. Therefore metal failure

through cyclic blows may be influenced.

Also as indicated in the literature, erosive wear varies with particle impact angle. When the angles are small (normal stress component is zero), cutting wear would occur while at large angles wear is attributed to deformation (shear component is zero). During hot forging the angles of impingement of the abrasives are uncertain but one suggestion is that they may impinge the die surface in both directions. Thus both cutting and deformation effects may be experienced by the die surface, both of which can result in subsurface deformation.

5.1.3 OXIDATIVE WEAR

One common feature of the worn die surface was the presence of smeared oxide. SEM observation of the as-forged die surface revealed several important details regarding the oxide layer (glaze). First, the thickness of the oxide glaze was not uniform over the entire die surface. This may be due to the fact that it was either not formed in the less dense areas or it may have been scrapped off during subsequent sliding. Second, the glaze was cracked leaving oxide islands on the die surface (Figs 33,34,40). Third, x-ray diffraction analysis of this glaze showed that it was made up of the compacted oxides of the constituent elements of the die insert (Table 5 a-c). Furthermore, electron probe micro analysis of the layer after hot forging suggested that the oxides contained the important wear resisting alloying elements (e.g. Cr and Mo) in approximately the same proportions as before forging (Fig 7). Thus this result indicates that, although oxidative wear occured, there was no transfer of material due to adhesion.

Stott and Wood [89] have recently suggested possible explanations for the development of this oxide glaze on several commercial alloys (including 5%Cr steel) during sliding in air at elevated temperatures. The three possibilities are -

1. Metallic wear particles which are formed during sliding may be fragmented and then oxidized and compacted until a smooth surface glaze is formed.
2. Transient oxide (e.g. oxide formed before sliding) may be scrapped off during sliding, giving rise to the formation and subsequent removal of more oxides until a sufficient amount is present to form a compacted oxide layer.
3. During the heating-up period rapid oxidation of the surface may occur, with the result that sufficient oxide may be formed to facilitate development of the glaze during subsequent sliding.

Thus, once the oxides are formed (by any of the three ways above) on the die surface, a relatively weak bond is developed between the oxide which causes them to adhere. This bonding is further increased due to compaction of the debris as a result of ram loading and slug sliding during subsequent forging cycles (Fig 40). As the number of forging cycles increases (i.e. cumulative increase in ram load) finer debris particles would be formed, giving rise to increased bonding strength. In addition, every stage of particle fragmentation during forging is associated with local grain redistribution and plastic flow of oxide due to relative sliding between slug and die.

Stott and Wood [89] have also suggested that such a glaze can considerably reduce friction and wear rates during sliding wear due to its smooth nature. However, it is worth noting that the glaze may be less effective in this respect in a complex wear situation as experienced during hot forging.

5.1.4 DELAMINATION WEAR

Other characteristic features of the worn die surfaces were the presence of micro voids and polygonal cracks. In addition there was evidence of sub-surface inclusions and deformation below the die surfaces before and after hot or cold forging.

Figs (19, 20, 21, 26, 30, 31, 35, 38, 41, 47) show some of the polygonal cracks and voids which were observed on various dies. It is worth noting that far more voids and cracks were observed on unplated No. 5 die inserts than on plated No.5 dies as well as surface treated and hardened and tempered BH13. This may be due to the relatively low resistance to deformation of unplated No.5 die. Micrographs of worn die surfaces and sub-surfaces (Figs. 14,16,18,22,23,27, 28,29,33 and 39) show that subsurfaces deformation occured during forging. In addition, Figs. (53 and 59) show that subsurface deformation of the inserts occured before forging due to machining. The amount of deformation which occured appeared to depend on the number of forging cycles, die material and its surface treatment. For example plough marks were observed on plasma nitrided BH13 inserts only after 100 forging cycles (Fig.44), where as they were observed after the first cycle on an unplated No.5 die insert (Fig. 14)

Figs. (21, 24, 26, 26, 50, 51) show some of the inclusions in both die steels, some of which were observed on the worn die surface after descaling. Two types of inclusions were observed, i.e. silicates and sulphides. Fig. 51 shows a typical elongated sulphide inclusion after forging. It can be seen from figs (19,26,43) that these inclusions act as void and cracks initiation sites during forging. Thus it will appear that the characteristic polygonal cracks originate in the steel substrate for both surface treated and, hardened and tempered dies. However, as subsurface deformation continues (with increasing forging cycles) these cracks grow and join neighbouring ones to form metal islands. Figs (19, 20, 23, 35, 38 and 39) show some of the dislodged and undislodged metal islands (flakes or platelets) formed by this process.

From the above it would seem that the wear platelets observed on the die surface after descaling were formed either by a two or three - step process. If pre-existing cracks were present in the steel then the process of wear

particle formation would involve only two steps, although this may be localized. Otherwise, the first step would be that of subsurface deformation followed by micro void nucleation at inclusions. Finally these voids would then open out as cracks which grow, ramify and join neighbouring cracks to form these wear platelets. However it is worth noting that both the two-step process (deformation plus crack propagation) and the three-step process may occur in the same die insert since several sites on an insert may be favourable to crack nucleation even though other local sites may contain pre-existing cracks. In addition, the inclusions mentioned above may include embedded scale, as in the case of unplated No. 5 die steel [101]. Such a scale would indeed act as additional subsurface crack nucleation site due to deformation during subsequent forging cycles.

The processes of wear particle formation described above are not in agreement with the older wear theories (i.e. abrasion, erosion and oxidation). In addition the shapes of the platelets are different. For example, abrasive wear would not produce the relatively smooth flat surfaces of the platelets (Figs 23, 32 and 39). Instead abrasive wear particles are generally curled, smooth backed and continuous as in cutting abrasion, although abrasion may sometimes leave only impression marks. It is, however, the delamination theory of wear proposed by Suh [22] which accounts for both the morphology and surface features of the metallic platelets.

5.1.5 GENERAL

From the foregoing it would appear that the wear modes which exist during forging may either act separately or together. Evidence of the latter possibility in a local die region is shown in figs (19,22), since the absence of flow of material around the crack edge suggests that the cracks were formed after deformation (including that due to erosion). However, of the mechanical wear modes, delamination wear appears to be dominant

since the majority of scars observed on die surface were those associated with delamination wear platelets. Indeed, while erosion and abrasion appear to be limited to HWR and MWR (Fig. 13), delamination wear may extend to LWR as indicated by the large number of polygonal cracks observed in this region. The latter wear theory proposes that wear particles are formed by successive removal of material in the form of flakes or platelets. Figs (30, 37) show typical wear edges left behind on the die surfaces after adjacent platelets had been removed. The delamination theory also suggests that the rate of formation of these platelets depends on subsurface deformation and crack nucleation as well as the crack propagation processes.

If all the wear modes operate together to produce the overall wear in the dies, then abrasion, erosion, and oxidation can be expected to do so by contributing to delamination wear in the following manner. Subsurface deformation during forging may be influenced by the normal ram cyclic impact load, and the plastic deformation and surface traction at asperities during sliding. Thus, since both erosion and abrasion can cause plastic deformation as explained earlier, they may also accelerate subsurface deformation.

The effect of oxidation on the declamination wear processes is less obvious since it may take place either during subsurface crack propagation or after the wear platelets have been formed. However the metallic luster of the platelets after descaling ((Fig. 32) suggests that the platelets were formed by subsurface crack propagation rather than along the oxide glaze - metal interface. Therefore it is thought that oxidation may effect declamination wear by accelerating crack propagation rate since the latter is essentially a fatigue type wear (i.e. a stress - corrosion phenomenum may be expected).

Before discussing the differences in wear volumes of the die steels, it should be noted that thermal fatigue cracking which occurs mainly in the LWR of the die may also influence the overall wear of the insert. However its effect on the delamination wear platelets is probably indirect. This is because thermal activation alone due to temperature stresses imposed during forging cannot assist in the production of disclocations which are required for the nucleation of voids and hence micro cracks in the delamination wear theory. For example it has been stated in the text [26] that even the smallest conceivable dislocation loop of 20^{o}A diameter requires an energy greater than 2 or 3 ev for its formation, which thermal activation cannot provide. As a result it was considered that the effect of thermal fatigue cracks may be simply that of joining neighbouring subsurface delamination cracks to accelerate the formation of platelets. This is because the former cracks normally propagates downwards from the surface while the latter grow at first in the slip direction and ramify later (separate thermal cycling test results will be discussed later).

5.1.5.1 EFFECT OF SURFACE TREATMENT ON WEAR VOLUMES

The experimental results presented in table 8, show that wear decreased in the increasing order of hardened and tempered No.5, hardened and tempered BH13, Co-Mo alloy plated No.5 and plasma nitrided BH13.

In order to explain these results the different wear modes may be assumed to act together as suggested above, since the values in table 8 represent the overall wear volumes rather than for the individual wear modes. This assumption can be better appreciated when it is remembered that each of the mechanical modes has its own mathematical formula which relates it to other parameters. Thus according to this assumption the effects of abrasion and erosion may be expected to accelerate subsurface deformation while those of oxidation and thermal fatigue may be to accelerate crack growth rate.

In all the conventional wear modes (abrasion, erosion) hardness is generally considered to be the most important property in assessing wear. But as indicated in the literature [12, 13], these theories lack the ability to explain the effect of microstructure on wear. The delamination theory, however, postulates that hardness is important since it influences the rate of plastic deformation and surface traction at each asperity which in turn controls its basic processes (subsurface deformation, crack nucleation and crack propagation). Thus both the hardness and microstructures of the die steels would be expected to play an important role in determining their wear volumes.

The delamination processes may either occur sequentially if the material can deform plastically and is free from pre-existing voids and cracks, or simultaneously if it contains these imperfections [91]. In the present investigation it was considered that these processes occured simultaneously since most commercial alloys contain imperfections. Thus the most dominant of the three processes will control the overall wear. But as previously indicated these processes are structure sensitive. Therefore in a pure metal (i.e. particle-free solid solution) subsurface deformation would be expected to dominate and hence control wear volume. In the case of a die steel which has a large number of favourable crack nucleation sites or in which particle-matrix decohesion to form voids can easily occur (e.g. No.5 die steel), the dominant process will be crack propagation. Whereas in BH13 die steel where crack propagation may be easier and void formation difficult, the controlling or dominant process is most likely crack initiation.

From the above it appears that the overall wear is a complicated function of the friction coefficient, the hardness, the bond strength of the particle-matrix interface, index of deformability of the inclusion, the crack growth rates - each of which may be dependent on other variables. It is therefore

difficult at present to predict the effect of all these variables on wear volume in a forging situation. Nevertheless the experimental results can be qualitatively discussed using some of the variables. First it may be helpful to recall the results of hardness measurements across and below the die inserts after forging. The results show that

(1) There is a general increase in hardness below and across worn die surface after a sufficient number of forging cycles, with the HWR always harder.

(2) this increase in hardness appears to depend on the number of forging cycles and surface treatment.

(3) the increase in hardness was probably due to transformation of retained austenite [92] into martensite (Fig 56), and the production of a hard compacted layer of metallic particles on the die surface (Fig 39) due to intermittent frictional contact [93,94,95].

It should be remembered also that increased hardness may have either the effect of reducing or increasing wear. For example if hardness is increased by the introduction of non-metallic inclusions which act as crack initiation sites, then wear may be expected to increase. However, if hardness is raised while crack nucleation and propagation are supressed then wear may be expected to decrease. A decrease in friction coefficient together with an increase in hardness will reduce subsurface deformation and hence crack initiation rate. Also an increase of toughness to an optimum value will lower crack propagation rate.

To explain the experiment result it is necessary to study the problem case by case.

5.1.5.2 WEAR OF NITRIDED BH13 VS UNNITRIDED BH13

The higher surface hardness of a nitrided BH13 insert (before and after forging) makes it experience less plastic deformation and ploughing than an unnitrided insert. Hence the former will have a lesser tendency to crack nucleation. The effect of increased roughness due to nitriding (Table 3) may increase this tendency, and hence wear volume. However the compressive stresses in the case appear to suppress crack nucleation and propagation. Thus a nitrided BH13 insert experiences less delamination wear than its unnitrided counterpart. It should be noted that this may only be true if all the failure modes (abrasion, erosion, oxidation thermal fatigue and delamination) act together. Otherwise, hardness and structural composition of the nitrided case can be expected to reduce the effect of each failure mode, which in turn would affect overall wear. As indicated later, nitriding can delay thermal fatigue cracking.

5.1.5.3 CO-MO ALLOY PLATED NO.5 DIE VS UNPLATED NO.5 DIE

A Co-Mo alloy plated electem No.5 die insert possesses higher surface hardness and lower surface roughness than it's unplated counterpart (tables 3 and 6). Therefore less subsurface deformation (through plastic deformation and surface traction) and hence void nucleation can be expected in the former. However, the tensile stresses often associated with the coating may increase crack propagation rate and so alter the rate of wear in comparison with its unplated counterpart. Therefore it would appear that it is the improved ductility (increased toughness) conferred by plating that overrides the above effect of tensile stresses. Thus crack growth rate may be reduced leading to less wear of the coated Electem by delamination.

Again, this explanation would hold if the abrasion, erosion, thermal fatigue and oxidation can be assumed to act together. Otherwise, hardness

microstructure and composition of coating can be expected to affect each failure mode as suggested above.

5.1.5.4 PLASMA NITRIDED AND UNNITRIDED BH13 VS CO-MO ALLOY PLATED AND UNPLATED ELECTEM

From the discussion above it would appear that it is the high surface hardness (reduced deformation) and the suppression of crack initiation and growth rate by the compressive stresses in the case, that makes plasma nitrided BH13 inserts wear less than Co-Mo alloy plated No.5 die inserts.

Similarly the reduced subsurface deformation (due to high hardness) and hence the difficulty of void and crack nucleaton may be responsible for the low wear in unnitrided BH13 inserts, whilst the increased subsurface deformation (due to low hardness) and the ease of void and crack nucleation may account for the high wear in unplated No.5 inserts.

It should be emphasized that many factors, some of which were mentioned in section(5.1.5.1), have been neglected in the discussion above. For example information is needed on the - particle matrix bond strength, friction coefficients and fatigue strengths and the effect of surface topography and integrity on initial die wear - to enable a more comprehensive explanation for the differences in wear volumes. An attempt was made in this investigation to obtain basic information (at room temperature) on some of these factors. Although these factors may affect the subsurface deformation, crack initiation and propagation processes somewhat they will not alter the mechanisms of wear (see fig 13A for a suggested wear model).

5.2 EFFECT OF SURFACE TOPOGRAPHY AND INTEGRITY ON DIE WEAR

In section 4.2 the results of the effect of surface roughness and integrity were discussed mainly from one standpoint, namely, the difference between

the roughness and integrities of the dies having the same surface treatment. Therefore, in the following discussion, attention will only be focused on the differences in surface treatment and machining.

Table 3 shows the comparative results for both steels and their surface treatments. It can be seen that wear decreased in the increasing order of hardened and tempered No.5,hardened and tempered BH13, Co-Mo alloy plated No.5, hard Cr plated No.5, Tufftrided and plasma nitrided BH13 die inserts.

Some of the possible reasons for the variation in wear due to surface treatment will now be discussed.

5.2.1 HARD CHROMIUM VS CO-MO ALLOY PLATED NO.5 DIE INSERT

As will be discussed later, hard Cr reduces the fatigue strength of No.5 die steel more than brush plated Co-Mo alloy. This is probably due to the high tensile stress and low ductility associated with hard chromium. Thus in a fatigue type wear (in which wear by delamination predominates), it can be expected that hard Cr plated inserts would wear more because of their higher crack propagation rate. Chromium is harder (more abrasion resistant) and confers better surface finish on No.5 die insert than brush plated Co-Mo alloy. Thus a hard Cr plated insert would undergo less subsurface deformation (due to reduced plastic deformation and surface traction at each asperity) than a Co-Mo alloy plated insert. Hence crack nucleation and therefore wear would be expected to be faster in the latter composite.

However it should be emphasized that after about 100 forging cycles it is highly probable that hard Cr plated inserts may become less wear resistant. This is because the hard Cr plate may become more susceptible to fragmentation due to its low ductility, thus exposing local areas of the less wear resistant underlying substrate to wear (Figs. 30 and 35).

5.2.3 PLASMA NITRIDED AND TUFFTRIDED BH13 INSERTS

Tufftriding generally confers resistance to abrasion (scratching, scuffing, etc) on steels due to the presence of a carbon-enriched ε-compound layer. Torsion tests [73] have shown, however, that such a layer would not withstand high dynamic and frictional stresses as much as a predominantly rich γ^1 - compound layer which is often associated with plasma nitrided BH13. It is thought that this property may be due to the hard layer ductility associated with the latter as against the more brittle layer of the former treatment which contains grain boundary precipitates. In addition nitriding confers a better surface finish and hardness on machined BH13 inserts than Tufftriding (table 3). Thus nitrided inserts would undergo less subsurface deformation and hence Tufftrided inserts would wear more initially.

5.2.4 VARIATION IN WEAR RESISTANCE DUE TO MACHINING

As in this investigation and elsewhere [92], it has been noted that hardened dies may contain patches of retained austenite. In general, machining can damage the surface and subsurface by (1) introducing defects such as voids, deformation and cracks, (2) residual stress and (3) inducing transformation of the retained austenite to fresh martensite (untempered) or overtempered martensite. Structural modification, hardness and the size and nature of the residual stress affecting the properties of the hardened dies, depend on the complex therom-mechanical processes occuring during machining.

Electrical discharge machining (EDM) may produce gradiently tempered surface layers containing annealed microstructures and carbides, although in some cases [96] additional fresh martensites have been reported for some die steels depending on their compositions. Cracks and residual stresses have also been reported in these layers due to cooling after heating caused by the melting action of the spark. The extent of damage depends on the

machining parameters employed e.g. rate of metal removal. However according to ASM [96] the metal surface after EDM generally possesses a lower endurance limit than obtained with conventional methods on the same steel. In addition a reduction in surface hardness was observed in this investigation (Figs. 59 a-d).

The surface integrity of a ground or turned die depends on machining conditions such as the type of grinding wheel (grit size, etc), or the wear land and the speed of cutter. Grinding at low speeds and at small depth of cut produces compressive residual stresses, whereas grinding at higher speeds and at larger depth of cut produces surface tensile stresses. In this investigation, the former condition was referred to as "fine ground" while the latter was called "rough ground". On the other hand, during turning it has been reported that the subsurface always contains tensile residual stresses, and that their size and depth increase with the size of the wear land of the cutter.

Generally fatigue failures invariably originate at the surface of a component. The ease with which it fails depends on the nature of the residual stress and the subsurface microstructional changes. Thus rough ground or turned (possessing tensile stresses) dies may be expected to fail easily due to the ease of crack initiation and propagation. In constrast fine ground dies (possessing compressive stresses) would have longer lives because of the suppression of crack nucleation. However, the change in hardness due to grinding and turning are indicated in figs 59 (a-d), and it can be seen that turning causes a greater reduction.

From the above discussion and the experimental results (table 3 and figs 58 (a-f)) it is clear that surface quality (roughness and integrity) plays an important role in the initial wear of hot forging dies. It is also clear that EDM would be expected to cause the highest initial wear while fine ground would cause the least wear.

5.3 PRACTICAL IMPLICATIONS AND REDUCTION OF DIE WEAR

Usually, wear investigation and analysis of a die in practice involves a number of stages which may include the selection of samples taken from the die followed by microscopic examination in order to establish the failure mechanisms. Thus for all practical purposes, the flat dies used in this investigation can be regarded as models of closed-dies used in drop forging practice. Consequently the results of this investigation can be regarded to represent what will be expected in practice. It is recognised, however, that mechanical stresses, scale formation, environmental conditions and the higher surface temperatures experienced by industrial dies [88]. may vary from job to job, and from one forging shop to the other. In any case these factors may only affect the wear processes (e.g. subsurface deformation, crack initiation and crack propagation) somewhat but they will not alter the mechanisms of wear. For example increased amount of scale formation due to large forgings in an industrial situation would not alter the mechanisms of abrasion and/or delamination, it may increase only the rate of wear.

Based on the results of this investigation and their discussion the likely methods of wear prevention or minimization can be summarised as follows:-

(1) The use of a suitable lubricant which would withstand the elevated temperature experienced during forging can considerably reduce surface traction (and hence die wear) by providing a low shear strength film between the die and slug (forging) asperities. This is particularly useful since interfacial frictional conditions may influence the plastic flow patterns of the deforming slug, which in turn controls the relative sliding motion between the slug and die.

(2) The use of solid solution hardening techniques to produce a die with a better surface hardness without introducing favourable crack nucleation sites in the die can minimize the ploughing action of

the tangential load during relative sliding between slug and die. Thus the use of an optimum fraction of very small and coherent particles (probably micron sizes) is desirable for good abrasion wear resistance. For example it may be necessary that the amount of each strong carbide forming elements in both BH13 and No.5 electem are reviewed. In addition thermo-chemical heat treatments like nitriding may be useful in this direction, as demonstrated by the results of this investigation. However, further modification of the process parameters may be needed to produce uniformly distributed nitrides in the case.

(3) Abrasive wear (and hence subsurface deformation) may be reduced by careful reduction of scale formed during heating of slugs in practice. This may be achieved by careful control of temperature and surface finish of slug, while trying to ensure optimum ductility for slug.

(4) In order to reduce wear by delamination, it is important that the basic processes leading to the formation of wear platelets are supressed. Increasing the surface hardness and decreasing friction coefficient would reduce subsurface deformation (due to plastic deformation and surface traction at each asperity) and hence crack initiation. On the other hand if the toughness of the die is increased to an optimum level without altering hardness then crack propagation rate can be minimized.

Diffusion and surface coatings may be used with advantage to reduce subsurface deformation, although their effectiveness would depend on their method of application and type. Plasma nitriding and Tufftriding may generally increase the surface hardness but increase the surface roughness (table 3). (It is recognised, however that the reports on

the effect of the former treatment on surface finish of BH13 has been rather varied [99]. This is probably due to the different surface preparation methods used by different investigators. However, there appears to be an agreement between the results obtained for the effect of Tufftriding in this investigation with those obtained by Child and Plumb [99]). Nonetheless in a lubricated forging situation, the valleys of the rougher die surfaces would act as reservoirs for lubricant to reduce friction. In addition the surface hardness together with the compressive stresses of their cases would normally suppress crack initiation and hence reduce wear by delamination. In a dry forging situation further improvement on wear resistance may be achieved by lowering friction coefficient and increasing surface hardness. This may be done by careful adjustment of the nitriding or Tufftriding parameters, e.g. pressure and temperature in the case of plasma nitriding.

Brush plated Co-Mo alloy and electrodeposited hard Cr may be used to improve surface hardness and to reduce friction which in turn will reduce subsurface deformation of both BH13 and Electem No.5 dies. The improved ductility confered by Co-Mo alloy on electem No.5 die steel may also increase the flow strength of the composite provided undersirable effects such as internal crack nucleation or propagation sites are minimized. Unfortunately Co-Mo alloy and hard Cr plates usually contain tensile stresses which can be detrimental in such applications as fatigue and sliding, since crack initiation and propagation could occur more easily. Therefore it may be desirable to use crack-free Cr or stress relieving Chromium (micro-cracked Cr) in place of hard Cr, while further modification of the Co-Mo alloy plating solution and its method of application may be needed to reduce tensile stresses. In addition composite coatings containing submicron particles (e.g. Co-Cr plus WC) may be suitable candidates.

Apart from surface modifications, delamination and indeed other types of wear mechanisms which occur during hot forging may be minimised by structural or subsurface modification. As identified in this investigation, the presence of an oxide glaze plus a compacted hard layer of fragmented wear particles can lead to reduced ploughing and adhesion. Thus it may be necessary to introduce an optimum quantity of high temperature oxidation resistant elements in the die matrix so that while they contribute to the loss of material they can also result in the formation of the glaze which may lead to wear reduction. In addition a sufficient amount of the essential elements should be added to the matrix so as to produce the hardface coating due to fragmentation.

The relationship between surface quality (roughness plus integrity) and wear is of frequent, practical concern to the design and production engineers in the development of forging dies. This concern is not only in relation to die performance but also in terms of design economics e.g. relative cost of various finishing operations. However, in this discussion only their direct effect on wear will be considered, since costing of the different machining methods is outside the scope of this investigation.

By using the appropriate machining technique die wear can be minimized. For example it can be seen from figs. 58(a-f) that irrespective of die material and the subsequent surface treatment, fine ground dies produced the least wear.

Finally, as part of an attempt to elucidate the physical and metallurgical paramenters that govern the wear of dies, it may be necessary to establish a mathematical model which can be used to predict wear. Thomas [3] has used multiple regression analysis to show that wear and composition can be related by an equation of the form:

$$\text{Wear} \triangleq K - \alpha_1 (M_o)^{\frac{1}{2}} - \alpha_2 (SS) - \alpha_3 (H)$$

Where K is a constant, α_1, α_2, α_3 are experimentally determined coefficients, (Mo) is the equivalent molybdenum content of the alloy, (SS) is the sum of the elements present in solid solution and H is the alloy hardness. This is of course a very general formula as it does not consider either the effects of Co, Cr and V additions or the number of forging cycles in detail. For example Holloway and Hopkins [100] have reported that Co additions may reduce wear by raising A_1 temperature, whilst in the present investigation it was observed that wear is a sensitive function of forging cycles. Thus it would appear that the cumulative increase in load due to successive forging plays an important role in determining wear rate (wear volume per forging cycle). Therefore, a modification of Thomas's equation to include a cumulative load term may enhance the prediction of wear in practice and hence its minimization.

Such a load term should account for the physics and physical metallurgy of the contacting slug and die surfaces. For example it should consider the shear strength and coefficient of friction between the sliding members.

5.4. THERMO-MECHANICAL PROPERTIES

5.4.1 THERMAL FATIGUE

The characteristics and nature of thermal cracks formed in dies during hot forging and die-casting were investigated over a wide range of temperatures and thermal cycles. The nature, shape and size of the cracks shown in figs. 60(a-d) are in agreeement with those reported by Still and Dennis [24]. The origin of such cracks has been discussed in the literature [97], and it is generally agreed that the cracks are of thermal origin. Once the cracks are formed they act as stress raisers and in some cases may lead to fatigue failures of dies.

Thus it is therefore likely that thermal cracks generated during hot forging propagate at right angle to the die surface and hence may accelerate the linking of polygonal cracks necessary for the formation of wear platelets by delamination.

The results of the thermal cycling tests (table 9) may be summarised as follows:-

1. Plasma nitriding and brush plated Co-Mo alloy appear to delay crack initiation and propagation in BH13 and electem No.5 die steels respectively.
2. Raising the number of thermal cycles and the testing temperature increased the crack density, although in some cases the cracks were limited to the coating or case.
3. Hardened and tempered, and Plasma nitrided BH13 showed better resistance to cracking than unplated and Co-Mo alloy plated No.5 die steel.

From the above it would seem that nitriding and Co-Mo alloy plating would minimize the risk of failure when BH13 or No.5 die steels are used in hot forging or die-casting applications. Also the number of forgings or shots produced by these applications respectively would influence the extent and degree of cracking.

It should be noted that since the normal industrial hot forging temperature is around 1250^{o}C, (compared with 1150^{o}C for this experimental condition), the surface temperature range induced on industrial dies may be expected to lie very close to the upper limit (e.g. between 650-750^{o}C) of the temperature range investigated. Thus for the same die materials and surface treatments the simulated thermal cycling test results for flat dies above may be extended with some confidence to shaped dies.

5.4.2. NOTCH TOUGHNESS

The results presented in section 4.3.2. and discussed here relate mainly to the treatment conditions chosen for this investigation. Care must therefore be exercised in applying the results to a general situation. This is because most engineering materials exhibit fracture mechanisms that are governed by their microstructure and the stress systems to which they are subjected in practice. Under a specified stress system the fracture mechanism of a component may be of a brittle or ductile nature. Very often such modes of failure may be observed on a macroscopic scale depending on the material. Microscipically, however, far more details concerning the features of the fractured surface may be revealed depending on the magnification employed. Classification of these modes therefore becomes difficult in practice since a single component may undergo varying fracture mechanisms in succession.

ASM[96] classifies fracture mechanisms into two groups - intergrannular and transgranular. In the present investigation only transgranular mechanisms were observed - void coalescence, tearing, cleavage - either acting separately or in conjunction with one another.

5.4.2.1. Ni - P ALLOY PLATED NO. 5 DIE STEEL

With the exception of the hardened and tempered testpieces, all the other fractured surfaces (surface treated) exhibited cleavage near the notch root. Figs. (68, 69) provide views of different areas in an electroless Ni-P alloy plated testpiece exhibiting fracture features that are typical of cleavage. It is apparent that the fracture plane changes orientation from grain to grain. Fig. 68 is a good example where a change in orientation occured between adjacent grains. The river patterns, which represent steps between local cleavage facets of the same cleavage plane, are well defined. They appear to run from left to right, thus indicating

that the notch corresponds to the top of the fractograph.

The upper portion of the fracture surface, shown in fig 69, is a result of cleavage while the lower portion is a result of fracture by microvoid coalesence. Again it would appear that although equiaxed dimples predominate, certain grain orientations near the top of the fractographic (i.e. nearer the notch root) were unfavourable for ductile fracture by microvoid coalesence, and so local cleavage occurred.

Scanning views of ductile fracture areas, generally further away from the notch root are shown in figs. 70 9a-c). The region shown in fig. 70. contains several shallow dimples. At higher magnification, in an adjacent area, stringer troughs were observed. Examples are shown in fig. 70(b-c) In fig. 70c an elongated sulphide inclusion (stringer) can be seen to be at the foot of its trough.

5.4.2.2. CO-MO ALLOY PLATED NO. 5 DIE STEEL

Figs. 66 (a,b) show some cleavage facets near the notch root, while figs 67 (a,b) illustrate intermingled brittle-cleavage and dimples. Fig 67b is an enlarged view of the central region in Fig.67a. At about the top left hand corner of the fractograph is a cleavage region with slightly developed rivers patterns of cleavage steps.

On other fractographs, not shown for the sake of economy of space, regions containing fine dimples on the walls of larger ones were observed.

5.4.2.3. HARD CR. PLATED NO.5 DIE STEEL

Fig. 61 shows a mixed fracture mechanism of micro void coalescence and cleavage some distance away from the notch. Successive cleavage steps and dimples can be seen, the latter being in the majority.

Fig. 62 shows several shallow and moderately large dimples in the steel subsurface, Fig. 63, on the other hand shows a mixture of dimples and a region of tearing. Fig. 64 (a-c) shows three views, at increasing

magnifications, of another area on the fracture surface which exhibits features that are typical of cleavage plus tearing. Fig. 64a shows part of the notch edge, while Figs. 64(b , c) show extensive regions of cleavage adjacent to two tear ridges which are typified by their sharpness.

Fig. 65 (a,b) shows a region taken ahead of the tear ridges in fig. 64. In this region ductile failure by micro void coalescence alone occured. Some of the inclusions that nucleated some of the dimples can be seen.

5.4.2.4 MICRO-CRACKED Cr PLATED NO. 5 DIE STEEL

Figs. 72 (a-c) are three magnification views of the steel core, illustrating extensive regions of microvoid coalescence. Fig.72a, shows a void opening out as a crack, while Fig. 72b is an enlarged view of the areas surrounding the crack. However, Fig.72c reveals the inclusion associated with the void in Fig.72a.

Figs. 73(a-b) show the brittle plus ductile nature of the composite near the notch.

5.4.2.5. HARDENED AND TEMPERED NO.5 DIE STEEL

Mainly ductile (dimple) areas were observed, slight brittle patches as in Figs.71 (a-b).

It should be pointed out that many of the fractographs described above indicate the same mechanisms, but very often in different areas of the same testpieces. They have all been included to illustrate.

(1) that a mixture of failure mechanisms can occur in a die steel under a given load and surface treatment condition.

(2) that the surface treatments may alter the initial fracture mode particularly near the notch.

5.4.2.6. G E N E R A L

The results portrayed in the fractographs above can not be directly used in discussing the quantitative results of the notch-toughness values obtained in

this investigation. For example, although cleavage cracks may originate at locations where crystallographic slip is prevented (e.g. at inclusions or second phase particles) cleavage simply describes a mechanism. It may not be indicative of the relative ductility of the steel. The relative ductility and toughness can be influenced by grain boundary and inclusion-matrix strengths. Therefore the relative ductility and toughness of a surface treated testpiece cannot be compared with those of the hardened and tempered testpiece, on the basis of the occurrence of a mechanism.

The quantitative results presented in table 10 represents notch toughness only and therefore do not quantify material behaviour or resistance during crack propagation. However the results indicates that all the surface treatments reduced the toughness of the hardened and tempered steel.

In the case of the coated testpieces there appeared to be a correlation between hardness and the toughness result. The susceptibility of a testpiece to brittle fracture increased with coating hardness.

5.4.3 DUCTILITY

The results presented in table 11 were partly disucssed in section 4.3.3. In general, the results indicate that there is probably a relationship between the effective ductility of the composite and the residual stresses of the coating, although it has an inverse relationship with hardnesss.

If the result of static slow bend tests are compared with those of cyclic bend fatigue tests (section 5.4.4), it can be seen that the surface coatings improved the ductility of the hardened tempered testpiece in the same way as they reduced its fatigue strength. Thus the higher the improvement in ductility the lower was the reduction in fatigue strength (Fig.74).

Therefore it appears that the internal stresses together with the diverse structural variations of the coatings may affect initiation and propagation

the most deletenions effect on fatigue as shown in fig. 74. That is, the reduction in fatigue strength of the hardened and tempered steel by brush plated Co-Mo alloy is less that those due to micro-cracked Cr and hard Cr.

Ni-P alloy, on the other hand, has a fine grained lamellar structure plus a small amount of tensile stress [64]. In addition the ductility which it confers on No.5 die steel is much higher than that due to brush plated Co-Mo alloy. Hence it can be expected to reduce fatigue strength less than Co-Mo alloy.

Macroscopic examination revealed cheveron marks converging towards specific region of the surface in all surface treated and untreated testpieces. Figs. 94 (a,b) show the typical mating fracture surfaces of a Co-Mo alloy plated testpiece. It can be seen that fatigue was initiated at the surface.

Microscopic examination using S.E.M. also confirmed that failure was initiated at the surface Figs (80, 83, 89, 77). S.E.M. x-ray analysis of suspected sites of crack nucleation did not suggest the presence of inclusions or second-phase particles. Therefore it appears that the initiation sites may have been extrusions or intrusions formed on the surface peaks or valleys during the fatigue process.

The fatigue failure mechanisms were rather mixed, but always of the trans-grannlar type as observed on impact testpieces. These mechanisms include void coalescence, cleavage and brittle failure. Evidence of void coalescence is shown in figs (76, 87, 88 and 90), while brittle failure and ductile failure are illustrated in figs. (77, 80, 81, 85, 89 and 91) and figs. (87, 89, 84, 79) respectively. In addition tearing and brittle-cleavage features observed on the fracture surfaces are shown in fig. (82) and figs (78 and 86) respectively.

of cracks during static slow bending of these composites. The higher the internal tensile stress (i.e. low fatigue strength) in the deposits the easier it may be for the initiation of multiple cracks which resulted in the failure of the composites at their maximum bend angles (Fig.12).

5.4.4. MECHANICAL FATIGUE

The fatigue data (table 12) and its analysis of variance, have already been partly discussed in sections (4.3.4 to 4.3.4.2). The mean fatigue strength estimates for the surface treated testpieces were shown to affect that of the hardened and tempered testpieces differently.

It was indicated that the causes of variation other than the assignable ones, may be due to internal stresses, microstructural differences in coatings, and the effective surface finish due to each treatment. Because of the lack of adequate knowledge of the structure of some of the coatings, the structural effects of these treatments will be omitted in the discussion below. In addition, on close examination of fig.74 it can be seen that the effect of surface finish (if any) was probably negligible. For example it can be seen that even though Cr plated parts generally have a better surface finish than parts brush plated with Co-Mo alloy, the former resulted in a higher reduction of the strength of unplated Electem No.5 die steel. Thus the most probable cause of variation is that die to internal redsidual stresses.

A large tensile residual stress can be deterimental in such applications as fatigue, since crack nucleation and crack growth may occur more readily. In contrast, a compressive residual stress may be beneficial only if no subsurface modification or phase transformations occured during post hardening and tempering treatment.

Hard Cr is usually associated with a higher internal tensile strees than micro-cracked Cr and Ni-P alloy [68]. Therefore it would be expected to have

However a discussion of these mechanisms will be omitted since they have already been discussed in section 5.4.2. In addition the processes leading to their occurrence are well documented in standard texts.

6.0 CONCLUSIONS

1. Optical and S.E.M. examination of worn die surfaces and subsurfaces has yielded information sufficient for the construction of a detailed description of the failure mechanisms of hardened and tempered, and surface treated BH13 and No.5 die steels during drop forging.

   (a) During hot forging several wear mechanisms are in operation, namely, erosion, abrasion, oxidation and delamination. These may either act separately or together. However, based on information gathered from the worn die surfaces, subsurfaces and wear debris the latter alternative appears to be favoured.

   (b) It was observed that apart from the oxidative wear component, the deformation-type wear (delamination) was the dominant mode of failure. This is because both erosive and abrasive mechanisms do not directly account for the platelike morphology of the wear particles observed. Experimental evidence suggest that the formation of these platelets involves either a two or three step process depending on the surface and subsurface state of the steel or composite before forging. This process may occur sequentially in the order of subsurface deformation, void or crack initiation and crack propagation.

   (c) It is concluded that while oxidation and thermal fatigue may accelerate crack propagation, both erosion and abrasion appear to accelerate subsurface deformation and hence wear.

   (d) During forging a smooth oxide glaze is formed over a hard metallic layer. This glaze consists of a compacted layer of oxides of almost all the elements in the die steel, while the hard layer is essentially formed by fragmentation of metallic platelets as

a result of intermittent frictional contact between slugs and die surface. It is thought that both layers may not only minimize metal-to-metal adhesion but also reduce the surface traction which in turn affects wear volume.

(e) Dies used for cold forging showed similar wear patterns to those used for hot forgings.

2. Die wear is considerably affected by both its surface and subsurface conditions.

(a) In general, surface treated and untreated BH13 dies showed less wear than their No.5 counterparts. Wear occurred in the following increasing order of merit - unplated electem No.5, unnitrided BH13, electem No.5 brush plated with a Co-Mo alloy, electem No.5 plated with electrodeposited hard cr, Tufftrided BH13 and plasma nitrided BH13 die insert.

(b) Initial wear increased with increasing roughness.

(c) The effect of roughness on initial wear appears to overshadow that due to the surface integrity generated by the machining parameters and the type of machining employed. Thus, although electrical discharge machining may produce less subsurface deformation than rough turning, it seems that for both die materials (and irrespective of surface treatment) the effect of roughness predominates. This is probably due to the easy removal of primary asperities by the high loads experienced during forging. Therefore it is concluded that the effect of surface integrity may be limited to steady state wear.

(d) Wear (weight loss and volume) is a sensitive function of forging cycles.

3. Surface treatments (plasma nitriding and bush plated Co-Mo alloy) can delay thermal fatigue cracking of BH13 and electem No.5 die steel

at surface temperatures below 750°C. This temperature range is relevant to both hot forging of steel and die casting of aluminium, zinc and magnesium. However, the nature of the cracks observed were very different from the polygonal cracks present on die surfaces and subsurfaces after hot forging. They ran perpendicular to the surface similar to grinding cracks.

4. Semi-range S-N curves for three-point bend fatigue conditions were established for Electem No.5 in the hardened and tempered condition, and after coating with electrodeposited hard and micro-cracked Cr, brush plated Co-Mo alloy and electroless Ni-P alloy. It was shown that for the specific conditions chosen, that the mean fatigue strength of the basis steel was reduced markedly by all the surface treatments in the decreasing order of electroless Ni-P alloy brush plated Co-Mo alloy, micro-cracked and hard Cr. It is apparent that the presence of internal tensile stresses in the platings adversely affected the fatigue strength of the hardened and tempered testpieces. A metallographic study of the fracture surfaces indicated that although the overall fatigue failure mechanisms were mixed, failure was initiated at the surface in all cases. At room temperature the mechanisms observed included, brittle and ductile failure, cleavage void coalescence. The latter being often associated with MnS inclusions.

5. Standard Izod impact test results qualitatively indicated reductions in toughness of between 1.7% to 12.3% for similar coatings to those applied to fatigue testpieces above. It is thought that this reduction was due to the brittle nature of the coating. Mixed failure mechanisms similar to those experienced with the three-point bend fatigue testpieces were observed. (It is worth noting that wear particle formation, due to cyclic impact loading during forging, occurred as a result of void coalescence at inclusions).

6. Finally results of the slow bend tests indicated that for similar testpieces to those used on the cyclic bend fatigue tests, at the limiting bend angle, multiple cracks were present. This showed that even under static loading, failure of these composites started at the surface by a process of multiple crack formation. Furthermore, all except hard Cr treatments improved ductility of the composite. Improvement was in the increasing order of electrodess Ni-P, Brush plated Co-Mo alloy and electrodeposited micro-cracked Cr.

7. SUGGESTION FOR FURTHER WORK

In order to explain fully the differences that exist in wear volume of both die steels due to surface treatment, further work is needed to quantify variables such as friction coefficients, particle-matrix bond strength, crack growth rates and hot hardness. It is recommended that these variables should be measured under conditions that are simulative of drop forging. If this gap in the knowledge can be bridged thus a more comprehensive explanation can be made to account for the differences in wear volume due to surface treatment, and also for the difference in volume which would be expected for closed-die forging.

8.0 ACKNOWLEDGEMENTS

The author wishes to thank his supervisors Mr. H.C. CHILD and Dr. J. K. DENNIS - for the interest and understanding which they demonstrated throughout the entire period of this project. The author also wishes to thank Mr. S. J. CROSS and other members of the technical staff in the machine shop of the Department of Metallurgy for their unfaltering assistance throughout this project. Finally the author wishes to thank Mrs. E. A. BURGISS for her speed in typing.

LIST OF REFERENCES

1. DENNIS J. K. and STILL F.A. The use of electrodeposited cobalt alloy coatings to enhance the wear resistance of hot forging dies. COBALT 1975 1, 17-28.

2. ASTON J.L., HOPKINS, A.D. and KIRKHAM, K.E. The wear testing of hot working die steels. Metallurgia and Metal forming Feb. 1972, 39, 46-49.

3. THOMAS A. D.F.R.A. Metal Treatment, 1965, vol 32, P.47.

4. LANCASTER, J.K. The influence of temperature on metallic wear Proc. Phys. Soc. London Section B, 70 (1957) 112-118.

5. LANCASTER J.K. T.I.M.F. winter 1978, 4, 145

6. ARCHARD J. Temperature of rubbing surfaces, Wear 2, 6 1959, 438-455.

7. BOWDEN F.P. and TABOR D. The friction and lubricant of solids, Oxford University press, London 1958.

8. TABOR, D. Friction and Wear. Proceedings int. Symp. on Lub. and Wear. McCUCHAM publishing, Berkeley and California 1965.

9. LANDHEER, D AND ZAAT, J.H. Wear 27, 1. 1974, 129-145.

10. HIRST, W. Engineering, 8 No.209, May 1970, 477-480.

11. WELCH, N.C. The dry wear of steels. Phil. Trans. Roy Soc. 1965 257 31-70.

12. ARCHARD J. Contact and rubbing of flat surfaces. J. app. phys. 24 (8) 1953 981-988.

13. RABINOWICZ E. Influence of surface energy on friction and wear phenomenon. J. app. 32 (8) 1961 1440 - 1444.

14. KRUSCHOV M.M. Resistance of metals to wear by abrasion, as related to hardness. Proc - Int. Conf. on Lub. and Wear. Inst. of Mech. Eng. London 1957.

15. KRUSCHOV and BABICHEV M.A. Resistance to abrasive wear of structurally inhomogeneous materials. Friction and wear in Mechinery 12 1958, 5

16. SERPIK N.M. and KANTOR M.M. Investigation on the wear of steel during rubbing against loose powder abrasive. Friction and Wear in Machinery 1965, 19. 28.

17. POPOV V.S. and Nagoray P.L. Influence of carbide on the abrasive wear resistance of alloys. Russian casting Prod. 1969 8, 337.

18. RABINOWICZ E. Friction and Wear of Materials, Wiley N.Y.1965.

19. SARKAR A.D. Wear of Metals. Pergamon Press Oxford 1976.

20. BADSE LARSEN J. The abrasion resistance of some hardened and tempered carbon steels. Trans. Metall. Soc. A.I.M.E. 236 1966 1461.

21. RICHARDSON R.C.D. "Wear of metals by relatively soft abrasives". Wear, (1968), 11, 245.

22. SUH, N.P. The delamination theory of wear. Wear 25 1973 111 - 124.

23. JOHNSON and MELLOR. "Indenting and Forging with a flat Punch", in Plasticity for Mechanical Engineers Oct. 1961.

24. STILL F.A. and DENNIS J.K. Electrodeposited wear-resistant coatings for hot forging dies. Metallurgia and Metal forming. 44 Jan. 1977 10 - 21.

25. JAHANMIR S. and SUH N.P. Mechanics of subsurface void nucleation in delamination wear. Wear, 44 1977 17-38.

26. D. KUHLMANN - Wilsdorf "Dislocation" in "Physical Metallurgy" edited by R.W. Cahn. Second revised edition 1970.

27. GURLAND J. and PLATEAU J. The mechanism of ductile rupture of metals containing inclusions. Trans. Am. Soc. Met., 56 1963 442-454.

28. TANAKA K, Mori T, Nakamura T, cavity formation at the interface of a spherical inclusion in a plastically deformed matrix, Philos. Mag., 21 1970 267-279.

29. ZENNER C. J. applied Phys. 1951, 22, 372.

30. STROT A.N. The formation of cracks as a result of plastic flow (2 papers). Proc. Roy. Soc. London Ser. A, 223 1954, 404-414 232 1955 548-560.

31. ASHBY M.F. Work hardening of dispersion- hardened crystals Philos. Mag., 14 1956.

32. BROWN L.M. and STOBBS W.M. The work-hardening of copper silica, Philos., Mag., 23 1971 1185-1233.

33. McCLINLOCK F.A., On the mechanics of fracture from inclusions. In Ductility Am Soc. Met. Metals Park, Ohio, 1968 255-277.

34. MIEDEMA, A.R., Surface energies of solid metals. Z. Metallkunde 69 1978, No.5 287-292.

35. DRAPAL S. Hutn, Listy, 1969 24, 12, 850 (R.D.D.T.11986).

36. GOLDSCHMDT H.J. J.I.S.I., 185, 1957, 297.

37. KUO, K. J.I.S.I. 1963, 173, 363

38. SMITH E., and NUTTING J. J.I.S.I. 187, 1957, 314

39. MuKherjee T. Relation between structure and Mechanics Properties in tempered chromium steels. Ph.D thesis Sheffield University 1967.

40. Field M., Khales J., and Cammett J.T., A review of the measuring methods for surface integrity, C.I.R.P. 21 2, 1972, 219.

41. Goddard J. and Wilman H., Wear, Vol.5, 1962, 114-135.

42. Queener C.A, Smith T.C., Mitchel W.L., Transient wear of machine parts. Wear, vol. 8, 1965, 391-400.

43. Rowe G.W., Kaliszer H, Trmal G, and Cotter A., Running-in of plane bearings. Wear, 34 1975 1-14

44. Abrahamson E.P., Jahanmir S., and Suh N.P. The effect of surface finish on the wear of sliding surfaces, C.I.R.P. Ann. Int. Inst. Prod. Eng. Res., 24 1975 513-514.

45. Ewing J.A. and Humphrey J.C.W., Phil. Trans. Roy. soc. 1903 200A, 241.

46. Gough H.J. and Hanson D., Proc. soc. 1923, 104A 538.

47. Gough H.J., Proc. ASTM 1933, 33, 3

48. GOUGH H.J. and SOPWITH D.G., J. Inst. of metals 1935 56,55

49. Taylor G.I., and ELAM, C.F., Proc. Roy. Soc 1925, 108A, 28

50. TAYLOR G.I., Proc. Roy Soc. (1927) 116A, 16.

51. QROWAN, E. Proc. Roy. Soc. 1939, 171A, 70.

52. WOOD W.A., BULL. Inst. of metals 1955, 3, 5.

53. THOMPSON. N, WADSWORTH N.J. and LOUAT N., Philos. Mag. 1956.

54. FORSYTH P.J.E., The physical basis of Metal Fatigue - Blackie and Sons, London 1969.

55. COTTRELL A.H. and Hull D., Proc. Roy. Soc. 1957, 242A, 211.

56. CHILD, H.C. The heat treatment of Tools and dies - a review of present status and future trends. The Metals Society, 1977, Book No. 185, 291-321.

57. MANSON, S.S. Nat Advis. Cttee. Aerenautics, Publ. (TN2933) 1953.

58. NORTHCOLT L. and BARON, H., J.I.S.I., 184, 385, (1956).

59. BARON and BLOOMFIELD in "Thermal Fatigue" by Glenny, E., Metallurgical Review 6, No. 24, 1961.

60. BETTERIDGE, W. "The Nimonic Alloys". 1959. London Edward Arnold.

61. BENGTSSON K.I. Metal Treatment, 1957, 28, 227.

62. CANNING HANDBOOK on electroplating - 21st edition (1970).

63. EDENHOFER, B., Physical and Metallurgical aspects of ionitriding heat treatments of metals. part 1. 1974, 1, 23-28.

64. BALDWIN and SUCH T.E., Trans. I.M.F. 46, 73 (1968)

65. PARKER and SHAH - Plating 58, (3), 230, (1971)

66. HAMMOND R.A.F. and WILLIAMS C., Metallurgical Review, 5, 165 1960

67. STILL F.A., DENNIS J.K., LODGE J.K., "The application of wear resistant coatings to hot forging dies." Proc. 2nd Int. Conf. on tool steels for hot working, st. Etienne France, Dec. 1977.

68. DENNIS J.K. and SUCH T.E., Nickel and Chromium plating Butterworth and Co. (publishers) Ltd.

69. INWOOD B.C. and GARWOOD A.E., Electroplated Coatings for wear resistance, Trib. Int., 11, 2, 1978 113-119.

70. JONES D., Application of wear resistant coatings by the brush plating technique. August 1978. Aston University internal report.

71. RUBINSTEIN, M. "A metal Put-on Tool for aircraft maintenance". Selectrons Ltd., Commercial Literature.

72. DENNIS J.K., LODGE K.J. and STILL Fi.A., Properties of Co-Mo and Co-W electrodeposits. Trans, I.M.F., 55, 1, 1977 17-33.

73. EDENHOFER B., Physical and Metallurgical aspects of ionitriding Heat treatment of metals, 2, 59-67, 1974.

74. TIBBETTS G.G., Role of Nitrogen atoms in ionitriding Applied phys. 44 1973, 11, 5072 - 5073.

75. JONES, C.K., STURGES, D.J. Hudis M., and Martin, S.W. Ion-Nitriding Paper presented at the conference of the heat treatment Joint Committee 'Heat treatment 73, Dec. 12.

76. JONES, C.K. and MARTIN S.W., 'Ionitriding - a modern case hardening technique'. Modern Machine Shop 1973, 9, 89-95.

77. JONES, B.K. and MARTIN, J.W., The metals technology Nov. (1977) 520-523.

78. SUTTON, H., Met., Technology, 1936, 2, 89.

79. BARDGETT, W.E., Met., Technology, 10, 87, 1943.

80. EDENOFFER, B., Production Ionitriding. Metal progress 1-9, 3976, 38-42.

81. ASTLEY P., Tufftride - a new development reduces treatment costs and process toxicity. Heat treatment of metals 2, 1975, 51-54.

82. ASTON, J.L. and MUIR, A.R. J.I.S.I. 207, 2, Feb. 1969.

83. EWERE, I., 'Plasma surface treatment", MSc thesis Aston University, 1975.

84. STEVEN G, AND CATLIN J.P., Journal of Materials, 1, No. 2, 293 June, 1966.

85. Sharp, W.F., Wear, 32, 1975, 315-325.

86. LIOTARD, H., ESTAMPE, Forge et Boulonnerie 1963.

87. BAYLISS, R.N.,PHD. thesis Fracture toughness of Electem No.5 die steel. Aston University 1974.

88. E. THOLANDER - Report to Euroforge Tech. Comm 1967.

89. STOTT and WOOD, G.C., The influence of oxides on the friction and

90. TRASOV L.P., Effect of grinding conditions and residual stress on the fatigue strength of hardened steels, American Machinist, 101 1957, 72.

91. SUH, N.P. An overview of the delamination theory of wear. Wear 4 (1977) 1-16

92. CROWTHER, P. Heat treatment of forging dies dies by the salt bath method. Metallurgia and Metal forming. Nov.499 1977.

93. FURUICHI, H. and YOSHIDA H. The formation of a thick hardened surface layer by repeated frictional contact. Wear, 50.

94. GARBAR I.I. and SKORININ J.V. Wear, 51, (1978) 327-336.

95. Inmar M.S. and Kohn E.M. Wear, 17, (1971) 33.

96. ASM metals handbook, 10 eight edition. page 504-505.

97. Glenny, E., "Thermal Fatigue" Metallurgical Review 6, No.24 1961, page 387.

98. ELLIOTT, T.L. Tribology international, April, 1978, 121.

99. CHILD, H.C. Plumb, S.A. Survey of the effect of heat treatment of dies on the dimensions and surface conditions S.R.C. project No. B/RG/96299, June 1978.

100. HOLLOWAY, J.R., and HOPKINS, A.D. COBALT, No.50, 3 1971.

101. K.E. KIRKHAM, MSc. Thesis Aston University 1968.

APPENDIX 1: CALCULATION OF WEAR VOLUME

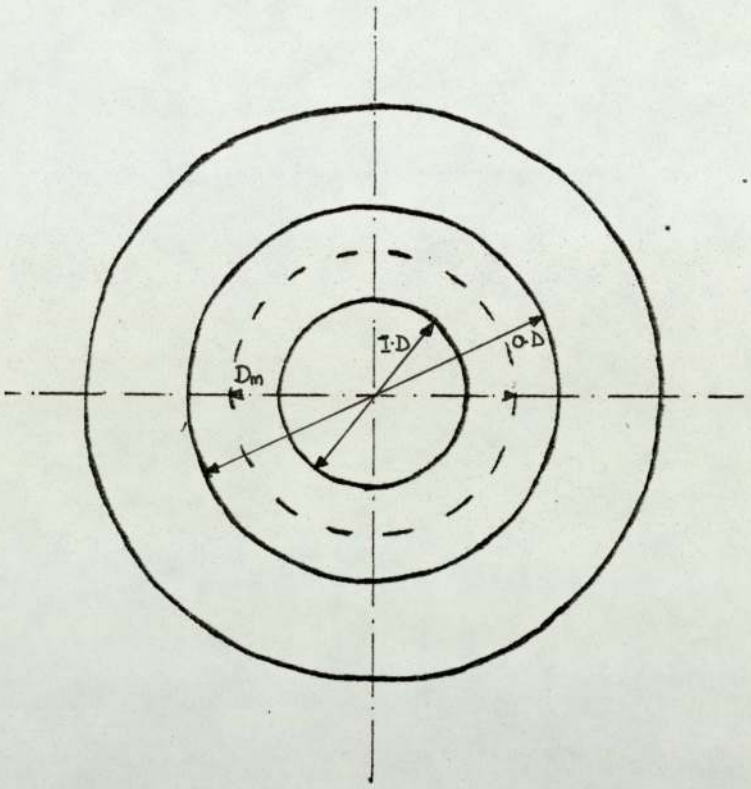

Mean diameter, Dm (imaginary circle) $= \dfrac{\text{O.D.} - \text{I.D.}}{2} + \text{I.D.}$

Half - Circumference $\dfrac{\Pi Dm}{2}$

Wear Trace area (A) $= \dfrac{\text{Planimeter Vernier Value x Calibration factor in}^2}{\text{Magnification (HM x VM)}}$

Inner Volume V_1 $\dfrac{\Pi Dm}{2} \times A_i \times 6.4516 \quad Cm^3$

Mean Volume, V $\sum_1^n V_i$

where i = 1, 2, 3 ..... n^{th} nos. of diameter traced.

BEJE

EX3 COSEC= 1.0353 ABS COEFF

SYSTEM FEK 1 0 KV

ANALYSIS NO. 1

	KV	MEASURED	Z	ABS	FLU	COR	TRUE	OXIDES	
FE	20.0	69.870	0.944	1.003	1.000	1.056	73.808	FE203	105.525

6 ITERATIONS TOTAL OXIDES 105.525

APPENDIX 2: COMPUTER ANALYSIS OF OXIDE FORMED ON SLUG BEFORE FORGING

A P E N D I X 3

THERMAL CYCLING APPARATUS AND PROCEDURE

The apparatus (Fig. 93) consists of an air cylinder, an H.F. Coil, a ceramic tube and a perforated hollow cylinder which lets in air during the cooling half of a cycle. The air cylinder which is normally attached to the experimental forging press (to enable simulation of forging cycle) controls the upward and downward stroke of the soldered testpiece via the ceramic tube. The testpiece has a smaller diameter peg machined at one of its end to enable attachment to the tube through a thread pin.

Before testing the required temperature and cycling time were set using controls on the press and H.F. unit. Chromel alumel thermocouples were used in conjunction with an X-Y graph recorder to monitor operating temperature.

The testpieces were heat treated, ground and surface treated (plasma nitrided, brush Co-Mo alloy plated) as described in section 3.

Appendix 4 : Analysis of Variance of Fatigue Data

Table 13a* : FATIGUE STRENGTH ESTIMATES AT 10^6 CYCLES FROM STEP LOADING DATA

Treatment / Test No	Hardened and Tempered (A)	Electroless Ni-P Alloy (B)	Brush Plated Co-Mo Alloy (C)	Bath Plated Micro-Cracked Cr (D)	Bath Plated Hard Cr (E)
1	.960	.811	.691	.652	.580
2	.914	.767	.668	.668	.587
3	.958	.852	.689	.637	.576
4	.929	.819	.637	.580	.612
5	.852	.845	.725	.673	.530
6	.942	.772	.714	.652	.585
7	.894	.840	.717	.594	.521

* All strength values in the table should be multiplied by 10^3 N/mm^2

Assumptions:

(1) the means of samples size n-7, drawn from each population (treatment) may be assumed to be normally distributed. Literature survey indicates that the region of the S-N Curve investigated is always normally distributed.

(2) the true mean of each treatment may be assumed to be equal, otherwise a difference exists, and the variability between the five mean values would estimate the true variance between the treatments (σm^2)

Null hypothesis (Ho) : That there is no real difference between treatments

ie $Ho \equiv \sigma m^2 = 0$

Replace entries (x) in table 13a by x^1, where $x^1 = (x - 0.894)\ 100$

Table 13b

TEST NO	A	B	C	D	E
1	6.6	-8.3	-20.3	-24.2	-31.4
2	2.0	-12.7	-22.6	-22.6	-30.7
3	6.4	-4.2	-20.5	-25.7	-31.8
4	3.5	-7.5	-25.7	-31.4	-28.2

Table 13b

TEST NO	A	B	C	D	E
5	-5.2	-4.9	-16.9	-22.1	-26.4
6	4.8	-12.2	-18.0	-24.2	-30.9
7	0.0	-5.4	-17.7	-30.0	-37.3
Σx^1	18.1	-55.2	-141.7	-180.2	-226.7
$(\Sigma x^1)^2$	327.61	3047.04	20078.89	32472.04	51392.69
$\Sigma (x^1)^2$	150.85	506.08	2926.49	4716.9	7405.99

Let K = the number of treatments
n = the number of observations per treatment
Kn = the total number of observations
x_i = and individual number of observations i = 1, 2, ... Kn
T_j = the total of the j^{th} treatment, j = 1, 2, ... K
G_2 = the grand total, i e total over Kn observations
G/Kn = the correction factor

Table 13c

Source of Variation	Degrees of Freedom (d f)	Sum of Squares (s s)	Mean Square (m s)
Between Treatments	K-1	$1/n \Sigma T^2 - \frac{G^2}{Kn}$	$1/n \Sigma T^2 - \frac{G^2}{Kn}$ (K-1)
Within Treatments (error)	K(n-1)	$\Sigma x^2 - \frac{1}{n}\Sigma T^2$	$\Sigma x - \frac{1}{n}\Sigma T^2$ (n-1)k
TOTAL	Kn-1	$\Sigma x^2 - \frac{G^2}{Kn}$	

Using the entries for x^1 in table 15b we have

$G = -585.7$; $G^2/Kn = 9801.27$

$\Sigma (x)^2 - \frac{G^2}{Kn} = 5905.04$; $\frac{1}{n} \Sigma T^2 - \frac{G^2}{Kn} = 5529.91$

Table 13d

Source of Variation	d.f.	ss	ms
Between Treatments	4	5529.91	1382.48
Within Treatments	30	375.13	12.50

Observed $F_{ratio\ (\phi_1,\ \phi_2)} = \frac{1382.48}{12.50} = 110.6,\ (4,\ 30)$

From the tables, $F_{0.01}\ (4,30) = 4.02$. That is there is a probability of 0.01 of an F_{ratio} of at least 4.02 arising by chance. The probability of value as high as 110.6 arising by chance is therefore very small and H_o can be rejected with confidence.

Thus it can be concluded that the surface coatings affect the fatigue strength of hardened and tempered Electem No 5 die steel differently.

In order to determine the extent of their bais with respect to each other, 95% confidence limits were calculated as follows using:-

$$\bar{x}^1 \pm \text{to } .025\ (\phi = \phi_o)\ \frac{\sigma_o}{n}$$

where $\phi_o = \phi_2 = 30$

For the hardened and tempered testpieces (A) we have;

$$2.59 \pm 2.042\ \frac{12.5}{7}$$ as the confidence limits

Reverting to the oringinal units

$$x = \bar{x}^1 + 0894\ ;\ \sigma_o^2 = 12.5 \times 10^{-4}$$

$$x = 0.0259 + 0.894$$

$$= 0.9199$$

Hence the actual confidence limits may be expressed as

$$0.9199 \pm 2.042\ \frac{12.5}{7}\ 10^{-2}$$

14 .893 to .947

or 893 to 947 N/mm^2

Similarly the 95% confidence limits due to the coatings

(B) are : 787.9 to 842.4 N/mm^2

(C) are : 664.3 to 718.9 N/mm^2

(D) are : 609.3 to 663.9 N/mm^2

(E) are : 542.9 to 597.4 N/mm^2

Table 1 : COMPOSITIONS OF DIE STEELS

STEEL	Chemical Analysis								
	C	Mn	P	Si	S	Ni	Cr	Mo	V
BH13	.35	.30	-	1.0	-	-	5	1.5	1.0
ELECTEM No 5	.55	.65	.04 (Max)	.3 (Max)	.04 (Max)	1.5	.65	.26	-

Table 2 : TESTS TO ESTABLISH WEAR MECHANISMS

SPECIMEN			TESTS AND DIE ANALYSIS							
No	TYPE	SURFACE CONDITION	FORGING		SEM	WEAR MEASUREMENT	SECTIONING	X-RAY DIFF	EPMA	MICRO-HARDNESS
			HOT	COLD						
A1	No 5	Brush Plated Co-Mo alloy	-	10 Cycles	✓	✓	✓	-	-	✓
A2	✓	✓	-	100 Cycles	✓	✓	✓	-	-	✓
A3	✓	Unplated Ground	-	10 Cycles	✓	✓	✓	-	-	✓
A4	✓	✓	-	100 Cycles	✓	✓	✓	-	-	✓
A5	✓	Brush Plated Co-Mo Bot	10 Cycles	-	✓	✓	✓	-	-	✓
A6	✓	✓(Top)	10 Cycles	-	✓	✓	✓	-		✓
A7	✓	✓(Bot)	100 Cycles	-	✓	✓	✓	-	-	✓
A8	✓	✓(Top)	100 Cycles	-	✓	✓	✓	-		✓

Table 2 : Continued

SPECIMEN			TESTS AND DIE ANALYSIS							
No	TYPE	SURFACE CONDITION	FORGING		SEM	WEAR MEASUREMENT	SECTIONING	X-RAY DIFF	EPMA	MICRO-HARDNESS
			HOT	COLD						
A9	✓	Unplated	1 Cycle	-	✓	✓	✓	-	-	✓
A10	✓	✓	2 Cycle	-	✓	✓	✓	-	-	✓
A11	✓	✓	5 Cycle	-	✓	✓	✓	-	-	✓
A12	✓	✓	7 Cycle	-	✓	✓	✓	-	-	✓
A13	✓	✓	10 Cycle	-	✓	✓	✓	✓	-	✓
A14	✓	✓	100 Cycle	-	✓	✓	✓	-	-	✓
A15	✓	✓ (Bot)	1000 Cycles	-	✓	✓	✓	-		✓
A16	✓	✓ (Top)	1000 Cycles	-	✓	✓	✓	✓	-	✓

Table 2 : Continued

SPECIMEN			TESTS AND DIE ANALYSIS							
No	TYPE	SURFACE CONDITION	FORGING		SEM	WEAR MEASUREMENT	SECTIONING	X-RAY DIFF	EPMA	MICRO-HARDNESS
			HOT	COLD						
A17	BH13	Un-nitrided	100 Cycles	-	✓	✓	✓	-	-	✓
A18	✓	✓(Bot)	1000 Cycles	-	✓	✓	✓	-	-	✓
A19	✓	✓(Top)	1000 Cycles	-	✓	✓	✓	✓	✓	✓
A20	✓	Plasma Nitrided	1 Cycle	-	✓	✓	✓	-	-	✓
A21	✓	✓	2 Cycles	-	✓	✓	✓	-	-	✓
A22	✓	✓	5 Cycles	-	✓	✓	✓	-	-	✓
A23	✓	✓	7 Cycles	-	✓	✓	✓	-	-	✓
A24	✓	✓	10 Cycles	-	✓	✓	✓	✓	-	✓

Table 2 : Continued

SPECIMEN			TESTS AND DIE ANALYSIS							
No	TYPE	SURFACE CONDITION	FORGING		SEM	WEAR MEASUREMENT	SECTIONING	X-RAY DIFF	EPMA	MICRO-HARDNESS
			HOT	COLD						
A25	✓	✓(Bot)	100 Cycles	-	✓	✓	✓	-	-	✓
A26	✓	✓(Top)	100 Cycles	-	✓	✓	✓	✓	✓	✓
A27*	BH13	Plasma Nitrided	100 Cycles	-	✓	✓	✓	✓	-	✓
A28	✓	✓(Bot)	1000 Cycles	-	✓	✓	✓	✓	-	✓
A29	✓	✓(Top)	1000 Cycles	-	✓	✓	✓	-	✓	✓
A30*	No 5	Brush Plated Co-Mo alloy	100 Cycles	-	✓	✓	✓	✓	-	✓
A31	✓	Ground	NOT FORGED		✓	-	✓	✓	-	-
A32	✓	Ground and H/Treated	✓		✓	-	✓	✓	-	-

Table 2 : Continued

SPECIMEN			TESTS AND DIE ANALYSIS						
No	TYPE	SURFACE CONDITION	FORGING		SEM	WEAR MEASUREMENT	SECTIONING	X-RAY DIFF	EPMA	MICRO-HARDNESS
			HOT	COLD						
A33	BH13	Ground	✓		✓	-	✓	✓	-	-
A34		Ground and H/Treated	✓		✓	-	✓	✓	-	-

* used for identification of oxide glaze

Table 3 : EFFECTS OF SURFACE TOPOGRAPHY AND INTEGRITY ON WEAR

MATERIAL		SURFACE CONDITION		SURFACE QUALITY		WEAR INDEX
No 1	TYPE	MACHINE OPERATION	SURFACE TREATMENT	ROUGHNESS (CLA) (m)	INTEGRITY (DEFORMATION INDEX)	
B1	BH13	EDM	Hardened and Tempered	4.50	2	2
B2		EDM	Tufftrided	4.70	2	5
B3		EDM	Plasma Nitrided	4.55	2	6
B4		RT	Hardened and Tempered	0.70	1	8
B5		RT	Tufftrided	1.80	1	11
B6		RT	Plasma Nitrided	1.20	1	12
B7		RG	Hardened and Tempered	0.49	3	14
B8		RG	Tufftrided	1.00	3	17
B9		RG	Plasma Nitrided	0.60	3	18
B10		FG	Hardened and Tempered	0.10	4	20
B11		FG	Tufftrided	0.58	4	23
B12		FG	Plasma Nitrided	0.24	4	24
B13		EDM	Hardened and Tempered	4.0	2	1
B14		EDM	Co-Mo Alloy Plated	3.57	2	3
B15		EDM	Hard Cr Plated	2.95	2	4

Table 3 continued

MATERIAL		SURFACE CONDITION		SURFACE QUALITY		WEAR INDEX
No 1	TYPE	MACHINE OPERATION	SURFACE TREATMENT	ROUGHNESS (CLA) (m)	INTEGRITY (DEFORMATION INDEX)	
B16	No 5	RT	Hardened and Tempered	0.84	1	7
B17		RT	Co-Mo Alloy Plated	0.54	1	9
B18		RT	Hard Cr Plated	0.40	1	10
B19		RG	Hardened and Tempered	0.70	3	13
B20		RG	Co-Mo Alloy Plated	0.52	3	15
B21		RG	Hard Cr Plated	0.32	3	16
B22		FG	Hardened and Tempered	0.35	4	19
B23		FG	Co-Mo Alloy Plated	0.30	4	21
B24		FG	Hard Cr Plated	0.20	4	22

EDM : Electrical Discharge Machining
RT : Rough Turn
RG : Rough Ground
FG : Fine Ground

Both the deformation and wear indices are arbitrary but an increase in their values reflects less deformation and wear respectively.
+ Deformation index represent hardness value before surface treatment.

Table 4 : TYPICAL HARDNESS VARIATION ACROSS SURFACE TREATED TESTPIECES USED FOR MECHANICAL TESTS

TREATMENT / REGION OF MEASUREMENT	CORRECTED DEPTH* BELOW SURFACE (μm)	HARD Cr	MICRO-CRACKED Cr	ELECTROLESS Ni-P ALLOY	BRUSH PLATED Co-Mo ALLOY
		HARDNESS			
COATING	Edge	1010	960	511	570
	8	1000	940	509	568
	12	950	893	498	561
SUBSTRATE	Interface	409	409	410	411
	20	409	408	408	409
	40	405	406	405	405
	60	401	406	400	401
	80	400	403	400	401

* Method of depth correction was discussed previously in the section relating to Wear.

Table 5a : OXIDE/PHASE GLAZE ON PLASMA NITRIDED H13 DIE AFTER 100 CYCLES FORGING

MATERIAL	X-RAY DATA			
	2θ	d-Spacing	Miller's Indices	Oxide/Phase
H13 Die	16.0	2.5180	311	γ'-Fe_2O_3
	16.3	2.4744	104	V_4O_7
	18.4	2.192	111	γ'-(Fe_4N) 4.25c
	18.8	2.1459	012	MoD_2
	19.0	2.1230	223	Cr_5O_{12}
	19.7	2.0484	202	Cr_2O_3
	21.3	1.8965	200	γ'-(Fe_4N) 4.25c
	25.4	1.594	102	ε-Fe_3-Fe_2N
	26.9	1.507		FeO
	27.6	1.469	100	ε-Fe_2O_3
	30.4	1.3368	403	MoO_2
	31.8	1.2791	533	Fe_3O_4
	33.0	1.2340	220	Cr_2O_3
	34.8	1.169	200	ε-Fe_3N-Fe_2N
	36.3	1.125	134	Cr_2O_3
	38.3	1.0658	133	(Fe_2N) 120
	40.8	1.0199	321	Likely γ'-(Fe_4N) 4.25c
	43.3	0.9491	400	$\gamma' Fe_2N$

Table 5b : OXIDE-PHASE GLAZE ON TUFFTRIDED H13 DIE AFTER 100 CYCLES FORGING

MATERIAL	X-RAY DATA			
	2θ	d-Spacing	Miller's Indices	Oxide/Phase
BH13	16	2.5180	311	$\gamma' Fe_2O_3$
	16.5	2.443	$\bar{2}11$, $\bar{2}02$	$(VO_2)z$
	18.8	2.1459	002	MoO_2
	19	2.123	223	Cr_5O_{12}
	19.7	2.0488	202	Cr_2O_3 (10R)
	20	2.0179	-	Likely Cr_3O_8
	25.3	1.6005	311	(Fe_2N) 120
	25.5	1.5870	100	Σ-Fe_2O_3
	26.9	1.507	-	FeO
	27.7	1.4641	214	Cr_2O_3 (10R)
	31.8	1.2791	533	Fe_3O_4
	33.2	1.2268	306, 036	Fe_2O_3
	35.2	1.1586	200	Σ-Fe_3N-Fe_2N
	38.4	1.0652	133	(Fe_2N) 120
	43.3	0.9491	400	γ'-Fe_4N

θ BRAGG ANGLE

- Not available in Reference Table

Table 5c : OXIDE-GLAZE ON UNPLATED ELECTEM No 5 DIE AFTER FORGING 100 CYCLES

MATERIAL	X-RAY DATA			
	2θ	d-Spacing	Miller's Indices	Oxide
Electron No 5 Die Steel		2.5181	311	γ-Fe_2O_3
		2.1459	012	MoO_2
		1.8155	024	(Cr_2O_3) 10R
		1.7001	422	γ-Fe_2O_3
		1.6110	511, 333	γ-Fe_2O_3
		1.5410	310	MoO_2
		1.5124	-	Likely Cr_3O_8
		1.3210	620	γ-Fe_2O_3
		1.2872	113	MoO_2
		1.2792	533	Fe_3O_4
		1.2339	220	Cr_2O_3
		1.1250	134	Cr_2O_3
		1.0891	553, 731	γ-Fe_2O_3

- indicates "not available"

Table 6 : HARDNESS VARIATION ACROSS AND BELOW WORN DIE SURFACE

MATERIAL		CORRECTED DEPTH (μm)	MICRO HARDNESS (VPN)			
TYPE	CONDITION		A+	B+	AVERAGE	REGION
No 5 Die Steel	100 Cycles Co-Mo Alloy Plated	EDGE	650	640	645	HWR
		35	455	425	440	
		60	430	430	435	
		80	430	434	432	
		EDGE	560	560	560	LWR
		35	428	436	432	
		45	430	434	432	
		75	430	430	430	
	1000 Cycles Unplated	EDGE	475	485	480	HWR
		20	446	434	440	
		55	432	432	432	
		70	430	434	432	
		EDGE	465	465	465	LWR
		20	429	435	432	
		43	428	436	432	
		65	428	428	428	
	100 Cycles Unplated	EDGE	430	430	430	LWR HWR
		15	426	434	430	
		25	426	430	428	
		40	428	432	430	

A and B represent the average of two readings[+]

Table 6 : Continued

MATERIAL		CORRECTED DEPTH ON TAPER SECTION (μm)	MICRO HARDNESS VPN			REGION OF MEASUREMENT
TYPE	CONDITION		A	B	AVERAGE	
BH13	100 Cycles Plasma Nitrided	Edge	1385	1395	1390	HWR
		50	1200	1200	1200	
		80	1115	1105	1110	
		115	1030	1030	1030	
		150	826	834	830	
		175	600	600	600	
		250	589	591	590	
		325	589	591	590	
		Edge	1215	1225	1220	LWR
		50	1140	1140	1140	
		75	690	710	700	
		125	589	591	590	
		160	580	580	580	
		200	575	585	580	
	100 Cycles Plasma Nitrided	Edge	1324	1336	1330	HWR
		75	1065	1075	1070	
		125	925	915	920	
		150	700	700	700	
		170	600	580	590	
		220	590	580	585	
		Edge	1181	1199	1190	LWR
		38	1036	1044	1040	
		100	791	809	800	
		137	585	595	590	
		192	580	580	580	

Table 6 : Continued

MATERIAL		CORRECTED DEPTH ON TAPER SECTION (μm)	MICRO HARDNESS VPN			REGION OF MEASUREMENT
TYPE	CONDITION		A	B	AVERAGE	
BH13 Die Steel	100 Cycles Unnitrided	Edge	635	645	640	HWR
		38	630	620	625	
		25	595	585	590	
		150	590	590	590	
		200	590	590	590	
		Edge	584	596	590	LWR
		50	586	594	590	
		75	589	591	590	
		125	590	590	590	

MATERIAL		DISTANCE FROM DIE CENTRE (μm)	MICROHARDNESS (VPN)		
TYPE	CONDITION		A	B	AVERAGE
No 5 Die Steel	100 Cycles Co-Mo Plated	20	556	554	555
		1000	555	555	555
		2000	558	562	560
		3000	558	562	560
		4000	561	559	560
		6000	576	584	580
		7900	596	614	605
		9000	600	600	600
		10000	645	645	645

Table 6 : Continued

MATERIAL		DISTANCE FROM DIE CENTRE (μm)	MICROHARDNESS (VPN)		
TYPE	CONDITION		A	B	AVERAGE
No.5	1000 Cycles Unplated	20	435	435	435
		750	429	431	430
		2000	431	439	435
		3000	438	442	440
		4500	440	440	440
		6500	447	453	450
		7400	462	468	465
		8550	484	486	485
		9550	470	470	470
		10150	479	481	480
No 5 Die Steel	100 Cycles Unplated	20	422	438	430
		500	420	440	430
		1500	420	440	430
		3500	434	430	432
		5500	440	440	440
		7000	455	445	450
		8500	455	455	455
		10000	455	455	455
BH13 Die Steel	100 Cycles Unnitrided	150	587	593	590
		450	591	593	592
		1100	591	593	592
		1800	582	580	581
		3150	605	595	600
		5000	610	590	600
		7700	610	590	600
		9100	675	585	680
		10150	670	670	670

Table 6 : Continued

MATERIAL		DISTANCE FROM DIE CENTRE (μm)	MICROHARDNESS (VPN)		
TYPE	CONDITION		A	B	AVERAGE
BH13	100 Cycles Nitrided	150	1185	1195	1190
		600	1182	1198	1190
		1000	1200	1200	1200
		1500	1200	1220	1210
		2500	1185	1175	1180
		3450	1175	1175	1175
		4400	1215	1225	1220
		5600	1225	1235	1230
		7000	1270	1270	1270
		8500	1325	1335	1330
		9000	1330	1330	1330
	1000 Cycles Nitrided	150	1215	1225	1220
		650	1220	1220	1220
		2000	1205	1215	1210
		3200	1179	1181	1180
		4250	1175	1185	1180
		4900	1218	1222	1220
		6100	1300	1300	1300
		7550	1335	1345	1340
		9050	1338	1342	1340
		11000	1390	1390	1390

Table 7 : X-RAY DIFFRACTION ANALYSIS FOR RETAINED AUSTENITE

MATERIAL	BRAGG'S 2θ	d-SPACING	HKL	PHASE[X]
No 5 Electem Die Steel Hardened and Tempered	19.80	2.065	011	α
	20.00	2.045	111	γ
	20.30	2.015	110	α
	27.30	1.5091	002	Likely α
	28.85	1.4257	020	α
	35.2	1.1735	121	α
	40.7	1.0208	222	γ
	41.2	1.0089	220	α
	46.0	0.9085	031	α
	46.35	0.9021	310	α
	55.4	0.7638	231	α
No 5 Electem Hardened and Tempered Still and Dennis [24]	19.8	2.065	011	α
	20.0	2.045	111	γ
	28.8	1.4274	020	α
	35.2	1.1735	121	α
	40.7	1.0208	222	γ
	41.2	1.0089	220	α
	47.8	0.880	400	γ
	50.7	0.8292	222	α
	54.8	0.7714	132	α
	55.4	0.7638	231	α
H13 Hardened and Tempered	19.8	2.065	011	α
	20.3	2.015	110	α
	28.4	1.4472	020	Likely α
	28.85	1.4251	021	α
	35.20	1.1735	121	α
	40.80	1.985	222	γ
	41.2	1.0089	220	α
	46.3	0.9029	310	α
	55.4	0.7638	231	α

α Martensite
γ Austenite
θ Bragg's angle

Table 8 : WEAR SCAR MEASUREMENT +

SPECIMEN		POSITIONS OF DIAMETER												AVERAGE VOLUME $Cm^3 \times 10^{-3}$
No	TYPE	1	2	3	4	5	6	7	8	9	10	11	12	
A1	No 5	.163	.042	.059	.055	-	.036	.060	.062	.042	-	-	-	.065
A2	"	.194	.086	.195	.136	.118	.146	.019	.113	.162	-	.119	-	.136
A3	"	.299	.223	.226	.122	.188	.233	.270	.227	.173	.143	.210	.243	.213
A4	"	.472	.413	.253	.358	.286	.474	.364	.323	-	-	.255	-	.355
A5	"	.021	.019	.018	.010	.029	.029	-	-	-	.027	.031	.012	.022
A6	"	.033	.021	.015	.011	.013	.013	.012	.009	-	-	.010	-	.015
A7	"	.162	.171	.201	.141	.220	.181	.194	.156	.191	.162	.191	.171	.178
A8	"	.142	.112	.146	.168	.130	-	-	.146	.154	.150	-	-	.144
A9	"	-	-	-	-	-	-	-	-	-	-	-	-	-
A10	"	-	-	-	-	-	-	-	-	-	-	-	-	-
A11	"	-	-	-	-	-	-	-	-	-	-	-	-	-
A12	"	-	-	-	-	-	-	-	-	-	-	-	-	-
A13	"	-	-	-	-	-	-	-	-	-	-	-	-	-
A14	"	.377	.394	.410	.610	-	.353	.421	-	-	.367	-	-	.419
A15	"	3.510	4.2.2	4.584	4.862	4.145	4.549	-	4.200	-	4.12	3.895	-	4.231
A16	"	3.605	3.223	3.712	3.414	3.661	3.571	-	3.617	3.312	3.341	-	3.710	3.517
A17	H13	-	-	.231	.195	.156	.187	.156	.243	-	.196	.215	.243	.202
A18	"	1.061	0.996	1.146	1.224	1.031	1.081	1.240	1.310	1.012	0.994	1.351	1.062	1.126

Table 8 : Continued

SPECIMEN		POSITIONS OF DIAMETER												AVERAGE VOLUME
No	TYPE	1	2	3	4	5	6	7	8	9	10	11	12	$Cm^3 \times 10^{-3}$
A19	H13	0.896	0.363	0.556	.457	.729	.901	.671	.662	.912	.443	.899	.512	0.669
A20	"	-	-	-	-	-	-	-	-	-	-	-	-	-
A21	"	-	-	-	-	-	-	-	-	-	-	-	-	-
A22	"	-	-	-	-	-	-	-	-	-	-	-	-	-
A23	"	-	-	-	-	-	-	-	-	-	-	-	-	-
A24	"	-	-	-	-	-	-	-	-	-	-	-	-	-
A25	"	.094	.123	.084	.142	.084	-	.131	.123	.117	-	.150	-	0.116
A26	"	.089	.035	.051	.059	.024	.051	.072	.035	.048	-	.101	.066	0.057
A27*	"	.094	.119	.138	.124	.091	.131	.148	.087	-	.091	-	-	0.114
A28	"	.678	.695	.474	.516	.503	.671	.489	.264	.411	.412	.431	.301	0.487
A29	"	.480	.351	.321	.401	.440	.391	.281	.300	.312	.451	.451	-	0.380
A30*	No 5	-	-	-	-	.184	.179	.191	.163	.174	.183	.180	.199	0.182

* used for identification of oxide glaze

\- indicates scar volume could not be measured using talylin trace method

\+ see table 2 for specimen treatment conditions

\÷ all values in the table are in $10^{-3} cm^3$

Table 9 : THERMAL CYCLING TEST RESULTS

MATERIAL		CONDITION BEFORE TEST		TEST CONDITION		OBSERVATION
No	TYPE	HEAT TREATMENT and MACHINGING	SURFACE TREATMENT	TEMPERATURE ^{O}C	NO OF CYCLES	
C1	BH13 Die Steel	See Section 3	A	500	100	Uncracked
C2			B	"	"	"
C3			A	"	500	"
C4			B	"	"	"
C5			A	"	1000	Case Slightly Cracked
C6			B	"	1000	Severely Cracked in Comparison with (A)
C7			A	65.0	"	Case Cracked, But Substrate Not Penetrated
C8			B	"	"	Crack Density Increased
C9			A	"	2000	Crack Slightly Penetrated Substrate
C10			B	"	"	Crack Density Amd Depth of Penetration Increased
C11			A	750	1000	Substrate Was Severely Cracked
C12			B	"	"	Far More Cracks Than Its Nitrided Counterpart
C13			A	"	1500	Crack Density in Case Was Increased
C14			B	"	"	More Cracks Were Observed Than After 1000 Cycles

Table 9 : Continued

MATERIAL		CONDITION BEFORE TEST		TEST CONDITION		OBSERVATION
No	TYPE	HEAT TREATMENT and MACHINING	SURFACE TREATMENT	TEMPERATURE ^{o}C	NO OF CYCLES	
C15	B13		A	750	2000	Crack Density and Depth of Penetration Of Substrate Increased
C16			A	"	"	Very Much the Same Crack Density and Penetration As After 1500 Cycles

A : Plasma Nitriding
B : Unnitrided

Table 9 : Continued

MATERIAL		CONDITION BEFORE TEST		TEST CONDITION		OBSERVATION
No	TYPE	HEAT TREATMENT and MACHINING	SURFACE TREATMENT	TEMPERATURE ^{o}C	NO OF CYCLES	
C17	No 5 Die Steel	See Section 3	E	500	100	Uncracked
C18			F	500	100	Uncracked
C19			E	"	500	Slightly Cracked
C20			F	"	500	Severely Cracked in Comparison With It's Costed Counterpart
C21			E	"	1000	Coating Was Cracked and Substrate Slightly Penetrated
C22			F	"	"	Severely Cracked
C23			E	650	1000	Coating Was Cracked, and Substrate Further Penetrated
C24			F	"	1000	Crack Intensity and Density Increased
C25			E	"	2000	Crack Density Was Increased
C26			F	"	"	Severely Cracked As At 1000 Cycles
C27			E	750	1000	Far More Cracks Than Observed After 2000 Cycles At $650^{o}C$
C28			F	"	"	Crack Density And Intensity Appeared To Have Substantially Increased

Table 9 : Continued

MATERIAL		CONDITION BEFORE TEST		TEST CONDITION		OBSERVATION
No	TYPE	HEAT TREATMENT and MACHINING	SURFACE TREATMENT	TEMPERATURE ^{O}C	NO OF CYCLES	
C29			E	750	1500	Crack Density And Intensity Was Increased
C30			F	"	"	Crack Density And Intensity Was Similar To Its Coated Counterparts
C31	No.5		E	"	2000	Crack Density And Intensity Was Similar To That Observed After 1500 Cycles at $750^{O}C$
C32			F	"	"	Crack Density And Intensity Was Similar To That Observed After 1000 Cycles

E : Brush Plated Co-Mo Alloy
F : Unplated

Table 10 : NOTCH TOUGHNESS RESULTS AT ROOM TEMPERATURE

SUBSTRATE			SURFACE CONDITION BEFORE TESTING					NOTCH TOUGHNESS (JOULES)		COMMENT
No	TYPE	CONDITION BEFORE MACHINING	TREATMENT	COATING OR SURFACE		NOTCH DEPTH (mm)		READING	AVERAGE	
				THICKNESS (μm)	HARDNESS (VPN)	BEFORE TREATMENT	AFTER TREATMENT			
I1	No 5 die steel	originally forged, reduced and annealed at 830°C for 2 hrs to BS131 Parts 1-3 Specification	Hardened and Tempered only	-	400-411	3.302	3.302	15.8, 16, 16.2	16.0	Similar to result obtained by Bayliss
I2			Electroless Ni-P alloy Plated	12.5	498-511	3.327	2.540	16.0, 15.8, 15.8	15.73	1.7% reduction
I3			Brush Plated Co-Mo alloy	12.5	561-570	3.302	3.319	15.4, 15.1, 15.0	15.17	5.3% reduction
I4			Electrodeposited Micro-Cracked Cr	12.5	950-1010	3.302	2.771	14.8, 14.8, 14.6		7.9% reduction

Table 10 : Continued

SUBSTRATE			SURFACE CONDITION BEFORE TESTING					NOTCH TOUGHNESS (JOULES)		COMMENT
No	TYPE	CONDITION BEFORE MACHINING	TREATMENT	COATING OR SURFACE		NOTCH DEPTH (mm)		READING	AVERAGE	
				THICKNESS (μm)	HARDNESS (VPN)	BEFORE TREATMENT	AFTER TREATMENT			
I5		No.5	Electrodeposited Hard Cr	12.5	950-1010	3.302	3.288	14.2, 14.0, 13.9	14.03	12.3% reduction

Heat Treatment : Quenched in oil from 830^{o}C and tempered at 480^{o}C

An Avery machine was used

Table 11 : SLOW BEND TEST RESULTS AT ROOM TEMPERATURE

SURFACE TREATMENT	BEND ANGLE (α) AT MAX. APPLIED LOAD TO FAILURE				HARDNESS* (VPN)		COMMENTS
	A	B	C	AVERAGE % CHANGE (α)	CASE/ COATING	CORE	
Hardened and Tempered	(45) 6.21+	(54) 6.51	(50) 6.18	NIL	NIL	400-411	Limited Cracking Failed by Cracking
Electroless Ni-P Alloy	(62) 7.21	(60) 6.86	(50) 6.86	22.2	498-511	400-410	Multiple Cracks Observed Improved Ductility
Brush Plated Co-Mo Alloy	(48) 6.61	(60) 7.02	(56) 6.80	10.1	561-570	401-411	Multiple Cracks Observed Improved Ductility
Electrodeposited Micro-Cracked Chromium	(46) 6.5	(54.5) 6.4	(51) 6.5	1.7	893-960	403-409	Multiple Cracks Observed Improved Ductility
Electrodeposited Hard Chromium	(50) 6.08	(46) 6.07	(47) 6.20	4.0	950-1010	400-409	Multiple Cracks Observed Reduced Ductility

( ) represent max. bend angle (α) in degrees

+ Load values are in KN

Table 12 : FATIGUE DATA AT ROOM TEMPERATURE

TESTPIECE+	(MAXIMUM) APPLIED LOAD (N)	DISTANCE OF FRACTURE SURFACE FROM ONE END (mm)	STRESS (N/mm^2)		FATIGUE LIFE (N) (KILOCYCLES)	MEAN FATIGUE STRENGTH
			NOMINAL STRESS (S)	ESTIMATED FATIGUE STRENGTH		
PF1	9600	55	981	960	150	921.3
PF2	8400	60	936	914	316	"
PF3	8800	60	981	958	170	"
PF4	8400	61	952	929	296	"
PF5	7600	62	875	852	944	"
PF6	8000	65	966	942	266	"
PF7	8800	56	915	894	490	"

+ Hardened and tempered fatigue test pieces
Assumed stress ratio (R) = 0.3
Pre-assigned No. of cycles = 10^6 Span length = 130mm
Load was increased in steps of 5%, starting at 2KN

Table 12 : Continued

TESTPIECE+	(MAXIMUM) APPLIED LOAD (N)	DISTANCE OF FRACTURE SURFACE FROM ONE END (mm)	STRESS (N/mm^2)		FATIGUE LIFE (Ni) KILOCYCLES	MEAN FATIGUE STRENGTH (N/mm^2)
			NOMINAL (S)	ESTIMATED FATIGUE STRENGTH		
NPF1	7600	59.0	826	811	447	815 (11.5% reduction on untreated testpieces)
NPF2	7200	59.0	786	767	631	
NPF3	7600	62.0	875	852	168	
NPF4	7200	63.0	842	819	246	
NPF5	7200	65.0	869	845	188	
NPF6	6800	63.0	796	772	794	
NPF7	7200	64.6	859	840	251	

Electroless Ni-P alloy plated test pieces

Table 12 : Continued

TESTPIECE+	(MAXIMUM) APPLIED LOAD (N)	DISTANCE OF FRACTURE SURFACE FROM ONE END (mm)	STRESS (N/mm^2)		FATIGUE LIFE (N) KILOCYCLES	MEAN FATIGUE STRENGTH N/mm^2
			NOMINAL (S)	ESTIMATED FATIGUE STRENGTH		
CMF1	6400	60.0	713	691	159	691.5 (24.9% reduction on untreated testpiece)
CMF2	6000	62.0	691	668	955	
CMF3	6000	64.0	713	689	211	
CMF4	5600	63.5	660	637	977	
CMF5	6800	63.0	749	725	240	
CMF6	6800	62.0	783	714	178	
CMF7	6400	63.5	755	717	171	

+ Brush plated Co-Mo alloy fatigue testpieces

Table 12 : Continued

TESTPIECE+	(MAXIMUM) APPLIED LOAD (N)	DISTANCE OF FRACTURE SURFACE FROM ONE END (mm)	STRESS (N/mm^2)		FATIGUE LIFE (Ni) KILOCYCLES	MEAN FATIGUE STRENGTH N/mm^2
			NOMINAL (S)	ESTIMATED FATIGUE STRENGTH		
MCF1	5600	65.0	676	652	331	636.6 (30.9% reduction on untreated testpiece)
MCF2	6000	62.0	691	668	191	
MCF3	5600	63.5	585	637	437	
MCF4	5200	62.5	604	580	299	
MCF5	6000	62.5	696	673	164	
MCF6	5600	65.0	676	652	257	
MCF7	5200	64.0	542	594	617	

+ Micro cracked chromium plated testpieces

Table 12 : Continued

TESTPIECE+	(MAXIMUM) APPLIED LOAD (N)	DISTANCE OF FRACTURE SURFACE FROM ONE END (mm)	STRESS (N/mm^2)		FATIGUE LIFE N	MEAN FATIGUE STRENGTH (N/mm^2)
			NOMINAL (S)	ESTIMATE FATIGUE STRENGTH (Ni)		
HCF1	5200	62.5	595	580	490	
HCF2	5600	58.0	603	581	227	
HCF3	5200	62.0	599	576	359	570.1
HCF4	5600	61.0	634	612	159	38.1% reduction on untreated testpiece
HCF5	4800	62.0	553	530	457	
HCF6	5200	63.0	608	585	174	
HCF7	4800	61.0	544	521	596	

+ Hard chromium plated testpieces

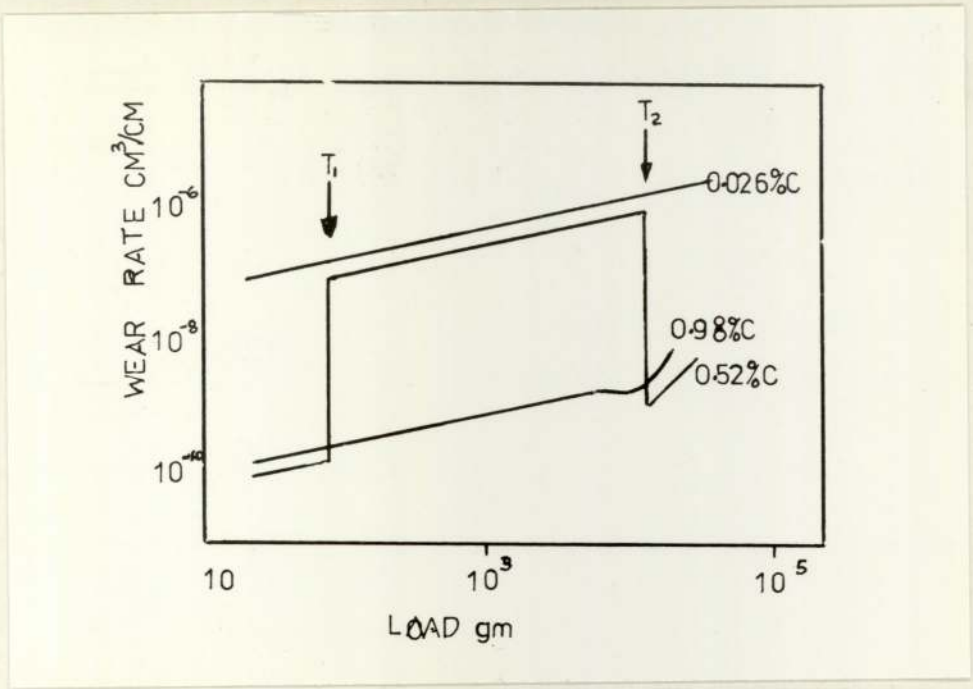

Fig. 1 Transition wear behaviour of steels.

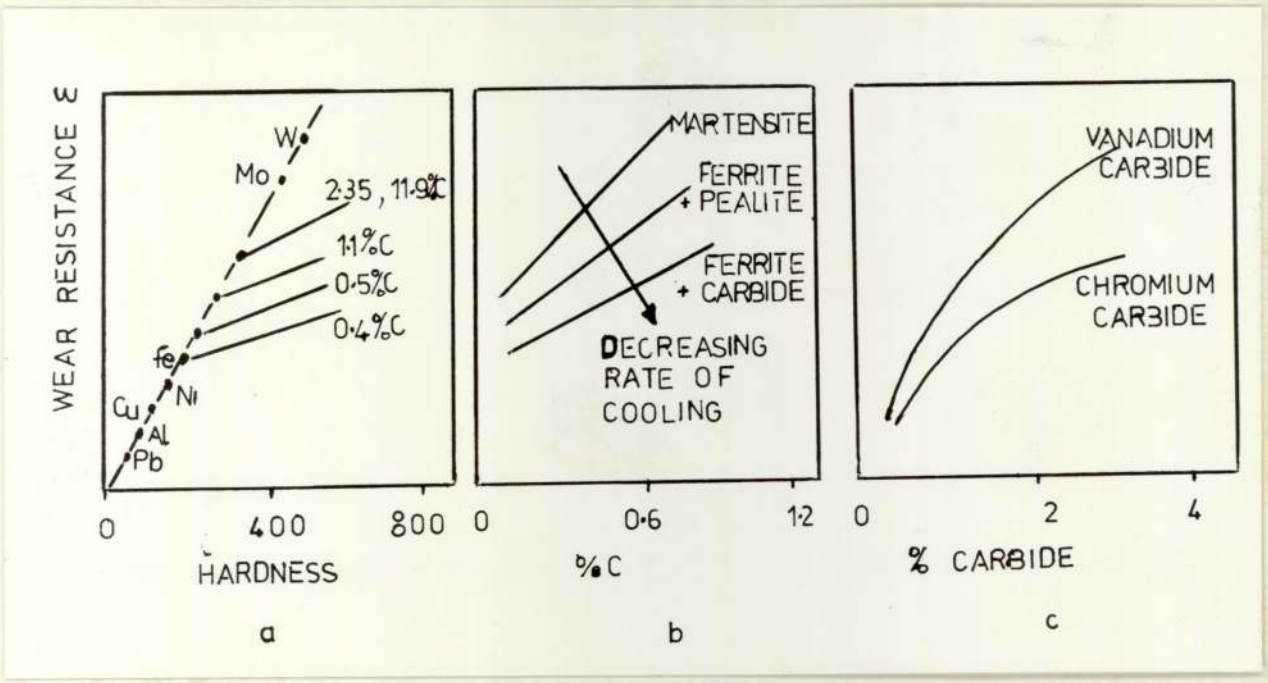

Fig. 2 Wear resistance as a function of

(a) hardness
(b) % carbon in steel
(c) % carbides in steel

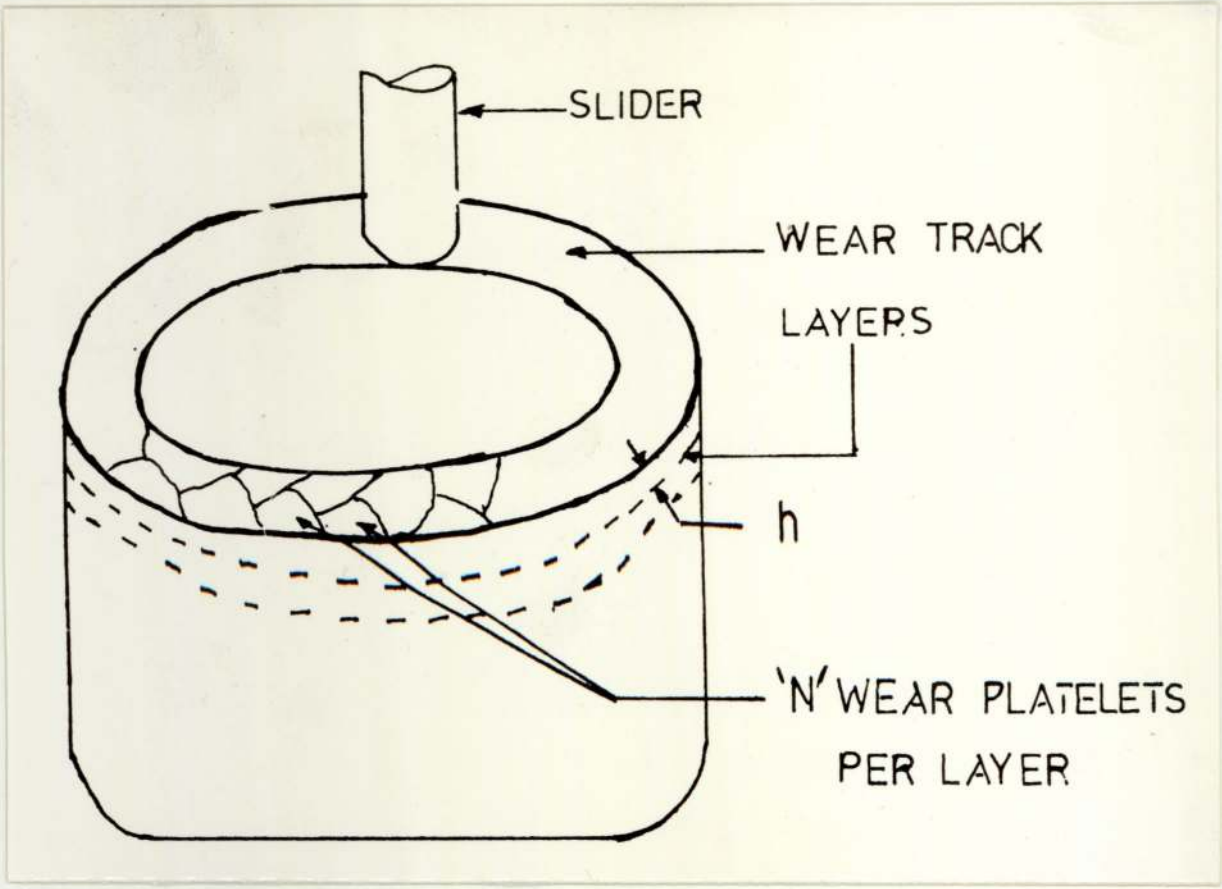

Fig. 3 Schematic representation of delamination wear model

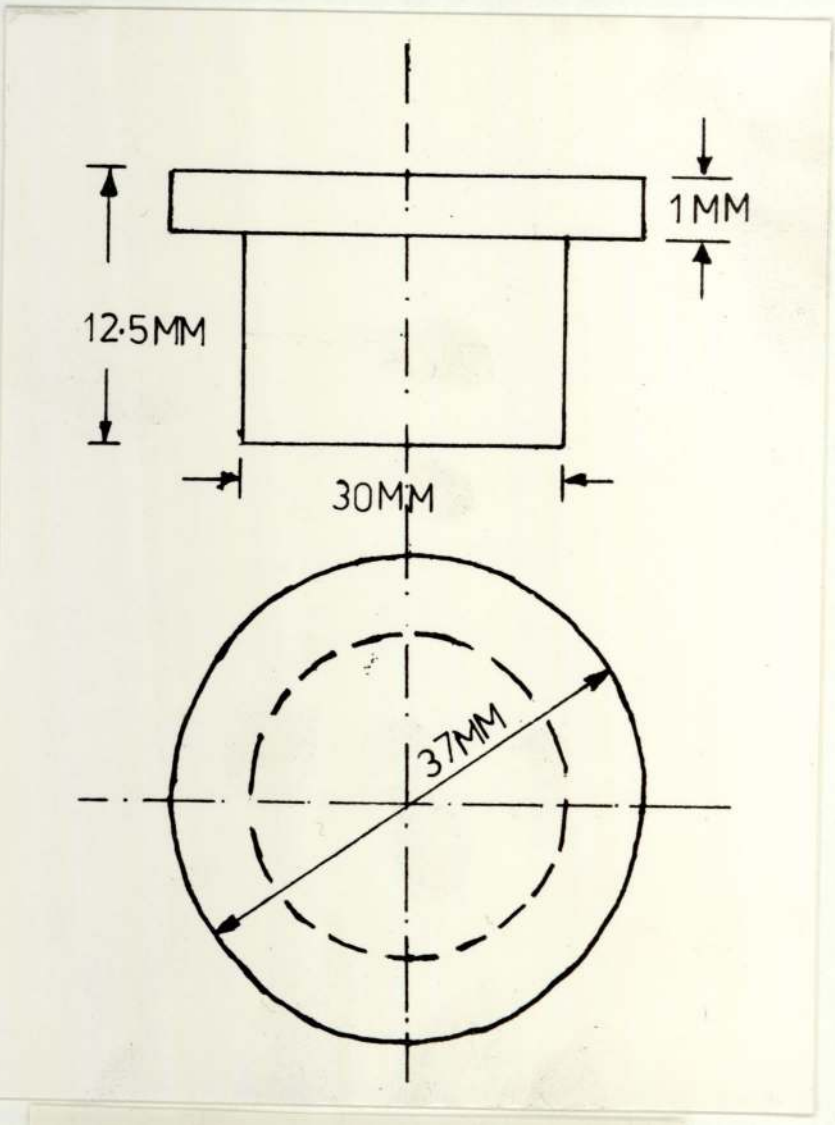

Fig.. 4 Experimental die insert

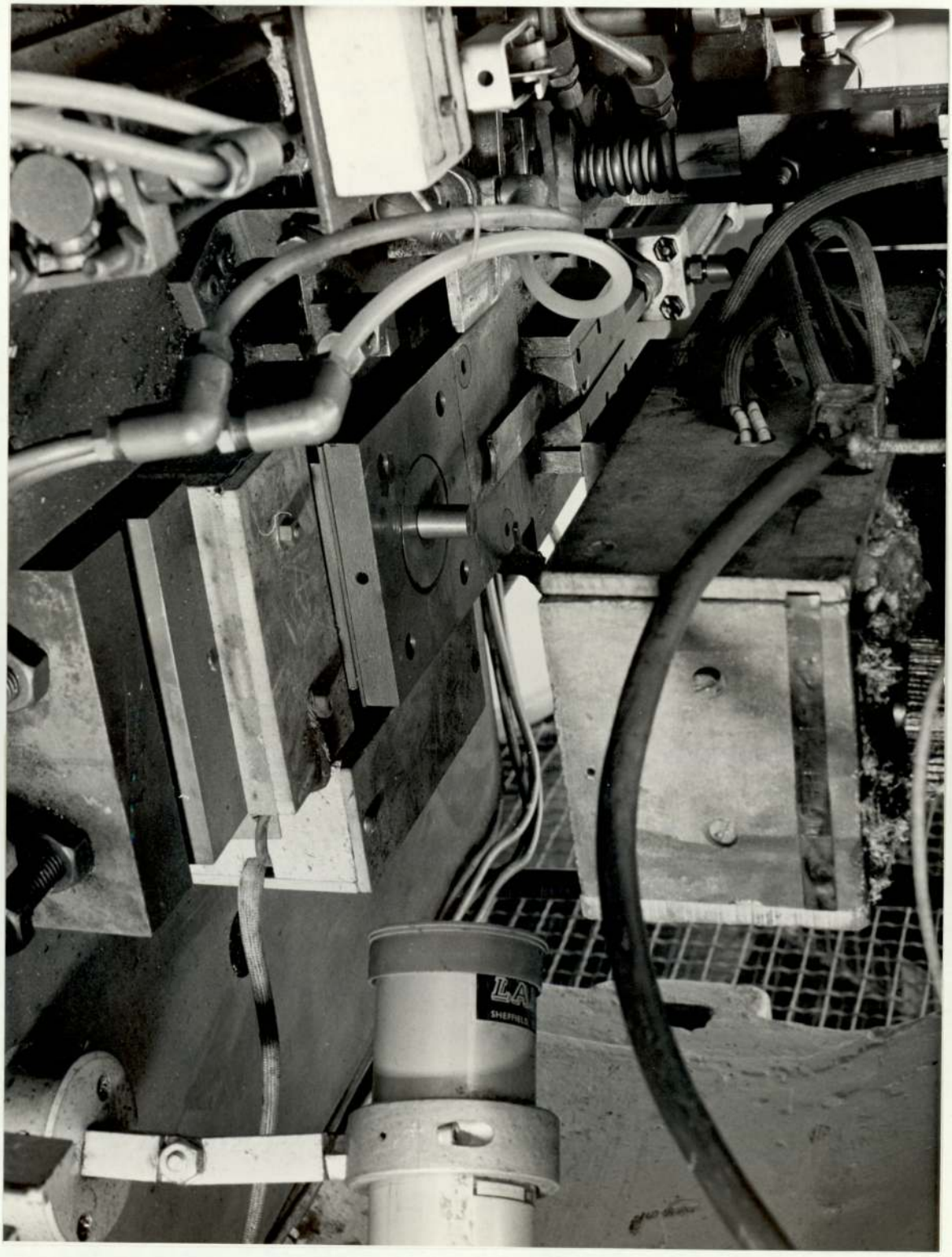

a

b

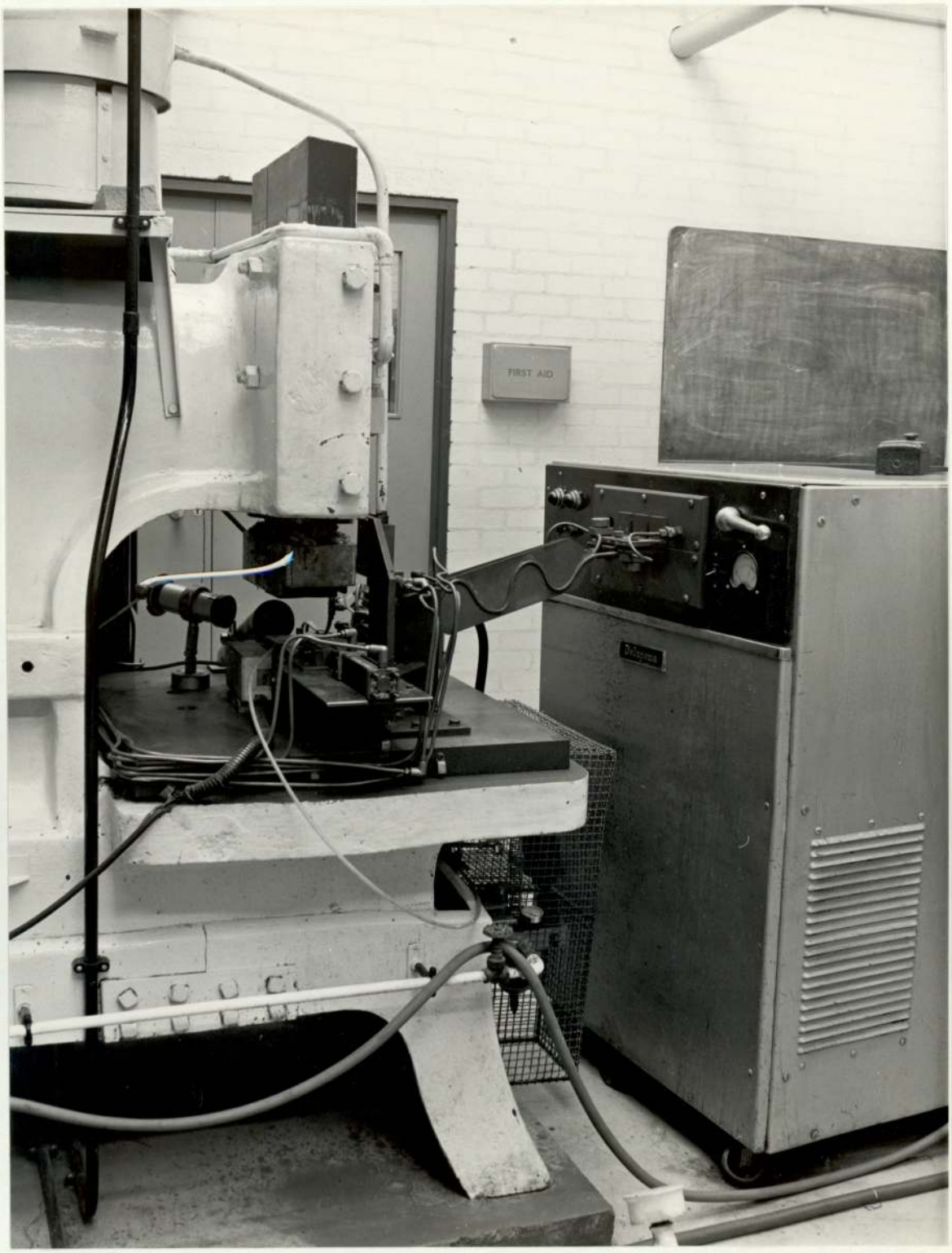

Fig. 5 Experimental forging press showing

(a) the feed mechanism
(b) a general view

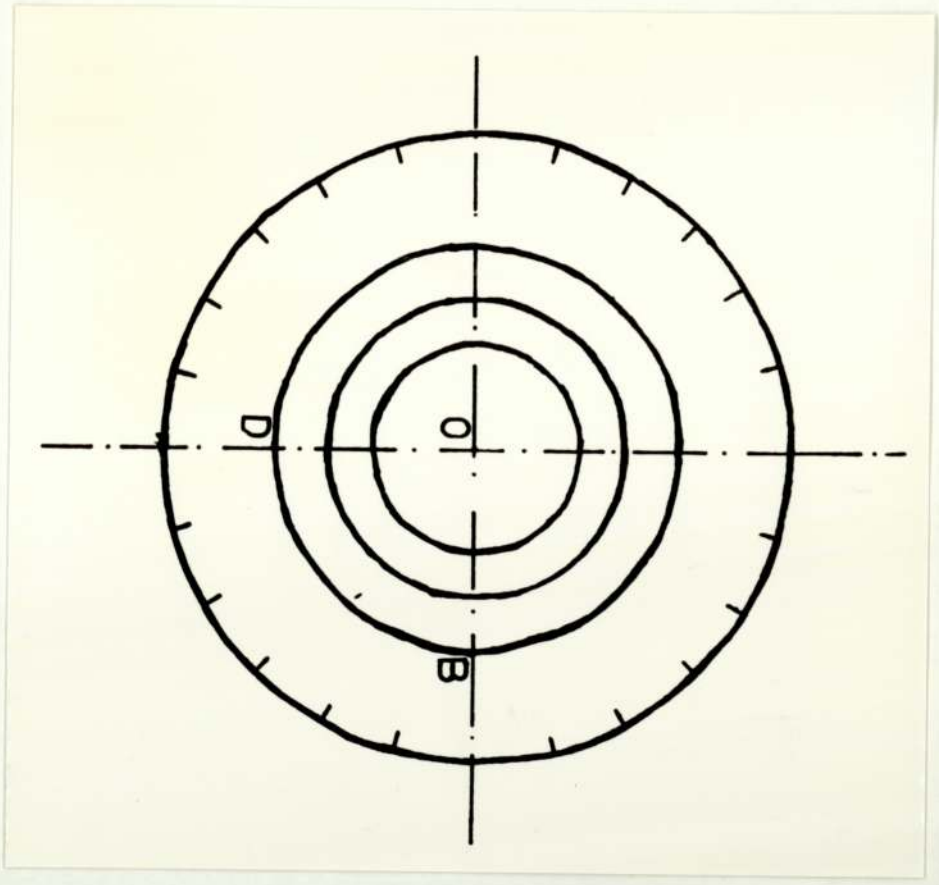

a

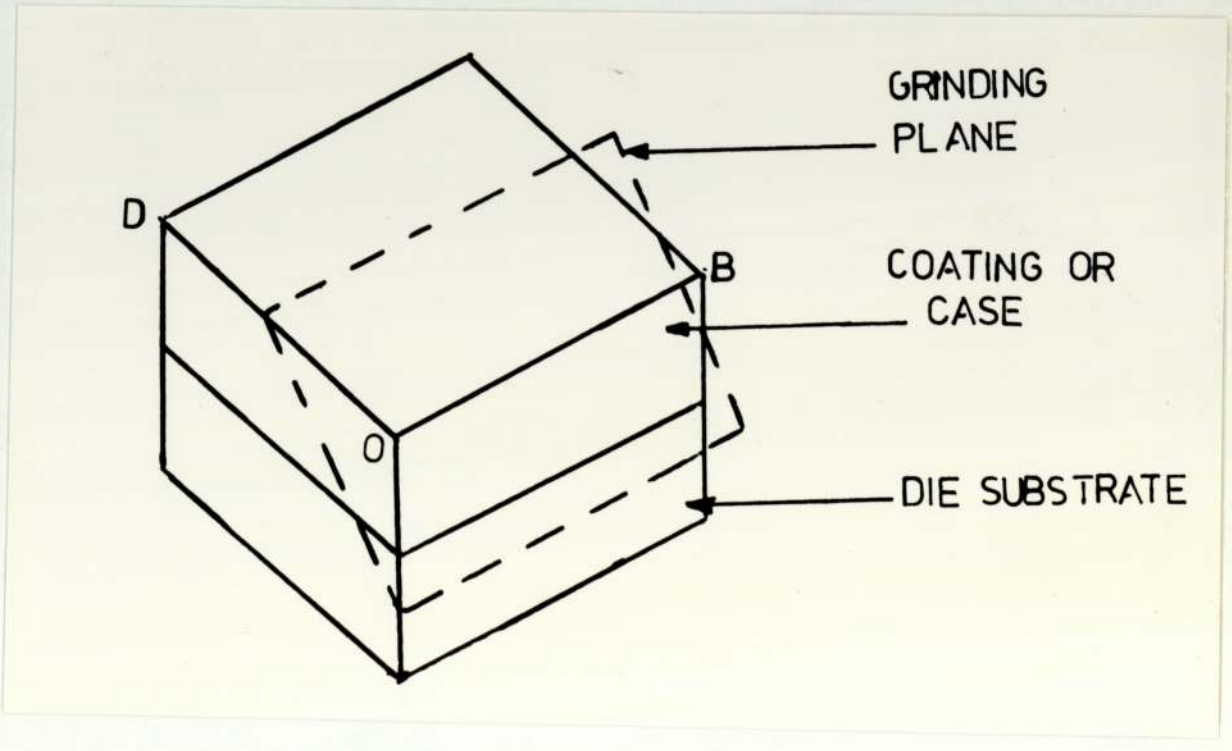

b

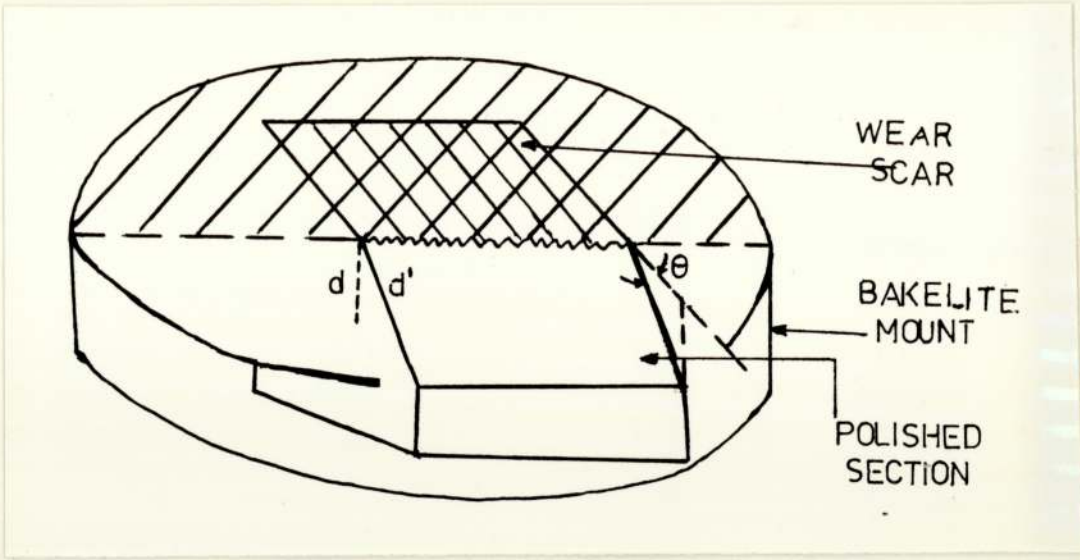

c

d

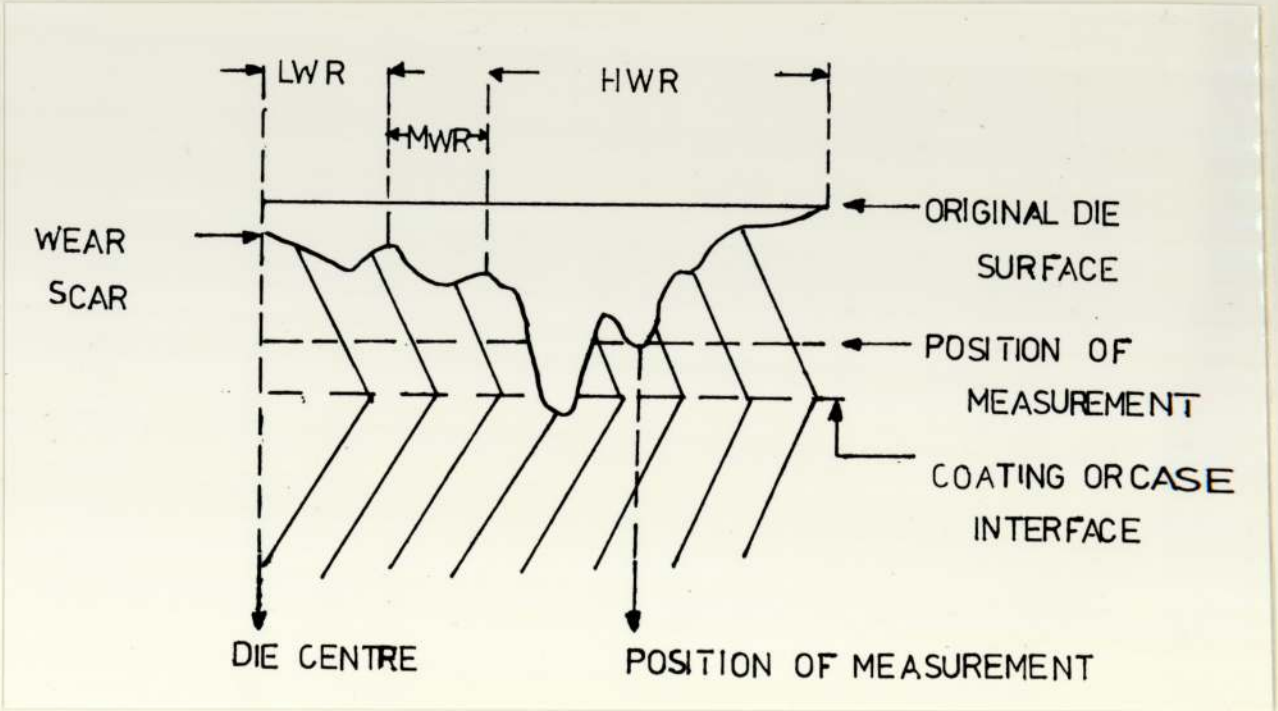

Fig. 6 Schenatic of the taper sectioning technique showing

(a) positions of wear measurements
(b) taper section
(c) section in bakelite mount after polishing
(d) positions of hardness measurement

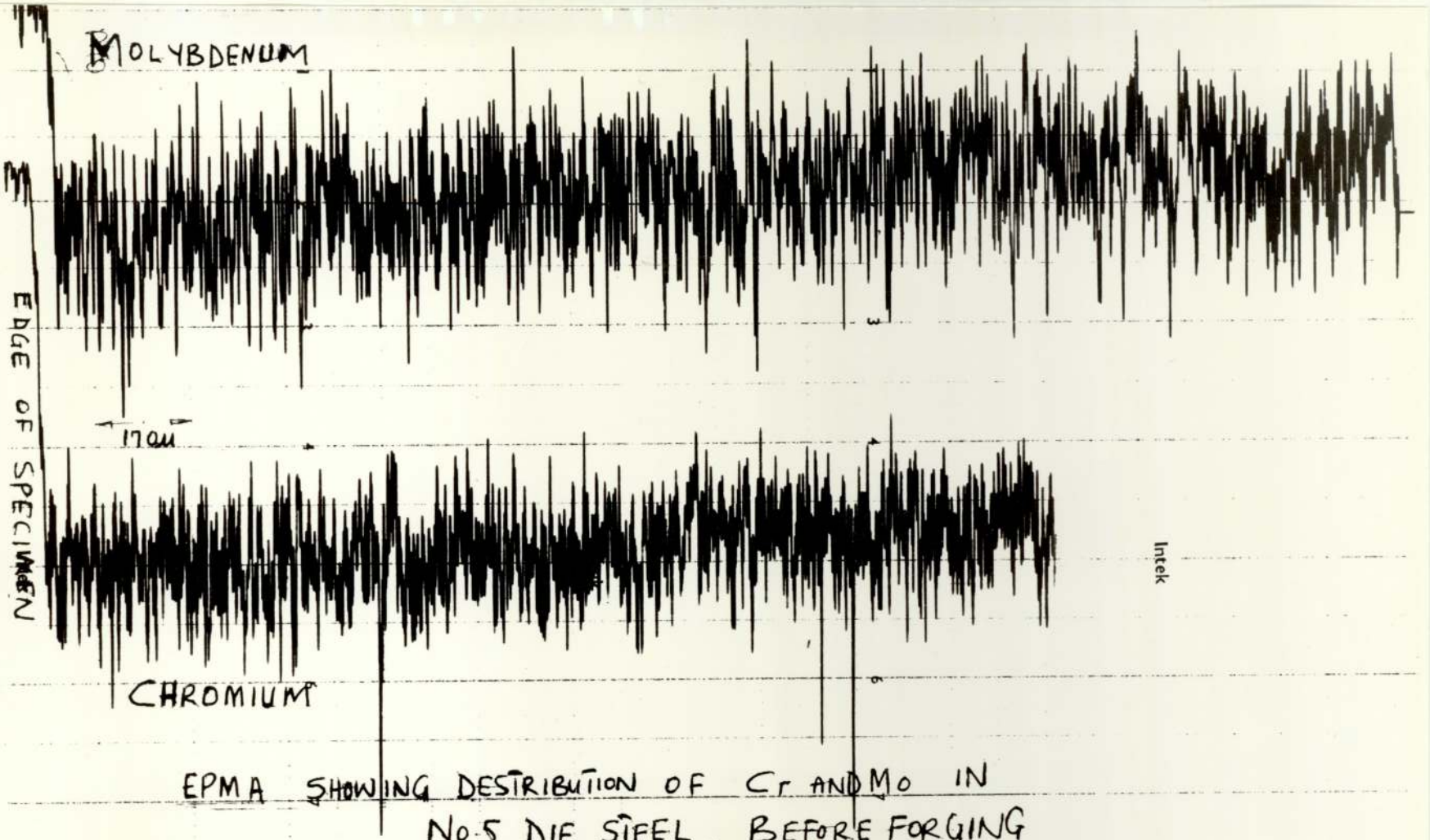

EPMA SHOWING DESTRIBUTION OF Cr AND Mo IN
No.5 DIE STEEL BEFORE FORGING

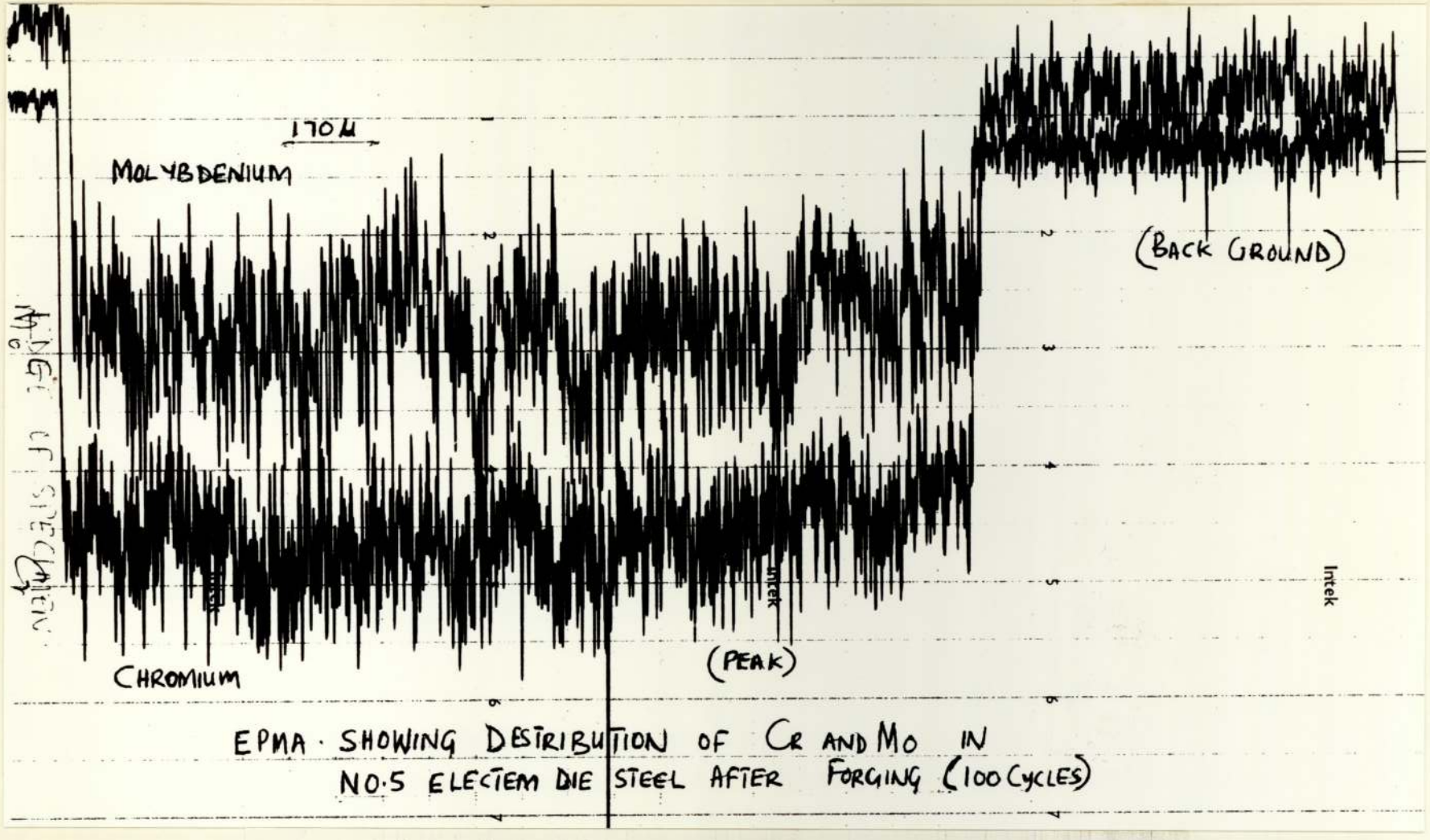

Fig. 7 Distribution of chromium and Molybdenum in No.5 die
(a) before, (b) after forging

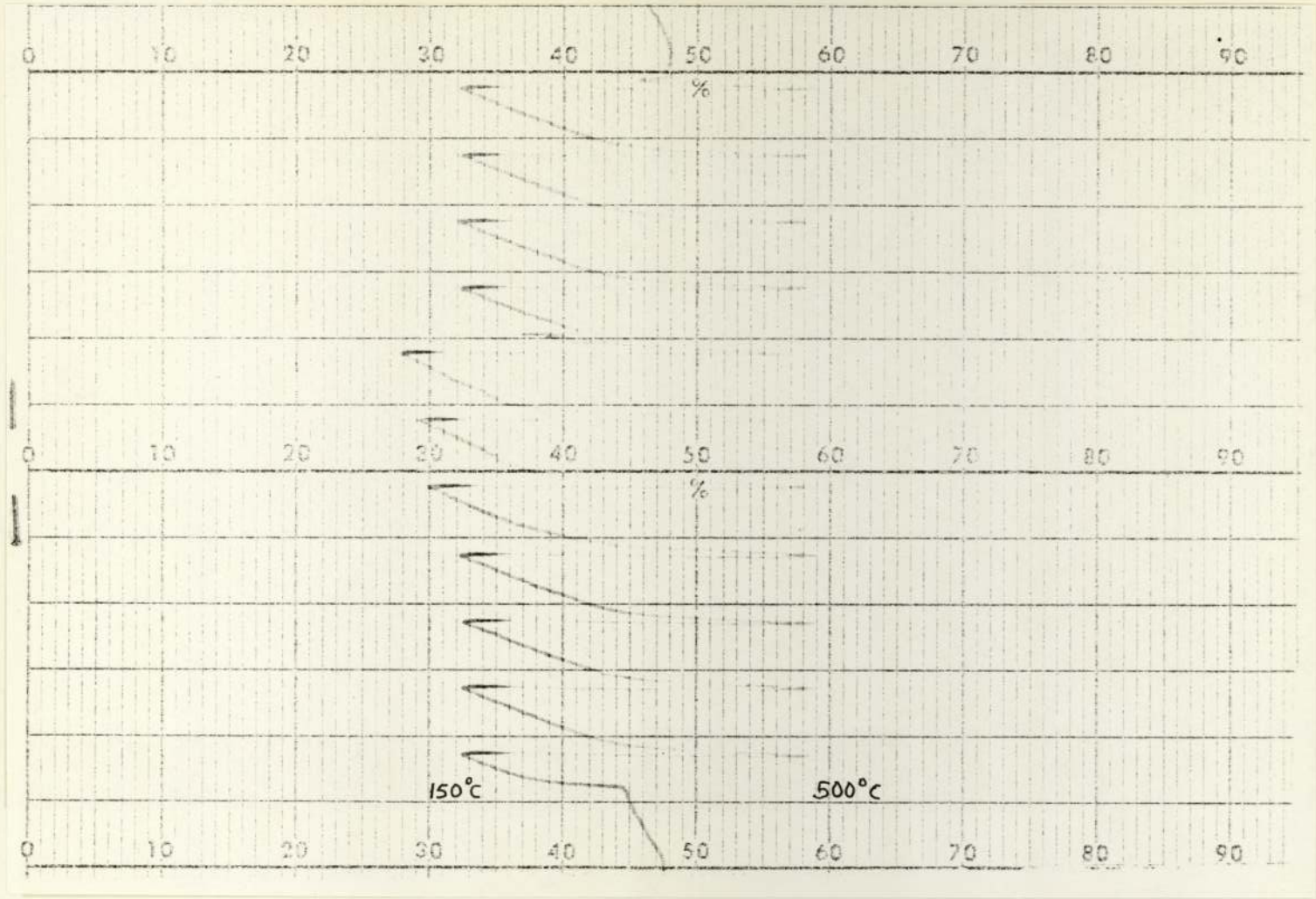

Fig. 8 Temperature distribution during thermal cycling

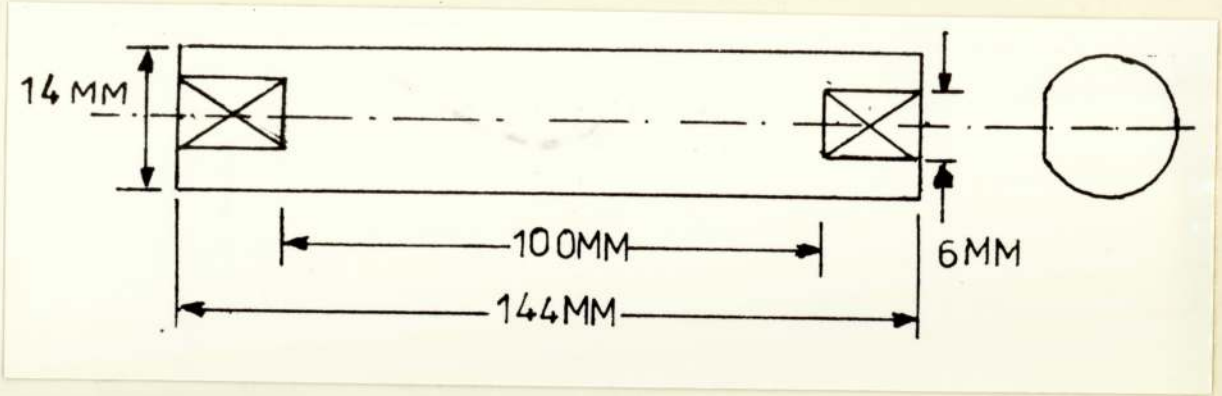

Fig. 9 Three-point bend fatigue testpiece

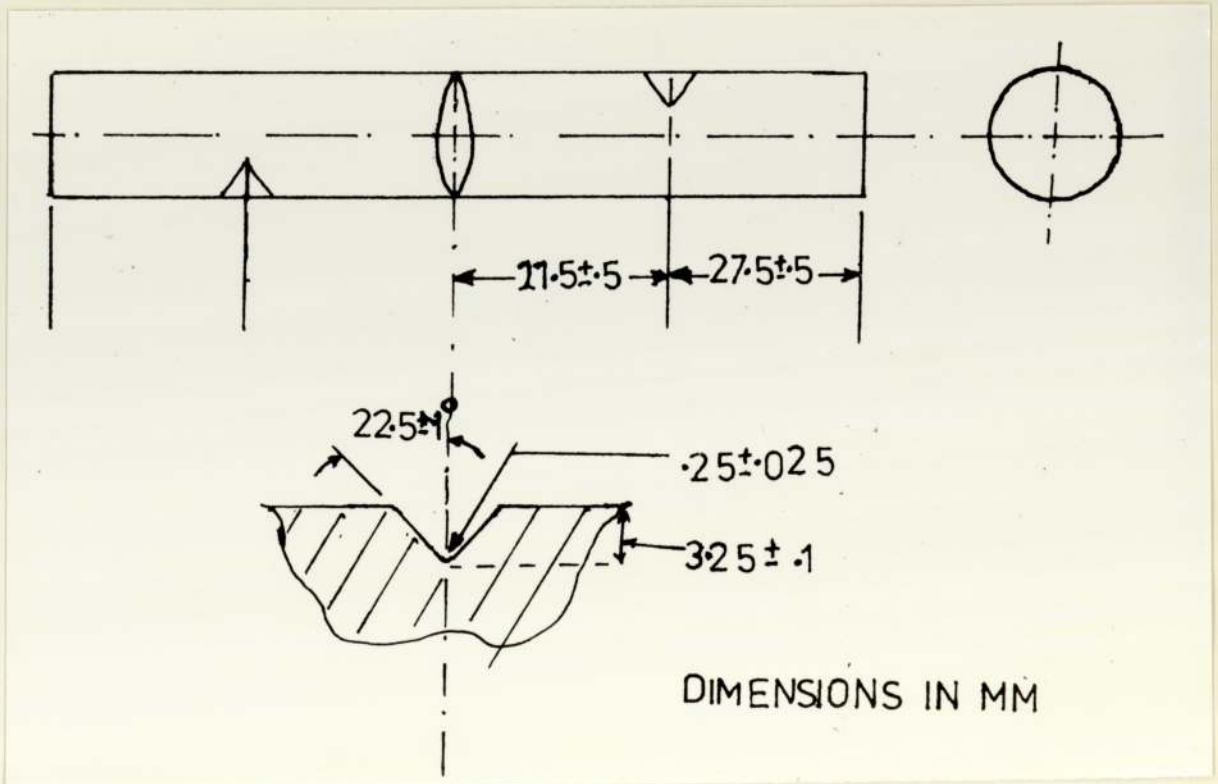

Fig. 11 Izod impact testpiece.

Fig. 10 Fatigue testing equipment showing the loading area

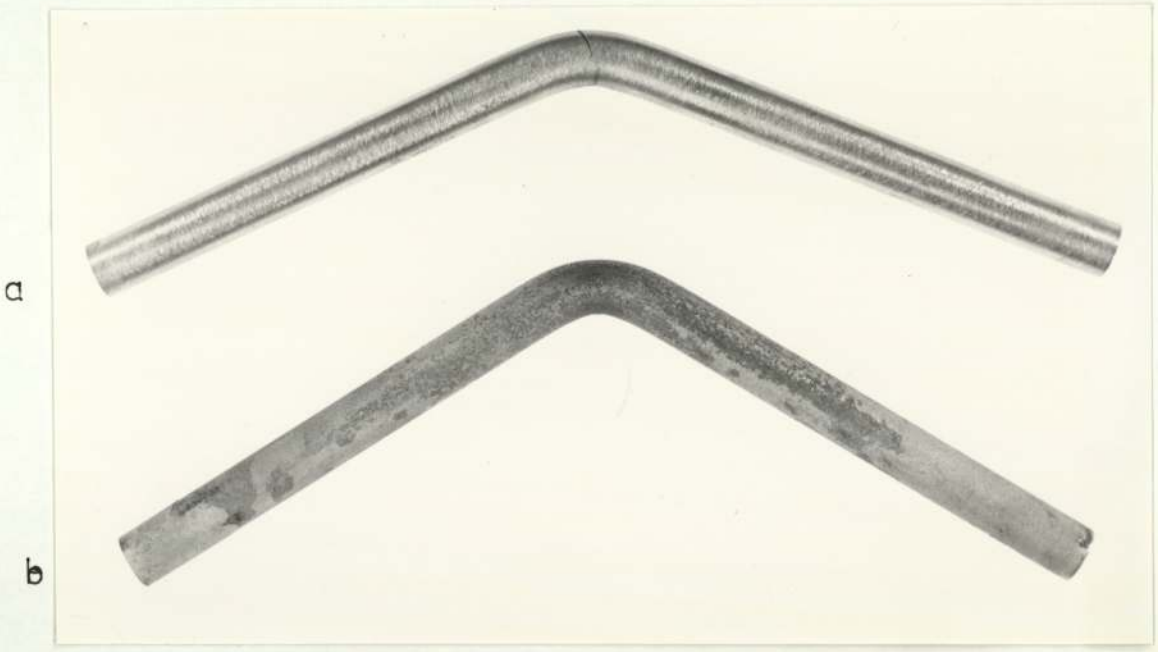

Fig. 12 Maximum angle of bend of
(a) hardened and tempered
and (b) brush plated Co-Mo alloy testpieces after slow bending

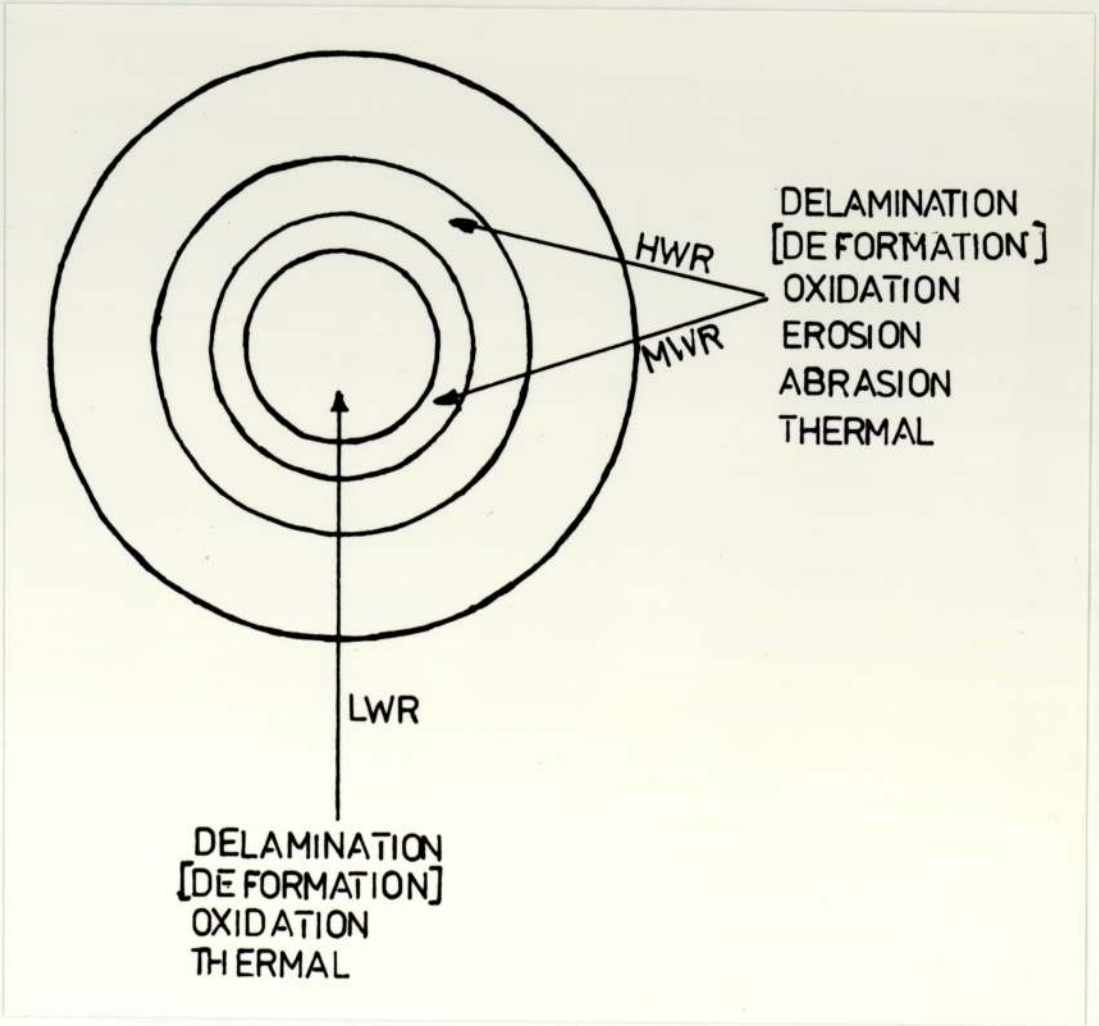

Fig. 13 (a) Variation of wear modes across die surface after forging.
(b) Plasma Nitrided die surface showing the wear regions in (a)

Fig. 14 Ploughing abrasion of a hardened and tempered No.5 die in the as-forged condition after 1 cycle hot forging.

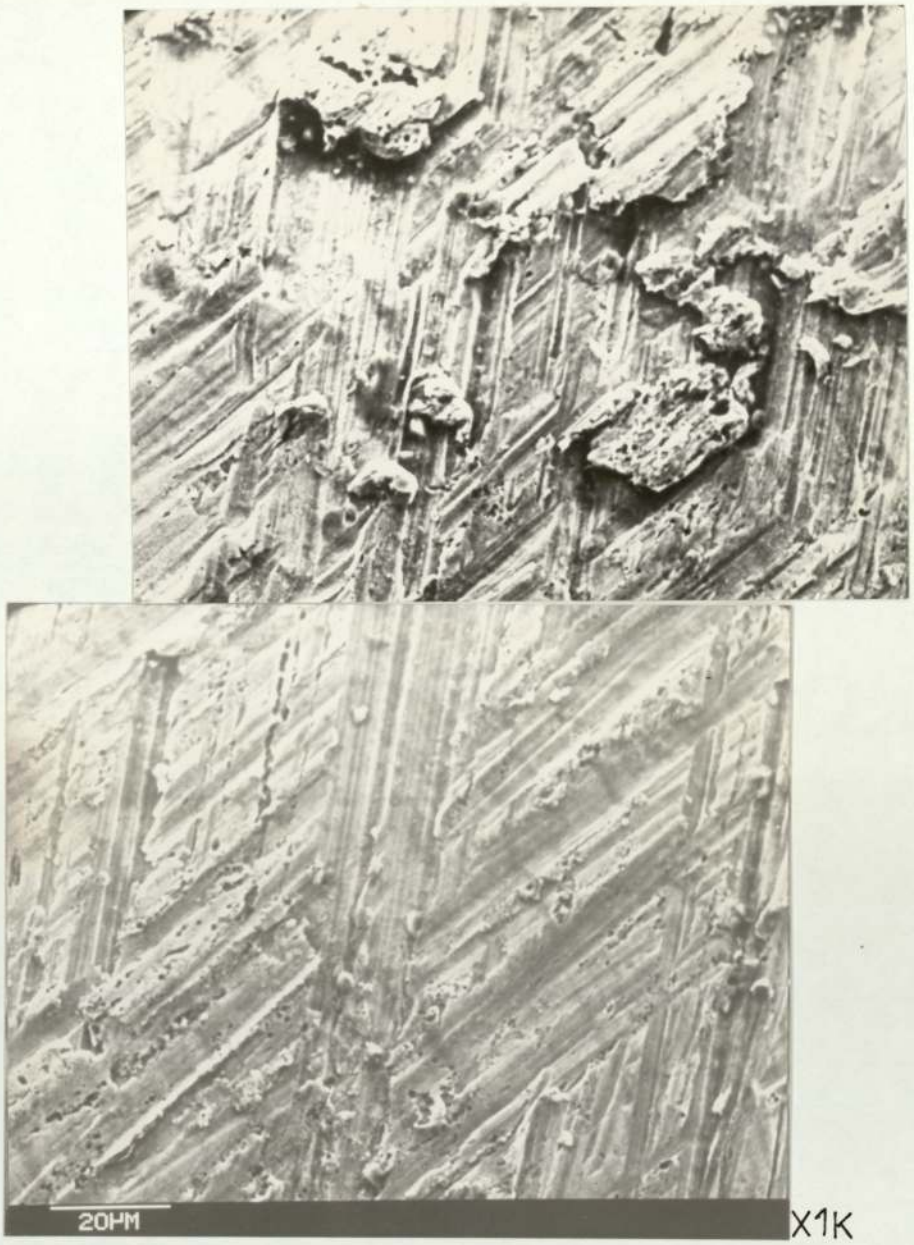

Fig. 15 Transition from ploughing to cutting abrasion of a hardened and tempered No.5 die after 2 cycles hot forging. Surface was descaled.

Fig. 16 Erosion of a hardened and tempered No.5 die after 5 cycles hot forging. Surface was descaled.

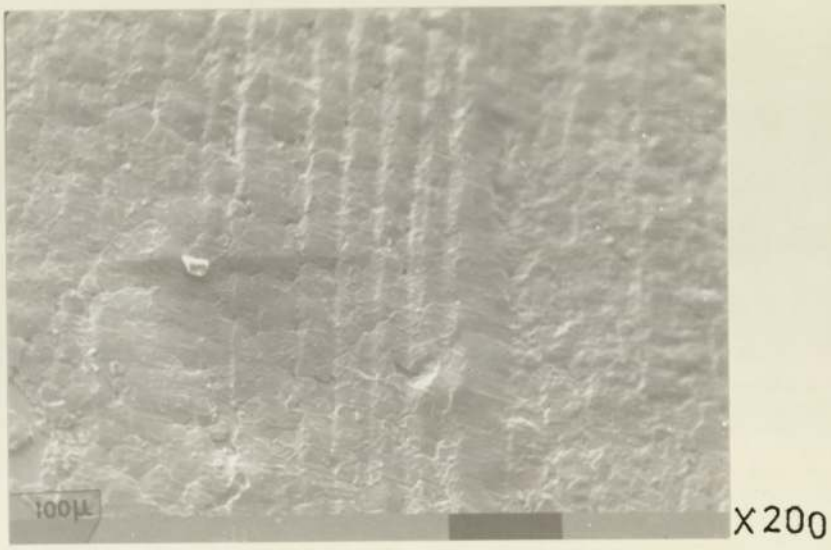

Fig. 17 Cutting abrasion of a hardened and tempered No.5 die after 10 cycles hot forging. Surface was descaled.

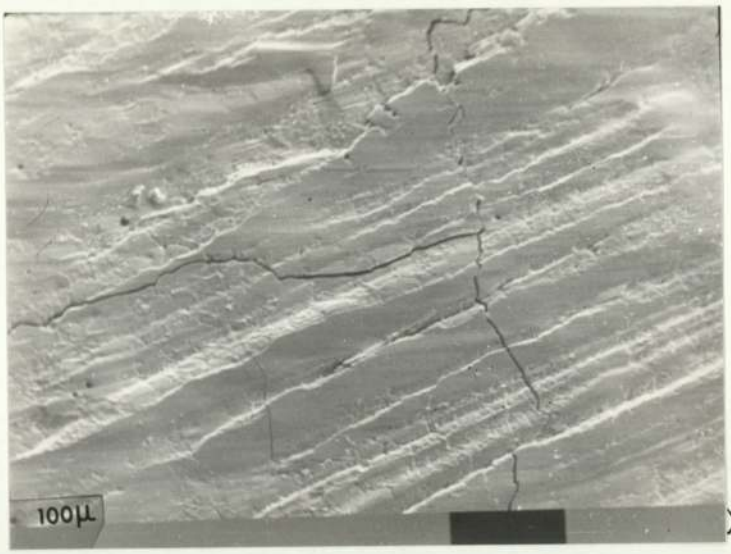

Fig. 18 Worn surface of a hardened and tempered No.5 die after 100 cycles hot forging showing

(a) cutting abrasion
(b) plastic deformation
(c) neighbouring cracks

Surface was descaled

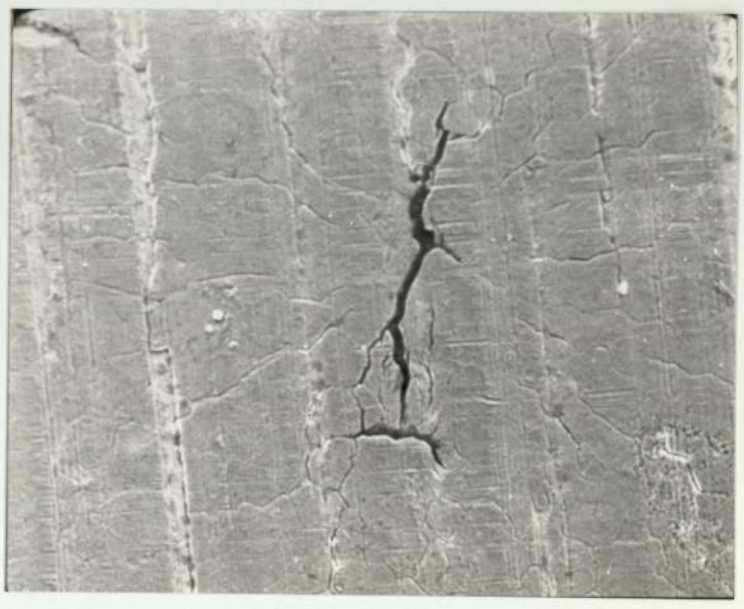

b

Fig. 19 Worn surface of a hardened and tempered No.5 die after 100 cycles hot forging showing

(a) undislodged metal island (Mag. x 500)
(b) several voids and cracks associated with them (Mag. x 1K) surface was descaled

Fig. 20 Worn surface of a hardened and tempered No.5 die after 100 cycles hot forging showing the linking of neighbouring cracks. (Mag. x 1K) surface was descaled.

a

b

Fig. 21 Similarity between surface and subsurface cracks in a hardened and tempered No.5 die after 1000 cycles hot forging.

(a) S.E.M. showing an inclusion and cracking of die surface. (Mag. x 2K). Surface was descaled.

(b) Optical micrograph showing subsurface inclusion and cracking. Magnification including that due to taper X1K (after Aston et al[2]).

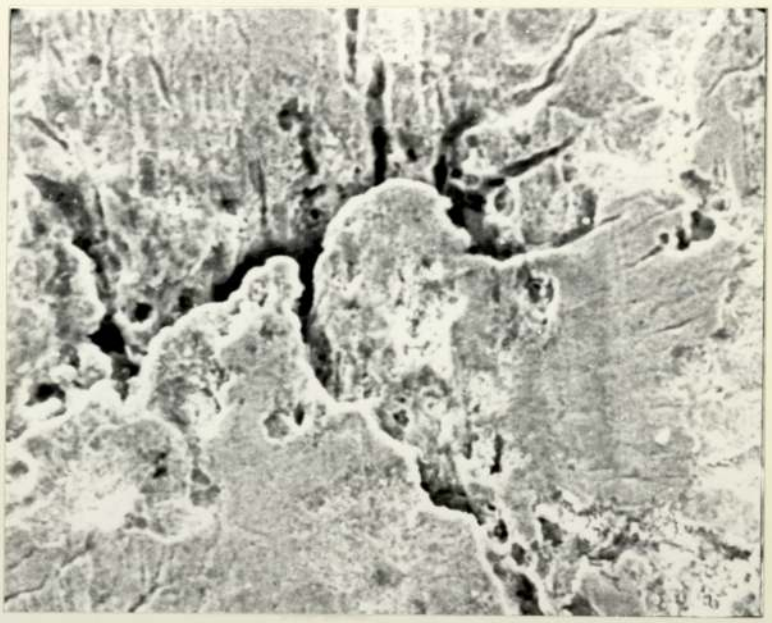

Fig. 22 Surface of a hardened and tempered No.5 die after 1000 cycles hot forging showing a combined effect of erosion and delamination wear. (Mag. x 1K) surface was descaled.

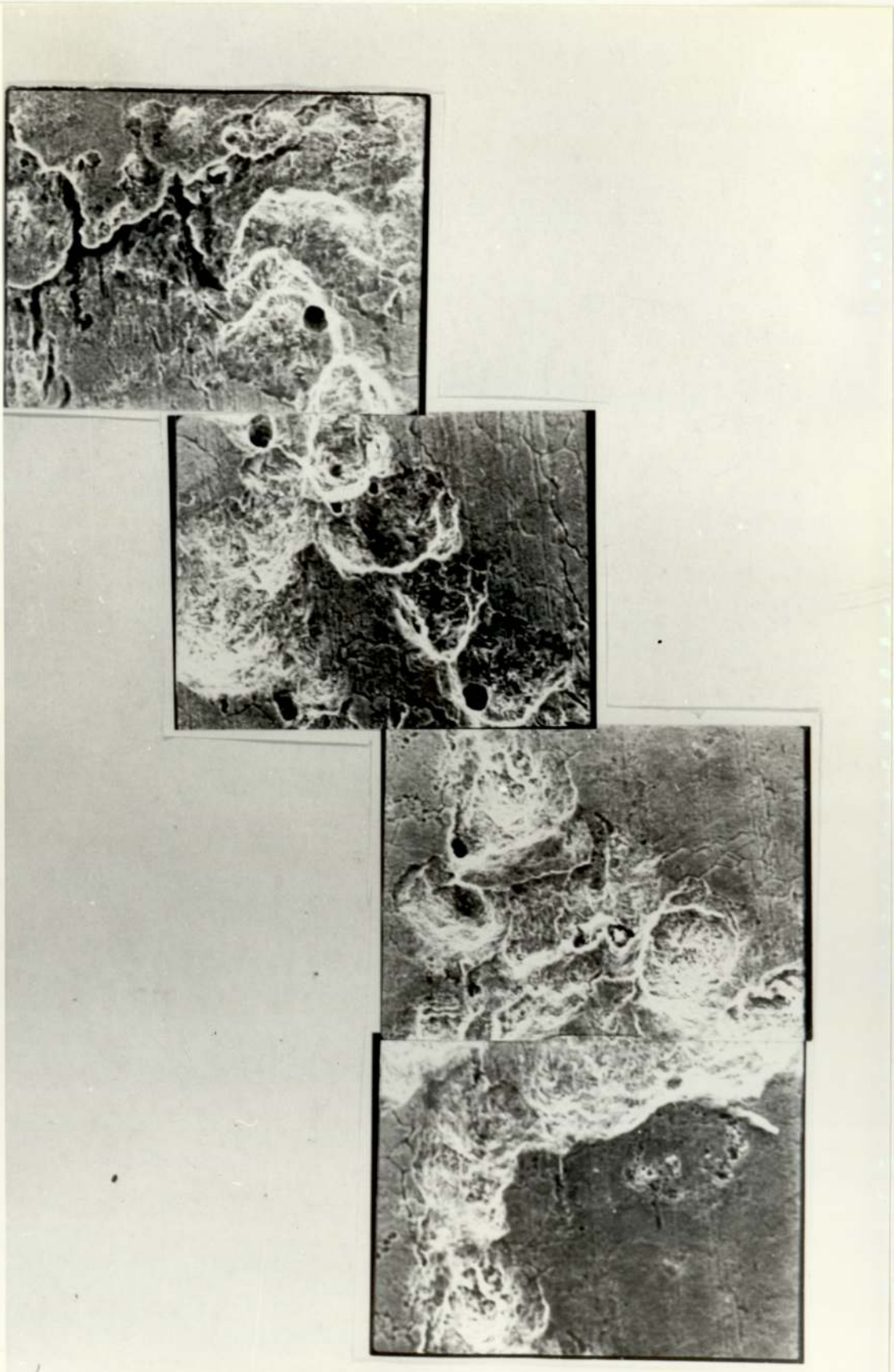

Fig. 23 A region below that in fig.22 showing

(a) severe erosion scars

(b) dislodged delamination platelets sitting on an eroded area suggesting that the latter probably occured first. (Mag. XlK)

Fig. 24 A view of the surface of a hardened and tempered No.5 die after 1000 cycles hot forging showing an exposed subsurface inclusion.

a

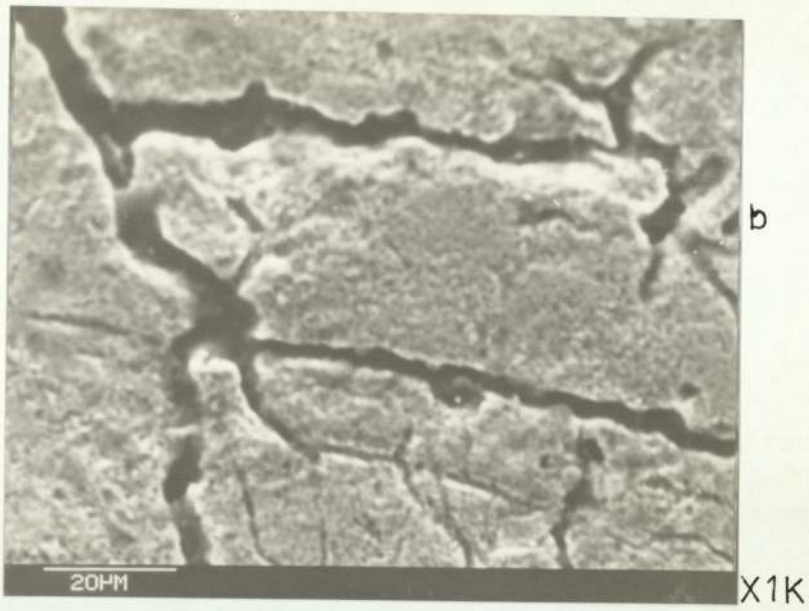

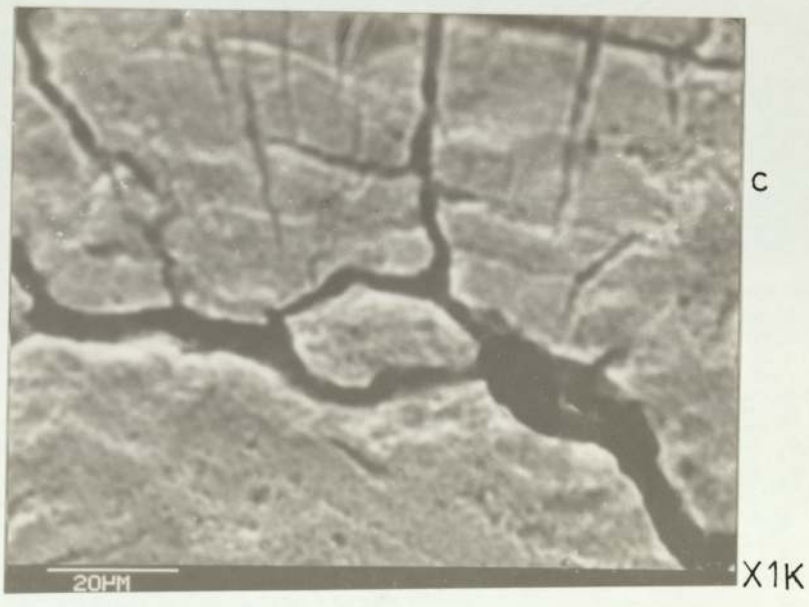

Fig. 25. Three views of the surface of a hardened and tempered No.5 die after 1000 cycles hot forging showing delamination platelets of varying dimensions. Surface was descaled.

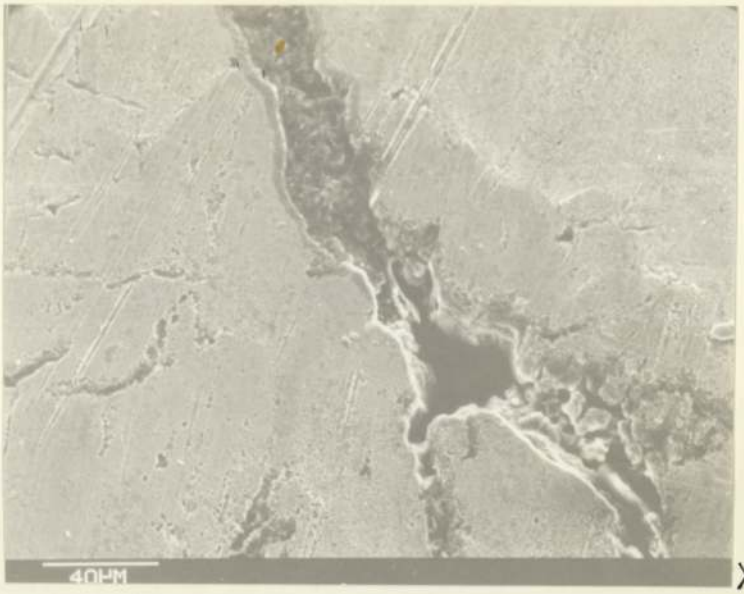

a

X500

b

X500

Fig. 26 A deformed region of the surface of a hardened and tempered No.5 die after 1000 cycles hot forging (a) shows the void and crack formed at an inclusion while, (b) is a further view of the region below (a)

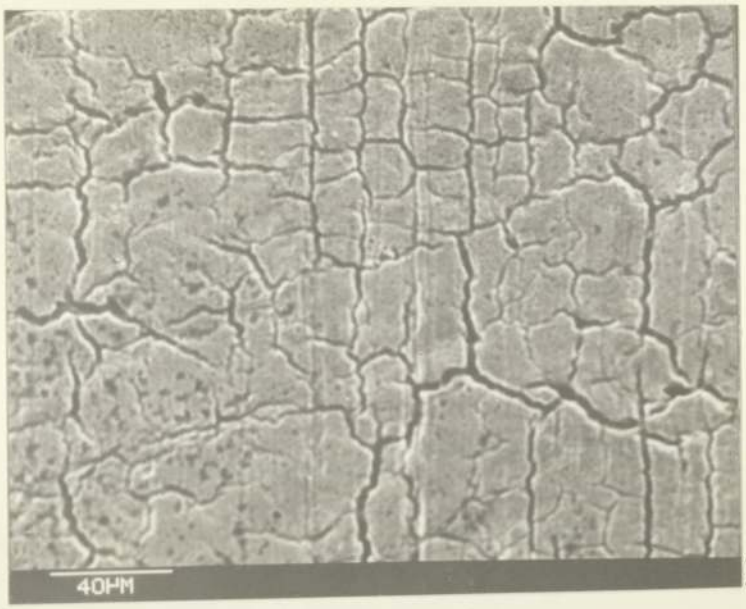

Fig. 27 Parallel grinding cracks on the surface of a hardened and tempered No.5 die after 1000 cycles hot forging.

Fig. 28 Scratch marks and original micro-cracks on the as-forged surface of a Co-Mo alloy plated No.5 die after 10 cycles cold forging.

Fig. 29 Two views of the as-forged surface of a Co-Mo alloy plated No.5 die after 10 cycles hot forging showing local flattening of coating due to intermittent frictional contact between slug and die.

Fig. 30 Two views of the as-forged surface of a Co-Mo alloy plated No.5 die after 100 cycles hot forging showing

(a) wear edge due to delamination

(b) further polygonal cracks on the exposed underlying substrate

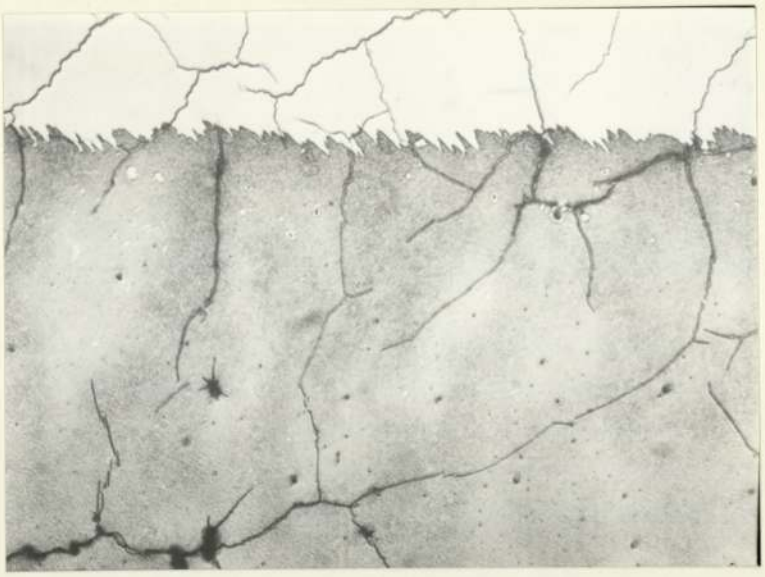

Fig. 31 Optical micrograph of the surface of a Co-Mo alloy plated No.5 die after 1000 cycles hot forging showing the linking of surface and subsurface.

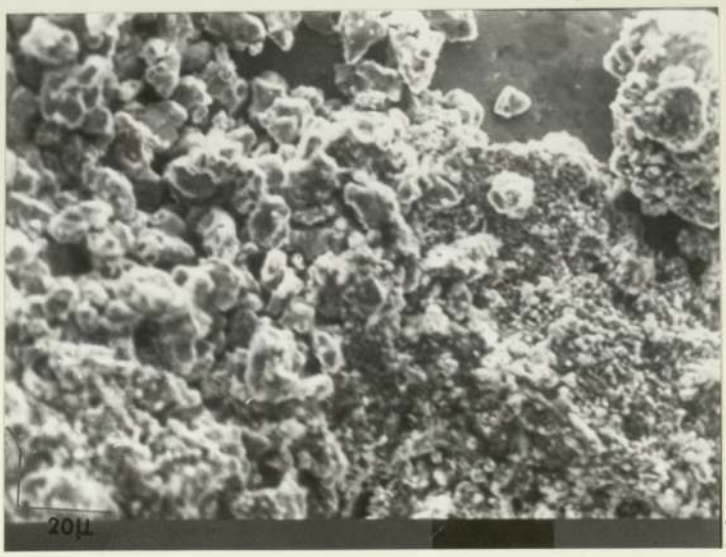

Fig. 32 A collection of wear platelets at the edge of the HWR of a hardened and tempered No.5 die after 1000 cycles hot forging. Surface was descaled.

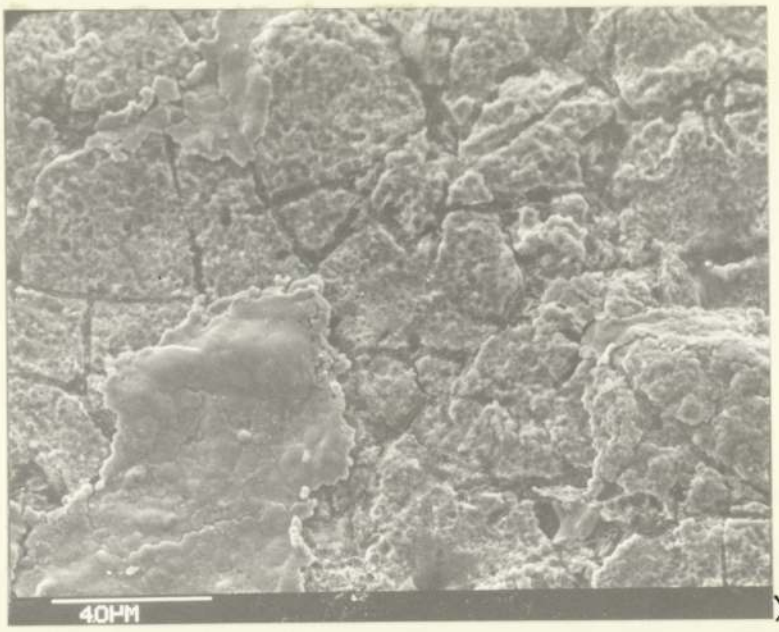

Fig. 33 A view of the surface of a hard Cr plated No.5 die after 100 cycles hot forging which was partially descaled to show how a mixture of compacted oxides and fragmented metallic particles may be formed.

Fig. 34 A view of the surface of a hard Cr plated No.5 die after 100 cycles hot forging showing a glaze of cracked oxide layer.

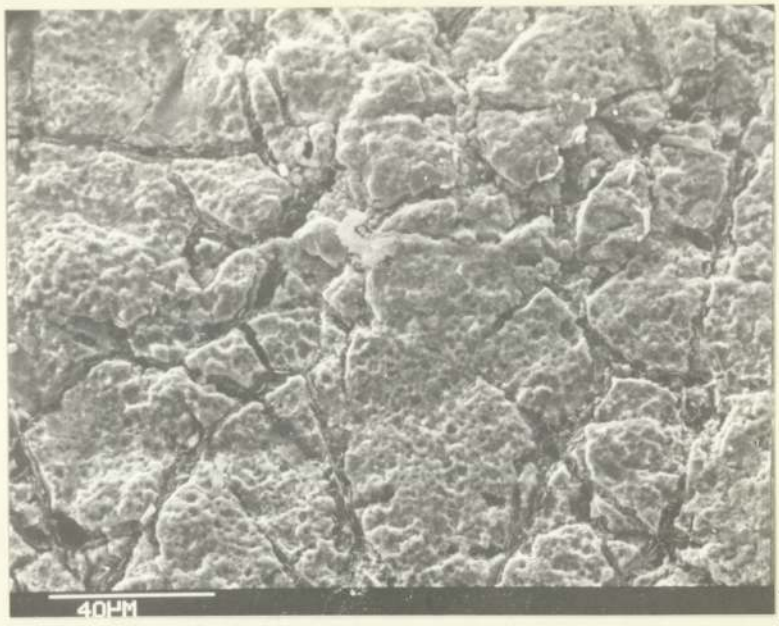

Fig. 35 A view of the surface of a hard Cr plated No.5 die after 100 cycles hot forging showing dislodged and undislodged fragmented platelets. Surface was descaled.

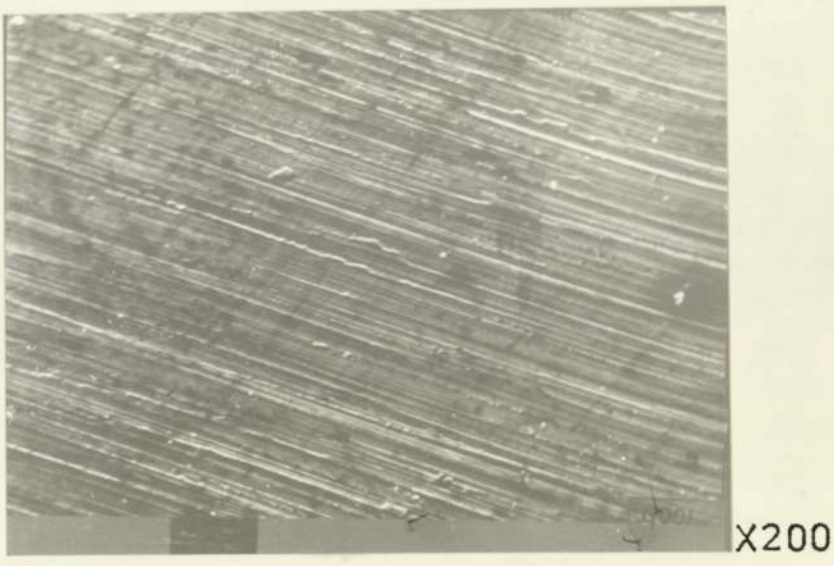

Fig. 36 Surface of a hardened and tempered BH13 die showing orginal grinding marks before forging.

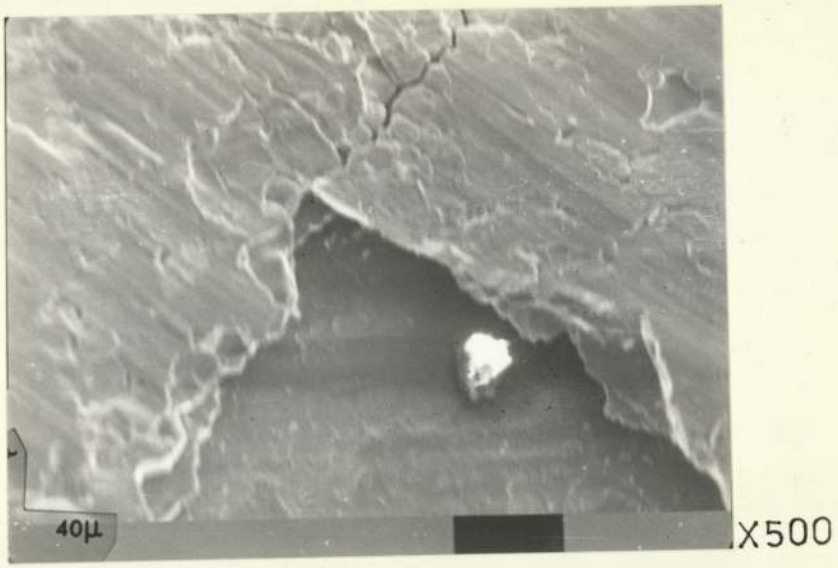

Fig. 37 A view of the as-forged surface of a hardened and tempered BH13 die after 100 cycles hot forging showing the layer-like appearance of a wear edge due to delamination.

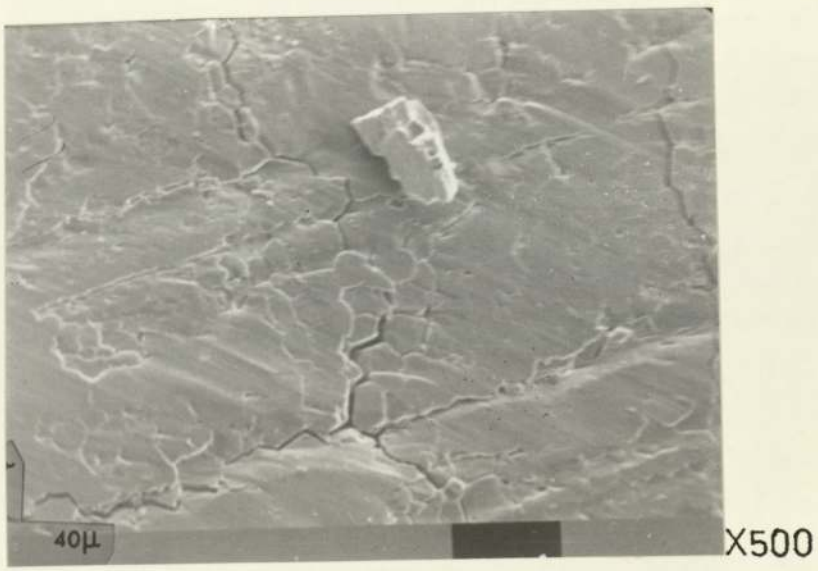

Fig. 38 A view of the as-forged surface of a hardened and tempered BH13 die after 100 cycles hot forging showing cracks and a dislodged wear platelet.

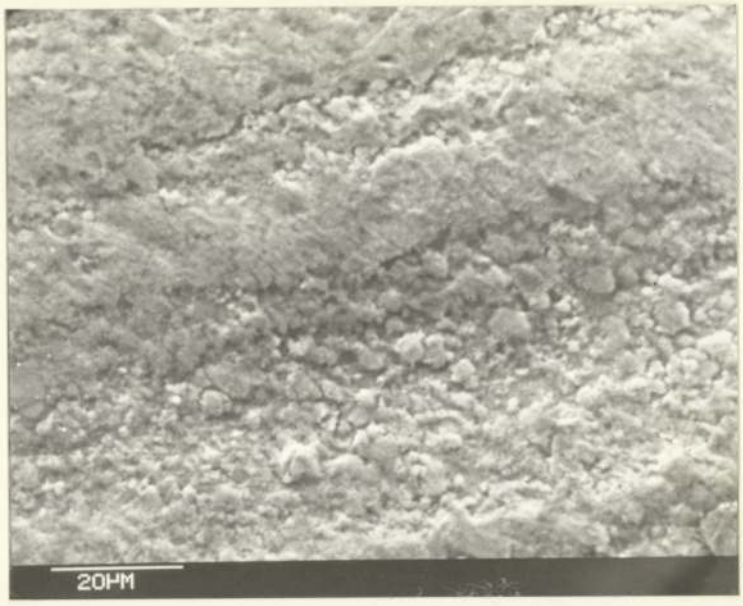

a

X1K

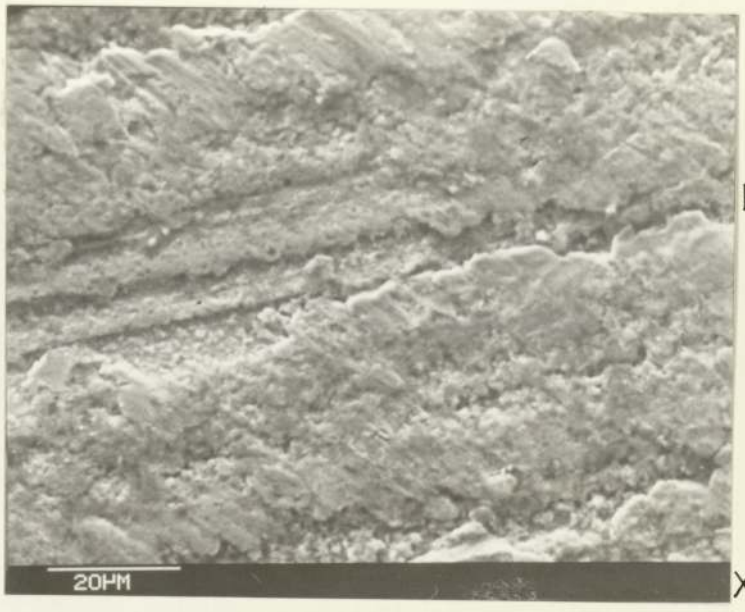

b

X1K

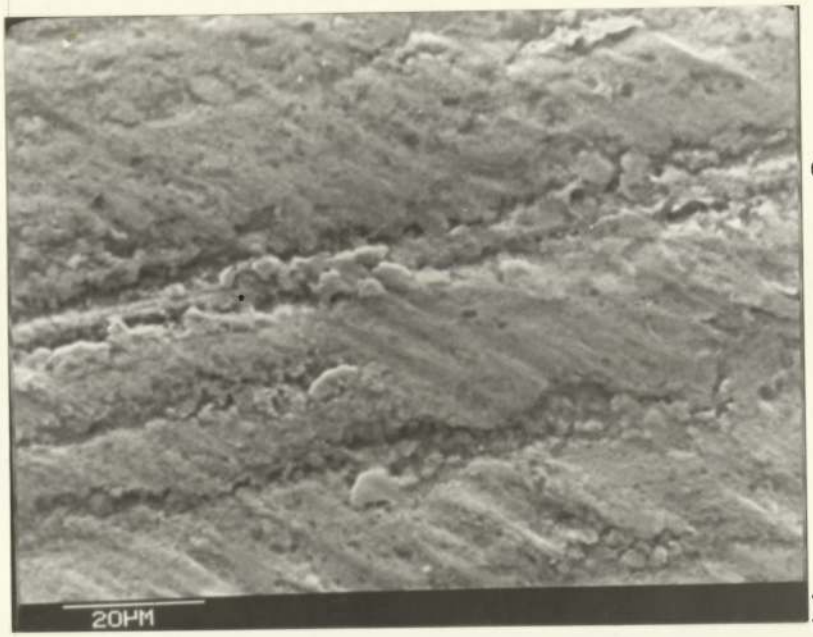

Fig. 39 Three views of the surface of a plasma nitrided BH13 die after 1000 cycles hot forging. (a) shows some fragmented wear platelets (b) and (c) show flattening of platelets of adjacent sites due to intermittent frictional contact between slug and die.

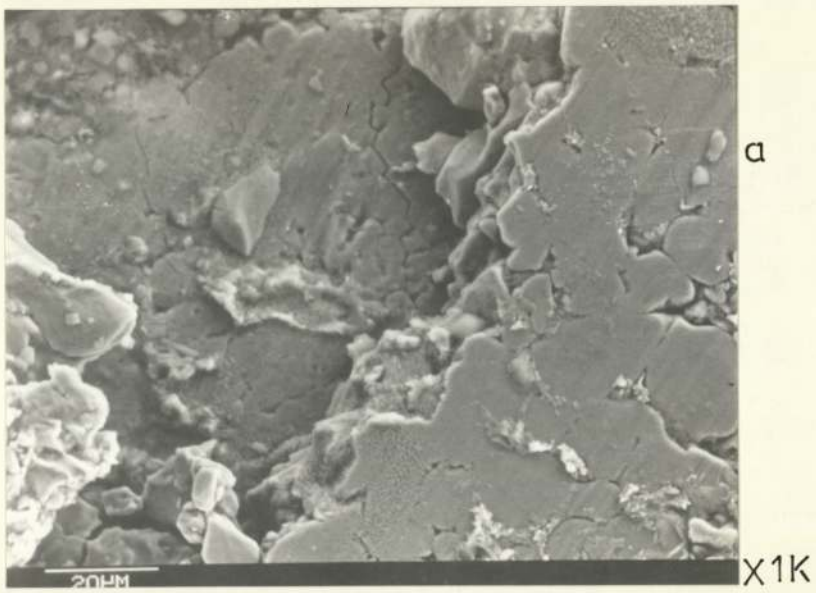

Fig. 40 Two views of the surface of a plasma nitrided BH13 die after 10 cycles hot forging showing

(a) a thick oxide layer (b) a cracked and flattened thin oxide layer.

Fig. 41 A view of the as-forged surface of a plasma nitrided BH13 die after 1000 cycles hot forging showing part of the polygonal cracks.

Fig. 42 A view of the as-forged surface of a plasma nitrided BH13 die after 1000 cycles hot forging showing cracks which penetrated the underlying steel.

Fig. 43 A view of the as-forged surface of a plasma nitrided BH13 die after 1000 cycles showing a void and the crack associated with it.

Fig. 44 A view of the surface of a plasma nitrided BH13 die after 100 cycles forging showing the effect of ploughing on a previously flattened layer, surface was descaled.

Fig. 45 A view of the surface of a plasma nitrided BH13 die after 1000 cycles hot forging showing polygonal cracks, slight erowion marks and a dislodged platelet. Surface was descaled.

Fig. 46 A view of the surface of a Tufftrided BH13 die after 100 cycles hot forging showing a typical crack associated with the formation of wear platelets by delamination. Surface was descaled.

Fig. 47 An enlarged view of the top right hand corner of die area in fig. 46, showing a void and cracks.

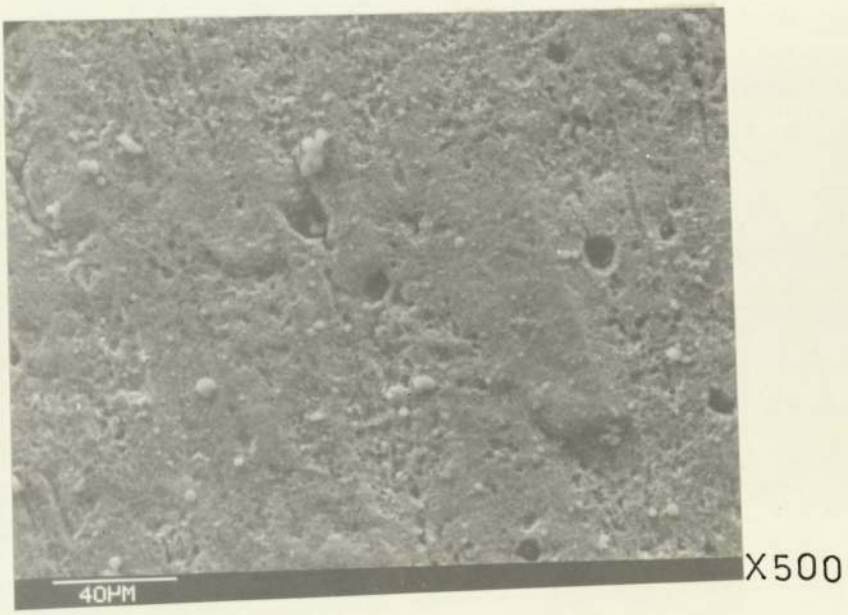

Fig. 48 General appearance of the MWR of the surface of a Tufftroded BH13 die after 100 cycles hot forging. Surface was descaled.

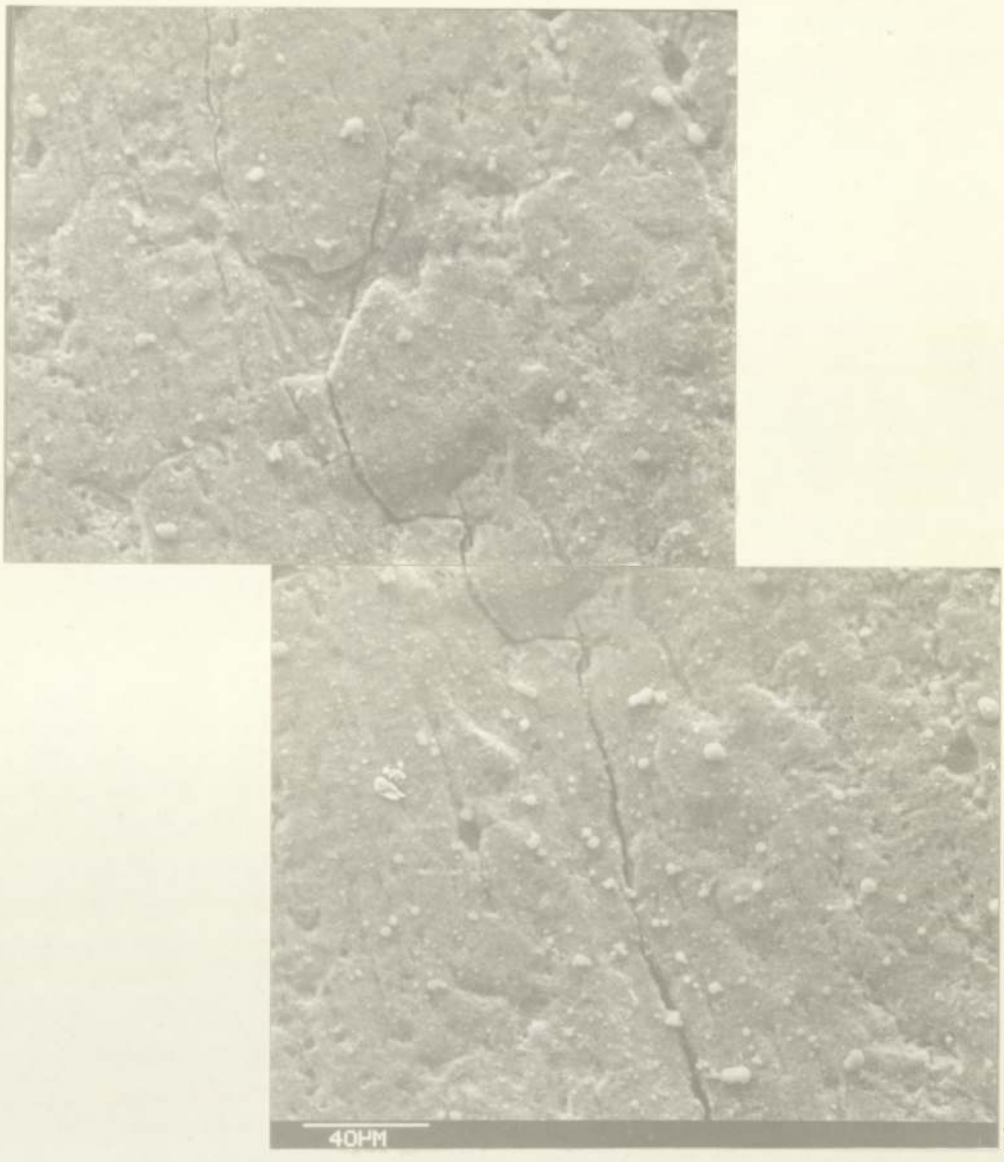

Fig. 49 A hugh crack running across the HWR of the surface of a Tufftrided BH13 die after 100 cycles hot forging. Surface was descaled.

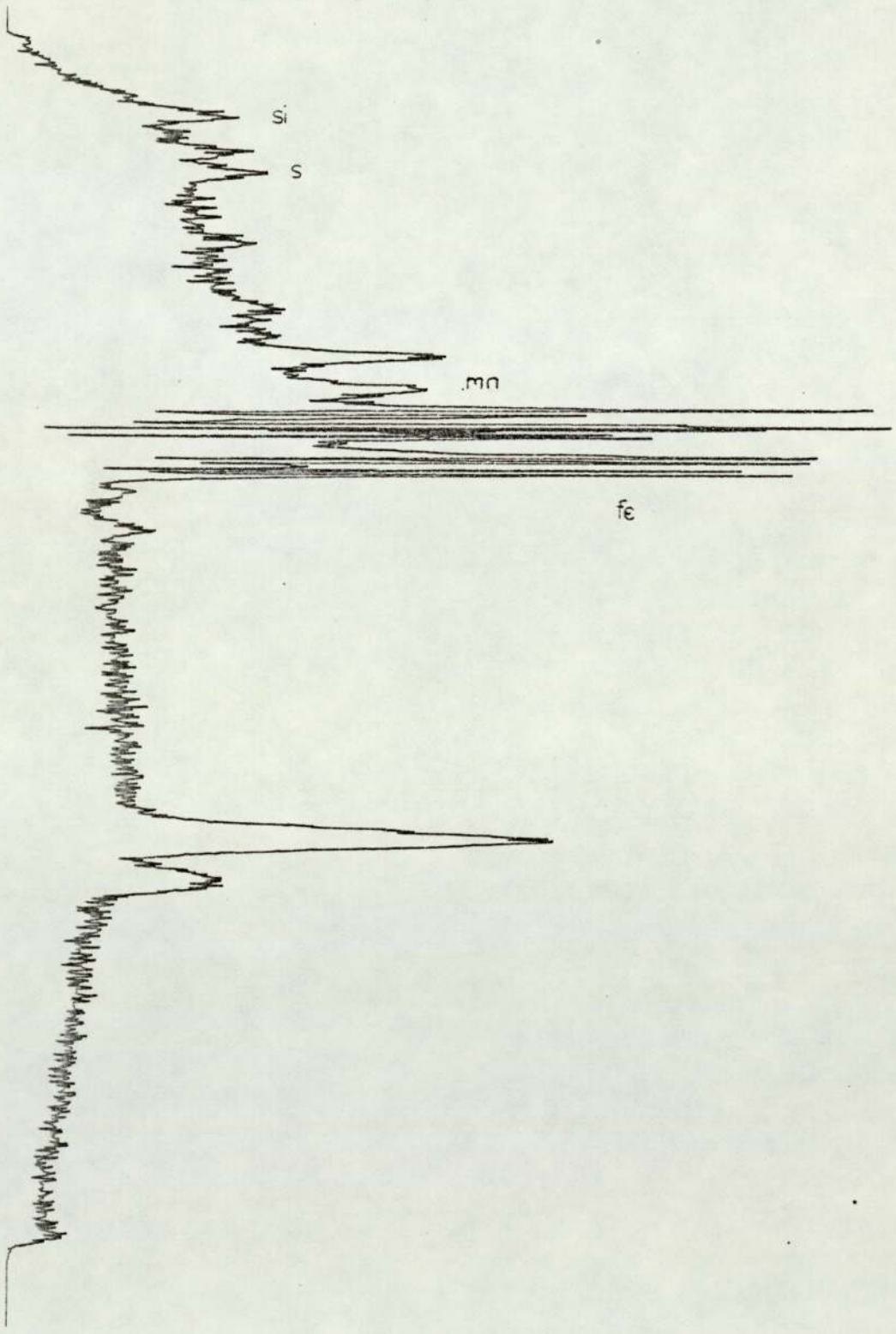

Fig. 50 S.E.M. x-ray analysis of an inclusion observed on the worn surface of No.5 die steel. Unidentified peaks are for elements of the surrounding die matrix.

Fig. 51 S.E.M. of an elongated MnS inclusion after forging.

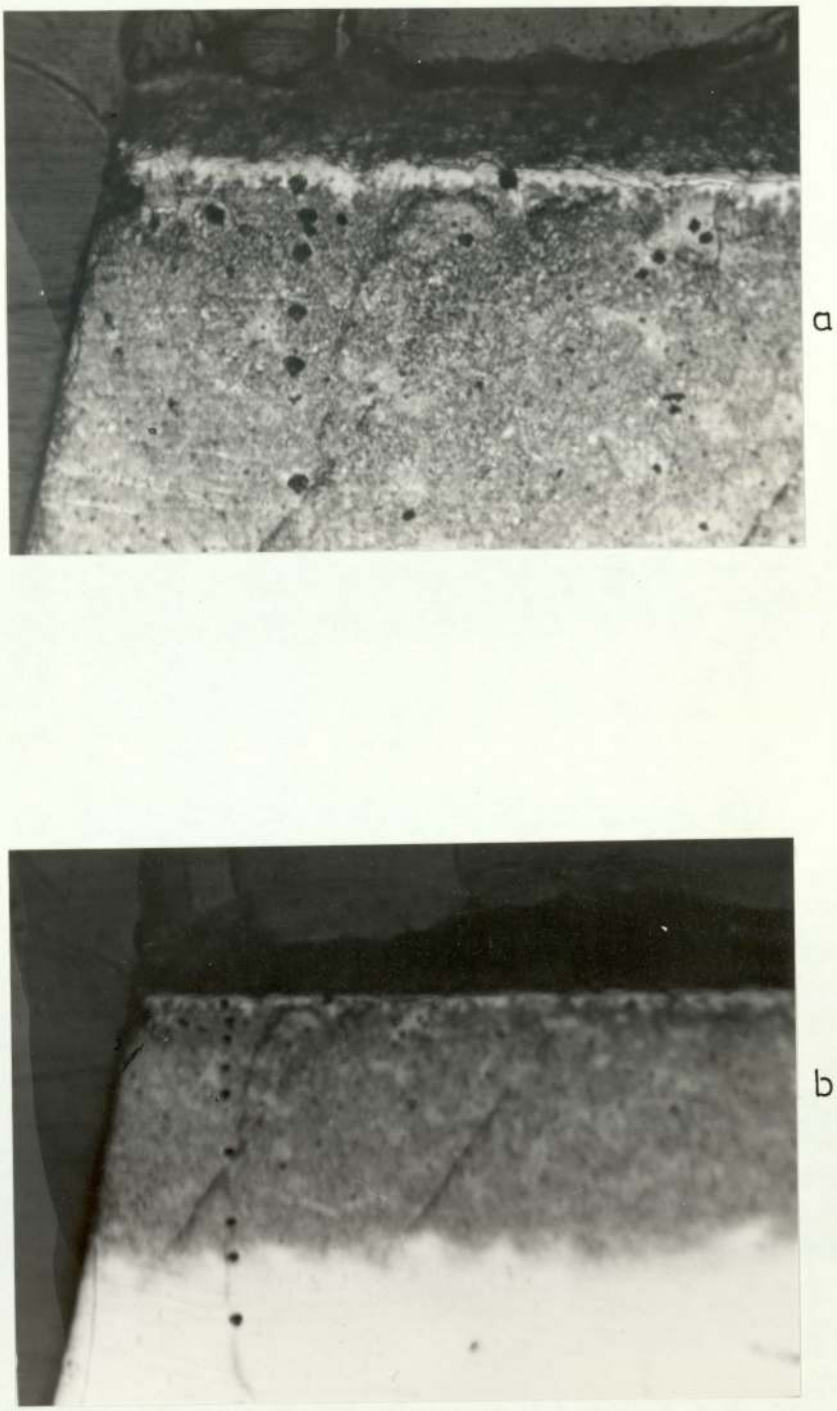

Fig. 52 Photomicrographs indicating regions of micro-hardness measurement on a BH13 die specimen. Magnifications including taper were (a) X990 (b) X510

Fig. 53 Vertical sections of (a) No.5 and (b) BH13 dies showing the the effects of grinding before forging.

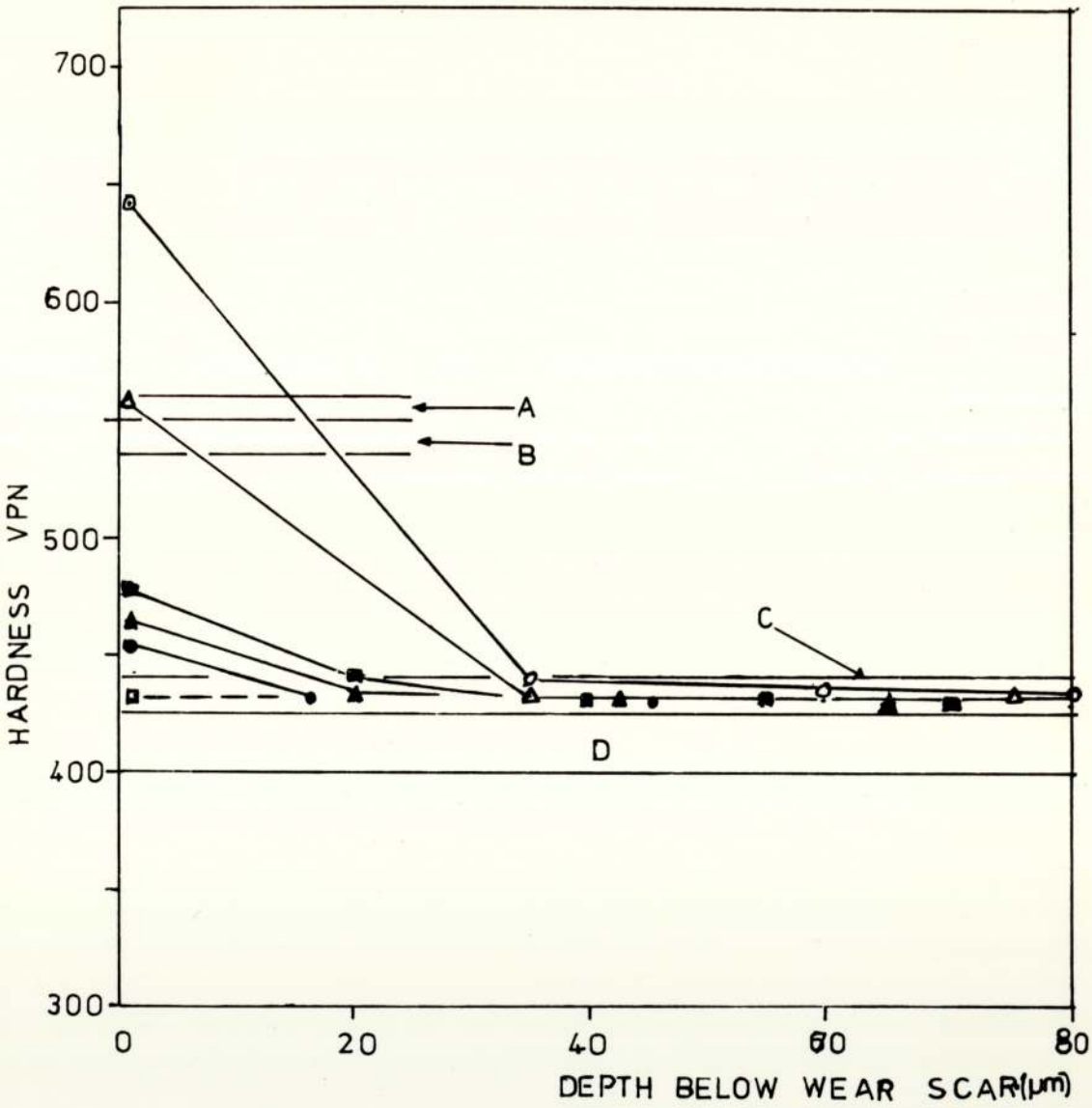

NOTATION	MATERIAL	NO OF CYCLE	CONDITION	REGION OF MEASUREMENT
—o—	NO·5	100	PLATED	HWR
—△—	"	100	"	LWR
—●—	"	1000	UNPLATED	HWR
—▲—	"	1000	"	LWR
—●—	"	100	"	HWR
—□—	"	100	"	LWR

a

Fig No

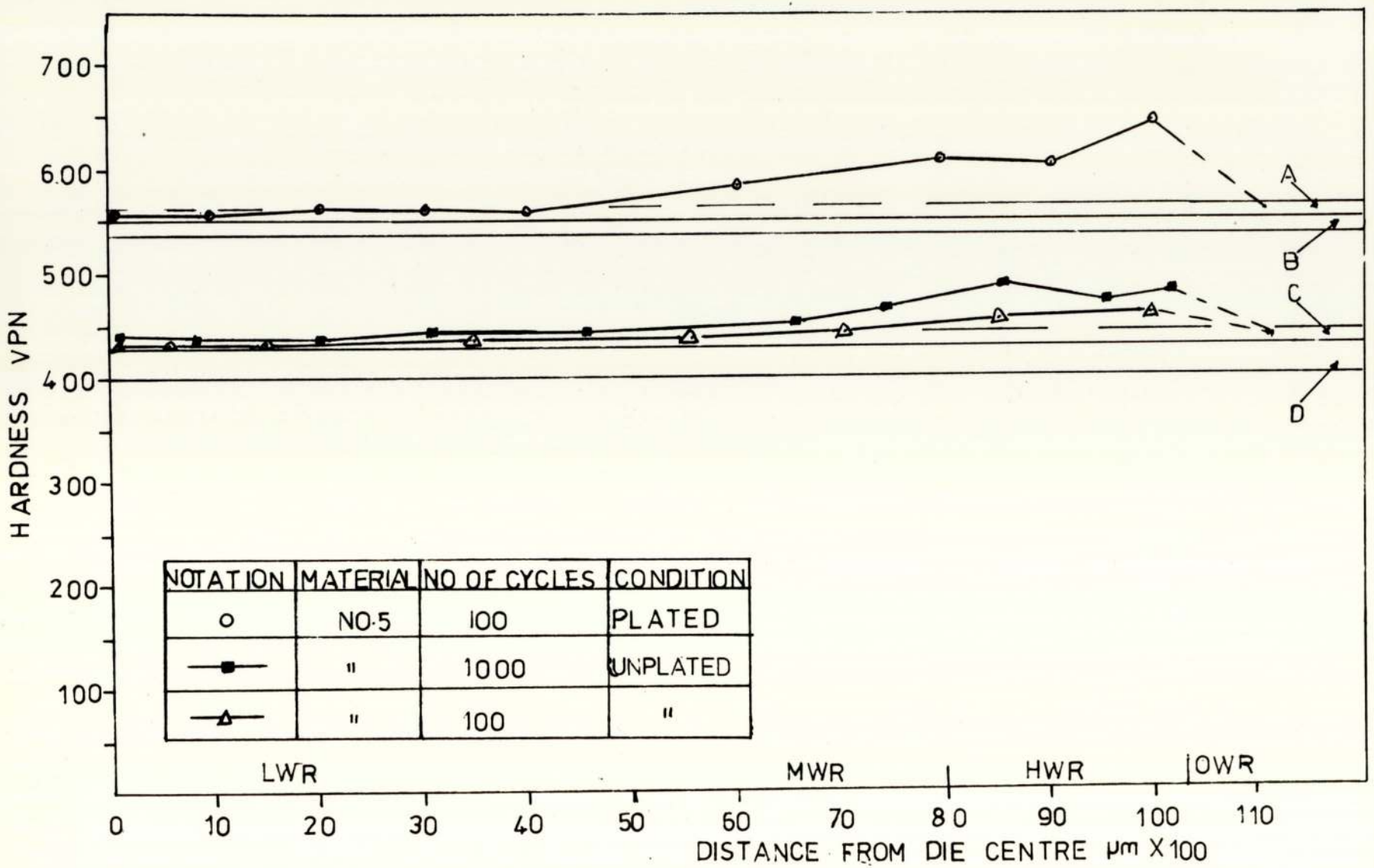
700
600
500
400
300
200
100
HARDNESS VPN
A
B
C
D
NOTATION | MATERIAL | NO OF CYCLES | CONDITION
o | NO·5 | 100 | PLATED
■ | " | 1000 | UNPLATED
△ | " | 100 | "
LWR
MWR
HWR
OWR
0 10 20 30 40 50 60 70 80 90 100 110
DISTANCE FROM DIE CENTRE μm X 100

b

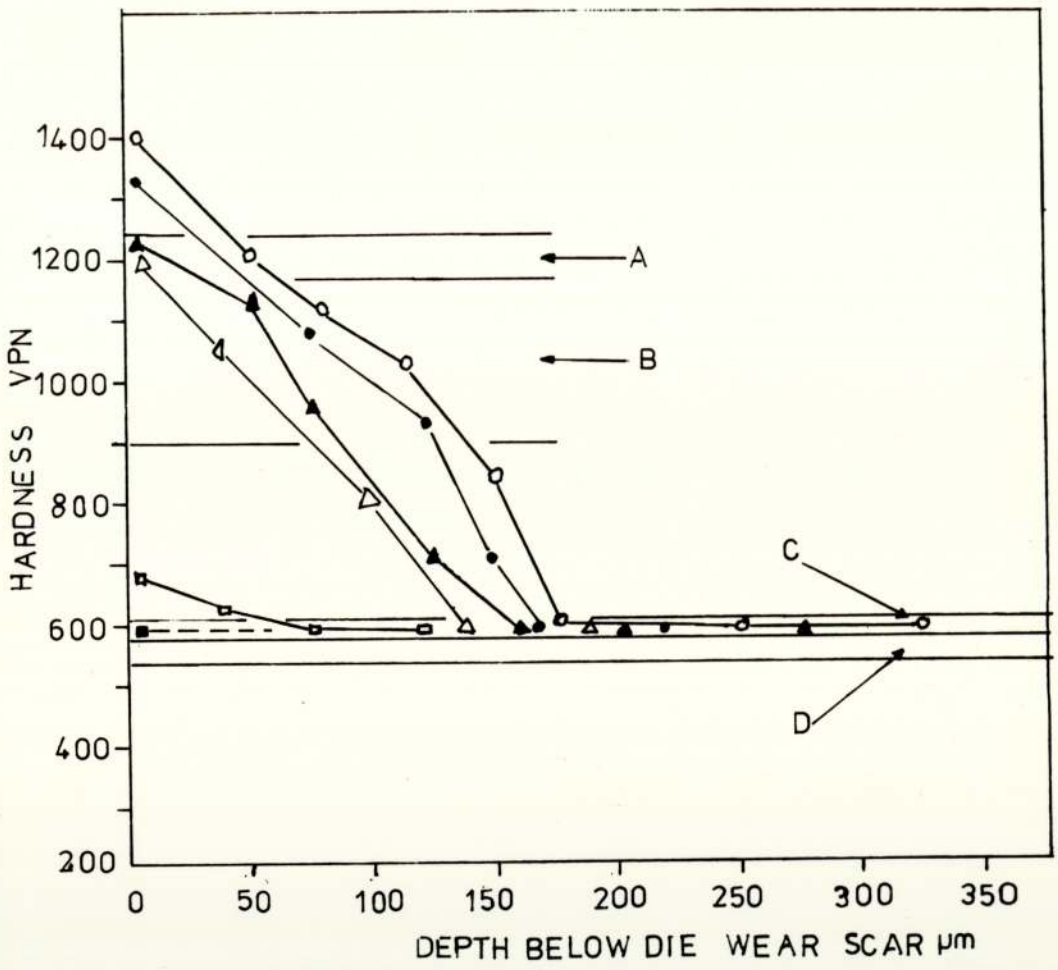

NOTATION	MATERIAL	NO OF CYCLE	CONDITION	REGION OF MEASUREMENT
—o—	HJ3	1000	NITRIDED	HWR
—▲—	"	1000	"	LWR
—●—	"	100	"	HWR
—△—	"	100	"	LWR
—□—	"	100	UNNITRIDED	HWR
--■--	"	100	"	LWR

C

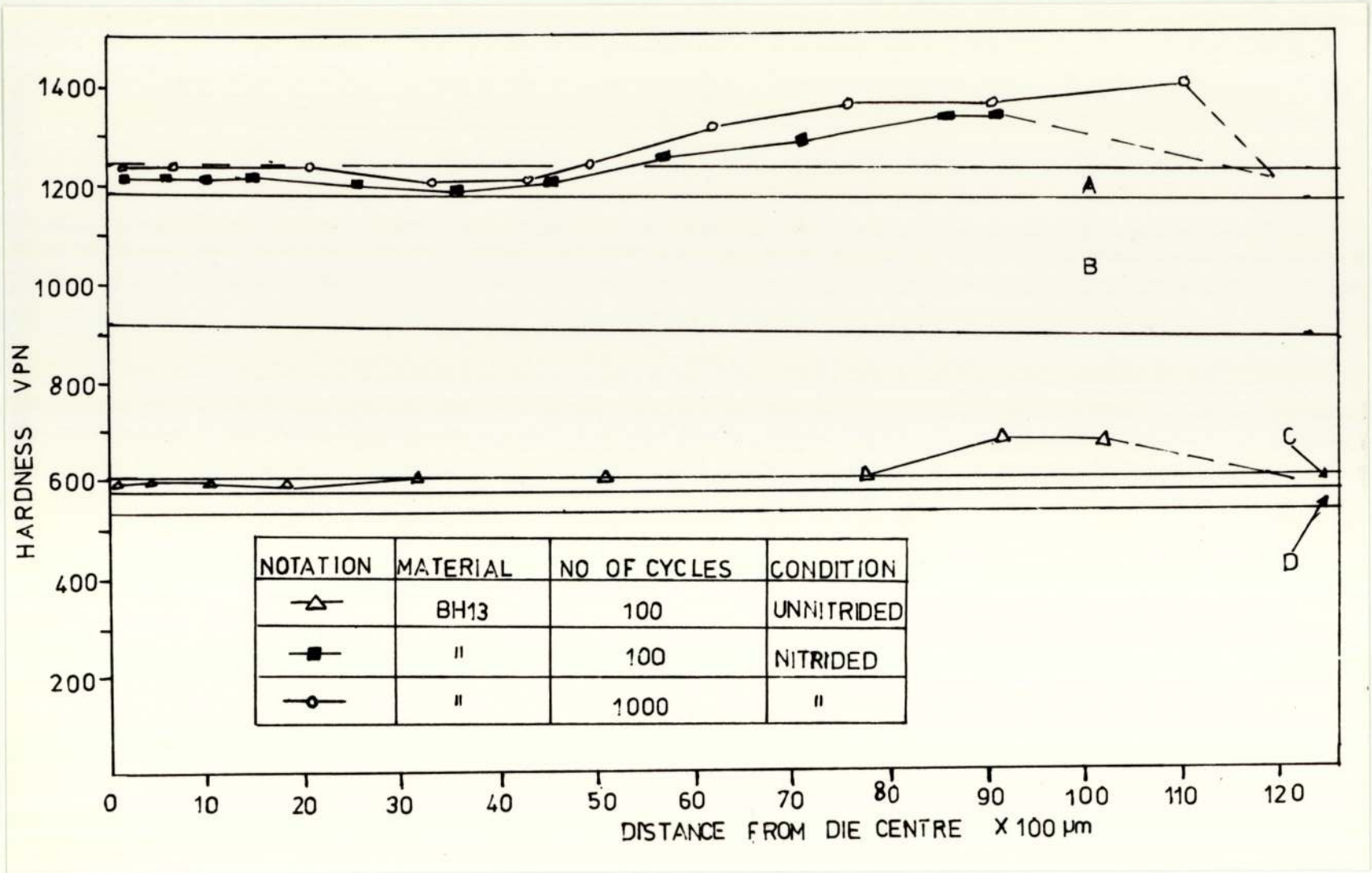
HARDNESS VPN
1400
1200
1000
800
600
400
200
A
B
C
D
0
10
20
30
40
50
60
70
80
90
100
110
120
DISTANCE FROM DIE CENTRE X 100 µm
NOTATION | MATERIAL | NO OF CYCLES | CONDITION
BH13 | 100 | UNNITRIDED
" | 100 | NITRIDED
" | 1000 | "

Fig. 54 Variation of hardness (a) below and (b) across the worn surface of No.5 die in its hardened and tempered and surface treated conditions.

Variation of hardness (c) below and (d) across the worn surface of BH13 die in its hardened and tempered and surface treated conditions.

A. Hardness range of coating or case of the region outside HWR after forging.

B. Hardness range of coating or case of the region outside HWR before forging.

C. Hardness range of the hardened and tempered die in the region outside HWR after forging.

D. Hardness range of the hardened and tempered die in the region outside HWR before forging.

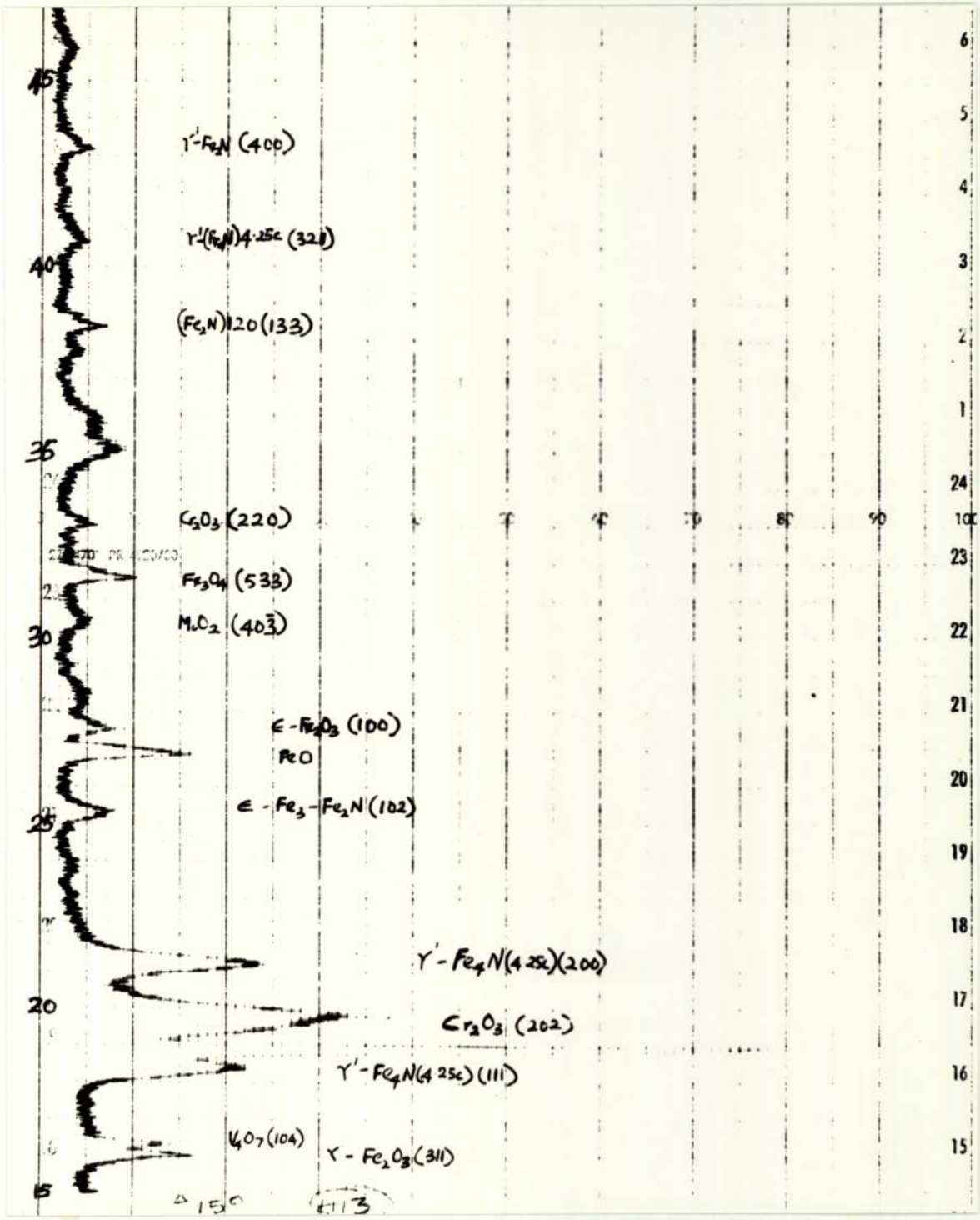
γ'-Fe4N (400)
γ'-(Fe4N)4.25c (328)
(Fe4N)120 (133)
Cr2O3 (220)
Fe3O4 (533)
MoO2 (403)
ε-Fe2O3 (100)
FeO
ε-Fe3-Fe2N (102)
γ'-Fe4N(4.25c)(200)
Cr2O3 (202)
γ'-Fe4N(4.25c)(111)
Mo4O7(104)
γ-Fe2O3(311)
45
40
35
30
25
20
15
6
5
4
3
2
1
24
23
22
21
20
19
18
17
16
15

a

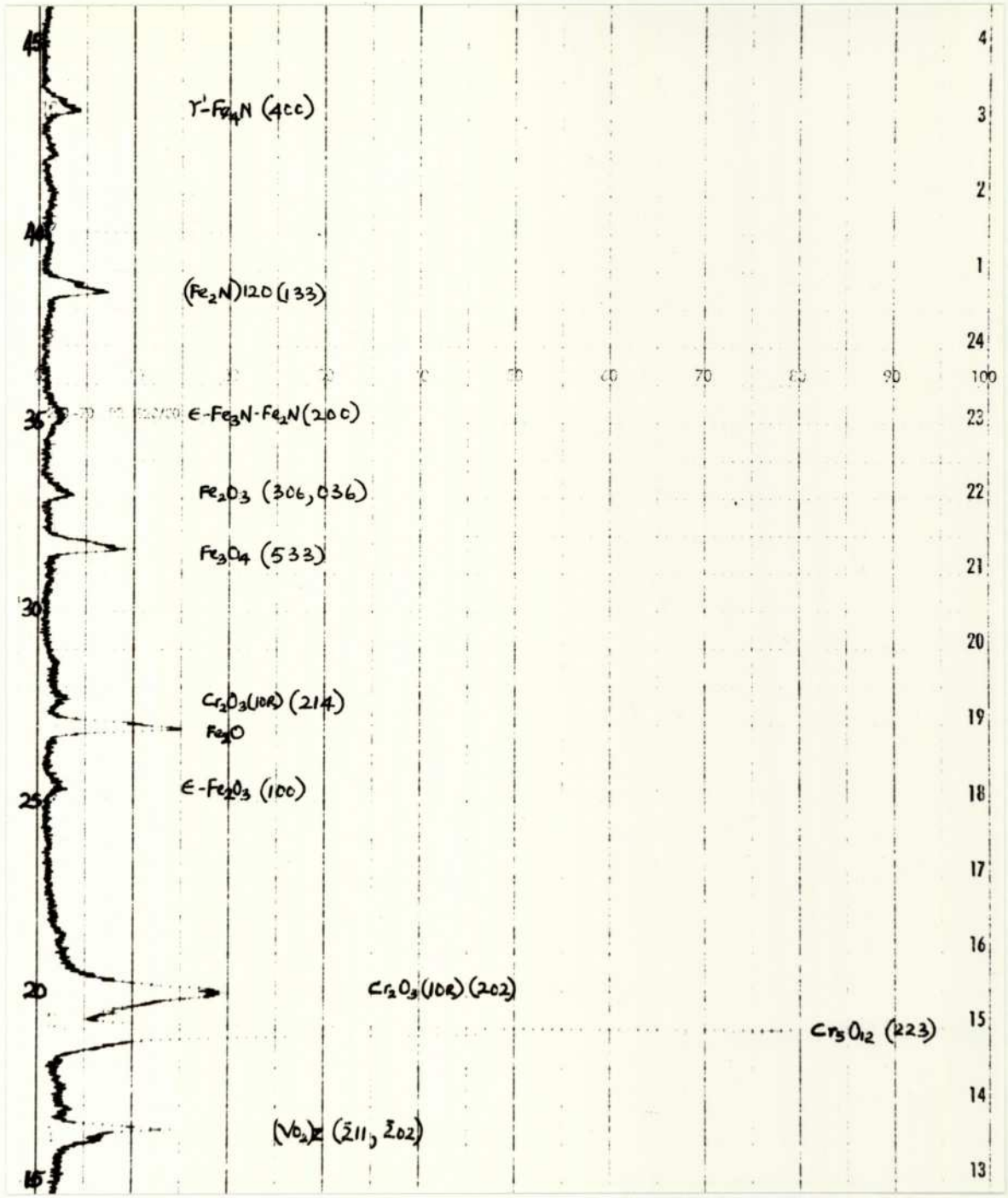
γ'-Fe4N (400)
(Fe2N)120 (133)
ε-Fe3N-Fe2N (200)
Fe2O3 (306, 036)
Fe3O4 (533)
Cr2O3(10R) (214)
Fe2O
ε-Fe2O3 (100)
Cr2O3(10R) (202)
Cr3O12 (223)
(VO2)2 (211, 202)
45
40
35
30
25
20
15
4
3
2
1
24
23
22
21
20
19
18
17
16
15
14
13

b

Fig. 55 X-ray powder diffraction traces of oxide glaze on
(a) plasma nitrided and
(b) Tufftrided BH13 die after 100 cycles hot forging.

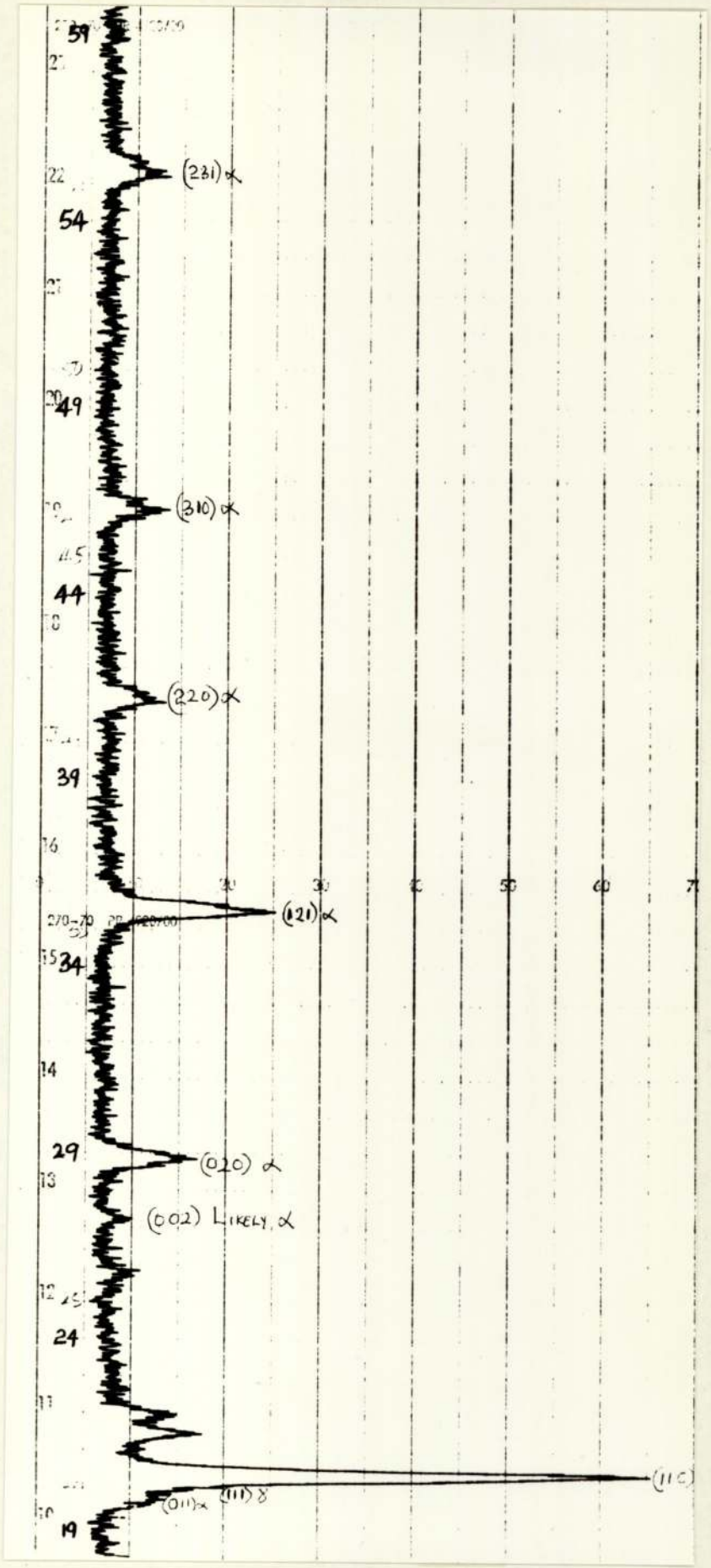
59
54
49
44
39
34
29
24
19
(231) α
(310) α
(220) α
(121) α
(020) α
(002) LIKELY α
(011) α
(111) β
(110)

a

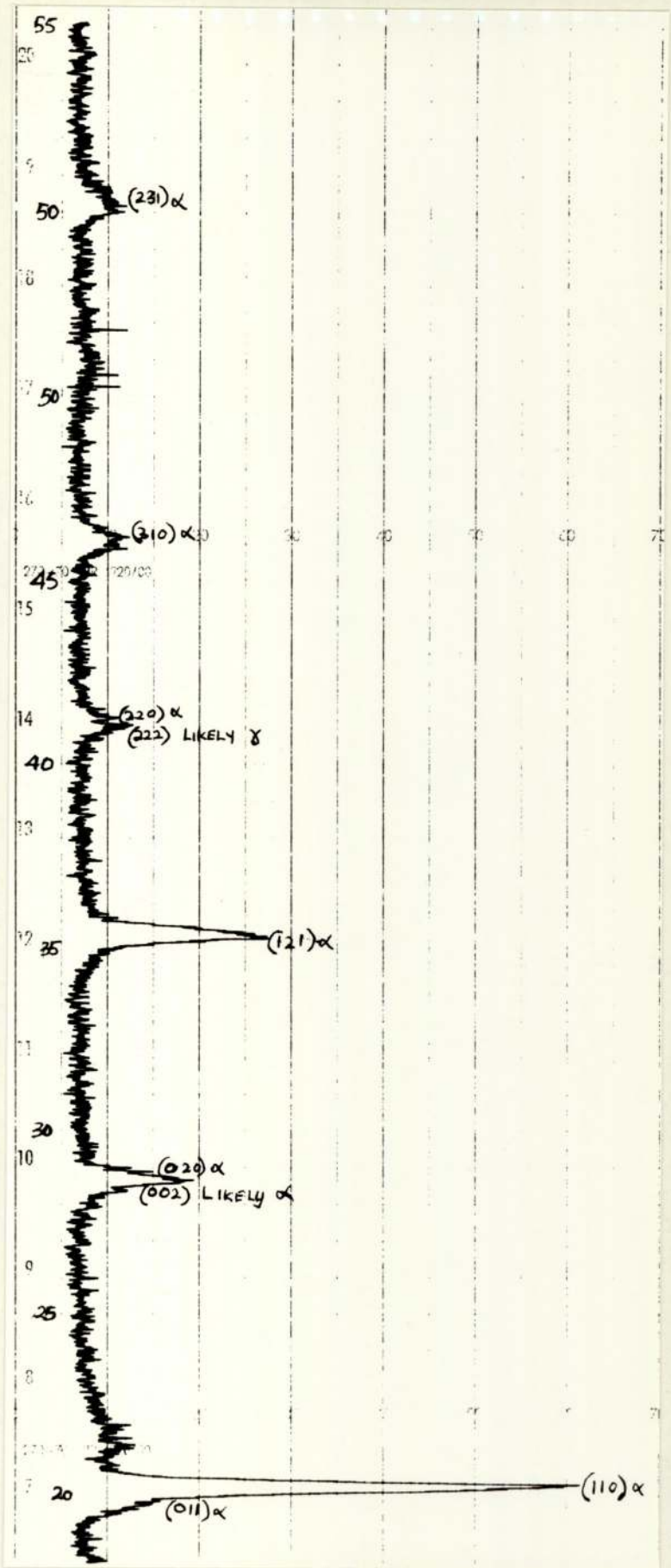
55
50
50
45
14
40
35
30
10
25
20
(231)α
(310)α
(220)α
(222) LIKELY γ
(121)α
(020)α
(002) LIKELY α
(110)α
(011)α

b

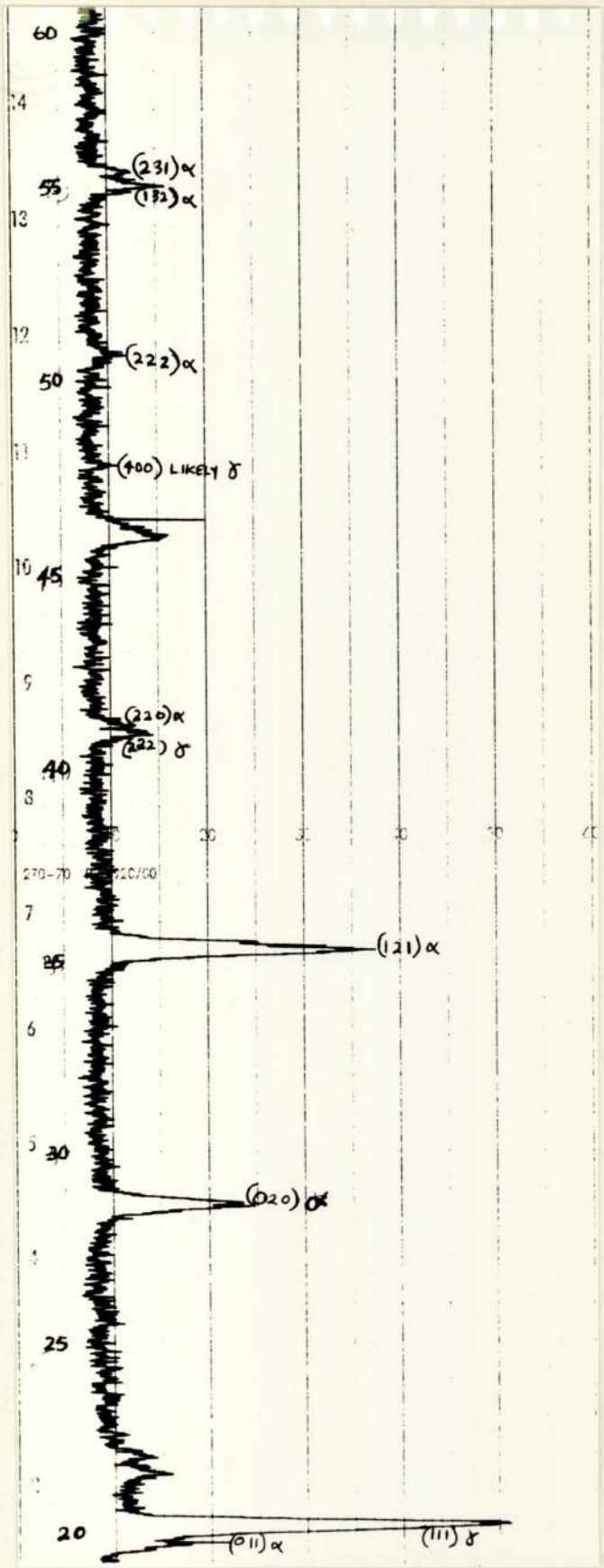

C

Fig. 56 X-ray powder diffraction traces of retained austenite in die after heat treatment.

(a) BH 13

(b) and (c)+ No.5

+ die was heat treated by Still and Dennis [24].

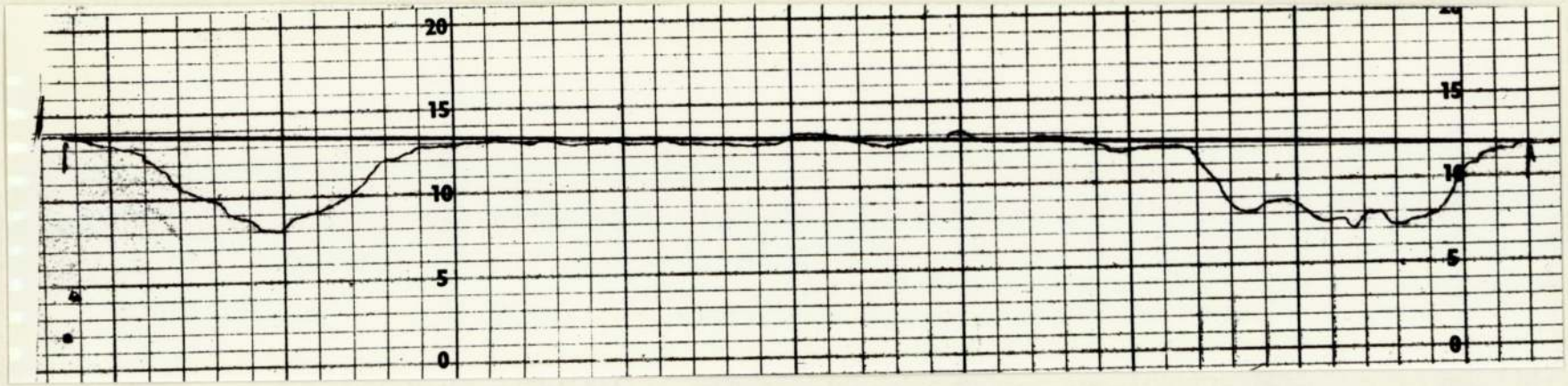
20
15
10
5
0
15
10
5
0

a

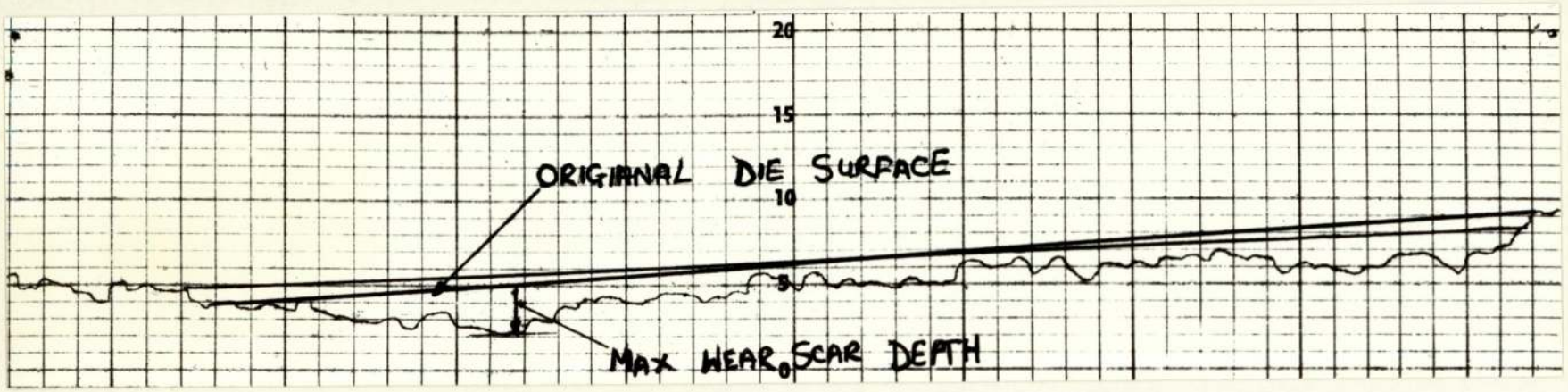
20
15
10
5
ORIGINAL DIE SURFACE
MAX WEAR SCAR DEPTH

b

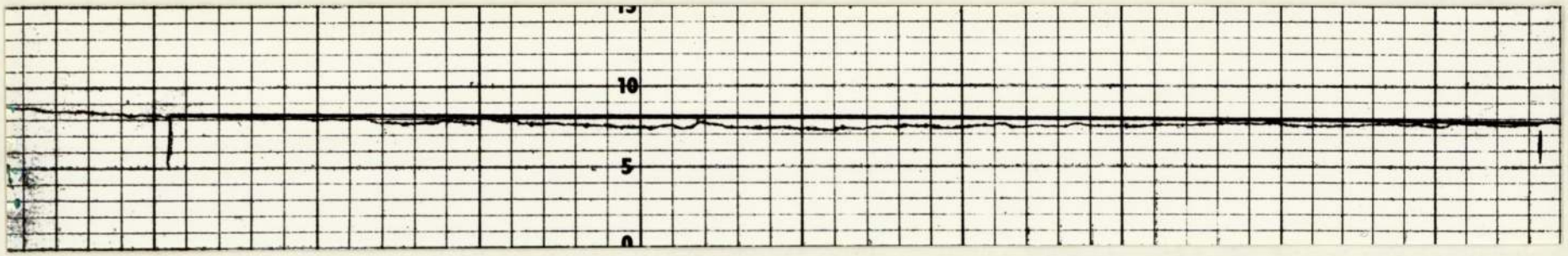

c

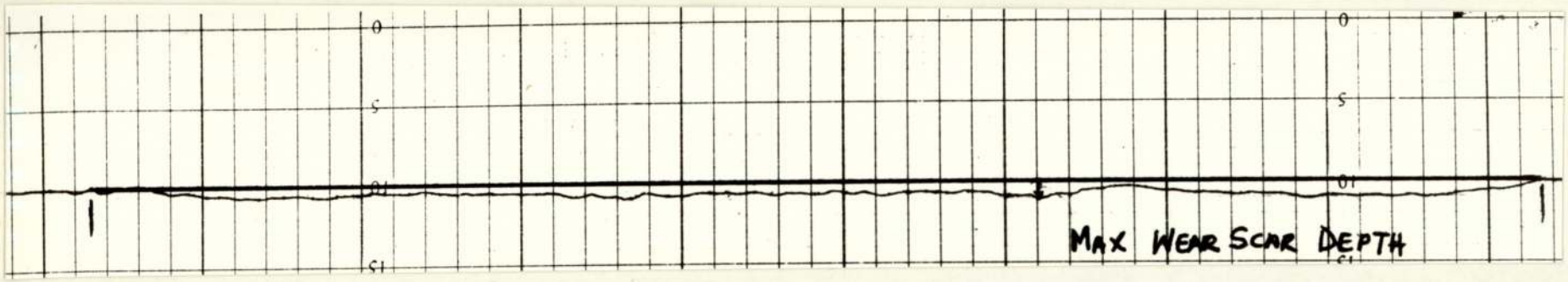

d

Fig. 57 Talylin wear scar traces of

(a) hardened and tempered No.5 die after 1000 cycles hot forging. Vertical Mag. X400

(b) Co-Mo alloy plated No.5 die after 100 cycles hot forging. Vertical Mag. X4000.

(c) hardened and tempered BH13 die after 100 cycles hot forging. Vertical mag. X1000.

(d) Plasma nitrided BH13 die after 1000 cycles hot forging. Vertical mag. X1000.

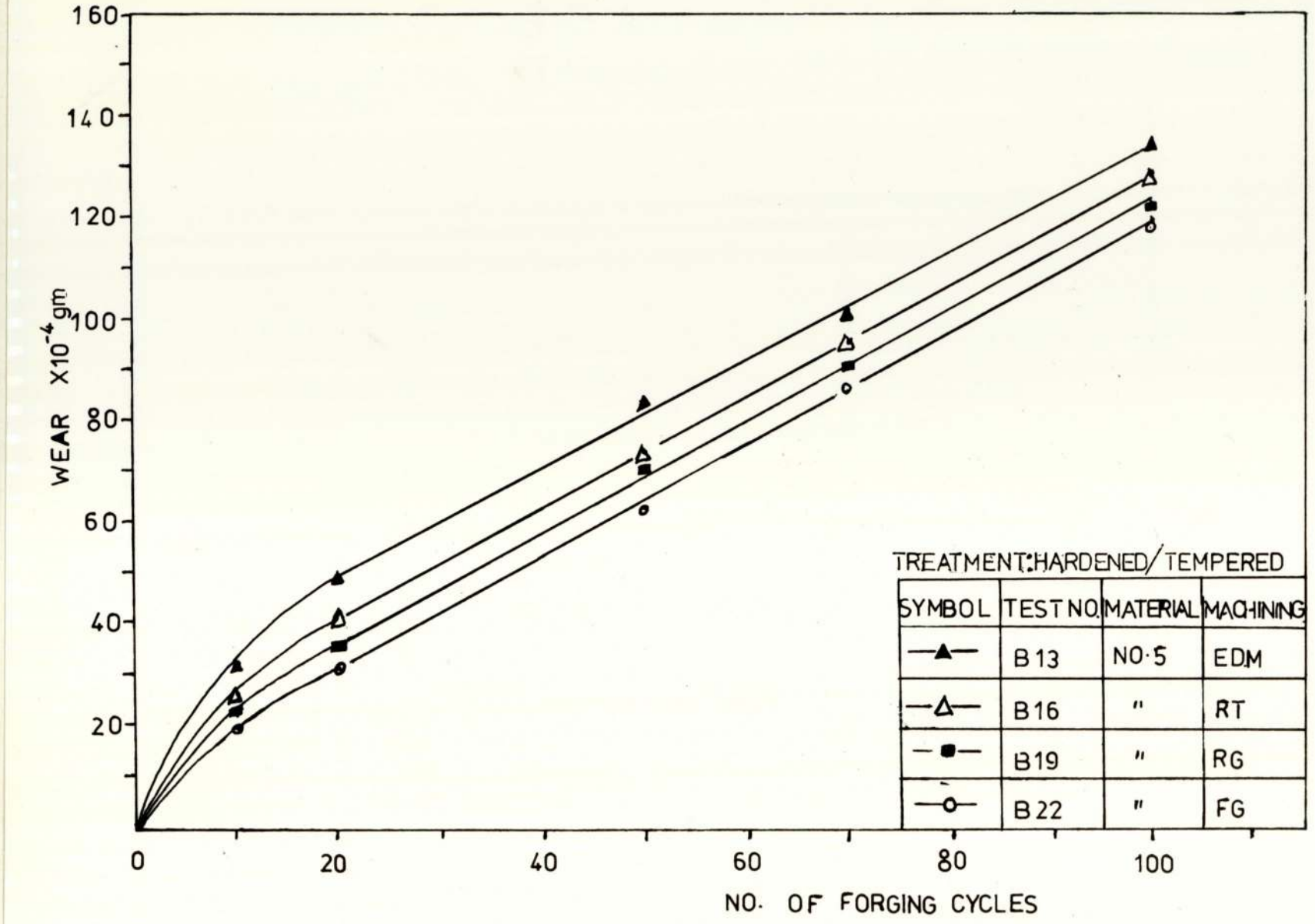
160
140
120
100
80
60
40
20
WEAR X10^{-4}gm
0
20
40
60
80
100
NO. OF FORGING CYCLES
TREATMENT: HARDENED/TEMPERED
SYMBOL | TEST NO. | MATERIAL | MACHINING
B13 | NO·5 | EDM
B16 | " | RT
B19 | " | RG
B22 | " | FG

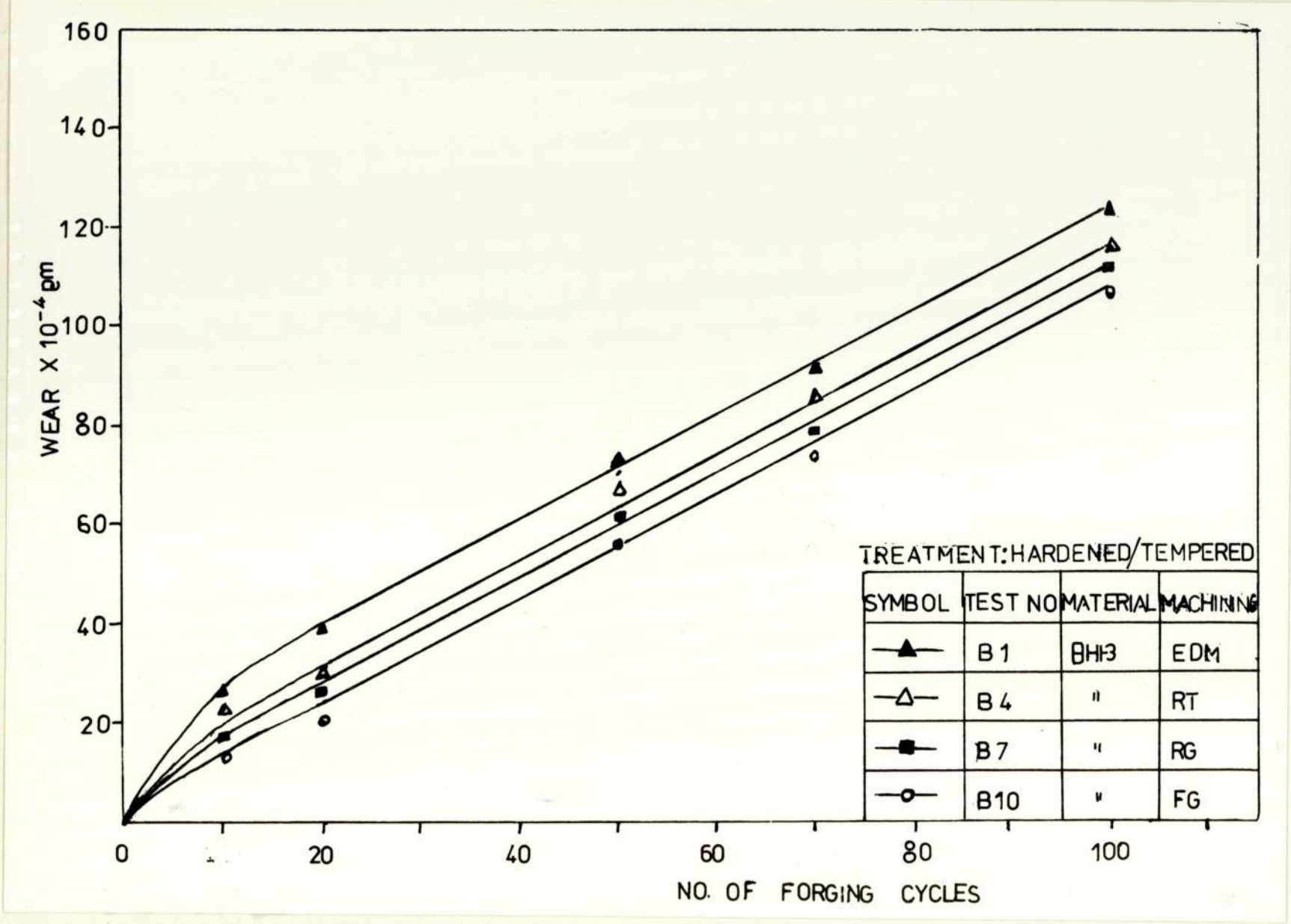
160
140
120
100
80
60
40
20
WEAR X 10^{-4} gm
0
20
40
60
80
100
NO. OF FORGING CYCLES
TREATMENT: HARDENED/TEMPERED
SYMBOL | TEST NO | MATERIAL | MACHINING
B1 | BHI3 | EDM
B4 | " | RT
B7 | " | RG
B10 | " | FG

b

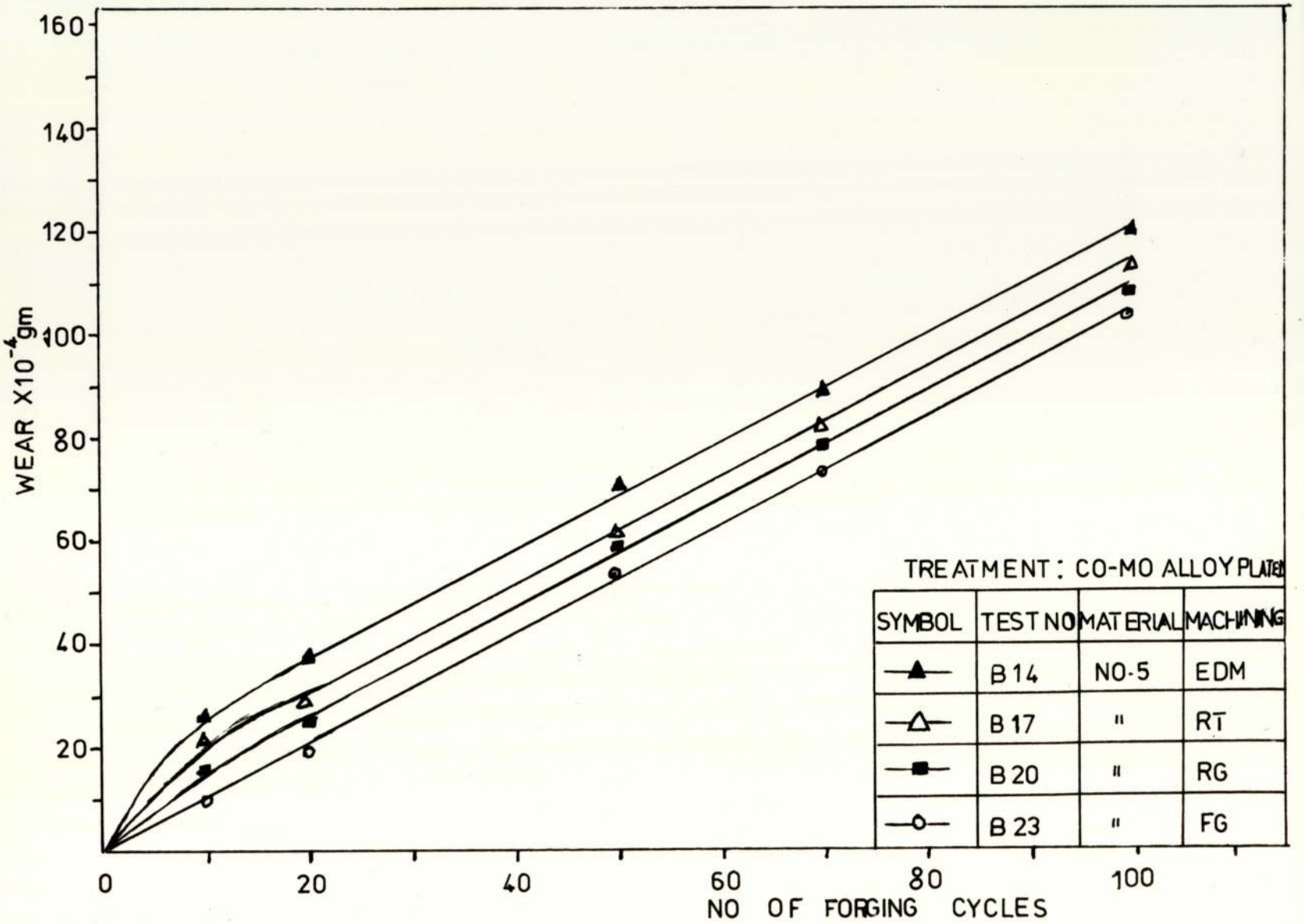
160
140
120
100
80
60
40
20
WEAR X10^{-4}gm
0
20
40
60
80
100
NO OF FORGING CYCLES
TREATMENT : CO-MO ALLOY PLATED
SYMBOL
TEST NO
MATERIAL
MACHINING
B 14
NO-5
EDM
B 17
"
RT
B 20
"
RG
B 23
"
FG

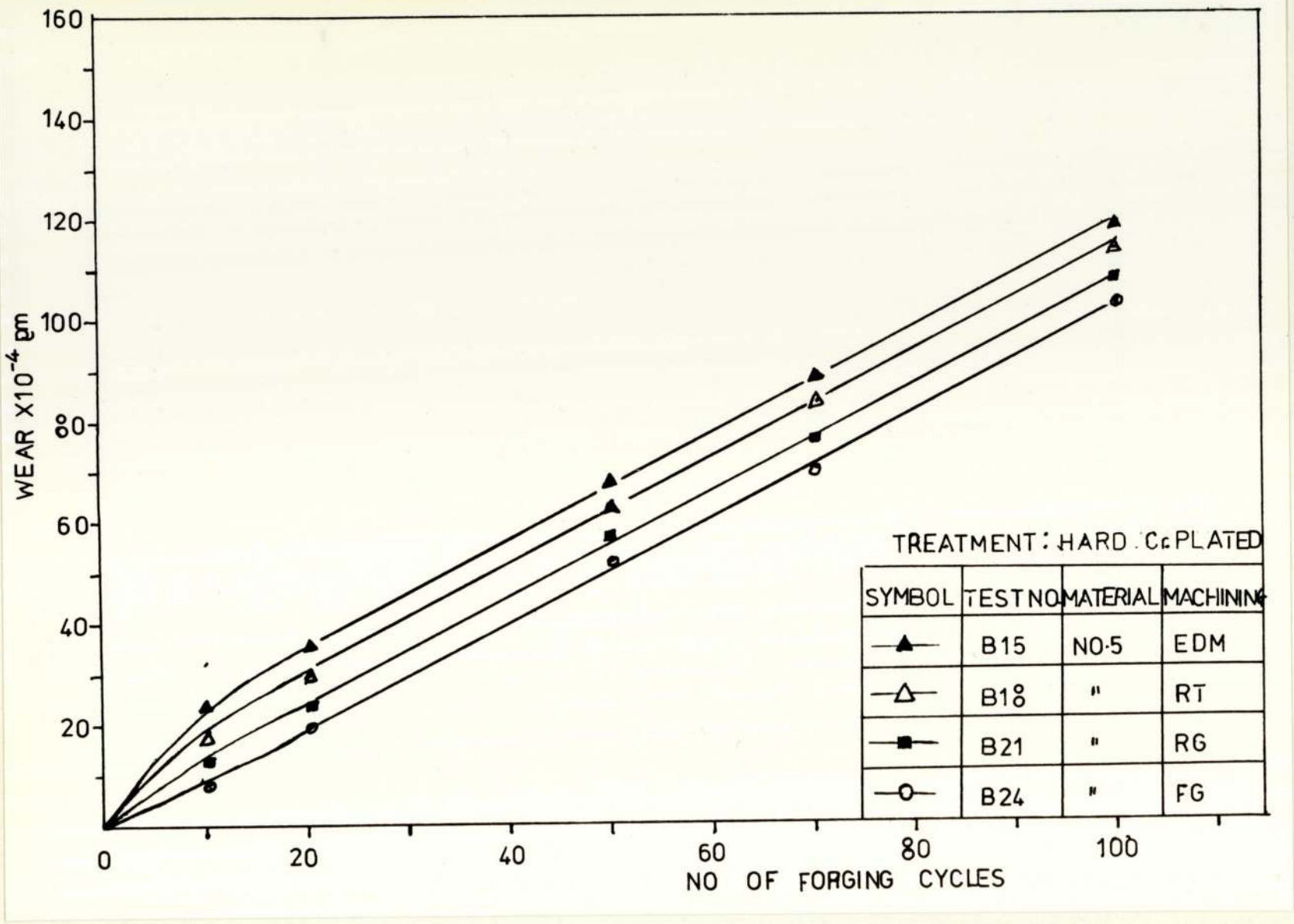
WEAR X10^{-4} gm
160
140
120
100
80
60
40
20
0
20
40
60
80
100
NO OF FORGING CYCLES
TREATMENT : HARD . Cr. PLATED
SYMBOL | TEST NO | MATERIAL | MACHINING
B15 | NO·5 | EDM
B18 | " | RT
B21 | " | RG
B24 | " | FG

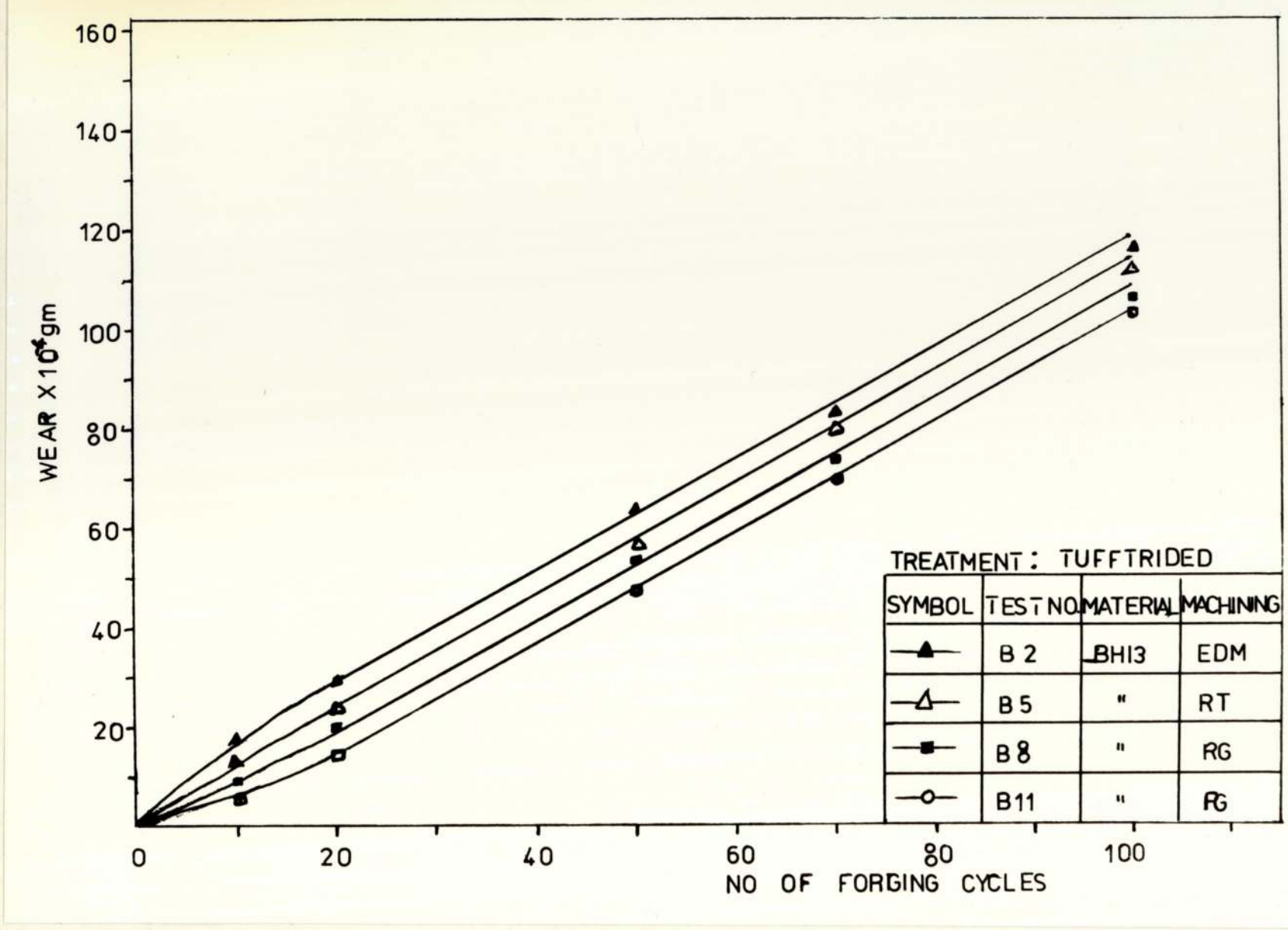
WEAR X 10⁴gm
160
140
120
100
80
60
40
20
0
20
40
60
80
100
NO OF FORGING CYCLES
TREATMENT : TUFFTRIDED
SYMBOL | TEST NO. | MATERIAL | MACHINING
B 2 | BH13 | EDM
B 5 | " | RT
B 8 | " | RG
B11 | " | RG

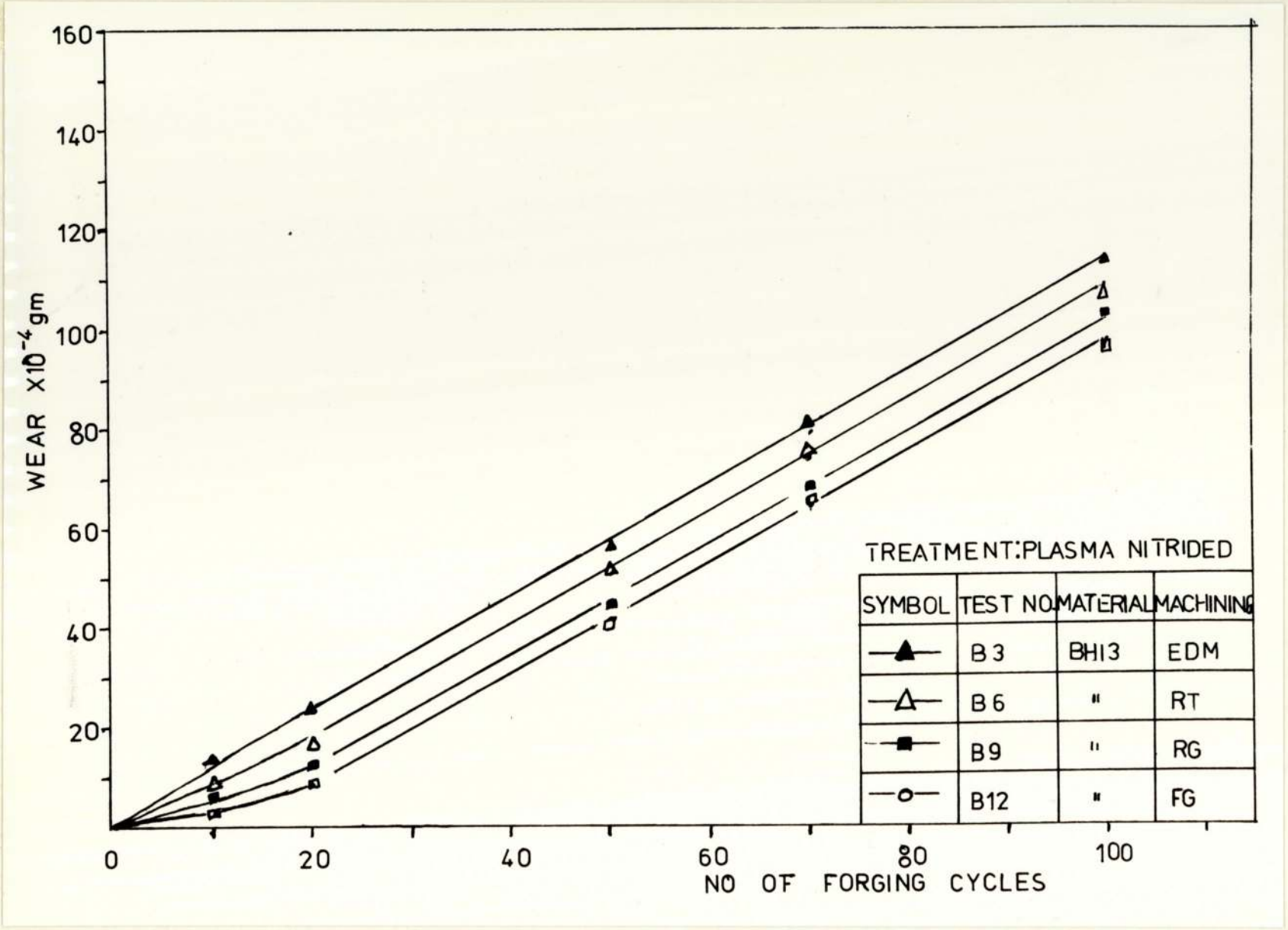
160
140
120
100
80
60
40
20
WEAR X10⁻⁴gm
0
20
40
60
80
100
NO OF FORGING CYCLES
TREATMENT:PLASMA NITRIDED
SYMBOL
TEST NO.
MATERIAL
MACHINING
B3
BHI3
EDM
B6
"
RT
B9
"
RG
B12
"
FG

Fig. 58 Die wear versus number of forging cycles

(a) hardened and tempered No.5

(b) hardened and tempered BH13

(c) Co-Mo alloy plated No.5

(d) hard Cr plated No.5

(e) Tufftrided BH13

(f) Plasma nitrided BH13

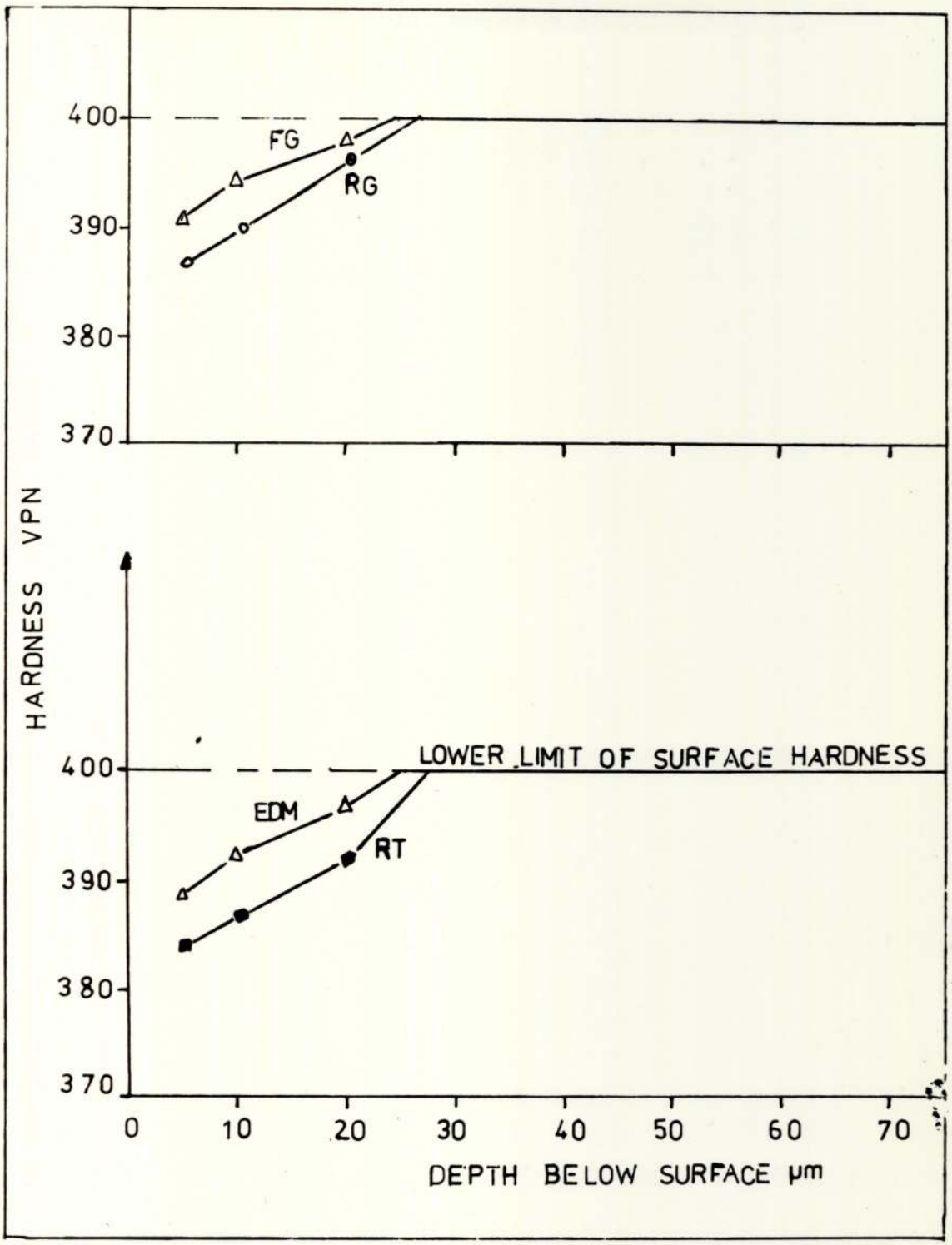
400
390
380
370
FG
RG
HARDNESS VPN
LOWER LIMIT OF SURFACE HARDNESS
EDM
RT
0
10
20
30
40
50
60
70
DEPTH BELOW SURFACE μm

a

b b

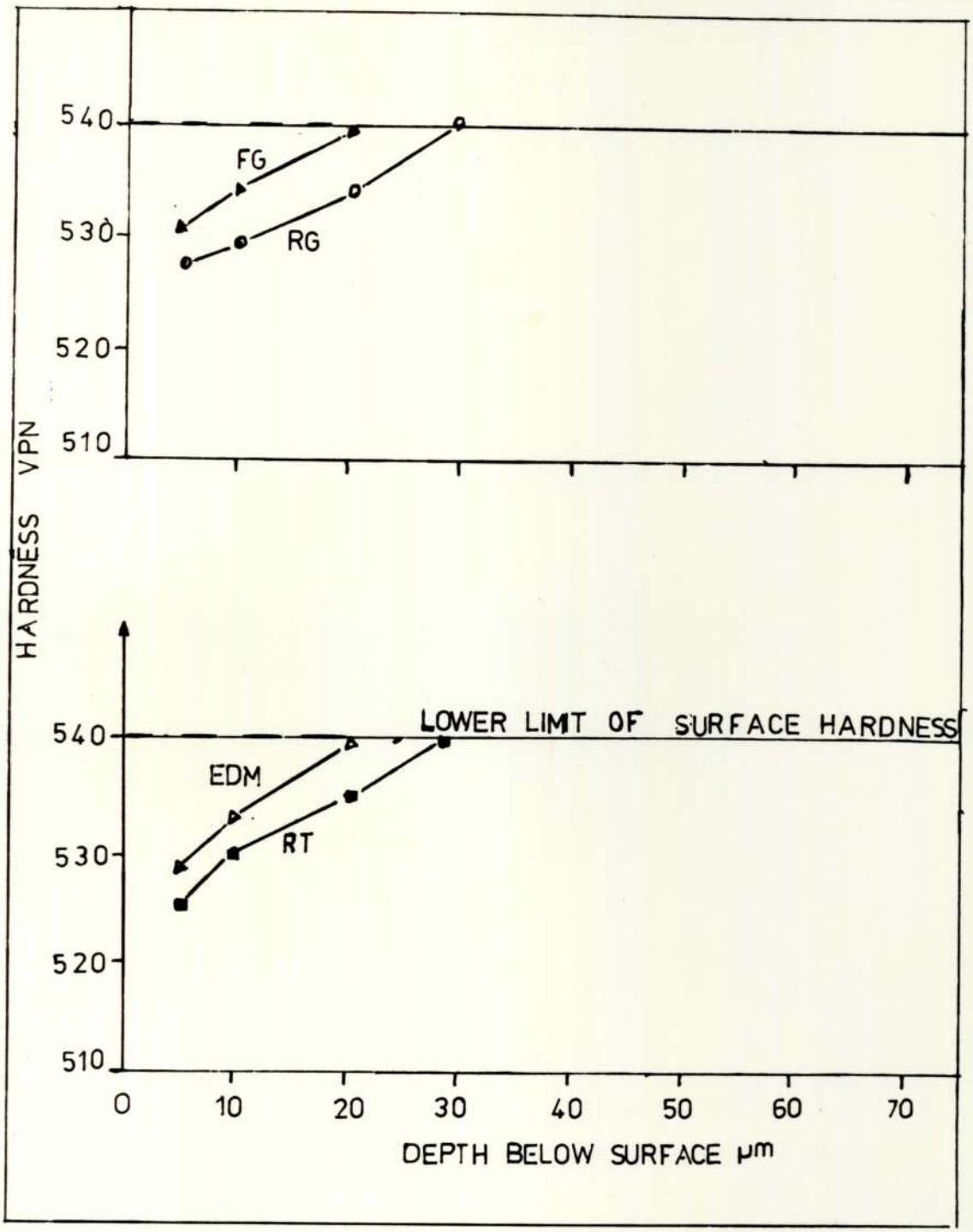
HARDNESS VPN
540
530
520
510
FG
RG
LOWER LIMIT OF SURFACE HARDNESS
EDM
RT
0
10
20
30
40
50
60
70
DEPTH BELOW SURFACE μm

c

d

Fig. 59 Effect of machining on subsurface hardness of dies before forging.

(a) and (b) show the variations in No.5 die, while

(c) and (d) show the variations in BH13

FG: Finish ground. RG: Rough ground

RT: Rough turn EDM: Electro-discharge machining.

a

b

c

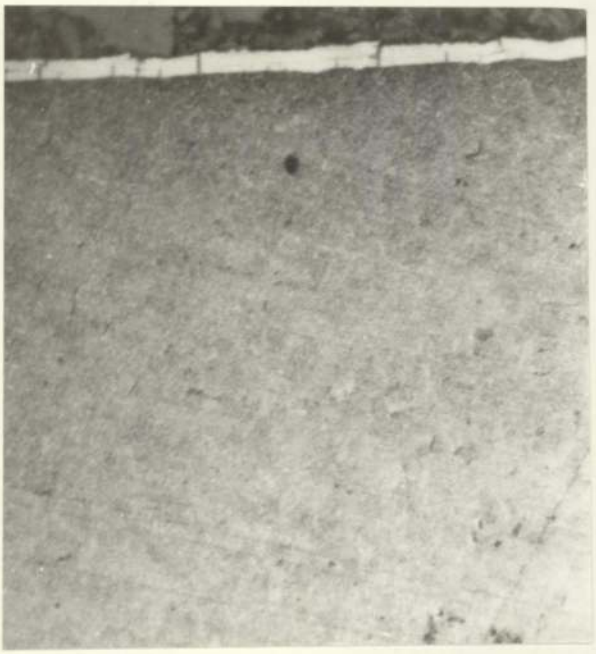

d

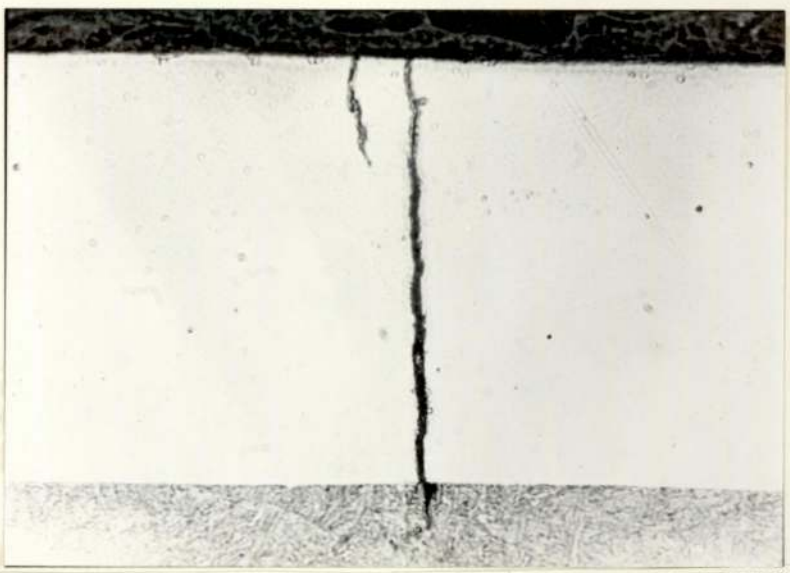

e

Fig. 60 Effect of thermal cycling on plasma nitrided BH13 die after

(a) 500 cycles at 500°C, mag x 249

(b) 1000 cycles at 750°C, Mag x 123

(c) 2000 cycles at 750°C, Mag x 123

(d) Co-Mo alloy brush plated No.5 die after 1000 cycles at 500°C. Mag. X345.

(e) bath plated Co-Mo alloy No.5 die after 1000 cycles at 500°C. Magnificant including taper x 1000 (after still and Dennis[24]).

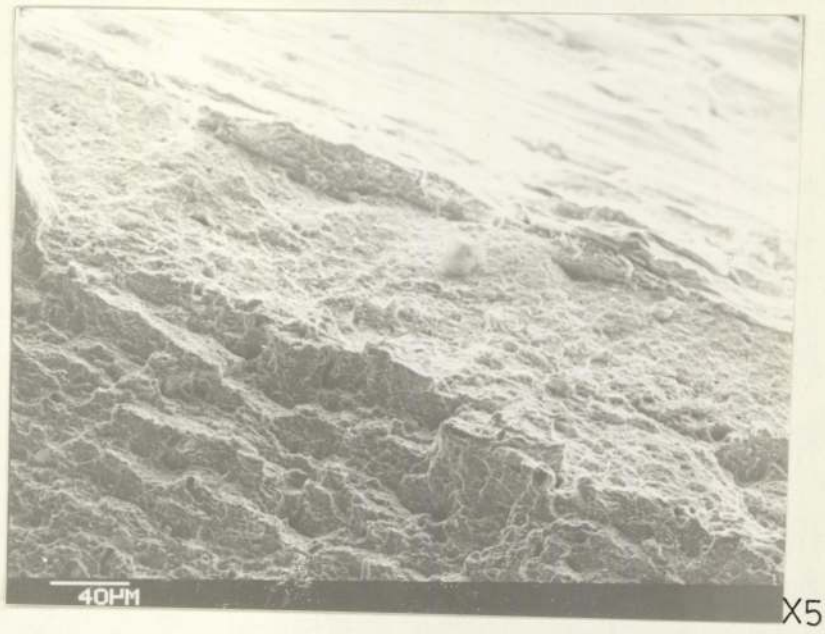

Fig. 61 S.E.M. fractograph showing a mixture of void coalescence and cleavage near the notch root of a hard Cr plated No.5 die steel impact testpiece.

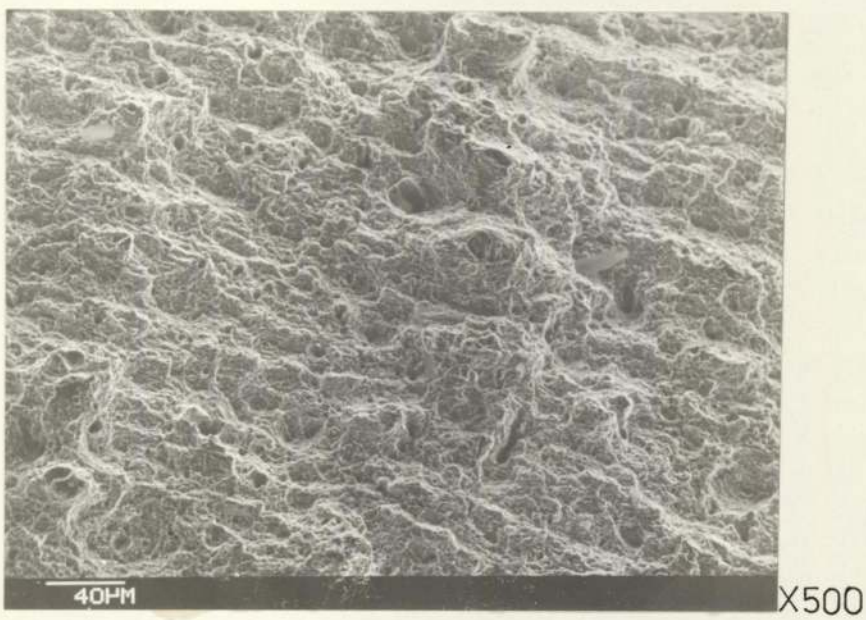

Fig. 62 S.E.M. fractograph showing large and small dimples in the core of a hard Cr plated No.5 die steel impact testpiece.

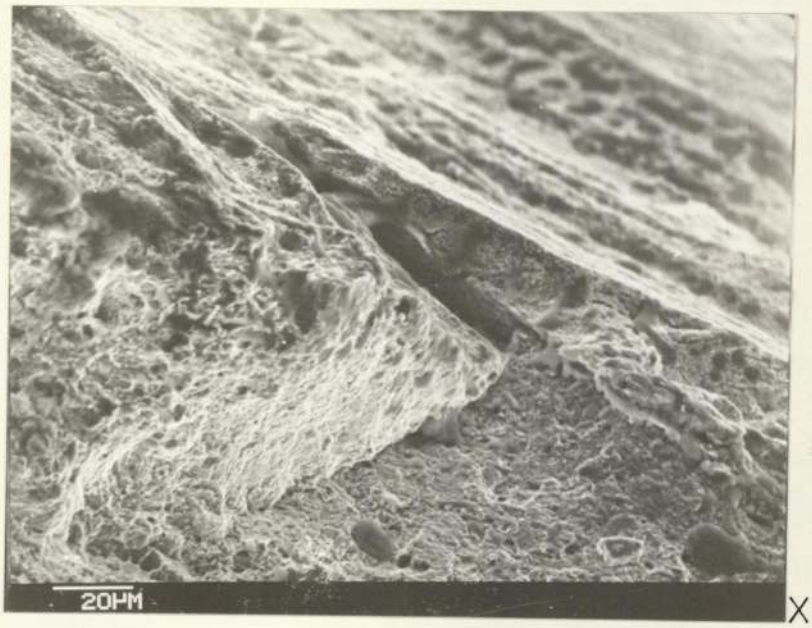

Fig.63 S.E.M. fractograph showing a mixture of dimples and tearing near the notch root of a hard Cr plated No.5 die steel impact testpiece.

a

Fig. 64 Three views of the fracture surface of a hard Cr plated No.5 die steel impact testpiece showing -

(a) the edge of the testpiece

(b) a mixture of cleavage plus tearing

(c) an enlargement of one of the tear ridges

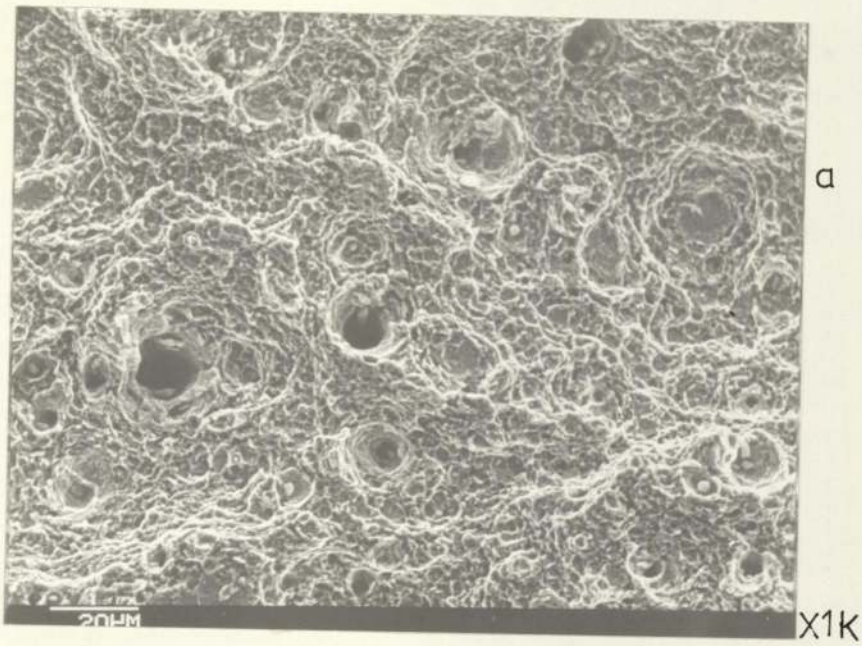

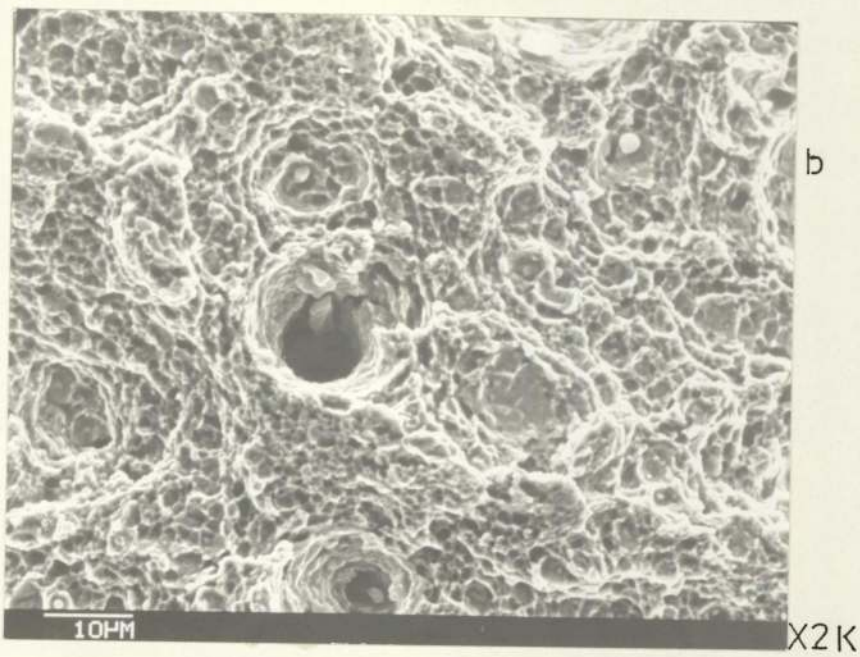

Fig. 65 Two views of the fracture surface of a hard Cr plated No.5 die steel impact testpiece showing -

(a) several large and small dimples

(b) an enlargement of the central dimples together with the inclusions associated with them taking ahead of the rear ridges in fig. 64.

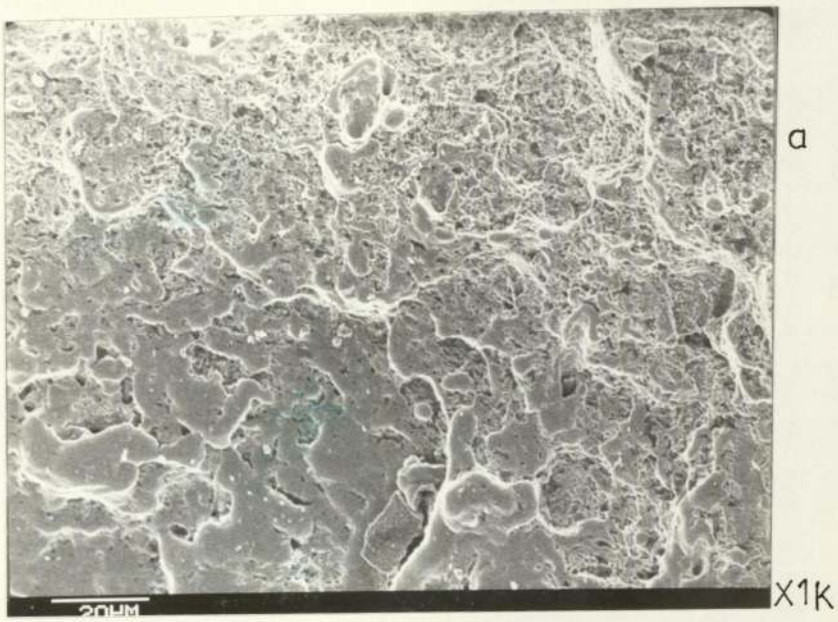

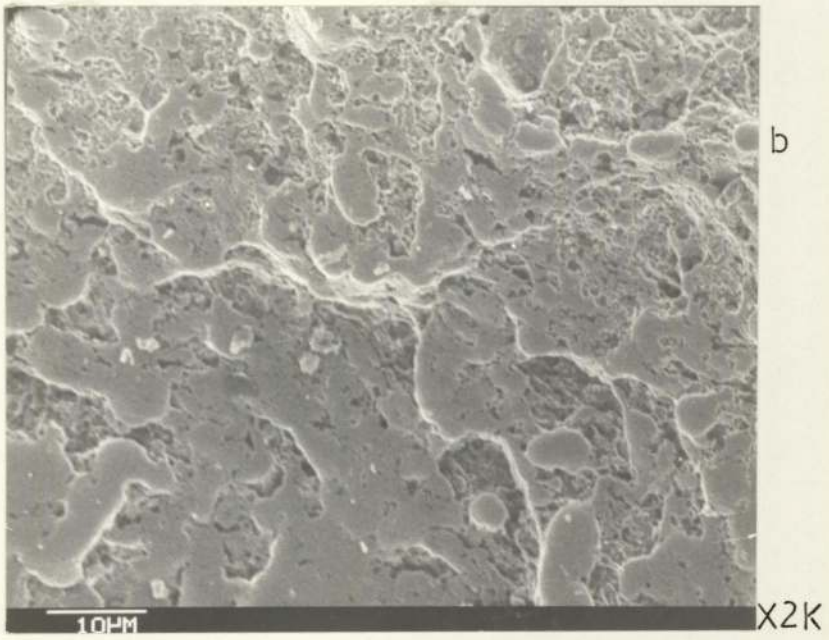

Fig. 66 Two views of the fracture surface of a Co-Mo alloy plated No.5 die steel impact testpiece, showing cleavage facets near the notch root. (b) is an enlargement of the central cleavage step in (a)

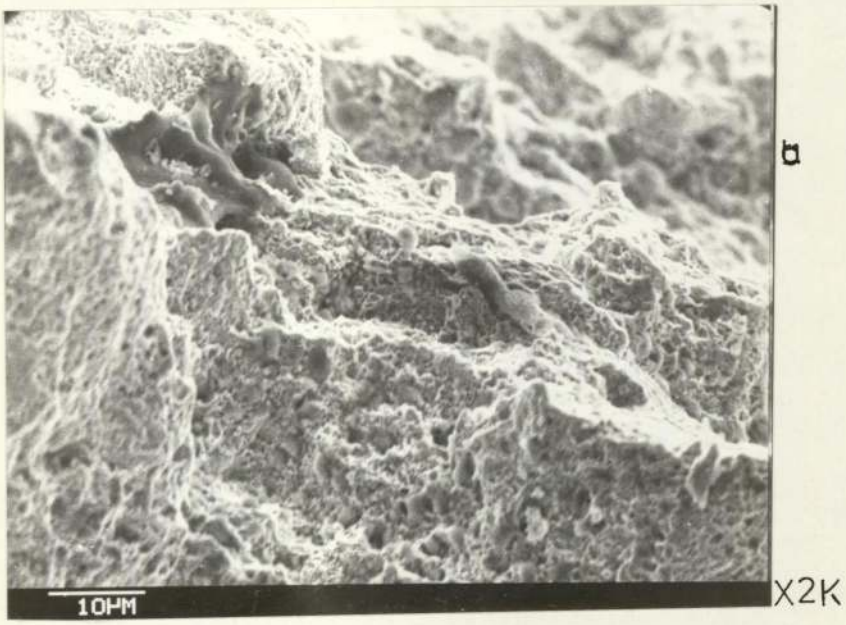

Fig. 67 Two views of the fracture surface of a Co-Mo alloy plated No.5 die steel impact testpiece showing intermingled brittle-cleavage plus dimples. (b) is an enlargement of the central region of (a) which further reveals the dimples.

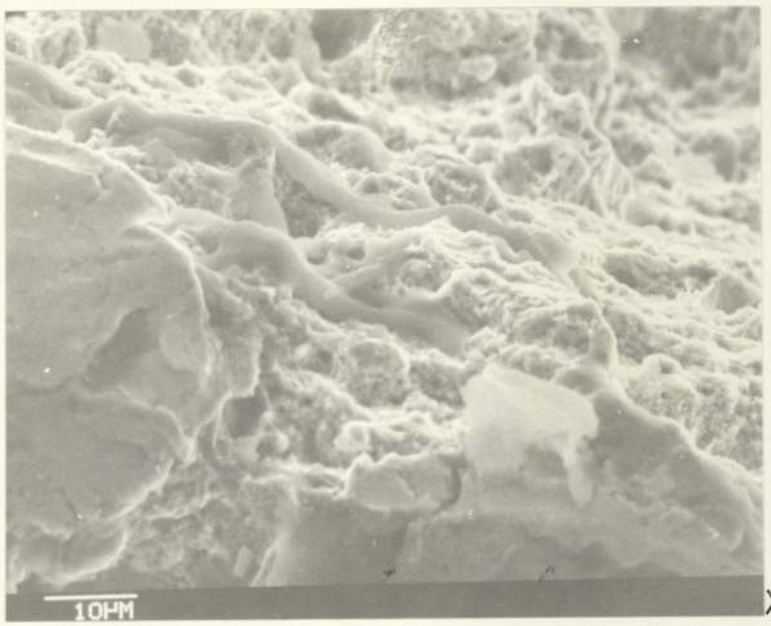

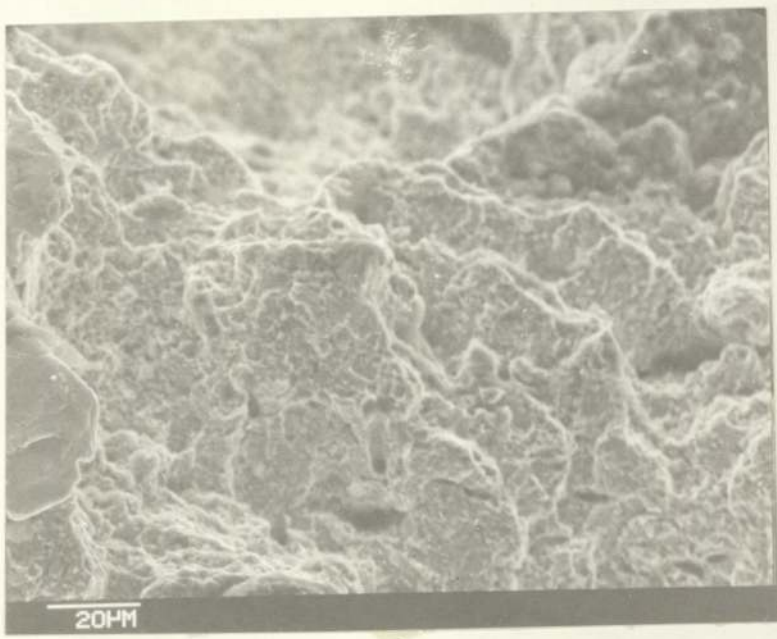

Fig. 68 Two views of the fracture surface of a Ni-Palloy plated No.5 die steel impact testpiece, showing -

(a) the river patterns of cleavage and the direction of crack propagation (corresponds to the direction in which the river pattern meet).

(b) brittle failure below region in (a).

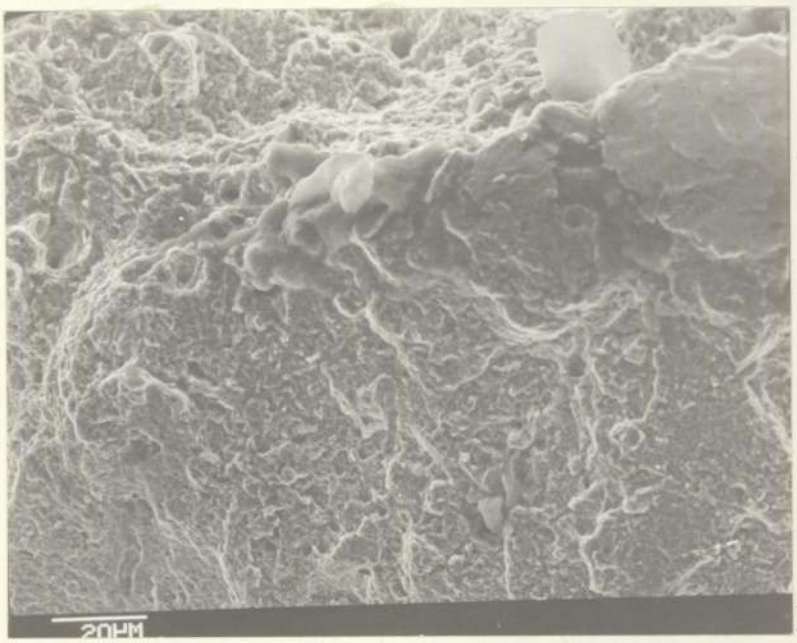

Fig. 69 S.E.M. fractograph of a Ni-P alloy plated No.5 die steel impact testpiece showing a mixture of cleavage plus dimples.

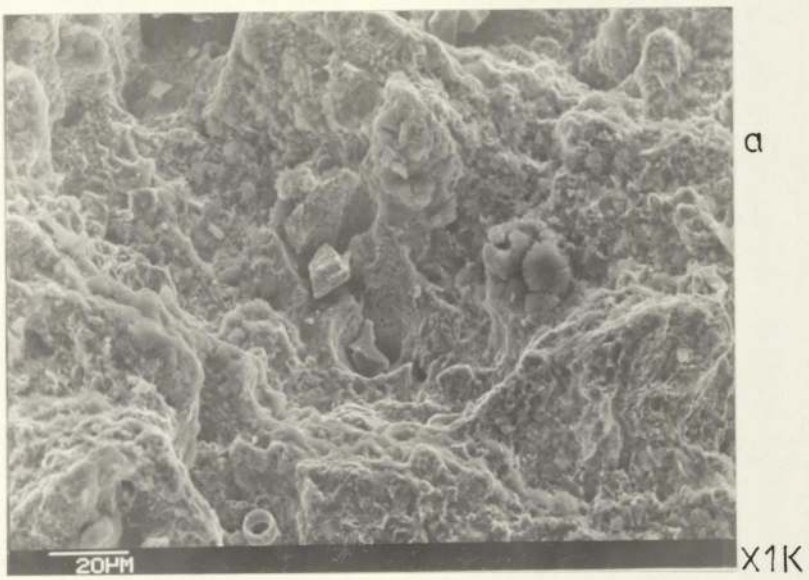

a

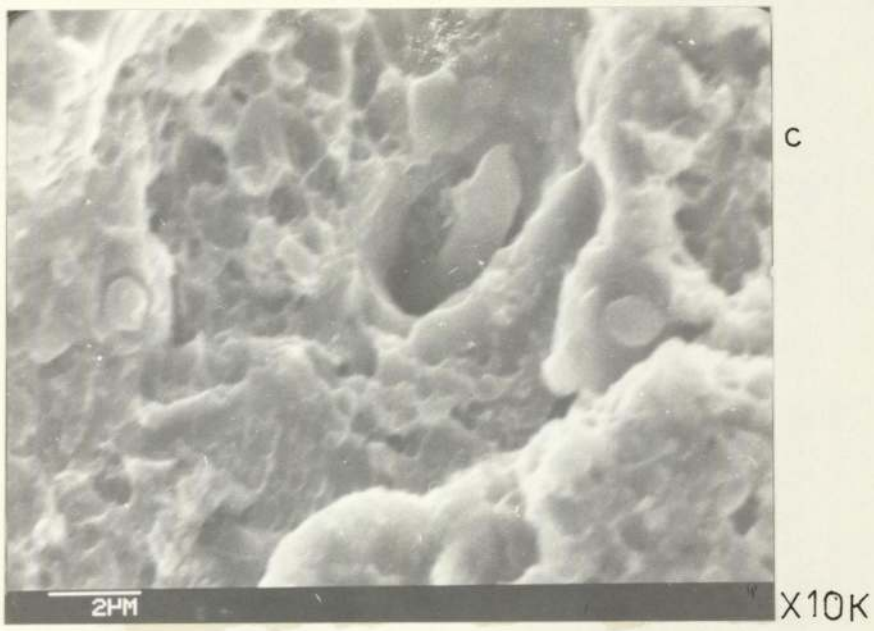

Fig. 70 S.E.M. fractographs of a Ni-P alloy plated No.5 die steel impact testpiece showing -

(a) ductile failure

(b) a stringer trough

(c) a fractured stringer of the base of its trough

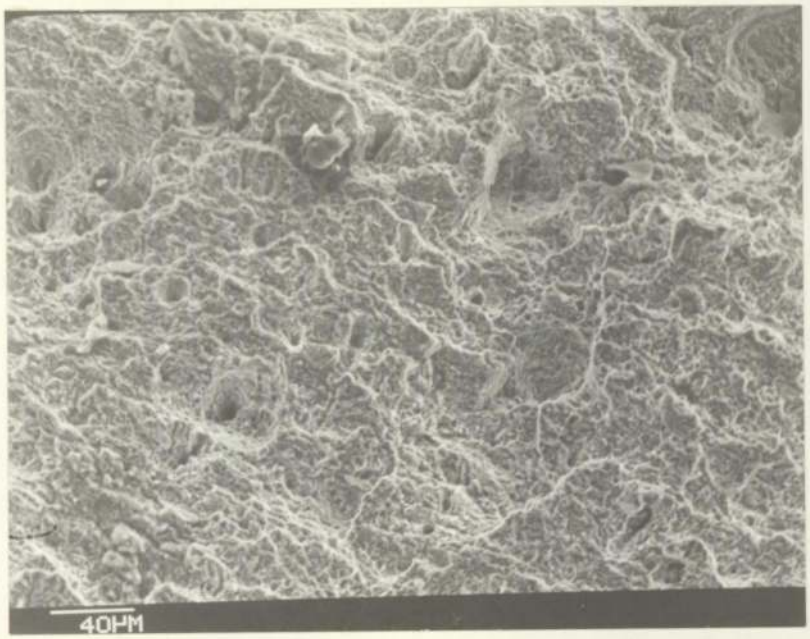

Fig. 71 S.E.M. fractographs of a hardened and tempered No.5 die steel impact testpiece showing ductile plus intermingled brittle failure areas. (b) is a higher magnification of the central region of (a)

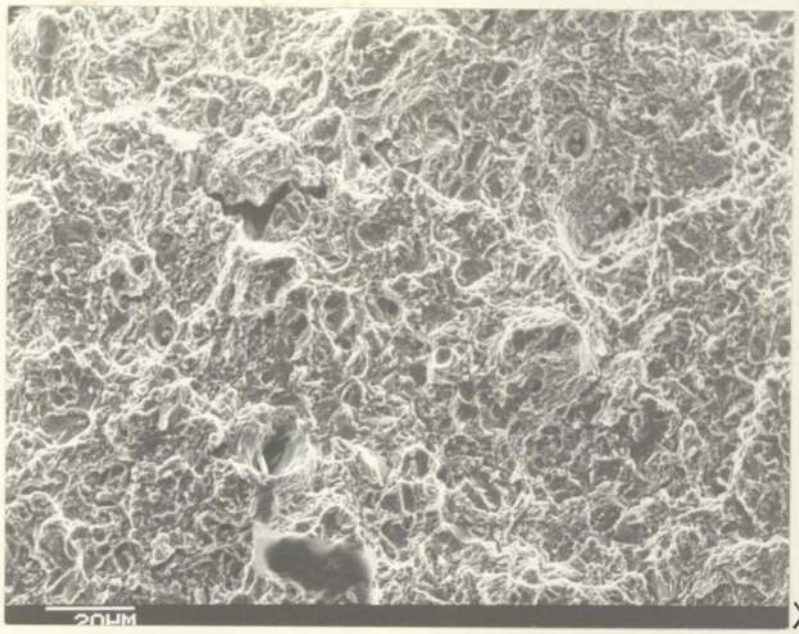

a

X1K

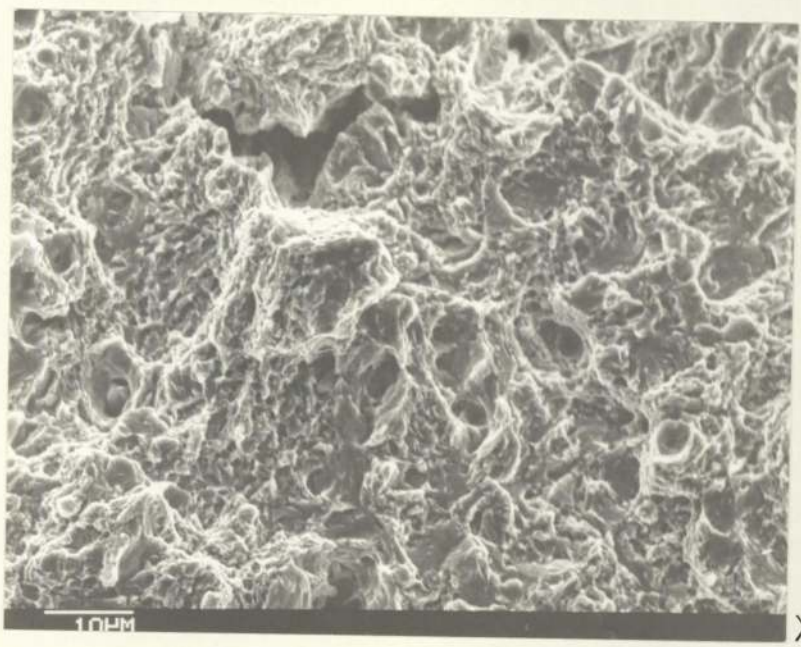

b

X2K

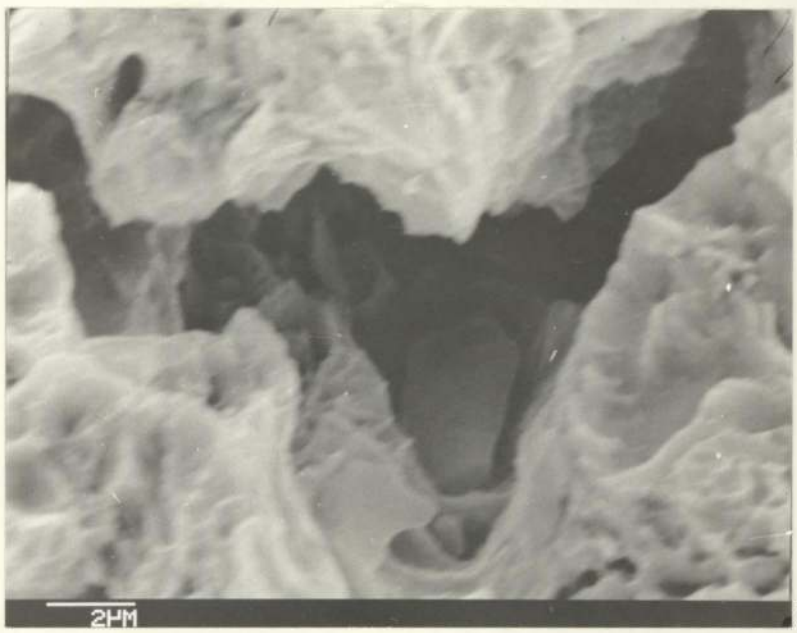

Fig. 72 S.E.M. fractographs of a micro-cracked Cr plated No.5 die steel impact testpiece showing void coalescence.

(a) shows a micro-void opening out as secondary crack

(b) is an enlargement of otherdimples around the void in (a)

(c) shows the inclusion associated with the void in (a)

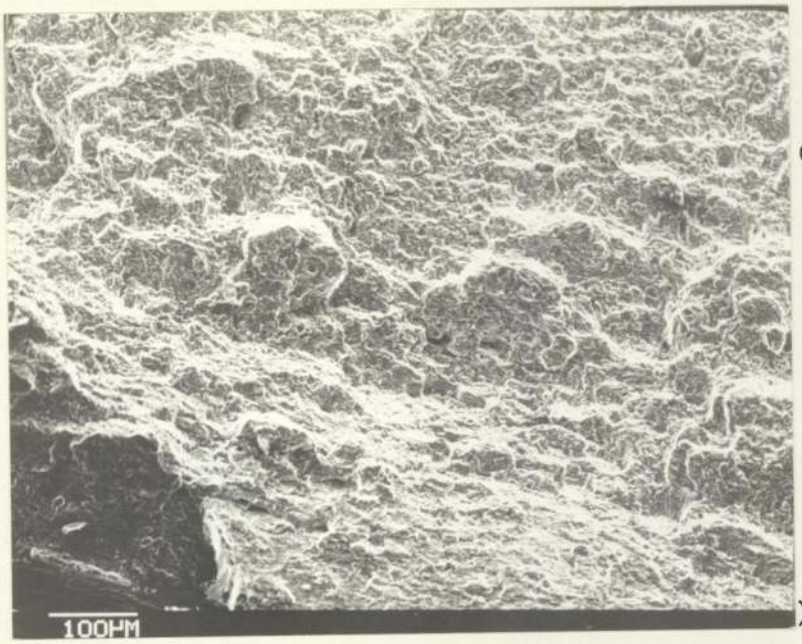

a

X200

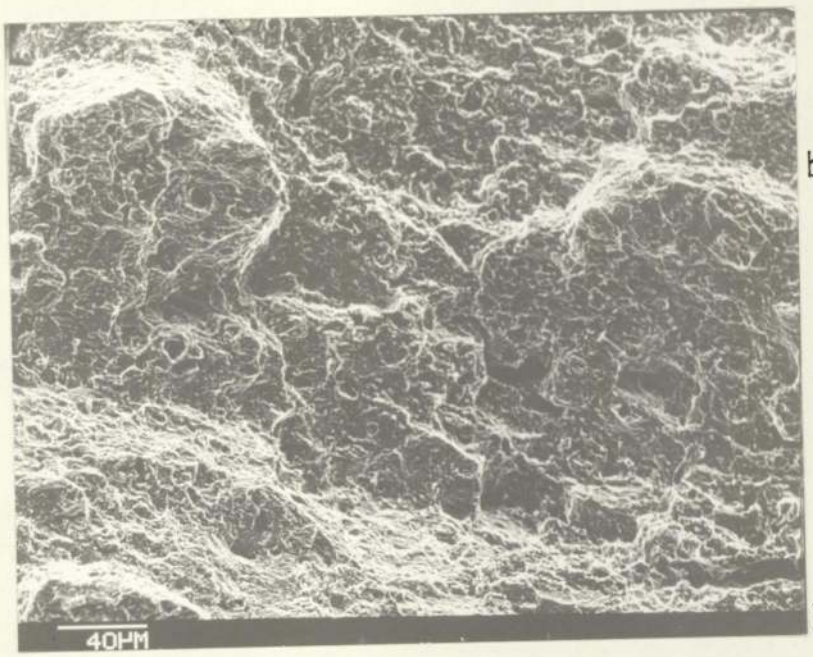

b

X500

Fig. 73 S.E.M. fractographs of a micro-cracked Cr plated No.5 die steel impact testpiece showing ductile plus brittle failure. (b) is a magnified view of the central region in (a), revealing some of the brittle areas further.

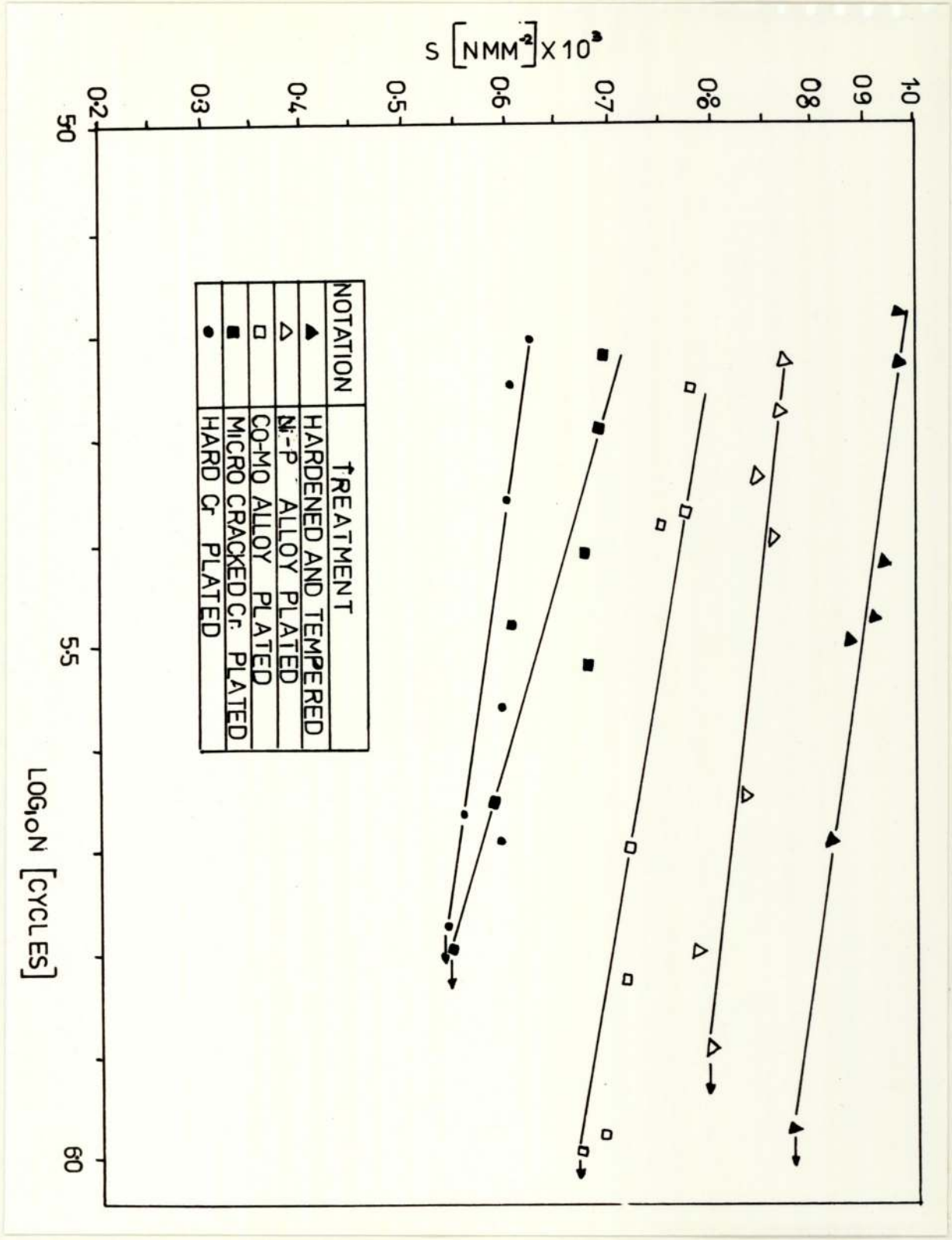

Fig. 74 Semi-range S-N curves for No.5 die steel in its hardened and tempered, and surface treated conditions. A three-point bend fatigue test was used.

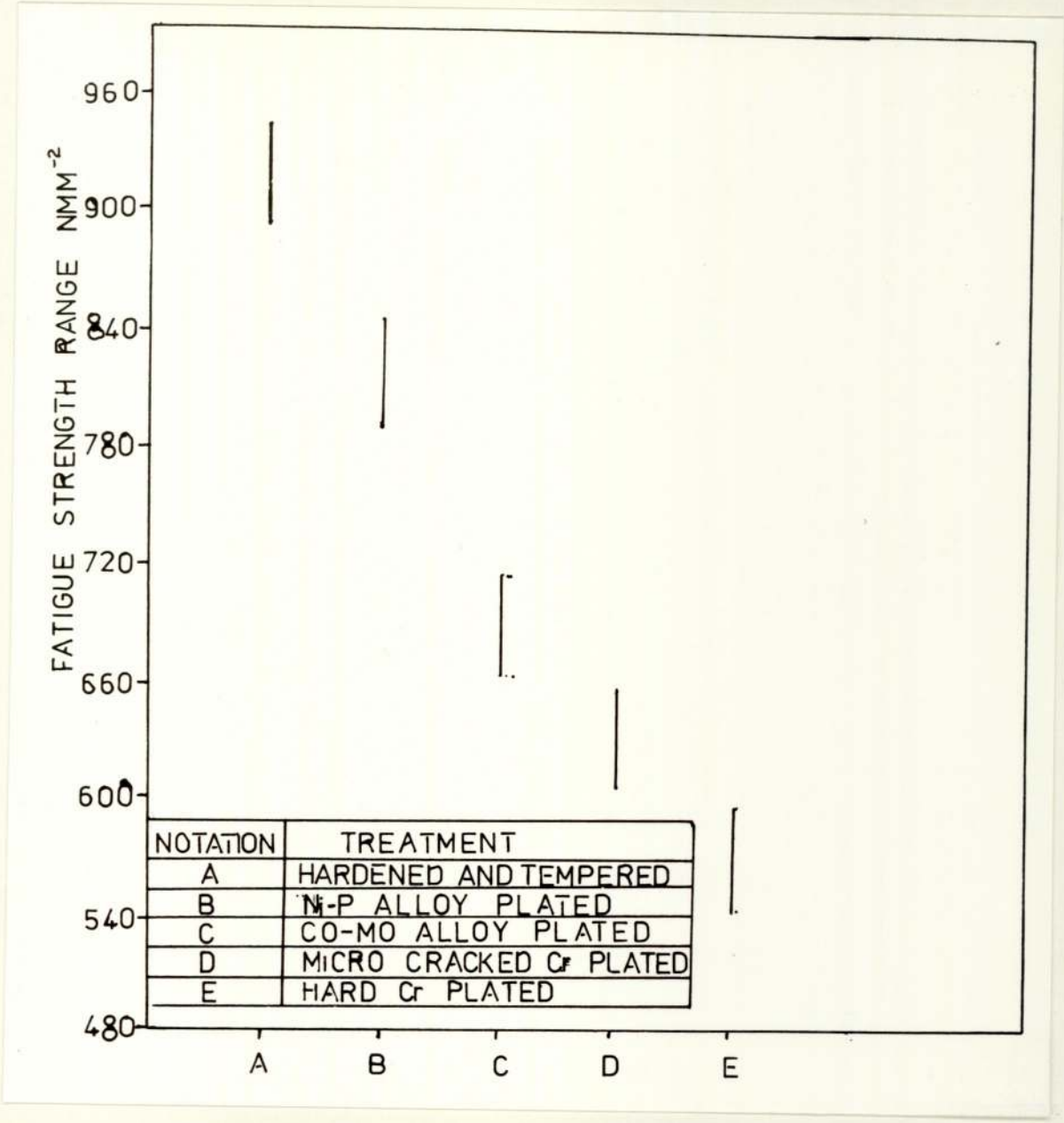

Fig. 75 Schematic representation of confidence limits for estimated fatigue strength data.

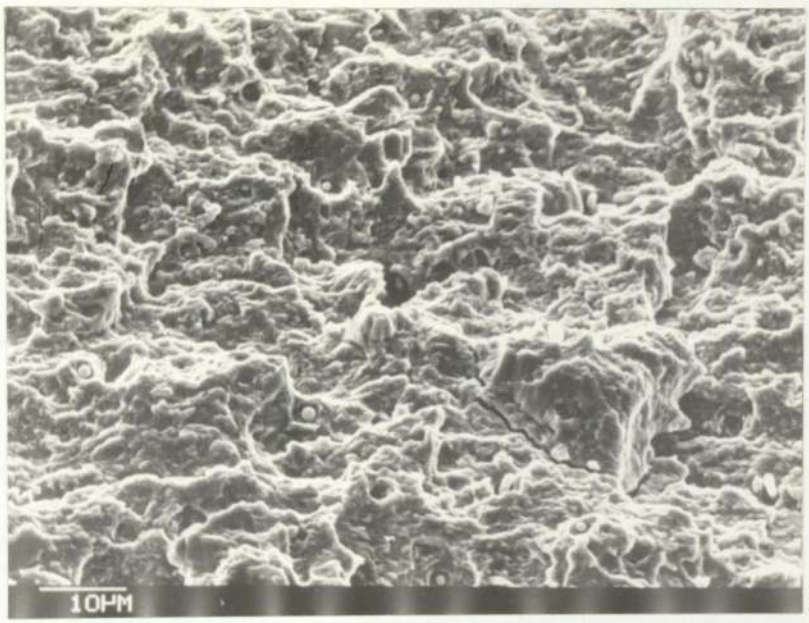

Fig. 76 S.E.M. fractographs of a Co-Mo alloy plated No.5 die steel fatigue testpiece showing void coalescence. (b) is a magnified view of (a) revealing some of the inclusions associated with the dimples.

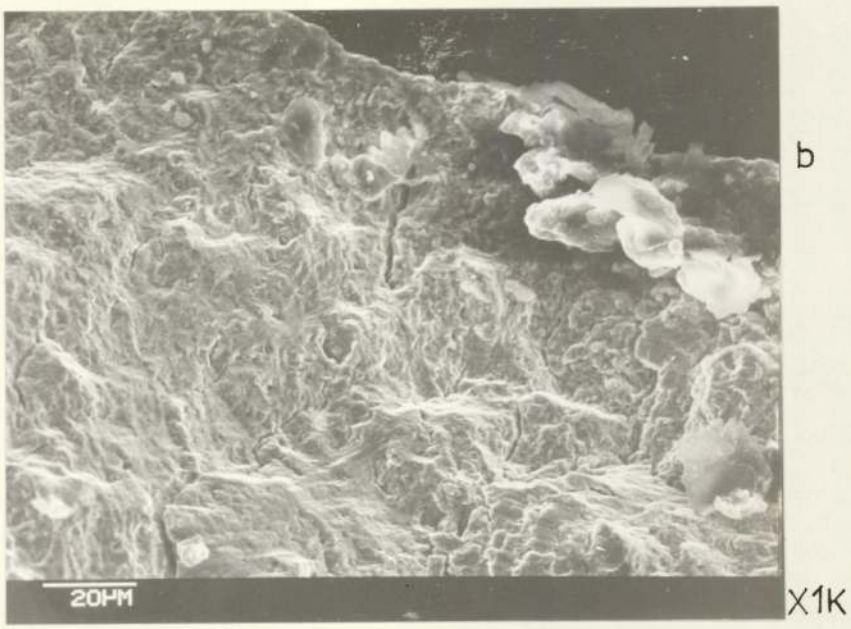

Fig. 77 S.E.M. Fractograph of a Co-Mo alloy plated No.5 die steel fatigue testpiece showing brittle failure and crack initiation at the surface (b) is a magnified view of (a)

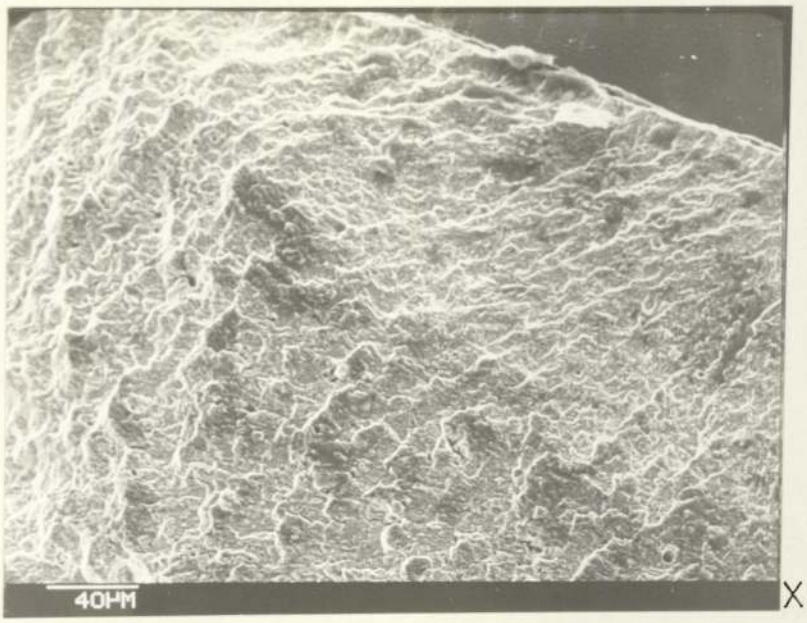

Fig. 78 S.E.M. fractograph of a hardened and tempered No.5 die steel fatigue testpiece showing brittle cleavage.

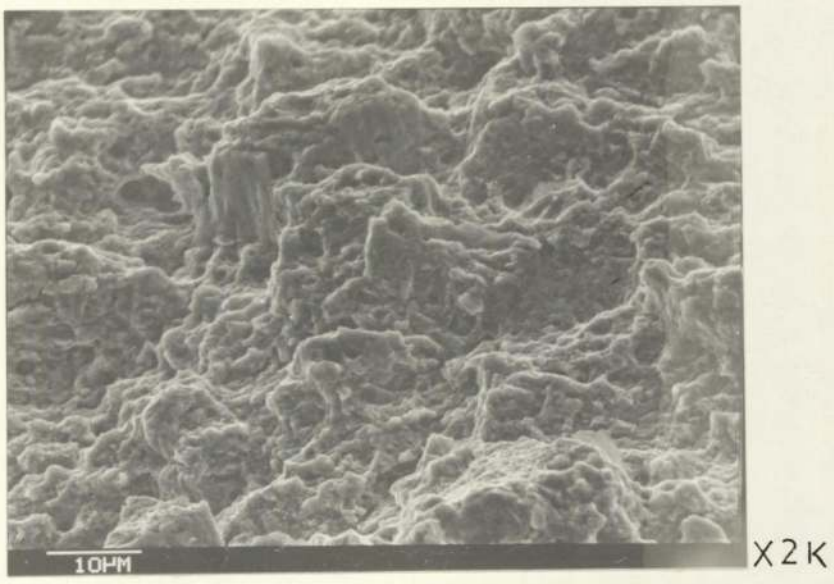

Fig. 79 S.E.M. fractograph of a hardened and tempered No.5 die steel fatigue testpiece showing ductile failure in the core.

Fig. 80 S.E.M. fractograph of a hardened and tempered No.5 die steel testpiece (having a life of 9.44 kilocycles) showing brittle failure and crack initiation at the surface.

Fig. 81 S.E.M. fractograph of a hardened and tempered No.5 die steel testpieces showing brittle failure and the direction of crack propagation (testpiece surface is nearer the top of the fractograph).

Fig. 82 S.E.M. fractograph of a hard Cr plated No.5 die steel fatigue testpiece showing a tear ridge and brittle failure at the coating-steel interface.

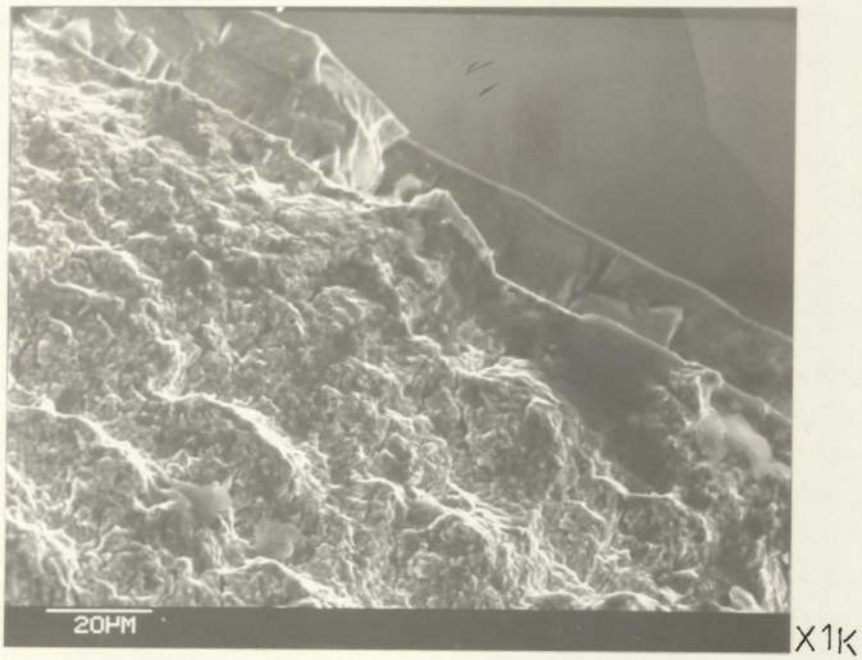

Fig. 83 S.E.M. fractograph of a hard Cr plated No.5 die steel fatigue testpiece showing crack initiation at the surface.

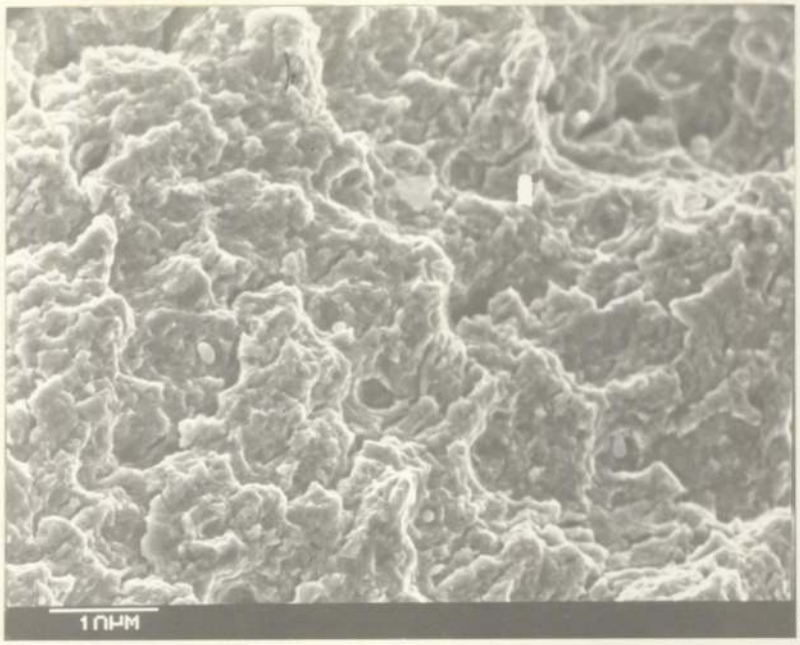

Fig. 84 S.E.M. fractograph of a hard Cr plated No.5 die steel fatigue showing ductile failure in the core.

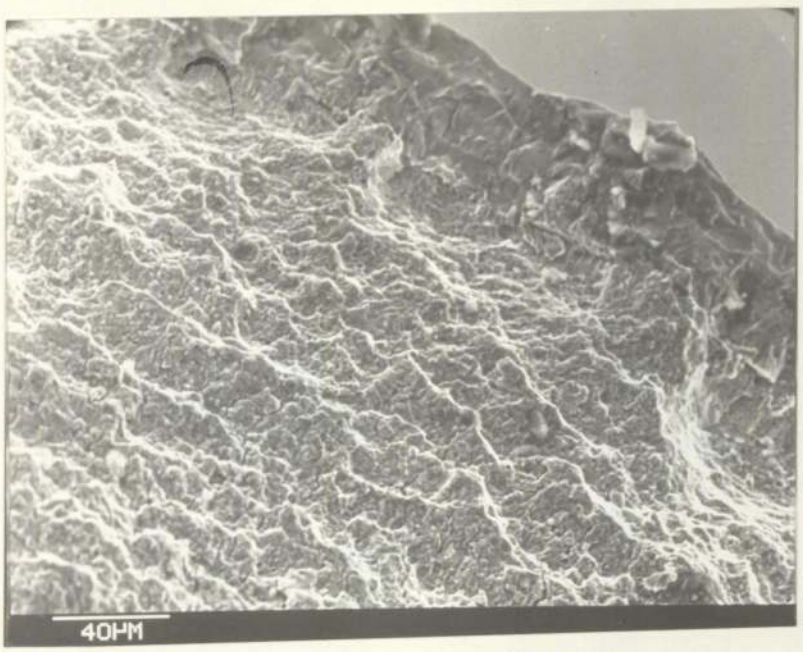

Fig. 85 S.E.M. fractograph of a micro-cracked Cr plated No.5 die steel fatigue testpiece showing brittle failure and crack initiation of the surface.

Fig. 86 S.E.M. fractograph of a micro-cracked Cr plated No.5 die steel fatigue testpiece showing cleavage steps and river patterns near the surface.

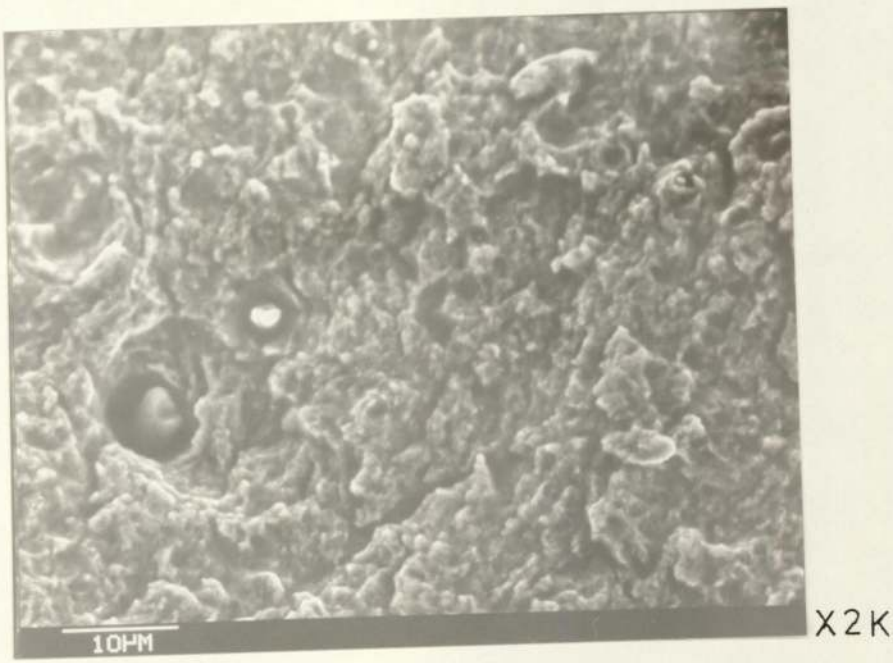

Fig. 87 S.E.M. fractograph of a micro-cracked Cr plated No.5 die steel fatigue testpiece ductile failure in the core. Note the equiaxed dimple and the secondary cracking associated with them. The inclusion was identified to be a silicate.

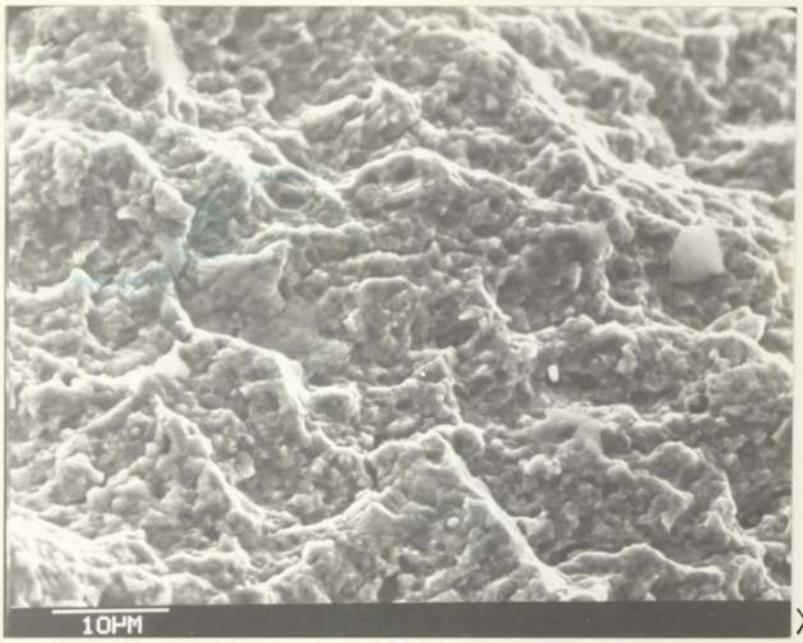

Fig. 88 S.E.M. fractograph of a micro-cracked Cr plated No.5 die steel fatigue testpiece showing inclusions and the network of cracks that are typical of transgranular failure by micro void coalescence.

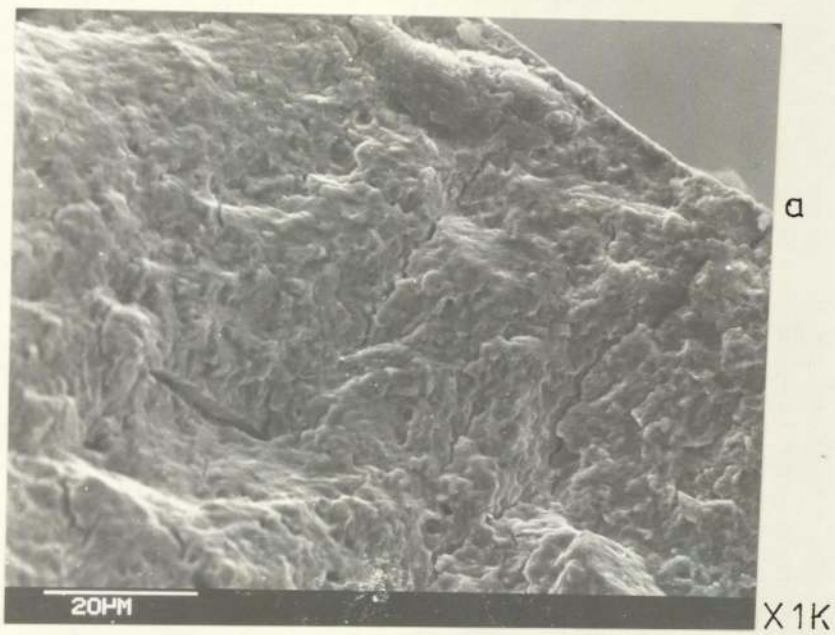

a

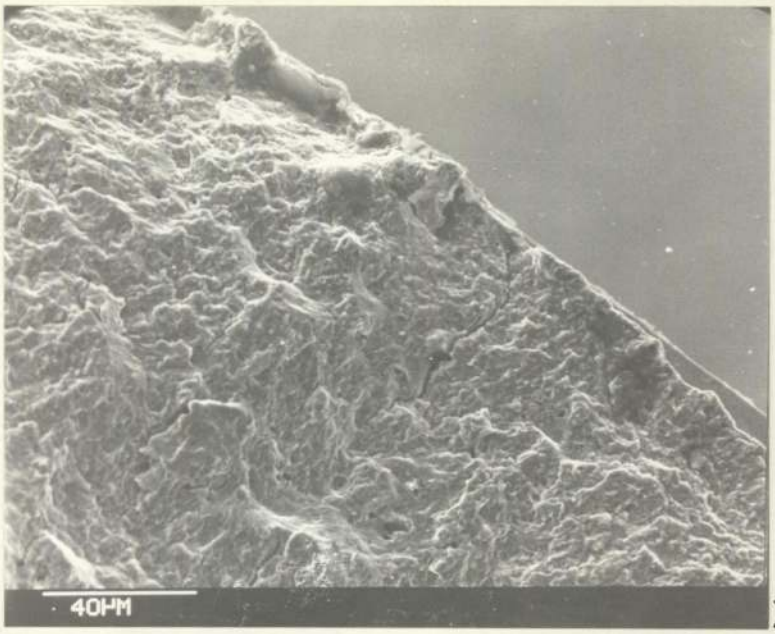

Fig. 89 S.E.M. fractograph of a Ni-P alloy plated No. 5 die steel fatigue testpiece showing (a) failure initiation at the surface, together with sites favourable to ductile and brittle failure. The life of the testpiece was 7.94 kilocycles. (b) is a lower manification of the area adjacent to that in (a) showing the coating which appears to be slightly obscured due to flow of material.

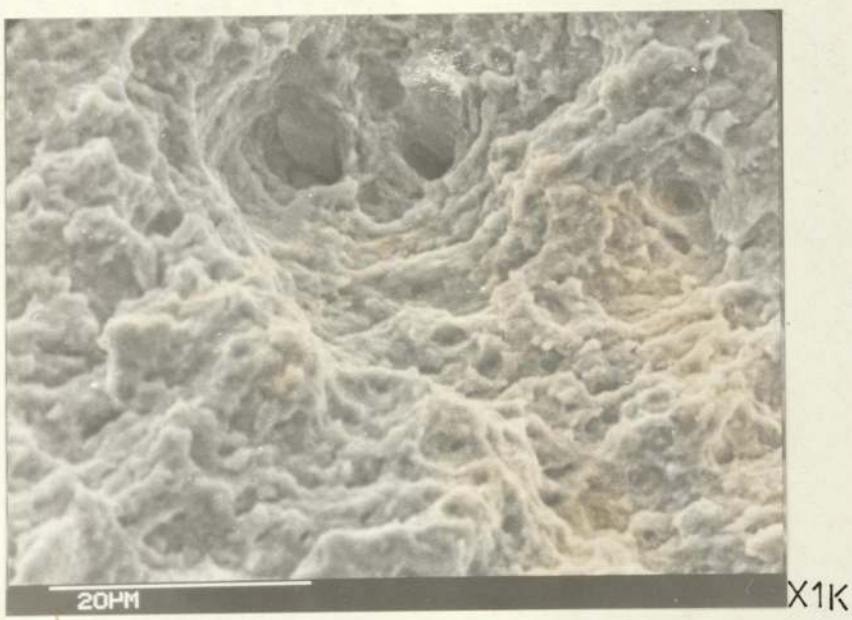

Fig. 90 S.E.M. fractograph of a Ni-P alloy plated No.5 die steel fatigue testpiece showing void coalescence in the core. Fracture is of the "Cup and Cone" type typified by the presence of equiaxed dimples. Note the tilting of cups and the cracks from them.

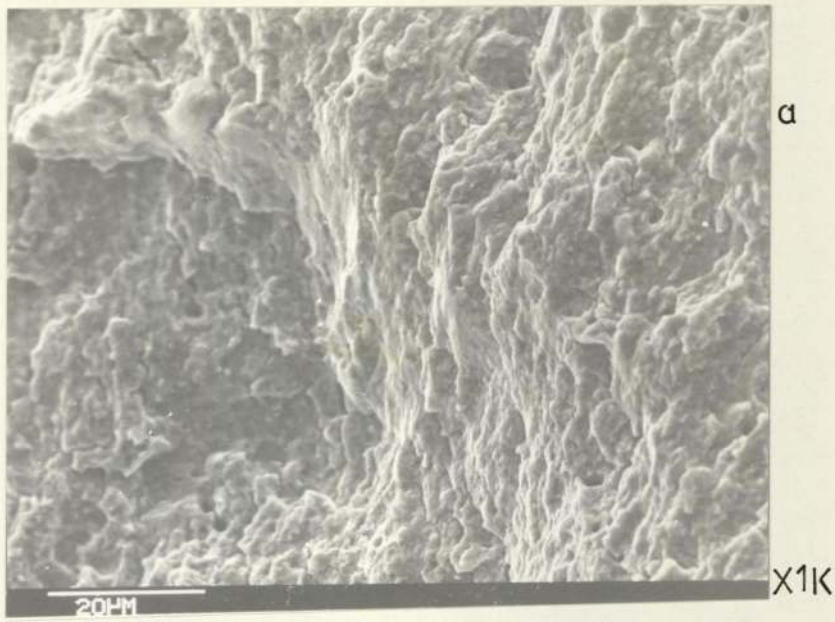

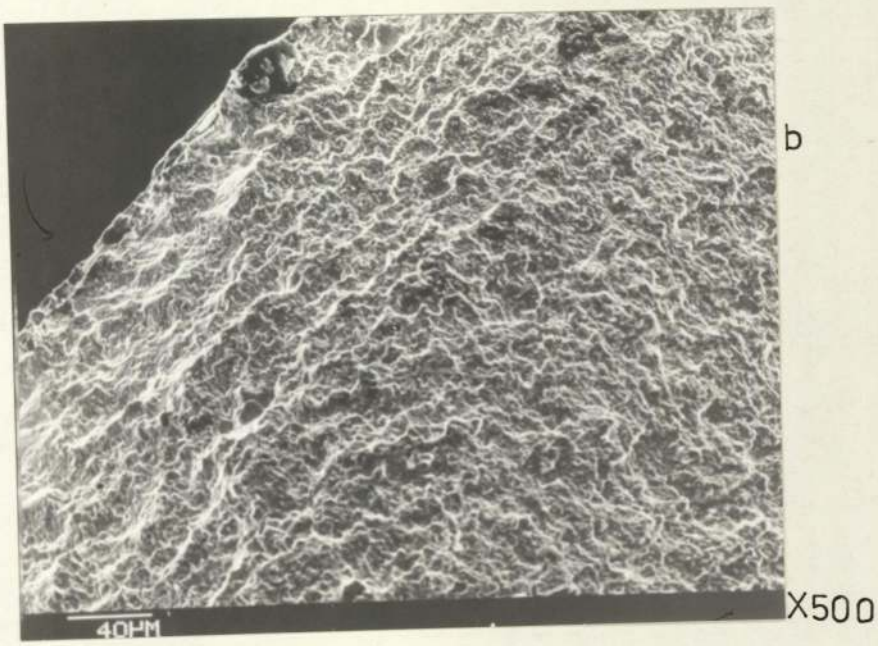

Fig. 91 S.E.M. fractographs of a Ni-P alloy plated No.5 die steel fatigue testpiece showing brittle failure in the slow fracture region (i.e. near the surface).

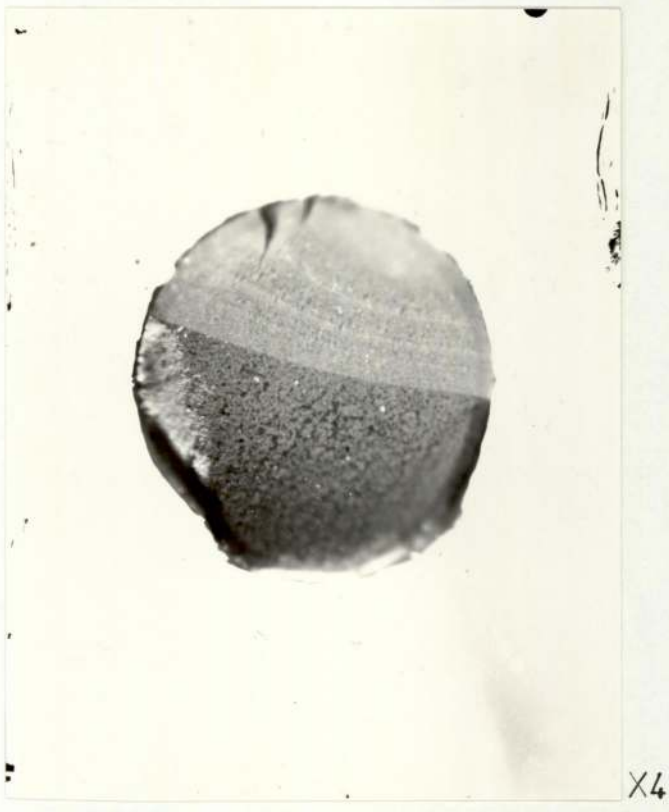

Fig. 92 Optical fractograph of the matching fracture surfaces of a Co-Mo alloy plated No.5 die steel fatigue testpiece. The life was 9.55 kilocycles. Note the initiation of failure of the surface.

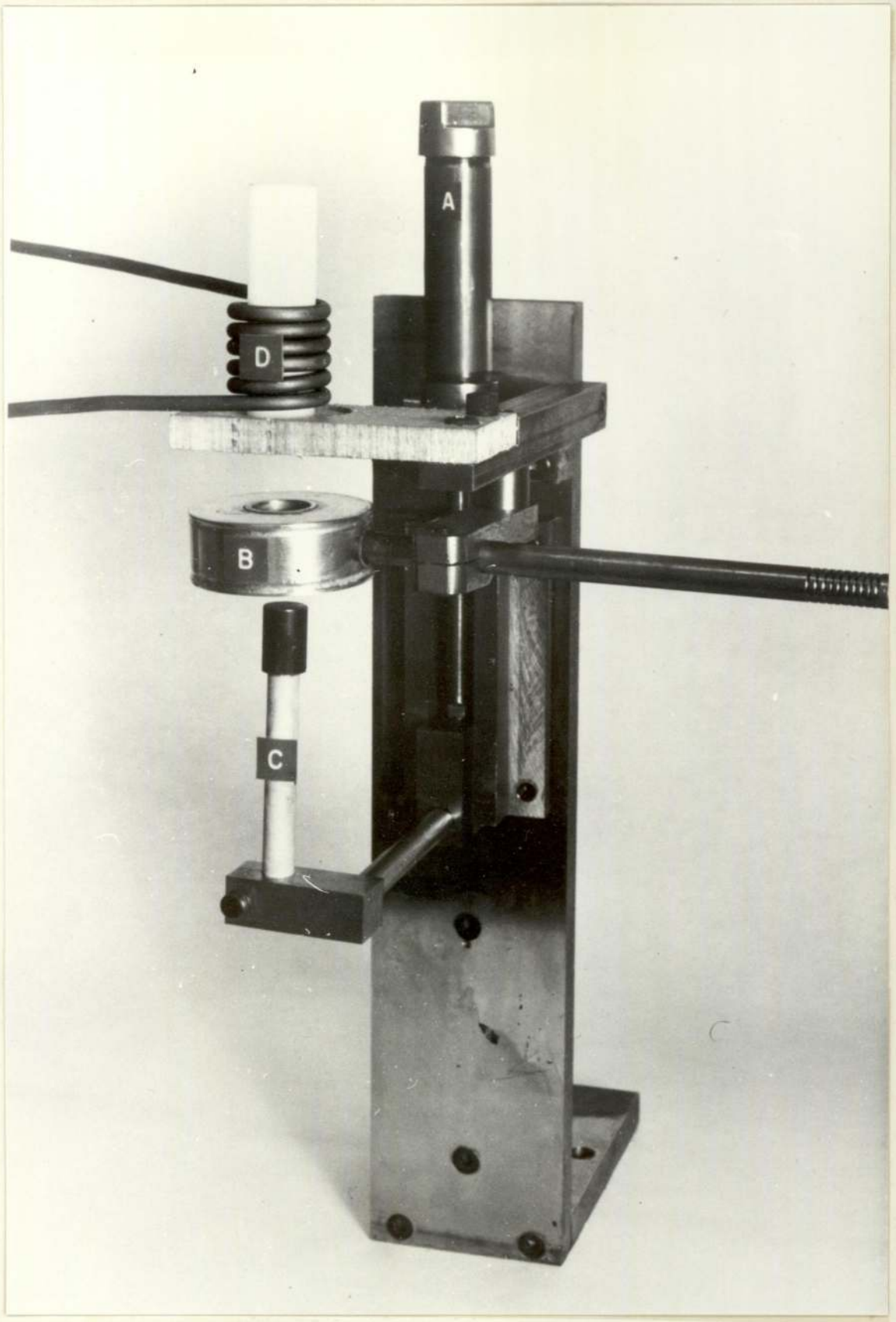

Fig. 93 Thermal Fatigue apparatus:

A: Air Cylinder

B: Air Spray

C: Ceramic Tube

D: H.F. Coil